

THE JOURNAL OF PHYSICAL CHEMISTRY

(Registered in U. S. Patent Office)

CONTENTS

Theoretical Pathways for the Reduction of N_2 Molecules in Aqueous Media: Thermodynamics of N_2H_4 : by Norman Bauer.....	833
Interactions in Aqueous Solutions III. On Statistical Thermodynamics of Colloidal Electrolytes: by D. Stigter.....	838
Interactions in Aqueous Solutions. IV. Light Scattering of Colloidal Electrolytes: by D. Stigter.....	842
Transmission Coefficients for Evaporation and Condensation: by Earl M. Mortensen and Henry Eyring.....	846
Heptane Isomerization: by G. M. Kramer and A. Schriesheim.....	849
The Sorption of Water Vapor by Native and Denatured Egg Albumin: by Robert L. Altman and Sidney W. Benson.....	851
The Phase Rule: The Significance of Negative Degrees of Freedom: by H. F. Halliwell and S. C. Nyburg.....	855
The Submonolayer Adsorption of Argon and Krypton on Molybdenum Disulfide: Phenomenological Comparison with Studies on Graphite: by Peter Cannon.....	858
The Heat of Fusion of Bismuth Trichloride—A Comparison of Calorimetric and Cryoscopic Determinations: by L. E. Topol, S. W. Mayer and L. D. Ransom.....	862
Phase Equilibria in the Systems BeF_2 - TbF_3 and LiF - BeF_2 - TbF_3 : by R. E. Thoma, H. Inaley, H. A. Friedman and C. F. Weaver.....	865
A Spectrophotometric Study of the Complexes Formed between Uranyl and Chloride Ions in Water and Water-Ethanol Solvents: by Jack D. Hefley and Edward S. Amis.....	870
Self-Diffusion in Molten Nitrates: by A. S. Dworkin, R. B. Escue and E. R. Van Artadalen.....	872
Anomalous Solvent Extraction Equilibria Due to Violence of Agitation: by Kenneth A. Allen and W. J. McDowell.....	877
Microwave Absorption and Molecular Structure in Liquids. XXXII. Analysis of the Relaxation Times of n -Alkyl Bromides in Terms of a Distribution between Limiting Values: by Keniti Higasi, Klaus Bergmann and Charles P. Smyth.....	880
Block-Polymers of Styrene and Isoprene with Variable Distribution of Monomers along the Polymeric Chain. Synthesis and Properties: by S. Schlick and M. Levy.....	883
Nuclear Magnetic Resonance Studies of Hydrogen Bonding. I. Carboxylic Acids: by Jeff C. Davis, Jr., and Kenneth S. Pitzer.....	886
Kinetics of n -Pentane Isomerization over $Pt-Al_2O_3$ Catalyst: by J. H. Sinfelt, H. Hurwitz and J. C. Rohrer.....	892
Kinetics of Hydrolysis of Polyethylene Terephthalate Films: by R. C. Golike and S. W. Lasoski, Jr.....	895
Analysis of Absorption Spectra of Multicomponent Systems: by Richard M. Wallace.....	899
Oscillating Temperatures in Reaction Kinetics. I. Activation Energy from Steady State Concentration: by Thomas I. Crowell.....	902
The Heat Capacity and Thermodynamic Functions of Uranium from 5 to 350° K.: by Howard E. Flotow and Harold R. Lohr.....	904
Chemical Thermodynamic Properties of Methylcyclopentane and 1- <i>cis</i> -3-Dimethylcyclopentane: by D. W. Scott, W. T. Berg and J. P. McCullough.....	906
The Mercury-Mercuric Chloride System: by S. J. Yosim and S. W. Mayer.....	909
High-Temperature Free Energy, Entropy, Enthalpy and Heat Capacity of Thorium Sulfate: by S. W. Mayer, B. B. Owens, T. H. Rutherford and R. B. Serrins.....	911
The Heat Content of Boron at High Temperatures: by Stephen S. Wise, John L. Margrave and Robert L. Altman.....	915
Comparative Studies on the Decarboxylation of Malonic Acid and the Trichloroacetate Ion: by Louis Watts Clark.....	917
Activity Coefficients for Thallous Sulfate in Aqueous Solution at 25°: by J. M. Creeth.....	920
Asbestos Ore Body Minerals Studied by Zeta Potential Measurements: by Edward Martinez and Gordon L. Zucker.....	924
Heats of Combustion, Formation and Isomerization of the <i>cis</i> and <i>trans</i> Isomers of Hexahydroindan: by Clarence C. Browne and Frederick D. Rossini.....	927
NOTES	
Effect of a Noble Gas on the Labeling of n -Hexane by Exposure to Tritium: by A. Y. Mottlau.....	931
An Approximate Method for Measuring the Self-Interaction Constant of Non-Electrolytes in Two-Component Solvents: by Ernest Grunwald and George Baughman.....	933
The Effect of Pressure on the Melting Points of Isotactic Polypropylene and Polyethylene Oxide: by L. R. Fortune and G. N. Malcolm.....	934
The Influence of Ethane on the Polymerization Rate of Ethylene: by Chiya Eden and Hans Feilchenfeld.....	935
Heat of Entropy of Fusion and Cryoscopic Constant of Silver Nitrate: by George J. Janz, David W. James and Jerome Goodkin.....	937
The Preparation of Single Crystals of Certain Transition Metal Fluorides: by H. Guggenheim.....	938
The Association Equilibrium in the Methyl Bromide-Aluminum Bromide System. Estimated Bonding Strengths of Aluminum Bromide-Addition Molecules with Methyl Bromide, Pentene and Benzene: by D. G. Walker.....	939
The Growth of Barium Titanate Single Crystals from Molten Barium Fluoride: by R. C. Linares.....	941
The Fluorescence of Acetaldehyde Vapor: by E. Murad.....	942
Dissociation Constant and Limiting Conductance of $LiBr$ in Liquid SO_2 at 0.22°: Evidence for the Solvation of Li^+ : by Norman N. Lichtin and K. Narayana Rao.....	945
On the Concentration-Dependence of the Mobility of Incompletely-Dissociated Unsymmetrical Electrolytes in Diffusion: by J. M. Creeth and R. H. Stokes.....	946
The Application of Gas-Liquid Partition Chromatography to Problems in Chemical Kinetics: Acid-Catalyzed Methanolysis of Enol Acetates: by E. V. Kring, G. I. Jenkins and V. L. Bacchetta.....	947
The Two Crystal Forms of (Ethylene-dinitrilo)-tetraacetic Acid: by R. B. LeBlanc and H. L. Spill.....	949
Flame Temperature and Composition in the Aluminum-Potassium Nitrate Reaction: by A. W. Berger, D. Golomb and J. O. Sullivan.....	949
The Calculation of Equilibrium Constants from Spectrophotometric Data: by C. P. Nash.....	950
Infrared Anisotropy of Triclinic <i>trans</i> -8-Octadecenoic Acid: by Anne S. Jahn and H. Susi.....	953
Evidence from Intrinsic Viscosity and Sedimentation for Hypercoiled Configurations of Styrene-Maleic Acid Copolymer: by Walter Dannhauser, William H. Glaze, Ray L. Dueltgen and Kazuhiko Ninomiya.....	954
Spectroscopic Evidence of an Alumina Catalyzed Surface Reaction between Ammonia and Carbon Disulfide: by E. P. Parry and H. Rubalcava.....	955
Reaction of N,N' -Disalicylidene-1,2-propanediamine with Copper(II) Ions in Aqueous Isopropyl Alcohol Solution: by Kermit B. Whetsel.....	956
The Volatility of Actinium: by K. W. Foster and L. G. Faimé.....	958
COMMUNICATION TO THE EDITOR	
Faradaic Rectification and Electrode Processes: by P. Delahay, M. Senda and C. H. Weiss.....	960

THE JOURNAL OF PHYSICAL CHEMISTRY

(Registered in U. S. Patent Office)

W. ALBERT NOYES, JR., EDITOR

ALLEN D. BLISS

ASSISTANT EDITORS

A. B. F. DUNCAN

A. O. ALLEN
C. E. H. BAWN
JOHN D. FERRY
S. C. LIND

EDITORIAL BOARD
R. G. W. NORRISH
R. E. RUNDLE
W. H. STOCKMAYER

G. B. B. M. SUTHERLAND
A. R. UBBELOHDE
E. R. VAN ARTSDALEN
EDGAR F. WESTRUM, JR.

Published monthly by the American Chemical Society at 20th and Northampton Sts., Easton, Pa.

Second-class mail privileges authorized at Easton, Pa. This publication is authorized to be mailed at the special rates of postage prescribed by Section 131.122.

The *Journal of Physical Chemistry* is devoted to the publication of selected symposia in the broad field of physical chemistry and to other contributed papers.

Manuscripts originating in the British Isles, Europe and Africa should be sent to F. C. Tompkins, The Faraday Society, 6 Gray's Inn Square, London W. C. 1, England.

Manuscripts originating elsewhere should be sent to W. Albert Noyes, Jr., Department of Chemistry, University of Rochester, Rochester 20, N. Y.

Correspondence regarding accepted papers, proofs and reprints should be directed to Assistant Editor, Allen D. Bliss, Department of Chemistry, Simmons College, 300 The Fenway, Boston 15, Mass.

Business Office: Alden H. Emery, Executive Secretary, American Chemical Society, 1155 Sixteenth St., N. W., Washington 6, D. C.

Advertising Office: Reinhold Publishing Corporation, 430 Park Avenue, New York 22, N. Y.

Articles must be submitted in duplicate, typed and double spaced. They should have at the beginning a brief Abstract, in no case exceeding 300 words. Original drawings should accompany the manuscript. Lettering at the sides of graphs (black on white or blue) may be pencilled in and will be typeset. Figures and tables should be held to a minimum consistent with adequate presentation of information. Photographs will not be printed on glossy paper except by special arrangement. All footnotes and references to the literature should be numbered consecutively and placed in the manuscript at the proper places. Initials of authors referred to in citations should be given. Nomenclature should conform to that used in *Chemical Abstracts*, mathematical characters be marked for italic, Greek letters carefully made or annotated, and subscripts and superscripts clearly shown. Articles should be written as briefly as possible consistent with clarity and should avoid historical background unnecessary for specialists.

Notes describe fragmentary or incomplete studies but do not otherwise differ fundamentally from articles and are subjected to the same editorial appraisal as are articles. In their preparation particular attention should be paid to brevity and conciseness. Material included in *Notes* must be definitive and may not be republished subsequently.

Communications to the Editor are designed to afford prompt preliminary publication of observations or discoveries whose value to science is so great that immediate publication is imperative. The appearance of related work from other laboratories is in itself not considered sufficient justification

for the publication of a Communication, which must in addition meet special requirements of timeliness and significance. Their total length may in no case exceed 500 words or their equivalent. They differ from Articles and Notes in that their subject matter may be republished.

Symposium papers should be sent in all cases to Secretaries of Divisions sponsoring the symposium, who will be responsible for their transmittal to the Editor. The Secretary of the Division by agreement with the Editor will specify a time after which symposium papers cannot be accepted. The Editor reserves the right to refuse to publish symposium articles, for valid scientific reasons. Each symposium paper may not exceed four printed pages (about sixteen double spaced typewritten pages) in length except by prior arrangement with the Editor.

Remittances and orders for subscriptions and for single copies, notices of changes of address and new professional connections, and claims for missing numbers should be sent to the American Chemical Society, 1155 Sixteenth St., N. W., Washington 6, D. C. Changes of address for the *Journal of Physical Chemistry* must be received on or before the 30th of the preceding month.

Claims for missing numbers will not be allowed (1) if received more than sixty days from date of issue (because of delivery hazards, no claims can be honored from subscribers in Central Europe, Asia, or Pacific Islands other than Hawaii), (2) if loss was due to failure of notice of change of address to be received before the date specified in the preceding paragraph, or (3) if the reason for the claim is "missing from files."

Subscription Rates (1960): members of American Chemical Society, \$12.00 for 1 year; to non-members, \$24.00 for 1 year. Postage to countries in the Pan-American Union \$0.80; Canada, \$0.40; all other countries, \$1.20. Single copies, current volume, \$2.50; foreign postage, \$0.15; Canadian postage, \$0.05; Pan-American Union, \$0.05. Back volumes (Vol. 56-59) \$25.00 per volume; (starting with Vol. 60) \$30.00 per volume; foreign postage per volume \$1.20, Canadian, \$0.15; Pan-American Union, \$0.25. Single copies: back issues, \$3.00; for current year, \$2.50; postage, single copies: foreign, \$0.15; Canadian, \$0.05; Pan American Union, \$0.05.

The American Chemical Society and the Editors of the *Journal of Physical Chemistry* assume no responsibility for the statements and opinions advanced by contributors to THIS JOURNAL.

The American Chemical Society also publishes *Journal of the American Chemical Society*, *Chemical Abstracts*, *Industrial and Engineering Chemistry*, International Edition of *Industrial and Engineering Chemistry*, *Chemical and Engineering News*, *Analytical Chemistry*, *Journal of Agricultural and Food Chemistry*, *Journal of Organic Chemistry*, *Journal of Chemical and Engineering Data* and *Chemical Reviews*. Rates on request.

THE JOURNAL OF PHYSICAL CHEMISTRY

(Registered in U. S. Patent Office) (© Copyright, 1960, by the American Chemical Society)

VOLUME 64

JULY 25, 1960

NUMBER 7

THEORETICAL PATHWAYS FOR THE REDUCTION OF N₂ MOLECULES IN AQUEOUS MEDIA: THERMODYNAMICS OF N₂H_n¹

BY NORMAN BAUER

Chemistry Department, Utah State University, Logan, Utah

Received April 1, 1969

From an estimate that the hypothetical gaseous anion N₂⁻ would lose its electron with the liberation of at least 63 kcal./mole, from the assumption that its free energy of hydration would equal that of O₂⁻, and from thermodynamic data on hydrazine and oxygen, it has been deduced that the as yet unobserved free radical N₂H should be moderately stable and should require at least 32 kcal./mole of free energy for the removal of its H atom. Estimates of electron affinities, of proton and of H-atom dissociation free energies for free radicals, molecules or anions of the type N₂H_n (n = 1 to 3) were also obtained; and these quantities proved to be consistent with the known reduction potential of the N₂, N₂H_{2aq}⁺ couple. The results suggest that, under special conditions favorable for the stabilization of the anions N_{2aq}⁻ and N₂H_{n, aq}⁻, the reduction of N₂ to N₂H_{2aq} may be able to proceed through free radical intermediates by a succession of electron, water, proton captures.

I. Introduction

The extraordinary stability of the N₂ molecule, reflected in its dissociation energy of 225 kcal./mole, indicates the difficulty of producing nitrogenous compounds from elementary nitrogen. Nevertheless, the fact that either nitric acid or ammonia in dilute aqueous solution is thermodynamically stable under ordinary conditions intrigues us with the possibility of oxidizing or reducing aqueous N₂. Furthermore the challenging fact of biological N₂-fixation tells us that the rate of some such process is not impracticably slow. The crucial mechanisms of the first several steps in this fixation are unknown.²⁻⁴

In the present study we attempt to deduce thermodynamic limitations on conceivable free radical mechanisms of biological N₂-fixation from theoretical estimates of electron affinities involved in a series of one-electron transfers which would yield N₂H_n in an aqueous system. The conception followed here is somewhat parallel to Gorin's

idea⁵ that the formation of the anion O_{2aq}⁻ is the first and slowest step in oxidations by hydrated molecular oxygen. The results below are only tentative (*cf.* Sec. V), but the combination of principles used should eventually yield definite answers.

II. "Electron Affinity" of Gaseous N₂.—The properties of N₂ and of nitrogen compounds imply that a large investment of energy would be required to create or stabilize the anion N₂⁻, if indeed it can exist. We shall try to estimate an upper limit for the hypothetical electron affinity of N₂, A_{N₂}, defined as the energy change for reaction 4, below. This requires an upper limit for D_{N₂}⁻, the dissociation energy of N_{2g}⁻ according to (1), which we shall assume is given by D_{NO} = 150 kcal./mole for the isoelectronic nitric oxide.⁶ It seems to be a reasonable working hypothesis that D_{N₂}⁻ should be no greater than D_{NO} because the nuclear or core charges in N₂⁻ are smaller than in NO, hence are less capable of keeping the outer electrons in the "binding region" defined by Berlin.⁷ The upper limit of A_N, the electron affinity of atomic nitrogen,

(1) Paper III of the series "Physical-chemical Studies of Biological Nitrogen Fixation," supported by a grant from the Herman Frasch Foundation. Ref. (4) is paper II.

(2) (a) W. D. McElroy and B. Glass, eds., "A Symposium on Nitrogen Metabolism. Function of Metallo-Flavoproteins," The Johns Hopkins Press, Baltimore, 1956; (b) M. K. Bach, *Biochim. et Biophys. Acta*, **26**, 104 (1957).

(3) J. E. Carnahan and J. E. Castle, *J. Bacteriol.*, **75**, 121 (1958).

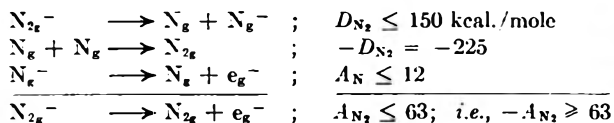
(4) N. Bauer and R. G. Mortimer, *Biochim. et Biophys. Acta*, **40**, 170 (1960).

(5) M. H. Gorin, *Ann. N. Y. Acad. Sci.*, **40**, 123 (1940).

(6) G. Herzberg, "Molecular Spectra and Molecular Structure. I. Spectra of Diatomic Molecules," D. Van Nostrand, Inc., New York, N. Y., 1953, p. 558; A. G. Gaydon, "Dissociation Energies and Spectra of Diatomic Molecules," John Wiley and Sons, Inc., New York, N. Y., 1947, pp. 164-165; G. G. Cloutier and H. I. Schiff, *J. Chem. Phys.*, **31**, 793 (1959).

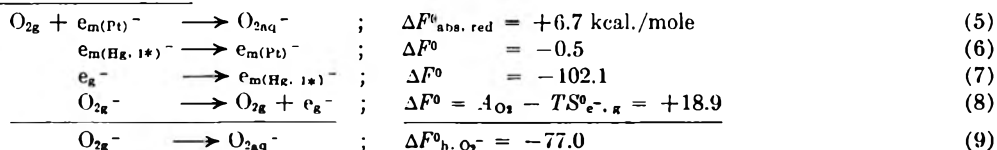
(7) T. Berlin, *J. Chem. Phys.*, **19**, 208 (1951).

in eq. 3 is set by the theory of Rohrlisch⁸ since a higher value is not compatible with other estimates⁹ or with the failure to observe N^- in mass spectra. Accordingly, we have



Equation 4, in harmony with general expectations, means that gaseous N_{2g}^- would be exceedingly unstable.

III. Possible Stabilization of N_{2g}^- and the N_{2aq}^- Electrode Potential.—An anion unstable in the gaseous state is not unprecedented in chemical reactions; and Fajans¹⁰ has stressed the role of cations or dipoles in stabilizing negative groups such as O^{2-} . In the case of N_{2g}^- we wish to see if the forces of hydration may be sufficient to give this anion sufficient stability in aqueous systems for its existence at least as a fleeting intermediate between N_2 and its protonated counterpart, N_2H .



This is conceivable because most known hydration energies of simple anions exceed the 63 kcal./mole required to stabilize N_{2g}^- .

We shall estimate the standard free energy of hydration of gaseous N_{2g}^- , $\Delta F_{h, N_2}^0$, by making the reasonable assumption that it equals $\Delta F_{h, O_2}^0$, i.e., is identical to that of the quite similar O_{2g}^- ion. Such an assumption should not be off by more than a few kcal./mole, in view of the fact that $\Delta F_{h, X}^0$ values for the halides¹¹ ($Cl^- = -84$, $Br^- = -78$, $I^- = -70$ kcal./mole) differ by so little in spite of large differences in size and polarizability.

Using the standard oxidation potential¹² for $(O_{2aq}^- \rightarrow O_{2g} + e_{m(Pt)}^-)$ of $E_{\text{rel}}^0 = +0.56$ v., one may deduce $\Delta F_{h, O_2}^0$ by following the reasoning of Latimer, Pitzer and Slansky,¹¹ and of Latimer,¹² according to eq. 5-9 below. We shall use $E_{\text{abs. ox}}^0 = -0.56$ v. for the absolute oxidation potential^{11,13} of the standard calomel electrode, where $E_{\text{rel. ox}}^0 = -0.2676$ v. for its potential relative to the hydrogen electrode. We also use $+0.02$ v. for the transfer of an electron from Hg to Pt metals (volta potential)¹³⁻¹⁵; i.e., $E_{\text{rel. ox}}^0(Pt) = E_{\text{abs. ox}}^0(Pt) + 0.272$ v. at 298°K. In accordance with Brewer¹⁶ we use

(8) F. Rohrlisch, *J. Chem. Phys.*, **30**, 1608 (1959).

(9) H. S. W. Massey, "Negative Ions," Cambridge University Press, Cambridge, 2nd Ed., 1950, p. 3, p. 20.

(10) K. Fajans, *Chimia*, **13**, 354 (1959).

(11) W. M. Latimer, K. S. Pitzer and C. M. Slansky, *J. Chem. Phys.*, **7**, 108 (1939).

(12) W. M. Latimer, "Oxidation Potentials. The Oxidation States of the Elements and Their Potentials in Aqueous Solutions," Prentice-Hall, Inc., New York, N. Y., 2nd Ed., 1952.

(13) R. E. Wood in "Electrochemical Constants," U. S. National Bureau of Standards Circular 524, U. S. Department of Commerce, Aug. 14, 1953.

(14) O. Klein and E. Lange, *Z. Elektrochem.*, **44**, 558 (1938).

(15) B. E. Conway, "Electrochemical Data," Elsevier Publ. Co., New York, N. Y., 1951, p. 31.

102.1 kcal./mole for the standard free energy of removal of an electron from Hg_{1*} in contact with water vapor, instead of 104.5 kcal./mole for removal from dry liquid Hg.

The electron affinity of O_{2g} , used to get $\Delta F_{(8)}^0$, is still subject to controversy.¹⁷ We are inclined to use $A = 20$ kcal./mole in the present study not because its absolute value is necessarily the correct one but because, being deduced from related thermochemical data, it is more apt to be consistent with the electrode potential E_{O_2, O_2}^0 used for $\Delta F_{(5)}^0$ than an electron affinity for O_{2g} deduced from spectroscopic arguments involving as yet unconfirmed excited states. This choice seems to be justified by the result that if the alternative value of A_{O_2} is used below, the unreasonably large value of 93.5 kcal./mole for $-\Delta F_{h, O_2}^0$ is obtained. To convert A_{O_2} to $\Delta F_{(8)}^0$, the Sackur equation was used for the standard entropy of an electron gas, $S_{e^-,g}^0 = 3.6$ e.u. Then, by ignoring the undoubtedly very small difference in vibrational and rotational entropy between O_2 and O_{2g}^- , we have at 298°K.

In this and following calculations we retain all numbers to the nearest 0.1 kcal./mole even though the absolute values in most cases are far from that reliable. In that way certain small differences or trends in relative quantities may be correctly calculated at a later stage. Also, a number of small terms (e.g., $\Delta F_{(6)}^0$) are included for clarity of thought and for showing how to make better predictions as improved data become available.

The above value of $\Delta F_{h, O_2}^0 = -77.0$ kcal./mole is quite reasonable when compared to those of the halide ions quoted above, considering that O_{2g}^- in aqueous systems should resemble the halide-like CN^- . Thus we can use $\Delta F_{h, N_2}^0 = -77.0$ and $-A_{N_2} \geq 63$ kcal./mole in equations analogous to (5)-(9) to calculate $-\Delta F^0 \geq 89.7$ kcal./mole for the electrode process $N_{2aq}^- \rightarrow N_{2g} + e_{m(Pt)}^-$. According to the above method of absolute electrode potentials, this means that the standard oxidation potential of the couple N_{2aq}^- , N_2 is $E_{\text{rel. ox}}^0 \geq +4.16$ v., relative to H_2 , H_{aq}^+ . Such a large $E_{\text{rel. ox}}^0$ value suggests that hydration alone is not sufficient to give N_{2g}^- an adequate stability for playing a role in chemical reactions; but that N_{2aq}^- may become moderately stable when situated near some additional positive charges.

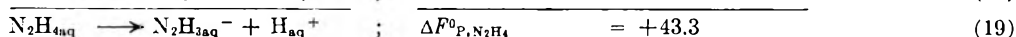
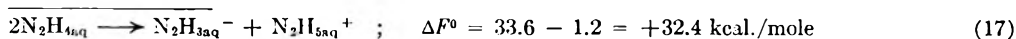
IV. Stabilities of N_2H_n -Type Molecules, Radicals and Anions.—We expect that molecules of the type N_2H_n , and their corresponding anions, would be produced from N_{2aq}^- by proton capture and subsequent further reduction by electrons or H-

(16) L. Brewer in "The Chemistry and Metallurgy of Miscellaneous Materials: Thermodynamics," L. L. Quill, ed., McGraw-Hill Book Co., New York, N. Y., 1950, p. 156.

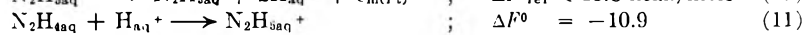
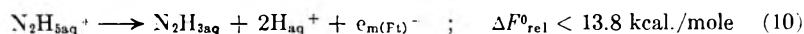
(17) R. S. Mulliken, *Phys. Rev.*, **115**, 1225 (1959); H. O. Pritchard, *Chem. Revs.*, **52**, 529 (1953). Note that Mulliken does not take into account the recent upward revision of D_{N_2} in criticizing Pritchard's application of the "Mulliken Rule."

atoms. In the following we will make an estimate of H-atom dissociation energies and other trends of behavior in the series N₂H, N₂H₂, N₂H₃, N₂H₄.

This is, as far as we know, the first attempt to evaluate the stability of the free radical N₂H. Concerning diimide (or "diazene"),¹³ N₂H₂, the molecule has been observed¹⁹ in mass spectra and it has been postulated¹³ as an intermediate in the oxidation of aqueous hydrazine; while Pauling²⁰ has speculated about the structure of N₂H₂. Dimide also has been postulated as the first intermediate in a reduction mechanism of N₂-fixation.²¹ The salt NaN₂H₃ is known and the radical ("hydrazyl,"¹⁸ or H₃N₂, "hydrogen pernitride") has also been postulated¹⁸ as an intermediate in hydrazine oxidation. However, the free energies of formation or of bond dissociation have not been established for the above three N₂H_n; and even the thermodynamics of N₂H₄ requires further analysis.



(a) **Free Energy of H-Atom Dissociation from N₂H₄.**—Latimer¹² has estimated an upper limit of 0.6 v. for the standard reduction potential of the N₂H₃, N₂H₅⁺ couple from the experiments of Cuy and Bray.²² The following equations 10–16 then give an upper limit for the dissociation free energy of H from N₂H₄, using data for ΔF⁰₍₁₁₎ and ΔF⁰₍₁₃₎ from standard reference works.^{12,23} For ΔF⁰₍₁₄₎, an estimate probably reliable to 0.1 kcal./mole was made from the known standard free energy of condensation of hydrazine (–2.4 kcal./mole)²³ and from the known heat of solution of hydrazine and water,²⁴ using the method of Hildebrand and Scott²⁵ which required the thermal expansivity of aqueous hydrazine.²³ It was assumed that –ΔF⁰₍₁₅₎ = 3ΔF⁰₍₁₄₎/4 because the free energies of hydration of N₂H_n,_{gas} must be almost entirely attributable to dipole interactions along N...H bonds. Then we have



In order to deduce the corresponding quantities for N₂H₃, N₂H₂ and N₂H we shall need estimates of

(18) J. W. Cahn and R. E. Powell, *J. Am. Chem. Soc.*, **76**, 2568 (1954).

(19) S. N. Foner and R. L. Hudson, *J. Chem. Phys.*, **28**, 719 (1958).

(20) L. Pauling, *J. Am. Chem. Soc.*, **53**, 3233 (1935).

(21) C. J. A. I. Virtanen and M. Hakala, *Acta Chem. Scand.*, **3**, 1044 (1949); and ref. 2a, p. 332.

(22) E. J. Cuy and W. C. Bray, *J. Am. Chem. Soc.*, **46**, 1796, 1810 (1924).

(23) L. F. Audrieth and R. A. Ogg, "The Chemistry of Hydrazine," John Wiley and Sons, Inc., New York, N. Y., 1951.

(24) V. C. Bushnell, A. M. Hughes and E. C. Gilbert, *J. Am. Chem. Soc.*, **59**, 2142 (1937).

(25) J. H. Hildebrand and R. L. Scott, "The Solubility of Non-electrolytes," Reinhold Publ. Corp., New York, N. Y., 3rd Ed., 1950, p. 139.

certain free energies of proton dissociation, of hydration and of electron capture, derived below.

(b) **Free Energy of Proton Dissociation from N₂H₄.**—We can estimate this quantity from Pleskov's²⁶ potentiometric studies of NaN₂H₃ in liquid hydrazine. He found $K^{298} = 2 \times 10^{-25}$ for $2\text{N}_2\text{H}_{4\text{solv}} \rightarrow \text{N}_2\text{H}_{3\text{solv}}^- + \text{N}_2\text{H}_{5\text{solv}}^+$, which is close to that for the corresponding reaction in water according to an application of the well-known Born theory of hydration energies. According to this theory, the free energy of proton dissociation from N₂H₄ should be only about $0.0065 \times 175 = 1.2$ kcal./mole more favorable in water than in liquid hydrazine owing to the similarity of dielectric constant ratios $(\epsilon - 1)/\epsilon$ for water (0.987₆) and hydrazine (0.981₀) if we assume the total solvation energy of N₂H₅⁺ and N₂H₃⁻ to be 175 kcal./mole (analogous to K⁺ and Br⁻) and neglect presumably small entropy differences. Then we can make the estimate

(c) **Free Energies of N₂H_n⁻ Anion Hydration.**—

We postulate that ΔF⁰_h of N₂H_n⁻ will increase slowly with increasing number of H-atoms because of the polarity of the N₂...H bond and the asymmetry of the N₂H₄ molecule ($\mu_{\text{N}_2\text{H}_4} = 1.8$ d.). Let us estimate the maximum polar effect per added H-atom as an average of $3.6/4 = 0.9$ kcal./mole, where 3.6 represents the known ΔF⁰ of mixing N₂H₄ and H₂O. Accordingly, for N₂H_n⁻ → N₂H_{n+1}⁻; ΔF⁰_h = –77.0 – 0.9 = –77.9 kcal./mole. For the other anions in the series the values of ΔF⁰_h are: N₂H₂⁻ = –78.8; N₂H₃⁻ = –79.7. The uncertainties in the above increments tend to cancel in applications below, such as in eq. 20–28.

(d) **Electron Affinities of Gaseous N₂H_n.**—We seek to place an upper limit on the electron affinity of N₂H, A_{N₂H}, for this will determine the lower limit of the N₂...H bond dissociation free energy.

A lower limit for the difference

$$\Delta A_{\text{N}_2, \text{N}_2\text{H}} = A_{\text{N}_2\text{H}} - A_{\text{N}_2} \text{ may be}$$

evaluated from the following evidence and combined with the

previously derived A_{N₂} to give

the limit for A_{N₂H}. In this part

(d), ΔE⁰_h refers to energy of hydration, not to a difference in

electrode potentials.

Uri²⁷ has deduced the value –136 kcal./mole for the sum (ΔE⁰_{h, HO₂⁻} – A_{HO₂⁻}}, which is in thermochemical accord with the H...O₂ dissociation energy of 36 kcal./mole and the H...O₂H dissociation energy of 102 kcal./mole. This provides a value of A_{HO₂⁻} ≤ 60.5 kcal./mole, if we take –ΔE⁰_{h, HO₂⁻} ≤ 75.5 which is the mean of the values estimated for O₂⁻ by Evans and Uri²⁸ and by this author from ΔF⁰_{h, O₂⁻} = –77.0 (Sec. III) and from ΔS⁰_{h, O₂⁻} = –15 e.u. We note that ΔE⁰_{h, O₂⁻}} provides a lower limit for the hydration energy of HO₂⁻ because the}}}}}

(26) V. A. Pleskov, *Acta Physicochim. U. R. S. S.*, **13**, 662 (1940).

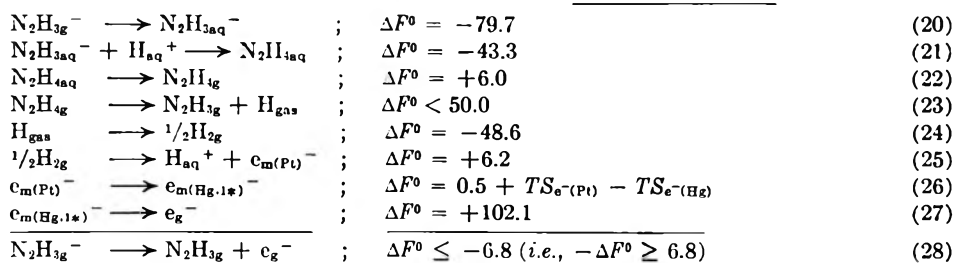
(27) N. Uri, *Chem. Revs.*, **50**, 375 (1952).

(28) M. G. Evans and N. Uri, *Trans. Faraday Soc.*, **45**, 224 (1949).

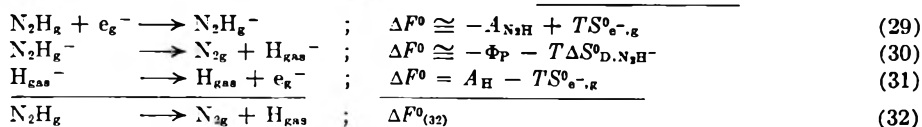
latter must have additional interaction with water owing to the polarity of $H \dots O_2^-$. Thus we know an upper limit for the difference in electron affinities of HO_2 and O_2 ; $\Delta A_{O_2,HO_2} \leq 60.5 - 20.0 = 40.5$ kcal./mole. That is, the result of adding an H-atom to O_2 is to enhance the electron affinity by about 40.5 kcal./mole, an effect we would expect from the fact that this is equivalent to embedding some positive charge within the electronic system of O_2^- . The corresponding effect of adding an H-atom to N_2 should not be as large as that of H in HO_2 . This follows from a consideration of the electronic charge which would be transferred to a proton penetrating the electronic system of N_2^- and of O_2^- . Fajans and Bauer²⁹ have shown that the charge transfer is an asymptotic function of the polarizability of the anion, for noble gas structures. In this analogous case the polarizability of N_2^- would be greater than that of O_2^- because of its lesser nuclear (core) charge; and would provide the greater neutralization of protonic charge.

We thus tentatively conclude that $\Delta A_{N_2,N_2H} < \Delta A_{O_2,HO_2}$; that is, $A_{N_2H} - A_{N_2} \leq 40.5$ kcal./mole. From Sec. I, $-A_{N_2} = 63.0$, so $-A_{N_2H} \geq 22.5$ kcal./mole.

Independent evidence that the above value of A_{N_2H} is substantially correct may be derived from equations (20) to (28), which give an estimate of the related quantity $A_{N_2H_1}$.



Neglecting the undoubtedly small differences in entropies between $N_2H_{3g}^-$ and N_2H_{3g} , the electron affinity of N_2H_{3g} is given by $-A_{N_2H_{3g}} = -\Delta F^0_{(28)} - TS_{e^-,g} \geq 6.8 - 1.1 = 5.7$ kcal./mole. This is consistent with the idea that the more H-atoms added to N_2 , the greater the electron affinity. It also gives the reasonable result that the first H-atom added shows a greater effect than subsequent ones. The consequent greater stability of $N_2H_3^-$, relative to that of N_2H^- , is consistent with the known properties of $Na.N_2H_3$. If we assume that $A_{N_2H_1}$ lies midway between that of N_2H and N_2H_3 we have these approximate values for the entire N_2H_n series: $-A_{N_2} \geq 63.0$; $-A_{N_2H} \geq 22.5$; $-A_{N_2H_1} \approx 14.1$; $-A_{N_2H_2} \geq 5.7$ kcal./mole.



(e) Free Energy of H-Atom Dissociation from N_2H_n .—From equations (29) to (32), the stability of N_2H with respect to H-atom dissociation may be evaluated.

(29) K. Fajans and N. Bauer, *J. Chem. Phys.*, **10**, 410 (1942).

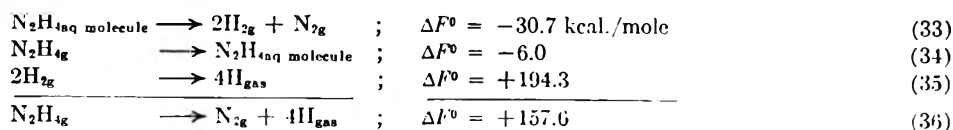
Since we need merely a lower limit for $\Delta F^0_{(32)}$ to establish the stability of N_2H , it suffices to approximate the lower limit of the potential energy liberated by polarization interaction between N_2 and H^- , Φ_P , as well to approximate the upper limit of the corresponding entropy change in reaction 30. Although at large $N_2 \dots H^-$ separations there must be a very small polarization attraction, the distance between H^- and N_2 cannot become sufficiently small for setting up an ordinary bond, owing to transfer of negative charge from H^- to the dipole induced in N_2 . This follows from the exceedingly great deformability of hydride ion (molar refraction = 37 cc./mole). Thus we have $-\Phi_P = 0.0$, or somewhat greater, as a condition for the lower limit of interest. A liberal estimate of the upper limit for $\Delta S^0_{(30)}$ would be the gain associated with three translational modes of H, since a small amount of rotational and vibrational entropy is also lost. That is, $\Delta S^0_{(30)} \leq 26$ e.u.; and $T\Delta S^0_{(30)} \leq 7.8$ kcal./mole at 298°K. Since in reaction (31) $A_H = 17.2$ kcal./mole is known,⁶ we have for the dissociation of H from N_2H : $\Delta F^0_{(32)} \geq 22.5 + 0.0 - 7.8 + 17.2$; $\Delta F^0_{D,N_2H} \geq 31.9$ kcal./mole.

We now know the $N_2 \dots H$ dissociation free energy for the two extremes in the series $N_2 \dots H$ (≥ 31.9); $N_2H \dots H$, $N_2H_2 \dots H$; $N_2H_3 \dots H$ (< 50.0). It seems reasonable to assume a uniform

gradation of ΔF^0_D values in the series in view of the small differences involved. In that case, the other values are: $\Delta F^0_{D,N_2H_1} = 37.9$ and $\Delta F^0_{D,N_2H_2} = 43.9$ kcal./mole. Fortunately, independent data are available for comparison with the average $N_2H_{n-1} \dots H$ dissociation free energy, $\overline{\Delta F^0_{D,N_2H_n,calcd}} = (31.9 + 37.9 + 43.9 + 50.0)/4 = 40.9$ kcal./mole calculated from the above theoretical estimates. The uncertainty in $\overline{\Delta F^0_{D,N_2H_n,calcd}}$ is at most only about ± 4 kcal./mole if $\Delta F^0_{D,N_2H} < \Delta F^0_{D,N_2H_1}$, as expected, for then the average value is confined within rather narrow lower and upper limits. The necessary thermodynamic data for $\overline{\Delta F^0_{D,N_2H_n,exp}}$ are to be found in the reference work

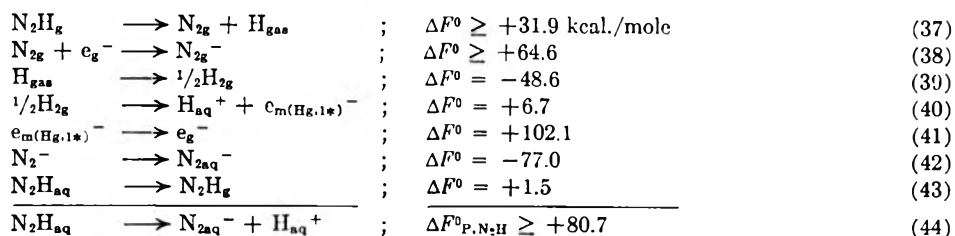
of Latimer¹² and of Audrieth and Ogg,²³ and are summarized in eq. 33-36; eq. 33 has been corrected for the hydrolysis of N_2H_4 .

Accordingly, the average per bond is $\overline{\Delta F^0_{D,N_2H_n,exp}} = 157.6/4 = 39.4$, which agrees well with the theo-

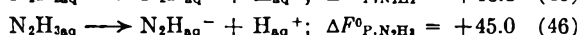
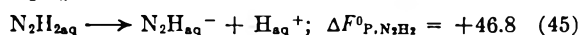


retical value of 40.9 kcal./mole.

(f) **Free Energy of Proton Dissociation from N_2H_n .**—The preceding results allow calculation of $\Delta F^0_{P,N_2H_n}$ for the dissociation of a proton from N_2H_n in an aqueous medium, according to the scheme



By the same method, the results for the other two N_2H_n are



It may be concluded that each of the $N_2H_n^-$ anions, and N_2^- , has an enormous affinity for a proton in an aqueous system; and that the proton affinity increases in the series $N_2H_{3aq}^-$, $N_2H_{2aq}^-$, $N_2H_{aq}^-$, N_{2aq}^- , with a large jump between the last two members.

V. Summary of Thermodynamic Properties and Conversion of N_2 to N_2H_n .—Table I summarizes the tentative values at 298°K. of electron affinities, A , the standard hydration free energies $\Delta F^0_{h,x}$ and $\Delta F^0_{h,x^-}$ of the neutral N_2H_n and $N_2H_n^-$ anion, respectively; the $N_2H_{n-1} \dots H$ bond dissociation free energies, ΔF^0_D ; and the $(N_2H_{n-1} \dots H^+)_{aq}$ proton dissociation free energies, ΔF^0_P , obtained above. Some of these quantities are upper or lower limits (*cf.* text). The absolute values of $\Delta F^0_{h,x}$ probably are correct within 0.1 kcal./mole; but the uncertainty in some of the other absolute values may be ten to hundreds of fold larger, depending on reliability of the assumptions and the data. However, all values are given to the nearest 0.1 kcal./mole to allow proper calculation of significant differences and trends.

It should be emphasized that major working hypotheses on which these results are based [(1) $D_{N_2} \leq D_{NO}$; (2) $\Delta F^0_{h,N_2} = \Delta F^0_{h,O_2}$; (3) $\Delta A_{N_2,N_2H} \leq \Delta A_{O_2,H_2O}$] have different degrees of plausibility, and as yet have to be assessed in terms of various trends and tests of self-consistency (*cf.* Secs. II-V) rather than on an absolute basis, since the molecules or ions in question are not directly observable. Likewise, certain especially important experimental values (*e.g.*, A_{O_2} relative to $E^0_{O_2 \cdot, O_2}$; A_{H_2O} relative to A_{O_2} ; $\Delta F^0_{(10)}$) are subject to substantial revision. However, the various quantities are locked together in such a way that the trends and over-all results do not

TABLE I

ESTIMATED THERMODYNAMIC PROPERTIES OF N_2 AND N_2H_n MOLECULES, RADICALS AND ANIONS

	N_2	N_2H	N_2H_2	N_2H_3	N_2H_4
A , kcal./mole	-64.1	-22.5	-14.1	-5.7	
$\Delta F^0_{h,x}$	-77.0	-77.9	-78.8	-79.7	
$\Delta F^0_{b,x}$		-1.5	-3.0	-4.5	-6.0
ΔF^0_D		31.9	37.9	43.9	50.0 ^a
ΔF^0_P		80.7	46.8	45.0	43.3 ^a

^a Experimental quantities.

seem very sensitive to revisions of absolute values.

The values in Table I can be used to predict the electrode potential for the reduction of N_2 to aqueous hydrazine by a succession of one-electron captures followed by hydration and proton capture. Following the method of absolute electrode potentials (*cf.* Sec. III) we have 19 steps similar to those given in eq. 37-44; and finally obtain $\Delta F^0_{abs} = -5.0$ kcal./mole for the reaction $N_2 + 5H_{aq}^+ + 4e_{m(Pl)}^- \rightarrow N_2H_{5aq}^+$, which is equivalent to +0.22 v. for the predicted standard oxidation potential, $E^0_{ox,rel,calc}$. This compares very favorably, but possibly fortuitously so, with the experimental value¹² $E^0_{ox,rel,exp} = +0.23$ v. for the $N_2H_{5aq}^+$, N_2 couple. At least, Table I represents a self-consistent set of thermodynamic quantities which provides a framework for the analysis of successive steps in the possible reduction of aqueous N_2 .

NOTE ADDED IN PROOF.—A recent generalization by K. Fajans [*Chimia*, 13, 360 (1959)], consistent with his quanticule theory of chemical binding, lends considerable support to the first major working hypothesis on which this paper is based (*i.e.*, to $D_{N_2} \leq D_{NO}$): "Of two core pairs, the one with the greater total positive charge (Σ^+) is bound more strongly by the same quanticule." This rule was derived from data on diatomic molecules and ions containing a total of 9, 10 or 11 valence electrons, hence should be applicable to the case of $N_2^-(\Sigma^+ = 10)$ and $NO(\Sigma^+ = 11)$.

Acknowledgments.—I wish to thank Dr. G. Wilse Robinson and the anonymous referees for their valuable criticisms and suggestions.

INTERACTIONS IN AQUEOUS SOLUTIONS. III. ON STATISTICAL THERMODYNAMICS OF COLLOIDAL ELECTROLYTES

BY D. STIGTER

Western Regional Research Laboratory,¹ Albany 10, California

Received October 20, 1959

This paper discusses the osmotic pressure and salt distribution coefficients in the Donnan membrane equilibrium. Relations are derived between these virial coefficients and the thermodynamic potential of the colloid. For spherical colloid particles the results in the Donnan, the Debye-Hückel and the Gouy-Chapman model are compared. The assumptions underlying these three models are found to be self consistent. In the Gouy-Chapman model the assumption of pairwise additivity of potentials of average force between three interacting ions leads to significant errors in the evaluation of the relevant virial coefficients.

Introduction

This paper extends a previous application² of the McMillan-Mayer-Hill statistical solution theory^{3,4} to the Donnan membrane equilibrium. We consider an aqueous colloid solution (inside solution), separated from a 1-1 salt solution (outside solution) by a semipermeable membrane through which only water (component 1) and small ions may pass. The electroneutral colloidal electrolyte (component 2) has one ion species in common with the salt (component 3). ρ_i is the number of molecules of component i per unit volume of inside solution, ρ_i^* is the corresponding concentration in the outside solution. The intensive thermodynamic properties of the system are described by ρ_2 , the uniform temperature T and the chemical potentials μ_1 and μ_2 which are also uniform in the system.

The excess osmotic pressure π across the membrane can be expanded in powers of ρ_2

$$\frac{\pi}{kT} = \rho_2 + \sum_{n \geq 2} B_n \rho_2^n \quad (1)$$

Similarly, the salt distribution can be expanded

$$\frac{\rho_3}{\rho_3^*} = 1 + \sum_{n \geq 1} A_n \rho_2^n \quad (2)$$

The virial coefficients B_n and A_n are related to "cluster integrals" depending on the potential of average force between certain sets of particles in the outside solution and, hence, are functions of T , μ_1 and μ_3 . Expressions for B_2 , B_3 , A_1 and A_2 are given in I.⁵ In the application of these exact, formal expressions to real systems one assumes a model for the potential of average force. Hill⁶ has given an elaborate discussion of the Donnan model and of the Debye-Hückel model of electrolyte solutions. The results are subject to the well known restriction that the variation of the local electrostatic potential (due to the non-uniform ion distribution) be sufficiently small. This restriction was removed in paper I which deals with the Gouy-Chapman model as applied to Donnan systems containing spherical particles with a high surface potential. In the fol-

lowing a numerical comparison is made between the results for B_2 and A_1 in the three models.

It appears that certain relations exist between the two sets of virial coefficients. At present these relations are used mainly to investigate some properties of the Gouy-Chapman model.

Thermodynamics

Equation 1 yields for the activity coefficient γ_2 of the colloid in the inside solution²

$$\ln \gamma_2 = \sum_{n \geq 2} \frac{n}{n-1} B_n \rho_2^{n-1} \quad (3)$$

and, therefore, the thermodynamic potential of the colloid ions component is

$$\frac{\mu_2}{kT} = \frac{\mu_2^0}{kT} + \ln \rho_2 + \sum_{n \geq 2} \frac{n}{n-1} B_n \rho_2^{n-1} \quad (4)$$

in which μ_2^0 and B_n depend on T , μ_1 and μ_3 .⁷

Equations 2 and 4 are rewritten in terms of weight concentrations which are more convenient in thermodynamic manipulations. m_2 is the number of moles of colloid per mole of water, m_3 and m_3^* are the numbers of moles of salt per mole of water in the inside and outside solution, respectively. It is assumed that the molecular volume of the colloid v_2 is independent of pressure and of composition. In addition, the small ions are considered as point charges ($v_3 = 0$). When v_1 is the molecular volume of water, eq. 2 and 4 become, respectively

$$\frac{m_3}{m_3^*} = 1 + \frac{A_1 + v_2}{v_1} m_2 + \frac{A_2}{v_1^2} m_2^2 + \frac{A_3 - A_2 v_2}{v_1^3} m_2^3 + \dots \quad (5)$$

$$\frac{\mu_2}{kT} = \frac{\mu_2^0}{kT} + \ln m_2 + \frac{2B_2 - v_2}{v_1} m_2 + \frac{\frac{3}{2} B_3 - 2B_2 v_2 + \frac{1}{2} v_2^2}{v_1^2} m_2^2 + \dots \quad (6)$$

(7) Equation 4 may not be obvious since γ_2 refers to the colloid ions (the non-equilibrium species) while μ_2 refers to the colloid component. One might introduce the electrochemical potential η_2 of the colloid ions

$$\eta_2 = \eta_2^0 + kT \ln \rho_2 \gamma_2 \quad (4a)$$

When the colloid ion carries Z elementary charges, μ_2 is obtained from η_2 by adding the electrochemical potential η_c of Z counterions

$$\mu_2 = \eta_2 + Z\eta_c \quad (4b)$$

Setting, furthermore

$$\mu_2^0 = \eta_2^0 + Z\eta_c \quad (4c)$$

eq. 4 is recovered. The present derivation of μ_2 starts with formulating interaction effects. In order to ascertain that μ_2^0 is indeed independent of ρ_2 , it is observed that in eq. 4c η_2^0 and η_c depend on T , μ_1 , μ_3 and on an electrostatic potential ϕ which may or may not be a function of ρ_2 . A possible dependence of ϕ on ρ_2 , however, is irrelevant since ϕ cancels in μ_2^0 . This renders μ_2^0 a function of T , μ_1 and μ_3 only.

(1) A laboratory of the Western Utilization Research and Development Division, Agricultural Research Service, U. S. Department of Agriculture.

(2) D. Stigter and T. L. Hill, THIS JOURNAL, **63**, 551 (1959); hereafter denoted by I.

(3) W. G. McMillan and J. E. Mayer, *J. Chem. Phys.*, **13**, 276 (1945).

(4) T. L. Hill, *J. Am. Chem. Soc.*, **80**, 2923 (1958).

(5) In the notation of I $A_1 = b_{11}$ and $A_2 = b_{21} - 2b_{20}b_{11}$.

(6) T. L. Hill, *Faraday Soc. Disc.*, **21**, 31 (1956).

In deriving relations between B_n and A_n , the (Debye-Hückel) activity coefficient of the salt is assumed to equal unity and we have

$$\frac{\mu_3}{kT} = \frac{\mu_3^0}{kT} + 2 \ln m_3^* \quad (7)$$

μ_3^0 depends on T and μ_1 only. The thermodynamic equality

$$\left(\frac{\partial \mu_2}{\partial m_3}\right)_{T, \mu_1, m_2} = - \left(\frac{\partial m_3}{\partial m_2}\right)_{T, \mu_1, \mu_3} \quad (8)$$

is converted with eq. 7 to

$$m_3^* \left(\frac{\partial \mu_2/kT}{\partial m_3^*}\right)_{T, \mu_1, m_2} = - 2 \left(\frac{\partial m_3}{\partial m_2}\right)_{T, \mu_1, m_3^*} \quad (9)$$

Using eq. 5 and 6, equating the coefficients of equal powers of m_2 on both sides of eq. 9, one obtains the desired set of relations

$$\left(\frac{\partial \mu_2^0/kT}{\partial m_3^*}\right)_{T, \mu_1} = - \frac{2A_1 + 2v_2}{v_1} \quad (10)$$

$$\left(\frac{\partial B_2}{\partial m_3^*}\right)_{T, \mu_1} = - 2 \frac{A_2}{v_1} \quad (11)$$

$$\left(\frac{\partial B_3}{\partial m_3^*}\right)_{T, \mu_1} = - \frac{4A_3 + 4A_2v_2/3}{v_1} \quad (12)$$

The present procedure also gives relations between higher virial coefficients.

The dependence of μ_2^0 on m_3^* requires some comment. It will be recalled that μ_2^0 relates to a single colloid molecule in the outside salt solution. Let us consider a colloid ion with a positive electric charge Ze . The colloid molecule then consists of the colloid ion and Z small negative ions whose concentration is m_3^* . These negative ions contribute to μ_2^0 the m_3^* -dependent term $ZkT \ln m_3^*$. The single ion activity coefficient is assumed equal to unity, as before. μ_2^0 also contains an electrostatic term, μ_{el} , which arises from the accumulation of Z elementary charges on the colloid ion. This term is usually called the electrical free energy of the double layer and has been discussed in various connections.⁸⁻¹⁰ Several equivalent expressions for μ_{el} can be derived from imaginary charging processes. For instance, the work required to charge a single colloid ion and its counterions in a reversible manner, all other ions retaining their normal charge, gives¹⁰

$$\mu_{el} = \int_0^Z \psi_0' edz \quad (13)$$

ψ_0' is the surface potential of the colloid ion with a charge ze . In general ψ_0' , and therefore μ_{el} , depends on m_3^* and we have

$$\frac{\mu_2^0}{kT} = K + Z \ln m_3^* + \frac{\mu_{el}}{kT} \quad (14)$$

μ_{el} depends on T , μ_1 , m_3^* and on the particular properties of the colloid ion. K is the m_3^* -independent part of μ_2^0 .

Results for Different Models

The *Donnan model* bypasses the statistical theory. Since this model has been used extensively in the literature the results are included for completeness. The electroneutrality condition is applied and no further interaction is assumed between colloid and

(8) E. J. W. Verwey and J. Th. G. Overbeek, "Theory of the Stability of Lyophobic Colloids," Elsevier Publ. Co., Amsterdam, 1948.

(9) D. Stigter, *Rec. trav. chim.*, **73**, 593 (1954).

(10) J. Th. G. Overbeek and D. Stigter, *ibid.*, **75**, 1263 (1956).

small ions. Consequently μ_{el} is independent of m_3^* and from eq. 4 one obtains

$$\left(\frac{\partial \mu_2^0/kT}{\partial m_3^*}\right)_{T, \mu_1} = \frac{Z}{m_3^*} \quad (15)$$

In addition, the usual treatment^{6,11} leads to

$$B_2 = \frac{Z^2v_1}{4m_3^*} \quad (16)$$

$$A_1 = - \frac{Zv_1}{2m_3^*} \quad (17)$$

$$A_2 = \frac{Z^2v_1^2}{8m_3^{*2}} \quad (18)$$

In the *Debye-Hückel model* one obtains⁹ for colloid spheres with radius a in a solution with dielectric constant ϵ

$$\mu_{el} = \frac{Z^2e^2}{2\epsilon\kappa(1 + \kappa a)} \quad (19)$$

with

$$\kappa^2 = \frac{8\pi e^2 m_3^*}{\epsilon kT v_1} \quad (20)$$

Equation 14 yields in this model

$$\left(\frac{\partial \mu_2^0/kT}{\partial m_3^*}\right)_{T, \mu_1} = \frac{Z}{m_3^*} - \frac{Z^2e^2\kappa}{4\epsilon kT(1 + \kappa a)^2 m_3^*} \quad (21)$$

Hill's expression⁶ for B_2 reads in the present notation

$$B_2 = 4v_2 + \frac{Z^2v_1}{4m_3^*} - \frac{Z^4e^2\kappa v_1}{16\epsilon kT(1 + 2\kappa a)^2 m_3^*} \quad (22)$$

In the same approximation the result for A_1 is found to be

$$A_1 = -v_2 - \frac{Zv_1}{2m_3^*} + \frac{Z^2e^2\kappa v_1}{8\epsilon kT(1 + \kappa a)^2 m_3^*} \quad (23)$$

For the *Gouy-Chapman model* μ_{el} can be written as¹⁰

$$\mu_{el} = \frac{1}{\delta} \frac{Z^2e^2}{2\epsilon a(1 + \kappa a)} \quad (24)$$

The symbols have the same meaning as in eq. 19. The correction factor δ depends on κa and on the surface potential of the colloid ion. Numerical results for B_2 , B_3 , A_1 and A_2 are given in I.

Inspection of eq. 15 to 23 shows that the Donnan model is essentially the limiting case of the Debye-Hückel model for $Zm_3^* \rightarrow 0$. Furthermore, the cross relations 10 and 11 are satisfied. This confirms the conclusion of, among others, Hill⁶ that the Debye-Hückel assumptions are self-consistent from a statistical thermodynamic point of view. The situation is less straightforward in the Gouy-Chapman model and discussion is deferred to the next section.

Numerical results for B_2 in the various models are compared in Fig. 1. It is noted that for increasing colloid charge the curves diverge rapidly. It was found that this divergence is even more pronounced at higher salt concentrations m_3^* . The same can be said of the results for A_1 in Fig. 2. Now, of the three models under discussion the Gouy-Chapman model is based on the least restrictive assumptions. Hence, the large differences observed in Figs. 1 and 2 indicate that both the Donnan and the Debye-Hückel model are unsatisfactory already in the case of moderately charged colloid ions.

(11) J. Th. G. Overbeek, "Progress in Biophysics and Biophysical Chemistry," Vol. 6, Pergamon Press, London, 1956, Ch. 3.

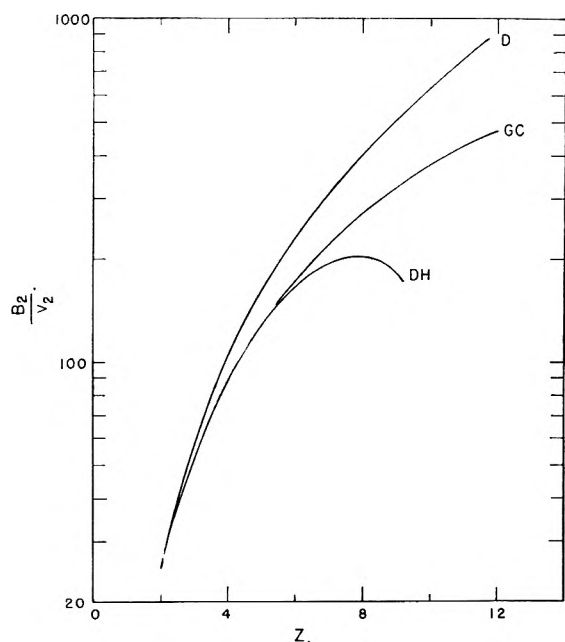


Fig. 1.— B_2/v_2 as a function of Z for $a = 25 \text{ \AA}$. and $m_3^*/1000N_0v_1 = 10^{-3}$ mole/l. of 1-1 salt in water at 25° : D = Donnan model; DH = Debye-Hückel model; GC = Gouy-Chapman model. (For purposes of comparison $v_2 = 4/3(\pi a^3)$ also in the Donnan model.)

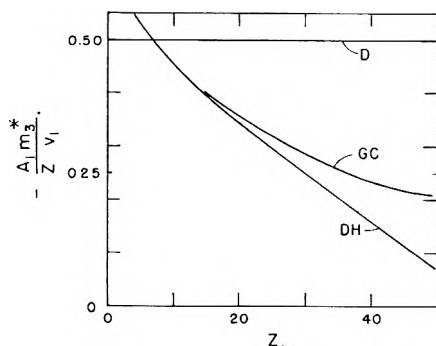


Fig. 2.— $A_1m_3^*/Zv_1$ as a function of Z for $a = 25 \text{ \AA}$. and $m_3^*/1000N_0v_1 = 10^{-2}$ mole/l. of 1-1 salt in water at 25° : D = Donnan model; DH = Debye-Hückel model; GC = Gouy-Chapman model.

Self-consistency of the Gouy-Chapman Model

The main assumptions in the Gouy-Chapman theory of the electrical double layer^{8,12-15} are: (1) small ions behave like point charges; (2) the (Debye-Hückel) activity coefficient of small ions equals unity; (3) the potential of average force of an ion may be identified with its average electrostatic potential in the Poisson-Boltzmann equation which governs the ion distribution.

The last assumption has been made also in the theory of strong electrolyte solutions and serious objections have been raised against it. Kirkwood¹⁶ has shown that assumption (3) is exact only under conditions that the Poisson-Boltzmann equation

may be linearized (Debye-Hückel model). When, however, higher terms must be retained, the Poisson-Boltzmann equation leads to thermodynamic inconsistencies.¹⁷

Equation 10 enables us to test the self-consistency of the Gouy-Chapman assumptions. For this purpose the case of $\kappa a \gg 1$ is particularly suitable. The ionic double layer, adjacent to the surface of the colloid particle, is essentially flat and the Poisson-Boltzmann equation can be solved analytically. It can be shown that (ref. 8, eq. 36 and p. 54)

$$\frac{\mu_{e1}}{kT} = Z\phi_0 - \frac{32\pi\epsilon^2m_3^*}{\kappa v_1} \left[\cosh\left(\frac{\phi_0}{2}\right) - 1 \right] \quad (25)$$

with $\phi_0 = e\psi_0/kT$. The relation between the surface potential ψ_0 of the colloid particle and Z is (ref. 8, eq. 12).

$$Z = \frac{4a^2}{e} \sqrt{\frac{2\pi\epsilon kTm_3^*}{v_1}} \sinh\left(\frac{\phi_0}{2}\right) \quad (26)$$

From eq. 14, 20, 25 and 26, and considering Z as a constant, one obtains

$$\left(\frac{\partial\mu_2^0/kT}{\partial m_3^*}\right)_{T,\mu_1} = \frac{16\pi a^2}{\kappa v_1} (1 - e^{-\phi_0/2}) \quad (27)$$

On the other hand, the expression for the negative adsorption of salt in a flat double layer derived by Klaarenbeek^{18,9,11} leads to

$$A_1 = -v_2 - \frac{8\pi a^2}{\kappa} (1 - e^{-\phi_0/2}) \quad (28)$$

It follows from eq. 27 and 28 that relation 10 is satisfied for the Gouy-Chapman model of the flat double layer, irrespective of the values of κ and the surface potential. This result makes it likely that the assumptions made in the customary treatment of the electrical double layer, are self-consistent not only for the flat double layer but in general. More particularly, it is surmised that assumption (2) justifies assumption (3).

A final remark may be made on the absolute errors introduced by assumptions (2) and (3). It has been shown that for spherical double layers the differences between results for the Gouy-Chapman model and the Debye-Hückel model (for which assumption (3) is exact) are smaller than for the flat double layer.^{9,10} Consequently, assumption (3) is less restrictive for spherical double layers than it is for the flat double layer. Now, in the latter case elimination of assumption (2) gives rise only to relatively small corrections.¹⁹ For spherical double layers such corrections are expected to be even smaller.

The present discussion confirms the general notion²⁰ that the Gouy-Chapman model is quite adequate for treating electrical interactions in colloidal solutions.

Virial Coefficients in the Gouy-Chapman Model

In paper I virial coefficients have been evaluated for colloid spheres surrounded by a Gouy-Chapman double layer. The results are, of course, subject

(12) G. Gouy, *J. phys.*, [4] **9**, 457 (1910); *Ann. Phys.*, [9] **7**, 129 (1917).

(13) D. L. Chapman, *Phil. Mag.*, **25**, 475 (1913).

(14) B. Derjaguin and L. Landau, *Acta Physicochim. U.R.S.S.*, **14**, 633 (1941); *J. Exptl. Theoret. Phys. (U.S.S.R.)*, **11**, 802 (1941).

(15) B. Derjaguin, *Acta Physicochim. U.R.S.S.*, **10**, 333 (1939).

(16) J. G. Kirkwood, *J. Chem. Phys.*, **2**, 767 (1934).

(17) See *e.g.*, R. H. Fowler and E. A. Guggenheim, "Statistical Thermodynamics," Cambridge Univ. Press, 1939, p. 405-409.

(18) F. W. Klaarenbeek, Thesis, Utrecht, 1946.

(19) W. E. Williams, *Proc. Phys. Soc. (London)*, **A66**, 372 (1953).

(20) See *e.g.*, ref. 8, p. 23; F. Booth, *J. Chem. Phys.*, **22**, 1956 (1954).

to assumptions (1) to (3). Moreover, it was assumed that (4) the results for the virial coefficients depend mainly on the (Debye-Hückel) potential field in the *outer* part of the double layer. In evaluating A_2 and B_3 the additional assumption was made that (5) the potentials of average force are pairwise additive. With relations 10 and 11 the assumptions (4) and (5) can be examined separately.

Results for eq. 10 are given in Table I. The dif-

TABLE I

κa	0.5	0.7	1.0	1.5	2	3	5
Ratio	1.018	1.004	0.991	1.012	0.990	1.001	1.013
Ratio of $-\frac{1}{2} \left\{ v_1 \left(\frac{\partial \mu_2^0/kT}{\partial m_2^*} \right)_{T, \mu_1} + 2v_2 \right\}$ and A_1 for $\phi_0 = 4$.							

ferentiation of μ_{e1} , eq. 24, is rather similar to that of B_2 which is detailed in the Appendix. Values of A_1 were taken from I. The table indicates that relation 10 is satisfied within the computational error of 1 or 2%. Hence the error introduced by assumption (4) is insignificant. This agrees with independent evidence presented in I.

We now turn to assumption (5). From the values of B_2 in I (which do not involve (5)), A_2 is obtained with eq. 11. (See Appendix.) Such results are compared in Fig. 3 with previous values of A_2 in I, based on (5). It is observed in Fig. 3 that the latter values are 10 to 30% too low. It can be shown that this trend is to be expected from assumption (5). In I A_2 is evaluated as a "cluster integral"^{4,2} relating to the interaction between one small ion and two colloid ions (all ions either positive or negative). Figure 4 shows a particular configuration. The pair potentials of average force are functions of the distance between the relevant pair of ions. In the Gouy-Chapman model, assumption (3), W_{12}' and W_{13}' are proportional with the electrostatic potential ψ in a single double layer around ions 2 and 3, respectively.

$$W_{12}' = e\psi_2(1) \quad W_{13}' = e\psi_3(1) \quad (29)$$

W_{23} relates to the interaction between two colloid particles and, hence, depends on properties of two overlapping double layers. A_2 depends on these pair potentials and also, through a term proportional with $\exp(-W_{123}/kT)$, on the interaction between *three* ions. The relevant potential of average force may be written as

$$W_{123} = W_{23} + e\psi_{23}(1) \quad (30)$$

$\psi_{23}(1)$ is the electrostatic potential in position 1 due to the interacting colloid particles at positions 2 and 3. Assumption (5) reads in the present case

$$W_{123} = W_{23} + W_{12}' + W_{13}' \quad (31)$$

or, with eq. 29 and 30

$$\psi_{23}(1) = \psi_2(1) + \psi_3(1) \quad (32)$$

However, the additivity of double layer potentials, as expressed in eq. 32, is not exactly true. In general (compare, e.g., ref. 8, Ch. X)

$$\psi_{23}(1) < \psi_2(1) + \psi_3(1) \quad (33)$$

It thus follows that assumption (5) yields too low values of $\exp(-W_{123}/kT)$. This may explain the observation in Fig. 3 that A_2 , as calculated in I, is too low. It is recommended that, in order to avoid assumption (5), A_2 be evaluated from B_2 through eq.

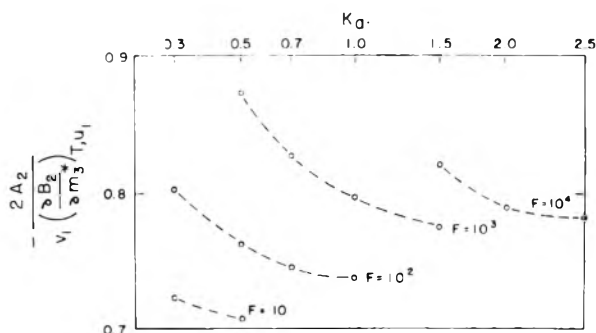


Fig. 3.—Ratio of A_2 and $-(v_1/2)(\partial B_2/\partial m_3^*)_{T, \mu_1}$ for various F and κa values. $\phi_0 = 4$ in all cases.

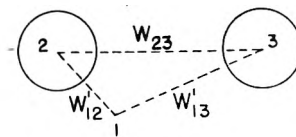


Fig. 4.

11. An accurate procedure is given in the Appendix.

The cluster integral for B_3^{21} contains a term proportional to $-\exp(-W_{123}/kT)$. Following the reasoning above, it is concluded that the results for B_3 in I, based on assumption (5), are somewhat too high.

Appendix

In I $\kappa^3 B_2$ has been derived as a function of the parameter

$$F = \frac{eakT}{e^2} \left(\frac{\phi_0}{\gamma} \right)^2 \kappa a e^{2\kappa a} \quad (34)$$

In the differentiation in eq. 11 Z and a are constant. Hence, one obtains with eq. 20 and 34

$$\kappa^3 \left(\frac{\partial B_2}{\partial m_3^*} \right)_{T, \mu_1} = \frac{\kappa^3 B_2}{2m_3^*} \left\{ \frac{d \ln \kappa^3 B_2}{d \ln F} \left(\frac{\partial \ln F}{\partial \ln \kappa a} \right)_{Z, a} - 3 \right\} \quad (35)$$

The differentiation of F requires further consideration. Equation 34 yields

$$\left(\frac{\partial \ln F}{\partial \ln \kappa a} \right)_{Z, a} = 1 + 2\kappa a - 2 \left(\frac{\partial \ln \gamma}{\partial \ln \kappa a} \right)_{Z, a} + 2 \left(\frac{\partial \ln \phi_0}{\partial \ln \kappa a} \right)_{Z, a} \quad (36)$$

γ is an explicit function²² of ϕ_0 and κa and we convert

$$\left(\frac{\partial \gamma}{\partial \kappa a} \right)_{Z, a} = \left(\frac{\partial \gamma}{\partial \kappa a} \right)_{\phi_0} + \left(\frac{\partial \gamma}{\partial \phi_0} \right)_{\kappa a} \left(\frac{\partial \phi_0}{\partial \kappa a} \right)_{Z, a} \quad (37)$$

The charge-potential relation can be written as²²

$$\phi_0 = \frac{Ze^2}{\beta eakT(1 + \kappa a)} \quad (38)$$

β depends on ϕ_0 and κa . With eq. 38 it can be shown that

$$\left(\frac{\partial \phi_0}{\partial \kappa a} \right)_{Z, a} = -\phi_0 \frac{1}{1 + \kappa a} + \left(\frac{\partial \ln \beta}{\partial \ln \kappa a} \right)_{\phi_0} \phi_0 \quad (39)$$

With eq. 37 and 39, eq. 36 now becomes

(21) Compare e.g., T. L. Hill, "Statistical Mechanics," McGraw-Hill Book Co., New York, N. Y., 1956, Ch. 5.
 (22) D. Stigter and K. J. Mysels, THIS JOURNAL, 89, 45 (1955).

$$\left(\frac{\partial \ln F}{\partial \ln \kappa a}\right)_{Z,a} = 1 + 2\kappa a - 2 \left(\frac{\partial \ln \gamma}{\partial \ln \kappa a}\right)_{\phi_0} + 2 \left[\left(\frac{\partial \ln \gamma}{\partial \ln \phi_0}\right)_{\kappa a} - 1 \right] \frac{\frac{\kappa a}{1 + \kappa a} + \left(\frac{\partial \ln \beta}{\partial \ln \kappa a}\right)_{\phi_0}}{1 + \left(\frac{\partial \ln \beta}{\partial \ln \phi_0}\right)_{\kappa a}} \quad (40)$$

Since the functions β and γ are quite similar²² we only discuss the differentiation of γ .

γ is a correction factor to the Debye-Hückel expression for the potential field in a spherical double layer. It is convenient to define a function D_ϕ with²²

$$\gamma(\phi_0, \kappa a) = 1 + D_\phi(\phi_0, \kappa a)[\gamma_f(\phi_0) - 1] \quad (41)$$

γ_f is the relevant correction factor for the flat double layer, for $\kappa a = \infty$ where $D_\phi = 1$. The analytical expression for γ_f is derived from the potential-distance function (ref. 8, eq. 6)

$$\phi = 2 \ln \frac{e^{\phi_0/2} + 1 + (e^{\phi_0/2} - 1)e^{-\kappa x}}{e^{\phi_0/2} + 1 - (e^{\phi_0/2} - 1)e^{-\kappa x}} \quad (42)$$

or

$$\phi = 4 \tanh(\phi_0/4)e^{-\kappa x} + \frac{4}{3} \tanh(\phi_0/4)e^{-3\kappa x} + \dots \quad (43)$$

κ is the distance from the charged flat surface. The relevant expression is in the Debye-Hückel approximation⁸

$$\phi_{DH} = \phi_0 e^{-\kappa x} \quad (44)$$

It follows from the definition²² of γ that, with eq. 43 and 44

$$\gamma_f = (\phi_0/4) \coth(\phi_0/4) \quad (45)$$

With eq. 41 the derivatives required in eq. 40 can be written as

$$\left(\frac{\partial \gamma}{\partial \kappa a}\right)_{\phi_0} = (\gamma_f - 1) \left(\frac{\partial D_\phi}{\partial \kappa a}\right)_{\phi_0} \quad (46)$$

$$\left(\frac{\partial \gamma}{\partial \phi_0}\right)_{\kappa a} = D_\phi \frac{d\gamma_f}{d\phi_0} + (\gamma_f - 1) \left(\frac{\partial D_\phi}{\partial \phi_0}\right)_{\kappa a} \quad (47)$$

With eq. 41, 45, 46, 47 and a graph²² of D_ϕ versus κa for various values of ϕ_0 , the factor γ and its derivatives are evaluated. The factor β and its derivatives are obtained in a similar way.²² Finally, with the help of eq. 40, 35 and 11 and a plot² of $\kappa^3 B_2$ vs. F the desired data on A_2 can be evaluated with an accuracy of a few per cent.

The method outlined above uses numerical values of functions relating to spherical double layers. Such data have been obtained with the help of an electronic computer by Hoskin²³ and, more recently, by Loeb, Overbeek and Wiersema.²⁴

(23) N. E. Hoskin, *Trans. Faraday Soc.*, **49**, 1471 (1953).

(24) A. L. Loeb, J. Th. G. Overbeek and P. Wiersema, to be published; A. Vrij, Thesis, Utrecht, 1959.

INTERACTIONS IN AQUEOUS SOLUTIONS. IV. LIGHT SCATTERING OF COLLOIDAL ELECTROLYTES

BY D. STIGTER

Western Regional Research Laboratory,¹ Albany 10, California

Received October 20, 1959

In the customary expansion of the excess turbidity in powers of the colloid concentration the coefficients of the three leading terms are connected with the virial coefficients of the Donnan membrane theory. The results are accurate for colloid solutions in which charge effects are predominant and which do not show depolarization or dissymmetry of the scattered light. Some literature data on bovine serum albumin are reinterpreted in terms of molecular weight. Current theories on the charge effect in light scattering are discussed briefly.

Introduction

The effect of electric charge on the light scattering by colloidal electrolyte solutions has received much attention in the literature.²⁻¹² In all treatments certain approximations are made which render the results unsuitable for general application. This paper concerns, in particular, solutions of highly charged colloid particles where charge effects are very pronounced. The treatment is based

on the exact light scattering equation for multi-component systems¹³⁻¹⁵ which connects the turbidity with thermodynamic properties of the solution. The statistical thermodynamic relations developed for the Donnan membrane system^{16,17} are employed to express the turbidity in terms of molecular parameters, *i.e.*, the size (and shape) and the surface potential (or the charge) of the colloid particles and the effective ionic strength of the solution.

The Light Scattering Equation.—We consider a solution consisting of the electroneutral colloidal electrolyte (component 2), water (component 1) and a 1-1 salt (component 3) which has one ion species in common with the colloid component. When τ^0 is the turbidity of the pure salt solution, the turbidity change $\tau - \tau^0$ caused by the introduction of the colloid is¹⁵

(13) H. C. Brinkman and J. J. Hermans, *J. Chem. Phys.*, **17**, 574 (1949).

(14) J. G. Kirkwood and R. J. Goldberg, *ibid.*, **18**, 54 (1950).

(15) W. H. Stockmayer, *ibid.*, **18**, 58 (1950).

(16) D. Stigter and T. L. Hill, *THIS JOURNAL*, **63**, 551 (1959).

(17) D. Stigter, *ibid.*, **64**, 838 (1960), hereafter denoted by III.

(1) A laboratory of the Western Utilization Research and Development Division, Agricultural Research Service, U. S. Department of Agriculture.

(2) P. Doty and R. F. Steiner, *J. Chem. Phys.*, **17**, 743 (1949).

(3) P. Doty and R. F. Steiner, *ibid.*, **20**, 85 (1952).

(4) J. T. Edsall, H. Edelhoeh, R. Lontie and P. R. Morrison, *J. Am. Chem. Soc.*, **72**, 4641 (1950).

(5) P. Doty and J. T. Edsall, "Advances in Protein Chemistry," Vol. VI, Academic Press, New York, N. Y., 1951, p. 35.

(6) K. J. Mysels, *THIS JOURNAL*, **58**, 303 (1954).

(7) K. J. Mysels, *J. Colloid Sci.*, **10**, 507 (1955).

(8) E. Hutchinson, *ibid.*, **9**, 191 (1954).

(9) L. H. Princen and K. J. Mysels, *ibid.*, **12**, 594 (1957).

(10) L. H. Princen, Thesis, Utrecht, 1959.

(11) W. Prins, Thesis, Leiden, 1955.

(12) W. Prins and J. J. Hermans, *Proc. Koninkl. Ned. Akad. Wetensch.*, **B59**, 162 (1956).

$$\frac{\tau - \tau^0}{H} = \frac{m_2}{\rho_2} \left[\frac{(\psi_2 - \psi_3 a_{23}/a_{33})^2}{a_{22} - a_{23}^2/a_{33}} + \psi_3^2 \left(\frac{1}{a_{33}} - \frac{1}{a_{33}^*} \right) \right] \quad (1)$$

$H = 32\pi^3 \nu^2 kT/3\lambda^4$; ν is the refractive index of the solution; $\psi_2 = (\partial\nu/\partial m_2)_{T,p,m_3}$; $\psi_3 = (\partial\nu/\partial m_3)_{T,p,m_2}$; m_i is the number of moles of component i per mole of water; ρ_i is the number of molecules of component i per unit volume of solution; a_{ij} is a partial derivative of the molecular chemical potential, μ_i , of component i with respect to m_j e.g.

$$a_{22} = (\partial\mu_2/\partial m_2)_{T,p,m_3} \quad (2)$$

a_{33}^* relates to the situation that $m_2 = 0$.

$$a_{33}^* = (\partial\mu_3/\partial m_3)_{T,p,m_2=0} \quad (3)$$

In eq. 1 the independent variables are T , p , m_2 and m_3 . A more convenient expression is obtained when μ_3 is introduced as independent variable instead of m_3 . With the equalities

$$a_{22} = (\partial\mu_2/\partial m_2)_{T,p,\mu_3} - a_{32}(\partial m_3/\partial m_2)_{T,p,\mu_3} \quad (4)$$

$$a_{23}/a_{33} = -(\partial m_3/\partial m_2)_{T,p,\mu_3} \quad (5)$$

eq. 1 is converted into

$$\frac{\tau - \tau^0}{H} = \frac{m_2}{\rho_2} \left[\frac{\{\psi_2 + \psi_3(\partial m_3/\partial m_2)_{T,p,\mu_3}\}^2}{(\partial\mu_2/\partial m_2)_{T,p,\mu_3}} + \psi_3^2 \left(\frac{1}{a_{33}} - \frac{1}{a_{33}^*} \right) \right] \quad (6)$$

This expression is general and exact for three-component systems (in the absence of depolarization and dissymmetry).

The second term in square brackets in eq. 6 is small compared with $\tau_2^0 \rho/Hm_2$. In most systems this term can be neglected without introducing a significant error. In addition, we change to volume concentrations which are more practical. Equation 6 becomes

$$\frac{\tau - \tau^0}{H} = \frac{m_2}{\rho_2} \left(\frac{\partial \rho_2}{\partial m_2} \right)_{T,p,\mu_3} \frac{[(\partial\nu/\partial \rho_2)_{T,p,\rho_3} + (\partial\nu/\partial \rho_3)_{T,p,\rho_2} (\partial \rho_3/\partial \rho_2)_{T,p,\mu_3}]^2}{(\partial\mu_2/\partial \rho_2)_{T,p,\mu_3}} \quad (7)$$

The derivatives of ρ_3 and μ_2 in eq. 7 refer to a (Donnan) system in which the pressure in the colloid solution is constant. In the conventional Donnan system, however, the pressure in the equilibrium salt solution is constant, that is, in the colloid solution μ_1 is constant, instead of p . At the present time the derivatives of ρ_3 and μ_2 can be connected with molecular parameters in a rigorous manner only in the latter case of constant μ_1 . For this reason we approximate

$$(\partial \rho_3/\partial \rho_2)_{T,p,\mu_3} = (\partial \rho_3/\partial \rho_2)_{T,\mu_1,\mu_3} \quad (8)$$

$$(\partial \mu_2/\partial \rho_2)_{T,p,\mu_3} = (\partial \mu_2/\partial \rho_2)_{T,\mu_1,\mu_4} \quad (9)$$

These approximations mean essentially that the pressure is dropped as an effective variable. The resulting minor errors in the final light scattering equation are discussed in the next section. Approximations 8 and 9 enable us to use in eq. 7 the virial expansions^{16,17} of ρ_3 and μ_2 in powers of ρ_2 .

The cofactor in eq. 7 can be derived from data on the solution density. Analytically, an expansion in powers of ρ_2 requires assumptions on the molecular volumes v_i of the components i . In most practical cases it suffices to set $v_3 = 0$ and consider v_1 and v_2 to be independent of the composition of the solution. In this case it is easy to show that

$$\frac{m_2}{\rho_2} \left(\frac{\partial \rho_2}{\partial m_2} \right)_{T,p,\mu_3} = (1 + v_2 \rho_2 + v_2^2 \rho_2^2 + \dots)^{-1} \quad (10)$$

With eq. 8 to 10 and eq. 2 and 4 of III, eq. 7 can be written as

$$\frac{H^* c_2}{\tau - \tau^0} = \frac{1 + (2B_2 + v_2)\rho_2 + (3B_3 + 2B_2 v_2 + v_2^2)\rho_2^2 + \dots}{M_2(1 + f\rho_3^* \sum_{n \geq 1} n A_n \rho_2^{n-1})^2} \quad (11)$$

$c_2 = \rho_2 M_2/N$ is the colloid concentration in grams per unit volume of solution. N is Avogadro's number.

$$H^* = \frac{32\pi^3 \nu^2}{3N\lambda^4} \left(\frac{\partial \nu}{\partial c_2} \right)_{T,p,\rho_3}^2 \quad (12)$$

$$f = \frac{(\partial \nu/\partial \rho_3)_{T,p,\rho_2}}{(\partial \nu/\partial \rho_2)_{T,p,\rho_3}} \quad (13)$$

ρ_3^* is the "effective" salt concentration in the colloid solution.^{16,17} Neglecting the (Debye-Hückel) activity coefficient, ρ_3^* can be defined with

$$\mu_3 = \mu_3^0(T,\mu_1) + 2kT \ln \rho_3^* \quad (14)$$

In the case of high concentrations of large salt ions it might be desirable to allow a finite value of v_3 . This substitutes for eq. 10 an expansion which is much more complicated and contains terms depending on A_n . It can be shown that the relevant correction terms in eq. 11, figuring in coefficients of ρ_2 and ρ_2^2 , are insignificant when $\rho_3^* v_3 \ll 1$.

In general the expansion in A_n in eq. 11 converges much more rapidly¹⁵ than that in B_n . Hence, in most applications of eq. 11, it is safe to replace the denominator by $M_2(1 + f\rho_3^* A_1)^2$.

Finally, the dependence¹⁶ of the virial coefficients on μ_3 , that is on ρ_3^* , deserves attention. Equation 11 is suitable for interpreting experimental data when the virial coefficients A_n and B_n are independent of ρ_2 . This means that ρ_3^* should be independent of ρ_2 as is the case, for instance, when all light scattering solutions have been dialyzed to equilibrium with the same salt solution. However, in most light scattering work information on ρ_3 , rather than on ρ_3^* , is available. To account for variation of ρ_3^* , the virial coefficients in eq. 11 are expanded in powers of ρ_2 , e.g.

$$B_2 = B_2^0 + \left(\frac{\partial B_2}{\partial \rho_3^*} \right)^0 \left(\frac{\partial \rho_3^*}{\partial \rho_2} \right)^0 \rho_2 + \dots \quad (15)$$

where the superscript 0 indicates solution properties at $\rho_2 = 0$. Neglecting minor terms, eq. 11 can now be converted into the more suitable expression

$$\frac{H^* c_2}{\tau - \tau^0} = \frac{1 + 2B_2^0 \rho_2 + \left[3B_3^0 + 2 \left(\frac{\partial B_2}{\partial \rho_3^*} \right)^0 \left(\frac{\partial \rho_3^*}{\partial \rho_2} \right)^0 \right] \rho_2^2 + \dots}{M_2(1 + f\rho_3^0 A_1^0)^2} \quad (16)$$

The coefficients of ρ_2 and of ρ_2^2 in eq. 16 are independent of ρ_2 . $2B_2^0$ is related to the limiting slope of the Debye plot of $Hc_2/(\tau - \tau^0)$ vs. c_2 . The coefficient of ρ_2^2 in eq. 16 determines the limiting curvature of a Debye plot. It is noted that the factor

$$\left(\frac{\partial B_2}{\partial \rho_3^*} \right)^0 = \left(\frac{\partial B_2}{\partial \rho_3} \right)^0 \quad (17)$$

can be derived from turbidity data at different salt concentrations. $(\partial\rho_3^*/\partial\rho_2)^0$ can be evaluated from ρ_3 with the relation^{16,17}

$$\rho_3^* = \rho_3(1 - A_1^0\rho_2 + \dots) \quad (18)$$

Comparison with Two-component Systems.—The main approximations in deriving eq. 11 have been made in eq. 8 and 9. In order to investigate the resulting errors, the limit of eq. 11 for $\rho_3^* = 0$, two-component colloid-water systems

$$\frac{H^*c_2}{\tau - \tau^0} = \frac{1}{M_2} [1 + (2B_2 + v_2)\rho_2 + \dots] \quad (19)$$

is compared with the *exact* expression for two-component systems¹⁸ at constant pressure

$$\frac{H^*c_2}{\tau - \tau^0} = \frac{1}{M_2} [1 + (2B_2 + \bar{v}_2^0 + b_{11})\rho_2 + \dots] \quad (20)$$

Since in eq. 19 v_2 has been assumed to be independent of composition, there is no difference with \bar{v}_2^0 in eq. 20. The additional term b_{11} in eq. 20 is related to the interaction between one solute (colloid) and one solvent (water) molecule in the outside solution of the Donnan system ($\rho_2 = 0$). On the basis of this comparison the rigorous treatment of three-component systems which replaces eq. 9 by an exact relation, is expected to substitute $2B_2 + b_{11}$ for $2B_2$ in eq. 11. It is expected that approximation 8 involves a correction similar to b_{11} but smaller. This term depends on the interaction between salt and water. Minor cross terms are also expected in an exact version of eq. 11.

It is likely that b_{11} is determined mainly by hydrogen bonding, hydration and volume effects. In the case of aqueous sucrose solutions¹⁹ b_{11} was found to be of order v_2 . It is anticipated that the same is true for colloidal solutions, the remaining correction terms in eq. 11 being smaller. In summary, eq. 11, and also eq. 16, are expected to be sufficiently accurate when $B_2 \gg v_2$.

Extrapolation of Turbidity Data to $c_2 = 0$.—In order to demonstrate the application of eq. 16, some literature data on bovine serum albumin (B.S.A.) are reinterpreted. Doty and Steiner³ report interesting data on solutions prepared by diluting a 0.9% BSA-HCl solution of pH 3.30 with a HCl-0.0054 M NaCl solution of pH 3.30. A Debye plot of their turbidity data shows a large limiting slope and, in addition, a strong curvature. Now, a fair estimate of the limiting curvature, from the last term of eq. 16, greatly improves the accuracy with which intercept and limiting slope can be determined in a Debye plot of experimental data. Furthermore, evaluation of the correction term $(1 + f\rho_3^0 A_1^0)^2$ in eq. 16 converts the reciprocal intercept into the accurate molecular weight of the colloid component.

First the choice of components is discussed. Strictly speaking, one should consider isoionic BSA, HCl and NaCl as separate components and apply a theory of four-component systems. However, one may apply the present three-component theory by combining isoionic BSA and bound HCl in the colloid component 2 and consider NaCl and unbound HCl as the (mixed) salt component 3. In this definition of components a colloid molecule

consists of a charged BSA ion and the appropriate number of Cl^- counterions. The protein charge which is positive at pH 3.30, derives from specifically bound Cl^- ions and an excess of bound H^+ ions.

It is evident that the factors H^* , M_2 and c_2 in eq. 16 should refer to the BSA-HCl component. Now, the refractive increments per gram are very nearly the same for HCl and for isoionic BSA. Therefore, one may employ the H^* referring to isoionic BSA³ without introducing a significant error. Denoting the molecular weight of isoionic BSA by M , we get $M_2 = (1 + \alpha)M$. The correction α depends on the composition of the BSA-HCl compound and is of the order of 0.03. Doty and Steiner³ report their protein concentrations in c grams isoionic BSA per ml. Obviously the concentration in eq. 16 is $c_2 = (1 + \alpha)c$.

We now turn to the term $(\partial\rho_3^*/\partial\rho_2)^0$ in eq. 16. The effective salt concentration is

$$\rho_3^* = \rho_{\text{HCl}}^* + \rho_{\text{NaCl}}^* \quad (21)$$

It is assumed that ρ_{HCl}^* is independent of the BSA concentration.²⁰ In the dilution procedure described above, the stoichiometric NaCl concentration depends on ρ_2 through

$$\rho_{\text{NaCl}} = \rho_{\text{NaCl}}^0 - 6 \times 10^{-4} M \rho_2 \quad (22)$$

It is easy to show²¹ that the relation between ρ_{NaCl} and ρ_{NaCl}^* can be expressed with

$$\rho_{\text{NaCl}}^* = \rho_{\text{NaCl}} (1 - A_1^0\rho_2 + \dots) \quad (23)$$

Equations 21, 22 and 23 yield the desired expansion of ρ_3^* in powers of ρ_2

$$\rho_3^* = \rho_{\text{HCl}}^* + \rho_{\text{NaCl}}^0 - (A_1^0\rho_{\text{NaCl}}^0 + 6 \times 10^{-4} M)\rho_2 + \dots \quad (24)$$

With eq. 24 and converting from c_2 , ρ_2 and M_2 to c and M , eq. 16 becomes

$$\frac{H^*c}{\tau - \tau^0} = T_1(1 + T_2c + T_3c^2 + \dots) \quad (25)$$

$$T_1 = M^{-1}(1 + \alpha)^{-2} (1 + fA_1^0\rho_3^0)^{-2} \quad (26)$$

$$T_2 = \frac{2NB_2^0}{M} \quad (27)$$

$$T_3 = \frac{3N^2B_3^0}{M^2} - \frac{2N^2}{M^2} \left(\frac{\partial B_2}{\partial \rho_3} \right)^0 (A_1^0\rho_{\text{NaCl}}^0 + 6 \times 10^{-4} M) \quad (28)$$

It is recalled the B_3^0 and A_1^0 can be evaluated from B_2^0 and ρ_3^0 . Furthermore, $(\partial B_2/\partial \rho_3)^0$ can be determined readily on a plot of $\ln B_2$ versus $\ln \rho_3^0$ which is nearly linear over a large range of ρ_3^0 (compare data in ref. 4). In this way T_3 can be derived from T_2 with eq. 28.

In the original paper³ $H^*/(\tau - \tau^0)$ is plotted *vs. c*. In order to take full advantage of eq. 25, a suitable value of T_1 is selected and the data are replotted as $[H^*/(\tau - \tau^0) - T_1]/c$ *vs. c*. Obviously, the curve through these points intercepts the abscissa at T_1T_3 with a limiting slope of T_1T_3 . The proper choice of T_1 should give a curve for which the observed limit-

(20) This implies that the pH does not change on mixing the BSA and the NaCl solutions of pH 3.30. A slight increase might be expected due to additional binding of H^+ and Cl^- by the BSA-ion with increased ionic strength. The relevant change of ρ_{HCl}^* and of the colloid component are ignored at present. The resulting errors are expected to be insignificant.

(18) T. L. Hill, *J. Chem. Phys.*, **30**, 93 (1959).

(19) D. Stigter, *This Journal*, **64**, 118 (1960).

ing slope agrees with the value $T_1 T_2$ calculated from $T_1 T_2$ with eqs. 26-28.

Figure 1 shows results for two choices of T_1 . The straight lines indicate the calculated limiting slopes. Table I gives values of various factors used in this calculation. In both cases we have employed $f = 0.74 \times 10^{-3}$; $\rho_3^0 = 5.9 \times 10^{-6} N$ and $\rho_{NaCl}^0 = 5.4 \times 10^{-6} N$ molecules/ml.; $M = T_1^{-1} (1 + f\rho_3^0 A_1^0)^2$, see eq. 26; $(\partial B_2 / \partial \rho_3)^0 = -B_2^0 / \rho_3^0$ as derived from a log-log plot of the best values of B_2 in 0.0054 and 0.0024 M NaCl at pH 3.30.³

TABLE I

T_1	$\frac{NB_2^0}{M}$ ml. g. ⁻¹	$\rho_3^0 A_1^0$	$\frac{(1 + f\rho_3^0 A_1^0)^2}{T_1}$	$\frac{N^2 B_2^0}{M^2}$ ml. ² g. ⁻²	T_2 ml. ² g. ⁻²
1.377×10^{-5}	76.3	-7.4	73500	0.23×10^4	2×10^4
1.320×10^{-5}	138	-12.5	77000	0.89×10^4	4.8×10^4

According to Fig. 1 the limiting slope obtained with eq. 28 is consistent with the experimental data for $T_1 = 1.377 \times 10^{-5}$ but definitely inconsistent when $T_1 = 1.320 \times 10^{-5}$ is assumed. Equation 26 and Table I give for the former value $M(1 + \alpha)^2 = 73500$. To estimate M , let us assume that $1/3$ of the adsorbed H^+ ions is neutralized by specifically adsorbed Cl^- ions (compare ref. 4, Table V). Then, for a net charge of 46 units,³ some 70 HCl molecules would be associated with one (isoionic) BSA molecule, corresponding to $\alpha = 0.036$ and $M = 68500$. This value compares with $M = 77000$ reported in the same investigation³ for pH 5.10 at which pH the corrections for interaction with small ions are probably very small. If no systematic errors are present in the $\tau - \tau^0$ data, for instance in the τ^0 employed, the dependence of M on the pH is real and is probably due to (increased) aggregation of BSA at pH 5.10.

The numerical method¹⁶ used above for deriving A_1^0 and B_2^0 from B_2^0 and ρ_3^0 refers to spherical colloids. There is evidence²¹ that the BSA molecule is not spherical, but more like a prolate ellipsoid with axial ratio 6 or 7 to 1. Now, the virial coefficients are essentially dependent on the outer part of the ionic double layer around a BSA ion which, for low ionic strength, approaches spherical symmetry. Hence the present results are rather insensitive to the actual size and shape of the BSA particle proper. Incidentally, these latter factors influence strongly the interpretation of B_2^0 in terms of surface potential or charge of the BSA ion. In view of these uncertainties such an interpretation of B_2^0 is omitted.

Discussion of Other Light Scattering Expressions.—Doty and Steiner³ have given an excellent semiquantitative discussion of light scattering by colloidal electrolyte solutions. The leading terms in eq. 11 are the same as in the expression of these authors. They discuss the Gouy-Chapman model of the ionic double layer and also point out the dependence of B_2 on the effective ionic strength. Their estimate of B_2 is based on a hard sphere cut off of the repulsion potential at a distance where the interaction energy is $1 kT$. It has been shown¹⁶ that such estimates of B_2 are considerably too low.

A number of other light scattering treatments are

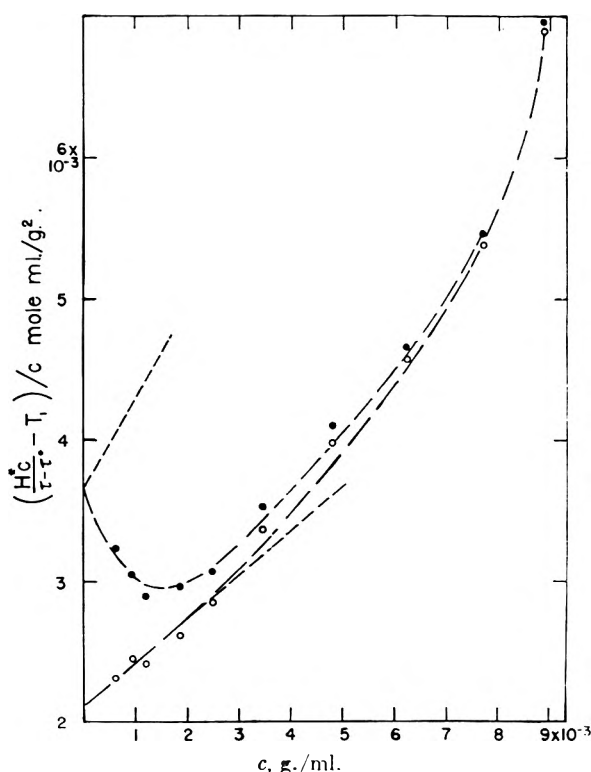


Fig. 1.— $[H^*c/(\tau - \tau_0) - T_1]/c$ vs. c for BSA in aqueous NaCl solutions at pH 3.30. Values of $H^*c/(\tau - \tau_0)$ from experiments by Doty and Steiner.³ Open circles, $T_1 = 1.377 \times 10^{-5}$; filled circles, $T_1 = 1.320 \times 10^{-5}$.

based on the Donnan model. With eq. 16 and 17 of III eq. 11 yields for this model

$$\frac{H^*c_2}{\tau - \tau^0} = M_2^{-1} \left(1 - f \frac{Z}{2} \right)^{-2} \left[1 + \frac{N}{M_2} \left(\frac{Z^2}{2\rho_3^*} + \text{minor terms} \right) c_2 + \dots \right] \quad (29)$$

The literature expressions are similar to eq. 29, showing the cofactor^{7,9-12} $(1 - f(Z/2))^{-2}$ and the term^{4-7,10-12} $Z^2/2\rho_3^*$. As shown in Figs. 1 and 2 of III the differences between the Donnan and the Gouy-Chapman model are quite marked. In general, the "effective charge" Z , as obtained from the slope of a Debye plot with eq. 29 is lower than the real colloid charge. Such a difference has indeed been found in work on detergent micelles where Z from eq. 29 could be compared with the electrophoretic charge.^{10,22} Preliminary calculations have shown that this difference is largely removed when eq. 11 is used with the Gouy-Chapman model of B_2 .

It is interesting to note that in some derivations both the electroneutrality of the colloid solution and the interaction between colloid particles (in terms of an activity coefficient of the colloid) are introduced. It has been shown, however, that the electro-neutrality condition leads to the Donnan model and already describes the interaction between the colloid particles.²³ Consequently the expressions under discussion^{4,7-10,11} contain the same interaction in two different terms. For self-consistent results one of these terms should be omitted. In fact, the extra term β_{22}^* of Edsall, *et al.*, (ref. 4,

(21) S. Krause and C. T. O'Konski, *J. Am. Chem. Soc.*, **81**, 5082 (1959).

(22) J. N. Phillips and K. J. Mysels, *This Journal*, **69**, 325 (1955).

(23) T. L. Hill, *Faraday Soc. Disc.*, **21**, 31 (1956).

Fig. 8) must be interpreted as an (approximate) measure of the inadequacy of the Donnan model for BSA solutions. Also, the very low "effective charges" of detergent micelles, reported by Prins¹¹ and by Prins and Hermans²⁴ are raised to more acceptable values if one of two main interaction terms is omitted from their light scattering expressions.

After completion of this work the author received a thorough treatise on light scattering by Vrij²⁵ in which an expression similar to eq. 11 is derived, except for the last term. Vrij's numerical results for A_1 and B_2 agree with ours¹⁶ but are given over a more extended range. Vrij simplifies the connection between light scattering and osmotic properties

(24) W. Prins and J. J. Hermans, *Proc. Koninkl. Ned. Akad. Wetensch.*, **B59**, 293 (1956).

(25) A. Vrij, Thesis, Utrecht, 1959.

by recommending that the factor $\partial\nu/\partial c_2$ in H^* be measured with reference to the equilibrium salt solution. This procedure eliminates terms due to colloid-salt interactions. Indeed, it is easily verified that in our eq. 7 the substitution

$$\left(\frac{\partial \nu}{\partial \rho_2}\right)_{T,p,\rho_3} + \left(\frac{\partial \nu}{\partial \rho_3}\right)_{T,p,\rho_2} \left(\frac{\partial \rho_3}{\partial \rho_2}\right)_{T,p,\mu_3} = \left(\frac{\partial \nu}{\partial \rho_2}\right)_{T,p,\mu_3} \quad (30)$$

yields essentially a two-component expression. Finally, Vrij shows that the connections with osmotic properties are exact if the colloid solution is subjected to the relevant osmotic pressure when $\partial\nu/\partial c_2$ and τ are measured. This is further evidence that our approximations 8 and 9, required in experiments at constant pressure, are rather good.

TRANSMISSION COEFFICIENTS FOR EVAPORATION AND CONDENSATION

BY EARL M. MORTENSEN¹ AND HENRY EYRING

Department of Chemistry, University of Utah, Salt Lake City, Utah

Received November 14, 1959

The theory of absolute reaction rates usually begins with the equilibrium calculation of the rate of surmounting a barrier and then corrects this by the transmission coefficient. In certain unimolecular reactions this transmission coefficient is less than unity. In such reactions there is often not sufficient time for the internal degrees of freedom to equilibrate in going from the initial to activated states. To correct for this non-equilibrium condition in evaporation and condensation the transmission coefficient is set equal to the ratio of the internal partition function in the initial state to the internal partition function in the activated state assuming equilibrium.

Introduction

The theory of absolute reaction rates corrects the approximation that equilibrium is maintained between the initial and activated states by introducing a factor κ .² In many reactions $\kappa = 1$ is a good approximation. We wish here to consider evaporation where κ differs considerably from unity in certain cases. Equilibrium is not always maintained in passing to the activated state. This is because the adjustment of energy between internal degrees of freedom cannot keep pace with the changes arising as the system passes to the top of the barrier. A similar situation arises when ultrasonic vibrations are passed through a substance. The heat capacity decreases at high frequencies of sound, indicating that there is not sufficient time for the internal degrees of freedom to equilibrate. Likewise, to explain the thermal conductivity of liquids Kincaid and Eyring³ were obliged to assume that translations, but not internal vibrations and rotations equilibrated on each collision.

During the unimolecular reaction the vibrational and rotational quantum levels may be altered so rapidly that there is insufficient time to re-establish a Boltzmann distribution. Thus, although levels may be altered, the population in these levels should be essentially the same as before the reaction oc-

curred, and so for the internal partition function of the activated complex we should write in such cases, the internal partition function F_e corresponding to the minimum along the reaction coordinate. This correction is most appropriately incorporated into the transmission coefficient κ so that we retain the original formation in which the rate constant k' is expressed by

$$k' = \kappa \frac{kT}{h} \frac{F^\ddagger}{F_i} e^{-\Delta E^\ddagger/RT} \quad (1)$$

where F_i is the molecular partition function per unit volume of the initial state, and F^\ddagger is the corresponding partition function of the activated complex assuming equilibrium, while for the transmission coefficient we write

$$\kappa = \frac{F_e}{F_i^\ddagger} \quad (2)$$

where F_i^\ddagger is the internal part of the molecular partition function in F^\ddagger which is to be replaced by the surface restricted internal partition function F_e . Gershinowitz and Rice's⁴ discussion of the activation energy of unimolecular reactions is of interest in this connection and Slater⁵ has brought together much valuable work of his own and others in his book.

Transmission Coefficients in the Evaporation and Condensation of Liquids.—Let us apply equation 1 to the evaporation of liquids. If there is no

(1) Supported by the Standard Oil Company of California through a predoctoral research fellowship.

(2) S. Glasstone, K. J. Laidler and H. Eyring, "The Theory of Rate Processes," McGraw-Hill Book Co., Inc., New York, N. Y., 1941, p. 185.

(3) J. F. Kincaid and H. Eyring, *J. Chem. Phys.*, **6**, 620 (1938).

(4) H. Gershinowitz and O. K. Rice, *J. Chem. Phys.*, **2**, 273 (1934).

(5) N. B. Slater, "Theory of Unimolecular Reactions," Cornell University Press, Ithaca, N. Y., 1959.

activation energy for condensation, then the activated state is the one in which the liquid surface and the evaporating molecule are separated. Then F^\ddagger is the gaseous partition function aside from the omitted translational motion away from the surface, while F_i is the partition function for the molecules on the surface. If F_i is related to the vapor pressure P , using the chemical potential, we obtain the usual Hertz-Knudsen equation for the rate of vaporization v where

$$v = \kappa c_g \left(\frac{kT}{2\pi m} \right)^{1/2} = \frac{\kappa P}{(2\pi mkT)^{1/2}} \quad (3)$$

and c_g is the concentration of gas molecules in the vapor. It is well known⁶ that the actual rate of vaporization in many cases is less than $P/(2\pi mkT)^{1/2}$ indicating a transmission coefficient or condensation coefficient as it is called of less than unity. To obtain this condensation coefficient we must evaluate the partition function F_e for the molecules on the liquid surface. Generally we do not need to consider the vibrational degrees of freedom because they are the same in the two states.⁷ However the rotational degrees of freedom between the two states are different because on the surface the rotations are hindered leading to a smaller rotational partition function. Therefore, κ in equation 3 is the ratio of rotational partition functions for the surface molecules to those in the vapor phase. Herzfeld⁸ was the first to point out the importance of rotation in evaporation.

One of the best methods for finding the ratio of rotational partition functions in liquid and gas was developed by Kincaid and Eyring.³ They called it the free angle ratio. It was G. Wyllie⁹ who pointed out the near equivalence of the free angle ratio with the observed condensation coefficient.

The rotational partition function for the molecules on the surface can be determined by considering either the potential energy between them as a function of their angle of rotation or by considering, as did Kincaid and Eyring, some measurable quantity which is related to the rotational partition function such as the entropy of vaporization. Since the free angle ratio requires certain data which are not always available in the literature, it was felt that it would be desirable to investigate other methods for determining the ratio of rotational partition functions to further illustrate equation 2.

Now, the entropy $\Delta S_{v,s}$ gained by a molecule in going from the surface of a liquid to the vapor phase is given by¹⁰

$$\Delta S_{v,s} = R \ln \frac{8\pi^2 f_g^v V_g}{\sigma f_s^v \left[\int \dots \int e^{-W/kT} \prod_i dq_i \right]^{1/N}} + RT \left\{ \frac{\partial}{\partial T} \ln \frac{f_g^v}{f_s^v \left[\int \dots \int e^{-W/kT} \prod_i dq_i \right]^{1/N}} \right.$$

where f_g^v and f_s^v are the vibrational partition functions and W is the potential energy of the molecules on the surface in terms of the coordinates q_i describing the translation and rotation of the molecules. Since the vibrational frequencies are generally the same in the two phases,⁷ they cancel and we obtain upon rearrangement

$$\frac{\sigma}{8\pi^2} \left[\int \dots \int e^{-W/RT} \prod_i dq_i \right]^{1/N} = V_g e^{-\Delta S_{v,s}/R} e^{-\bar{W}/RT} \quad (4)$$

where \bar{W} is the average potential energy of the molecules on the surface and is given by

$$\bar{W} = \frac{\int \dots \int W e^{-W/kT} \prod_i dq_i}{\int \dots \int e^{-W/kT} \prod_i dq_i}$$

If the average potential energy of the bulk liquid is taken to be the zero of potential energy, then $\Delta S_{v,s} + \bar{W}/T$ is to a good approximation the entropy of vaporization ΔS_v from the bulk phase. Now, if the rotational and translational degrees of freedom can be separated so that equation 4 may be written in terms of the molecular partition functions f_g^r and f_s^r for rotation and the molar partition function Q_s^t for translation, we obtain

$$\frac{f_s^r}{f_g^r} (Q_s^t)^{1/N} = V_g e^{-\Delta S_v/R} \quad (5)$$

By comparing equation 5 with the one used by Kincaid and Eyring³ we see that $(Q_s^t)^{1/N}$ corresponds to their free volume V_f and f_s^r/f_g^r to their free angle ratio δ_r .

Now, in order to obtain the condensation coefficient or ratio of rotational partition functions of a liquid, let us first consider a liquid having a condensation coefficient of unity such as CCl_4 . For CCl_4 equation 5 becomes

$$(Q_s^t)_{\text{CCl}_4}^{1/N} = V_{g,\text{CCl}_4} e^{-\Delta S_{v,\text{CCl}_4}/R} \quad (6)$$

If we can find a temperature T_{CCl_4} at which CCl_4 is in the same standard state for translation as the liquid being considered such that $(Q_s^t)^{1/N}$ for the liquid equals $(Q_s^t)^{1/N}_{\text{CCl}_4}$, then the free angle ratio or condensation coefficient can be determined. By combining equations 5 and 6 we obtain

$$\delta_r = \frac{f_s^r}{f_g^r} = \frac{V_g}{V_{g,\text{CCl}_4}} e^{-\delta \Delta S_{v,R}} = \frac{P_{\text{CCl}_4} T}{P T_{\text{CCl}_4}} e^{-\delta \Delta S_{v,R}} \quad (7)$$

where $\delta S = \Delta S_v - \Delta S_{v,\text{CCl}_4}$ and the p 's are the vapor pressures of the liquids. We shall now investigate a few of the more common measures of the standard state.

One measure of the corresponding state of a liquid is its reduced temperature T_r . The ratio f_s^r/f_g^r obtained from the reduced temperature will be indicated by δ_2 . In the fifth column of Table I we have listed values of δ_2 for thirteen liquids at two different temperatures. The critical temperature T_c is given in column two.

In 1939 Hildebrand¹¹ suggested that the entropies of vaporization should be compared at equal vapor concentrations. For Hildebrand's rule the ratio will be indicated by δ_3 and is listed in column six of Table I.

(11) J. H. Hildebrand, *J. Chem. Phys.*, **7**, 233 (1939).

(6) O. Knacke and I. N. Stranski, "Progress in Metal Physics," Vol. 6, Pergamon Press Ltd., London, 1956, p. 181.

(7) G. Herzberg, "Infrared and Raman Spectra of Polyatomic Molecules," D. Van Nostrand Co., Inc., New York, N. Y., 1945, p. 534.

(8) K. F. Herzfeld, *J. Chem. Phys.*, **3**, 319 (1935).

(9) G. Wyllie, *Proc. Roy. Soc. (London)*, **A197**, 383 (1949).

(10) For linear molecules the $8\pi^2$ should be replaced by 4π .

TABLE I
 COMPARISON OF FREE ANGLE RATIOS

Molecule	T_c , °K.	t , °C.	δ_1 (K & E)	δ_2 (Tr)	δ_3 (H)	δ_4 (P)	Obsd. ^a
CCl ₄	556.31	0	1.02	1.00	1.00	1.00	1(0) ^{b,c,d,e}
		50	1.31	1.00	1.00	1.00	
C ₆ H ₆	561.7	0	0.86	0.70	0.74	1.42	0.85-0.95(6) ^f
		50	1.14	.77	.79	0.82	
CHCl ₃	536	0	0.26	.25	.20	.22	.16(2) ^f
		50	.99	.59	.58	.66	
CH ₃ I	528	0	.37	.31	.21	.32	
		40	1.25	.84	.57	.77	
CH ₃ OH	513.4	0	0.034	.078	.14	.20	.045(0) ^f
		50	.048	.20	.21	.17	
C ₂ H ₅ OH	516.3	0	.019	.021	.053	.064	.024(13) ^g
		50	.028	.024	.047	.061	
H ₂ O	647.31	0	.022	.11	.099	.17	.036(15) ^h
		100	.17	.11	.067	.17	
CH ₃ COCH ₃	508.2	0	.16	.10	.13	.15	
		50	.54	.30	.35	.42	
Cyclo-C ₆ H ₁₂	553.9	10	.69	.74	.82	.78	
		80	1.55	.97	1.09	1.02	
<i>n</i> -C ₈ H ₁₈	507.9	0	0.57	.57	0.84	0.70	
		50	.99	.65	1.01	.86	
<i>n</i> -C ₇ H ₁₆	540.17	0	.23	.32	0.65	.54	
		50	.36	.45	.83	.65	
C ₈ H ₈ CH ₃	594.0	0	.60	.59	.74	.71	
		50	.91	.67	.85	.80	
<i>n</i> -C ₇ H ₇ OH	536.9	0	.008	.007	.028	.024	.037 ^f
		100	.050	.030	.051	.059	

^a A number in parentheses in the last column is the temperature (°C.) at which the condensation coefficient was measured. ^b T. Alty and F. H. Nicoll, *Can. J. Research*, **4**, 547 (1931). ^c T. Alty, *Phil. Mag.*, **15**, 82 (1933). ^d W. Prüger, *Z. Physik*, **115**, 202 (1940). ^e L. von Bogdandy, H. C. Kleist and O. Knake, *Z. Electrochem.*, **59**, 460 (1955). ^f M. Baranaev, *J. Phys. Chem. (U. S. S. R.)*, **13**, 1035 (1939). ^g H. Bucka, *Z. physik. Chem.*, **195**, 260 (1950). ^h T. Alty and C. A. Mackay, *Proc. Roy. Soc. (London)*, **A149**, 104 (1935).

Pitzer¹² suggested that since the entropy of a gas is particularly volume dependent while the liquid volume is quite insensitive to imperfections of the liquid, that entropies of vaporization should be compared at equal vapor to liquid volume ratios. The ratio f_s^r/f_g^r using Pitzer's rule will be indicated by δ_4 and is listed in column seven of Table I.

Calculated values of δ greater than unity indicate a limitation in the method of calculation in that case.

For purposes of comparison free angle ratios as calculated by the method of Kincaid and Eyring³ are indicated in column four of Table I and will be indicated by δ_1 .

The observed condensation coefficients are listed in column eight. In most instances the calculated values of δ agree reasonably well with the observed condensation coefficients considering the approximations which were made; thus indicating the validity of equation 2 in treating problems of evaporation. It is also seen that the agreement is fair between the various methods particularly at the lower temperatures. It should be noted that in going from *n*-hexane to *n*-heptane the free angle ratio indicates that there is more restriction to rotation in heptane. If this trend continues, we might expect that long chain hydrocarbons would have small free angle ratios; however, it is found that the observed condensation coefficients in larger molecules containing many atoms appear to be unity.^{13,14} This discrepancy should be antici-

pated because as a large molecule evaporates, we should expect it to do so in segments. Each of these segments which has broken loose from the surface gains additional freedom of motion. By the time the molecule breaks away from the surface its internal motion is essentially like those of the molecules in the vapor phase, and, hence, the condensation coefficient is near unity. This stepwise process of evaporation is certainly not included in the calculated free angle ratios given in Table I. We should, therefore, be careful about interpreting the calculated free angle ratios of large molecules by methods similar to those used in obtaining Table I to be the same as the measured condensation coefficients. However, equation 2 is still valid because F_0 should then be put equal to the gaseous internal partition function and not the corresponding internal partition function for the surface because this is not the final position of equilibrium prior to evaporation.

From Table I we note that polar molecules have small free angle ratios or condensation coefficients indicating a small rotational partition function on the surface as compared with the one for the vapor phase. Classically the rotational partition function f^r may be written

$$f^r = \frac{1}{h^3} \int \dots \int e^{-H_r/RT} \prod_i dp_i dq_i \quad (8)$$

(13) R. S. Bradley and A. D. Shellard, *Proc. Roy. Soc. (London)*, **A198**, 239 (1949).

(14) R. S. Bradley and G. C. S. Waghorn, *ibid.*, **A206**, 65 (1951).

(12) K. S. Pitzer, *J. Chem. Phys.*, **7**, 583 (1939).

where H_r is the rotational part of the Hamiltonian and q_i and p_i are the conjugate coordinates and momenta. Since the potential energy does not depend upon the momenta, the contribution of the kinetic energy to the partition function in equation 8; just cancels in determining the free angle ratios, δ_r and so we obtain

$$\delta_r = \frac{\sigma}{8\pi^2} \int \int \int e^{-V/RT} \sin \theta \, d\theta \, d\varphi \, d\chi \quad (9)$$

where θ and χ , are Euler's angles and σ is the symmetry number. We expect, as did Harkins, Davies, and Clark¹⁵ that polar molecules are oriented because of the strong electrostatic forces which act on them so that for appreciable portions of the solid angle, V is large, and, hence, the free angle ratio in equation 9 is small.

For symmetrical top molecules such as benzene and chloroform we can estimate the amount of orientation if we can write a potential energy function for rotation. We shall first assume that rotation about the figure axis is essentially free. For rotations at right angles to this figure axis we shall assume that we can approximate the potential energy by a function of the form $\frac{1}{2}V_0(1 - \cos n\theta)$ where n is the symmetry number about this axis. For benzene $n = 2$ and for chloroform $n = 1$. Substituting this potential function into equation 9 we obtain

$$\delta_r = \frac{\sigma}{8\pi^2} \int_{\chi=0}^{2\pi/m} \int_{\varphi=0}^{2\pi} \int_{\theta=0}^{\pi/n} e^{-V_0(\cos n\theta)/2RT} \sin \theta \, d\theta \, d\varphi \, d\chi = \frac{1}{2} n \int_0^{\pi/n} e^{-V_0(1-\cos n\theta)/2RT} \sin \theta \, d\theta \quad (10)$$

since $\sigma = m_n$ where m is the symmetry number about the figure axis. For the case where $n = 1$, equation 10 reduces to

$$\delta_r = \frac{RT}{V_0} (1 - e^{-V_0/RT}) \quad (n = 1) \quad (11)$$

while for $n = 2$, we obtain

(15) W. D. Harkins, E. C. H. Davies and G. L. Clark, *J. Am. Chem. Soc.*, **39**, 541 (1917).

$$\delta_r = e^{-V_0/RT} \sum_{v=0}^{\infty} \frac{1}{(2v+1)v!} \left(\frac{V_0}{RT}\right)^2 \quad (n = 2) \quad (12)$$

For benzene we take $\sigma_r = 0.90$ (see Table I) at 279°K. Using equation 12 we obtain

$$V_0 = 90 \text{ cal./mole (benzene)}$$

This very small value of V_0 indicates that on the surface there is very little interaction upon the rotational degrees of freedom indicating perhaps a loose structure on the surface. On the other hand, for chloroform, we have $\delta = 0.16$ at 273°K. and equation 11 gives

$$V_0 = 3400 \text{ cal./mole (chloroform)}$$

which indicates an appreciably oriented structure on the liquid surface. Since several of the free angle ratios or condensation coefficients are smaller than for chloroform, we would expect an even greater orientation for these molecules. Although the condensation coefficients indicate that there is orientation on the surface, we have not considered the surface structure in sufficient detail to determine whether this order is long or short range.

Liquid molecules possess a cooperative structure which is quite different from that of solid or gas so that it is not surprising that a molecule whose rotation cannot pass adiabatically into the liquid structure should be rejected. This incompatibility between the structures of the liquid and other phases is reflected in the extraordinary difficulty in nucleating both crystallization and boiling in pure liquids as exhibited by pronounced supercooling and superheating. The theory of significant liquid structure¹⁶ which has had marked quantitative success in characterizing liquids pictures the average molecule as executing solid-like motions when it occupies the solid volume which changes over to gas-like motions in strict proportion to the fractional increase in volume.

(16) H. Eyring, T. Ree and N. Hirai, *Proc. Natl. Acad. Sci.*, **44**, 7, 683 (1958), *et seq.*

HEPTANE ISOMERIZATION

By G. M. KRAMER AND A. SCHRIESHEIM

Esso Research & Engineering Company, Linden, New Jersey

Received November 21, 1959

The equilibrium composition of the isomeric heptanes was experimentally determined at 36.8°. This study was conducted because of the scarcity of experimental data on the heptane isomer equilibrium composition, and because of the conflict between existing data and calculated equilibrium values. Equilibrium was reached among seven of the nine heptane isomers, starting with *n*-heptane, 3-methylhexane, 2,3-dimethylpentane and 2,4-dimethylpentane. Side reactions prevented an accurate determination of the 2,2- and 3,3-dimethylpentane equilibrium values. The experimental and calculated equilibrium values of the heptane isomers were in good agreement. A discrepancy, outside the respective limits of uncertainty, was found only in the case of 2,3-dimethylpentane.

Paraffin isomerization studies¹ have pointed out the existence of discrepancies between experimentally obtained isomer equilibria, and that cal-

culated from thermodynamic data.² As the number of carbon atoms is increased, the possible oc-

(1) (a) F. E. Condon in P. H. Emmett, "Catalysis," Vol. VI, Reinhold Publ. Corp., New York, N. Y., 1958, chapter 2; (b) G. Egloff, G. Hulla and V. I. Komarewsky, "Isomerization of Pure Hydrocarbons," Reinhold Publ. Corp., New York, N. Y., 1942.

(2) (a) F. D. Rossini, E. J. Prosen and K. S. Pitzer, *J. Research Natl. Bur. Standards*, **27**, 529 (1941); (b) F. D. Rossini, K. S. Pitzer, R. L. Arnett, R. M. Braun and G. C. Pimentel, "Selected Values of Physical and Thermodynamic Properties of Hydrocarbons and Related Compounds," Carnegie Press, Pittsburgh, Pa., 1953.

currence of discrepancies increases and reliable experimental values are not usually available. Thus, only a limited amount of experimental data on the isomerization of heptane has been reported.³

This paper discusses the results of an investigation of the equilibrium isomerization composition of the heptanes. Two acid catalysts were used and five of the nine heptane isomers were employed as starting materials.

Apparatus and Experimental

Phillips Research Grade heptane isomers were used, except for 2,2-dimethylpentane which was kindly supplied by Dr. M. R. Fenske of the Petroleum Refining Laboratory of the Pennsylvania State University. The isomers were passed over a zeolitic adsorbent to remove water and olefins. Isobutane (Matheson) was used without further treatment. Benzene containing 0.004% sulfur was used, as supplied by the Baker Company. The aluminum halide was purified by repeated distillations in a vacuum system and handled in a dry box. Phosphoric acid, (87.4%), was used as a co-catalyst,⁴ with a metallic oxide as a catalyst support.⁵ The oxide was calcined at 590°.

One catalyst consisting of an aluminum halide and phosphoric acid was inhibited with 10 vol. % benzene (on the heptane), and reactions were carried out in stirred glass flasks at 36.8°. A gas bag attached to the end of a reflux condenser collected any light material. Samples were periodically withdrawn from the reaction flask with a hypodermic syringe for gas chromatographic analysis. A squalene column on firebrick at 0° was used to separate and identify all the C₇ isomers.

A second system consisting of aluminum halide supported on a metallic oxide, with isobutane as an inhibitor^{1a} was studied in a stainless steel reactor. Samples were periodically removed for analysis through a product withdrawal line.

Results

In order to secure accurate equilibrium data, two conditions must be met. One is the achievement of equilibrium and the second is the knowledge that side reactions have not perturbed the experimental equilibrium. In these studies, both catalytic systems produced the same isomer distribution from *n*-heptane, 3-methylhexane, 2,3-dimethylpentane and 2,4-dimethylpentane with less than 5% conversion to side products. However, 2,2-dimethylpentane could not be isomerized to equilibrium over these catalysts because of interfering side reactions. Interaction of the hydrocarbons with the catalyst leading to adsorption of the heptanes could not be prevented. It is unlikely that selective adsorption was important since both catalytic systems yielded similar products.

Table I shows the isomer distribution reached at 36.8°. The experimental values are averages from the four starting isomers. The reproducibility of the individual values is in the neighborhood of ±15% of the numbers shown.

The aluminum halide-metal oxide catalyst caused side reactions and the indicated product distribution was obtained by extrapolating the data to zero degradation. Good agreement was obtained over both catalysts. However, there are apparent differences between the experimental values and those calculated from thermodynamic data. These differences are due mainly to the fact that equilibrium

(3) J. J. B. van Eijk van Voorthuisen, *Rec. trav. chim.*, **66**, 323 (1947).

(4) V. N. Ipatieff and L. Schmerling, U. S. Patent 2,358,011, U. S. Patent 2,402,051.

(5) J. J. Owen and E. E. Stahly, U. S. Patent 2,349,458.

TABLE I

Isomer, mole %	AlX ₃ -H ₂ FO ₄		AlX ₃ -Oxide Liquid	—Calculated α—	
	Liquid	Vapor		Liquid	Vapor
22 DMP	5.0	7	4.4	23.0	29.4
24 DMP	17.0	22	19.7	8.0	9.6
23 DMP	9.0	8	8.2	30.1	26.3
33 DMP	9.5	10	8.2	11.4	11.2
223 TMB	8.0	10	5.4	4.4	5.5
2 MH	26.0	22	30.0	11.9	9.9
3 MH	18.5	16	17.2	7.6	6.0
<i>n</i> C ₇	6.0	4	5.9	2.7	1.5
3 EP	1.0	1	1.0	0.9	0.6

^a Vapor phase calculations are made using vapor pressure data from API Research Project 44, revised December 31, 1952,^{2b} and Raoult's law. The thermodynamic values are calculated from equilibrium data in source.^{2a}

has been reached only among seven of the nine isomers. This point is explained more fully in the following paragraphs.

In comparing experimental equilibrium data with the values calculated from thermodynamics, an experimental or calculated error in one compound will introduce errors into the composition values of the other isomers. In order to avoid this, a standard technique is to compare equilibrium values of pairs of isomers. 2,4-Dimethylpentane was picked as the reference compound (Table III). This compound was chosen because of its high equilibrium concentration, which in turn, provides confidence in its relative value. The ratios of *n*-heptane, 2-methylhexane, 3-methylhexane, 3-ethylpentane and 2,2,3-trimethylbutane to this common base are in good agreement with values calculated from thermodynamic data.

TABLE II

RELATIVE RATIOS OF C ₇ ISOMERS (36.8°)		
Ratio	Exptl.	Thermodynamic ^{2a}
<i>n</i> -C ₇		
$\frac{2,4\text{-DMP}}{n\text{-C}_7}$	0.18	0.16
$\frac{3\text{-MH}}{n\text{-C}_7}$		
$\frac{2,4\text{-DMP}}{3\text{-MH}}$	0.73	0.62
$\frac{2\text{-MH}}{n\text{-C}_7}$		
$\frac{2,4\text{-DMP}}{2\text{-MH}}$	1.00	1.03
$\frac{2,2,3\text{-TMB}}{n\text{-C}_7}$		
$\frac{2,4\text{-DMP}}{2,2,3\text{-TMB}}$	0.46	0.57
$\frac{3\text{-EP}}{n\text{-C}_7}$		
$\frac{2,4\text{-DMP}}{3\text{-EP}}$	0.05	0.06

The remaining isomer ratios differ considerably from the thermodynamic ratios, as shown in Table III.

TABLE III

RELATIVE RATIOS OF C ₇ ISOMERS (36.8°)		
Ratio	Exptl.	Thermodynamic ^{2a}
$\frac{2,2\text{-DMP}}{2,4\text{-DMP}}$		
$\frac{2,2\text{-DMP}}{2,4\text{-DMP}}$	0.32	3.06
$\frac{3,3\text{-DMP}}{2,4\text{-DMP}}$.46	1.66
$\frac{2,3\text{-DMP}}{2,4\text{-DMP}}$.36	2.74

2,2-Dimethylpentane could not be isomerized without degrading. Therefore, it is not known whether the differences between experimental and calculated isomer ratios are due to errors in thermodynamic data or to interfering side reactions.

Since the isomerization of 3,3-dimethylpentane was not attempted, it is also not known whether this isomer was at equilibrium.

However, 2,3-dimethylpentane was isomerized without side reactions, and its concentration was found to check that produced from the other isomers under conditions of little degradation. Thus, it is felt that the differences in the ratios for 2,3-dimethylpentane are due to errors in the thermodynamic values.

It is important to determine what causes the differences between the experimental and calculated equilibrium values. The calculated values are derived from the equation $\Delta F^0 = -RT \ln K_{eq}$ where ΔF^0 is obtained from thermodynamic measurements. Values of $\Delta F^0/T$ may be experimentally determined using equilibrium constants based on 2,4-dimethylpentane as the reference isomer. These experimental $\Delta F^0/T$ values are compared with the calculated values in Table IV. There is excellent agreement in all cases except 2,3-dimethylpentane, where a discrepancy outside the respective limits of uncertainty was found. The cause of this discrepancy probably is an error in

the thermodynamic data and the subject bears further investigation.

TABLE IV

VAPOR PHASE EQUILIBRIUM OF SEVEN HEPTANES, 36.8°

Isomer	Mole %		$\Delta F^0/T$	
	Obsd.	Calcd. ^a	Obsd. ^b	Calcd. ^{a, c}
2,3-Dimethylpentane	9.6	44.3	2.02	-2.02
2,4-Dimethylpentane	26.5	16.2	0	0
3-Methylhexane	19.3	10.0	0.63	0.94
2-Methylhexane	26.5	16.7	0	-0.06
2,2,3-Trimethylbutane	12.1	9.3	1.57	1.11
3-Ethylpentane	1.2	1.0	6.17	5.54
n-Heptane	4.8	2.5	3.39	3.70

^a Ref. 2a. ^b Probable experimental error is ± 0.46 cal./deg. mole. ^c The uncertainty is ± 1.3 cal./deg. mole.

Acknowledgment.—The authors wish to thank Esso Research and Engineering Company for permission to publish this work. They also wish to thank Mr. D. L. Baeder and Dr. P. J. Luchesi for their helpful suggestions, and Mr. J. L. Carter who participated in much of the experimental program.

THE SORPTION OF WATER VAPOR BY NATIVE AND DENATURED EGG ALBUMIN¹

BY ROBERT L. ALTMAN² AND SIDNEY W. BENSON

Department of Chemistry, University of Southern California, Los Angeles 7, California

Received December 8, 1959

The sorption-desorption cycles for water on native and on steam, heat and alcohol-denatured egg albumins have been studied from 25 to 70° for the first and up to 100° for the latter three. The amount of water sorbed is a very weak function of the temperature at high relative humidity and only slightly more sensitive at low humidities. The size of the hysteresis loop decreases with increasing temperature and for denatured albumin at 100° it has almost disappeared. Between 70 and 100° denatured albumin shows no hysteresis above a relative humidity of 0.7. The sorption isotherms of the three denatured egg albumins were significantly different both at 25 and 40° indicating that denatured albumin is not a uniquely defined material.

Introduction

The sorption of water vapor on solid proteins is different from the sorption of non-polar gases on these solids. For non-polar gases the adsorption and desorption paths of non-polar gases coincide and there is no hysteresis loop.^{3,4}

(1) This work has been supported by a grant (G-3541) from the U. S. Public Health Service of the National Institutes of Health.

(2) The material in this paper has been included in a dissertation submitted by R. L. Altman to the Graduate School of the University of Southern California (1958) in partial fulfillment of the requirements for the degree of Doctor of Philosophy.

(3) S. W. Benson and D. A. Ellis, *J. Am. Chem. Soc.*, **70**, 3563 (1948).

(4) S. W. Benson and D. A. Ellis, *ibid.*, **72**, 2095 (1950).

Experimental data on the sorption of water vapor by egg albumin are relatively complete only in the room temperature region. Barker⁵ provides sorption and desorption isotherms at 20° for both native and heat denatured egg albumin, and Mellon, Korn and Hoover⁶ have done the same at 30°. Further observations on water sorption in this temperature range are reported by Benson and Ellis,^{3,4} Shaw,⁷ Bull,⁸ and Benson and Richardson.⁹

(5) H. A. Barker, *J. Gen. Physiol.*, **17**, 21 (1933).

(6) E. F. Mellon, A. H. Korr and S. R. Hoover, *J. Am. Chem. Soc.*, **71**, 2761 (1949).

(7) T. M. Shaw, *J. Chem. Phys.*, **12**, 391 (1944).

(8) H. B. Bull, *J. Am. Chem. Soc.*, **66**, 1499 (1944).

(9) S. W. Benson and R. L. Richardson, *ibid.*, **77**, 2585 (1955).

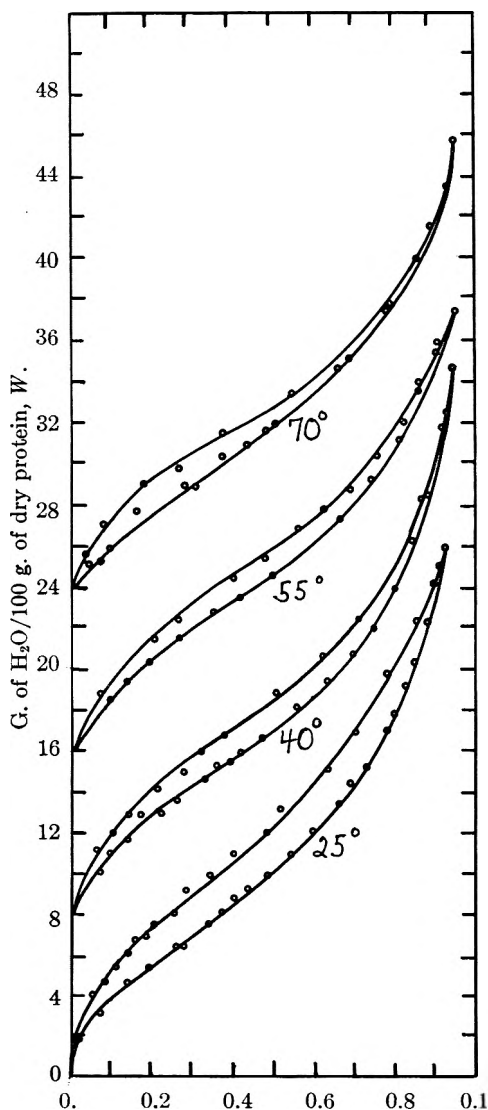


Fig. 1.—Water sorption on native egg albumin. Lower half of each curve represents adsorption and upper half desorption. The ordinates have been shifted by 8 units in W for each succeeding temperature (*i.e.*, subtract 8 units from 40° curve, 16 units from 55° curve, etc.). Points are experimental values.

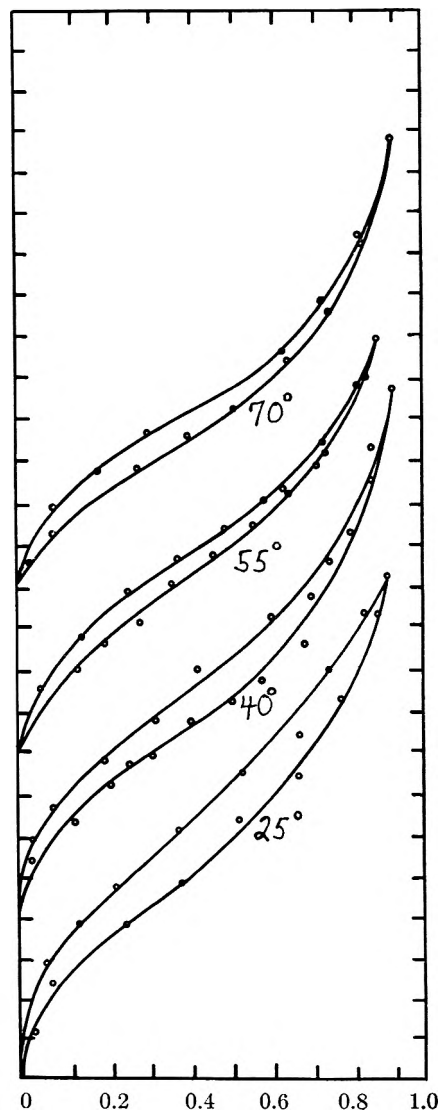


Fig. 2.—Water sorption on denatured egg albumin. Lower half of each curve represents adsorption and upper half desorption. The ordinates have been shifted by 8 units in W for each succeeding temperature (*i.e.*, subtract 8 units from 40° curve, 16 units from 55° curve, etc.). Points are experimental values.

Benson and Richardson report the most complete sorption data on egg albumin taken at 25°, and Bull has reported further experimental observations at 40°.

Sorption hysteresis is a phenomenon of great interest¹⁰⁻¹³ in proteins. Because all previous data have been obtained at relatively low temperatures little is known about the effect of temperature on water sorption and upon sorption hysteresis. Therefore, an extensive investigation of water sorption by native and denatured egg albumin seemed worthy of study.

(10) D. H. Everett and W. I. Whitton, *Trans. Faraday Soc.*, **48**, 749 (1952).

(11) D. H. Everett and F. W. Smith, *ibid.*, **50**, 187 (1954).

(12) D. H. Everett, *ibid.*, **50**, 1077 (1954).

(13) J. A. Enderby, *ibid.*, **51**, 835 (1955).

Experimental

Materials and Reagents—The various forms of egg albumin and other reagents used in this research are briefly described as: (1) native egg albumin, powdered, Armour and Company, Lot E 81116; (2) denatured egg albumin prepared by passing hot steam over native egg albumin, source: Armour and Company, Lot E 81116. The insoluble fraction was separated from any remaining soluble egg albumin by adding water, suction-filtering, and evacuating any remaining water; (3) coagulated egg albumin, made by boiling native egg albumin, source: Armour and Company, Lot E 81116; (4) alcohol denatured egg albumin, made by pouring a saturated solution of native egg albumin into absolute alcohol. The precipitate was filtered, washed with water, and evacuated. The native egg albumin was from Armour and Company, Lot E 81116, and the USP absolute ethyl alcohol was from U. S. Industrial Chemicals Company.

Apparatus—A McBain sorption balance was con-

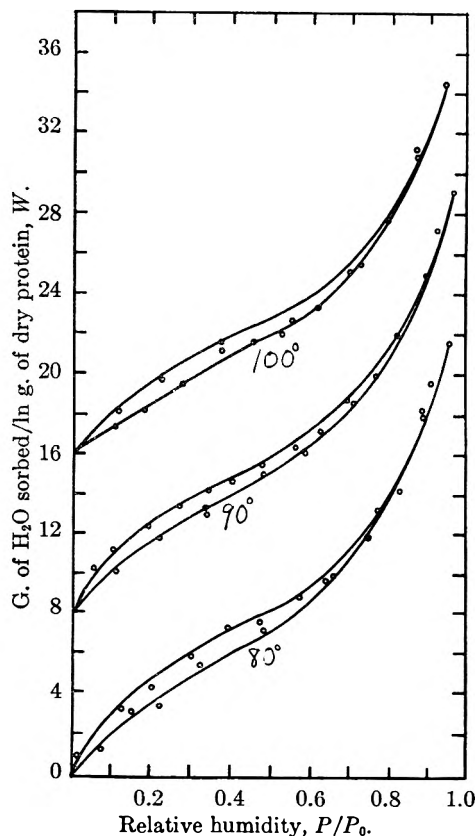


Fig. 3.—Water sorption on denatured egg albumin. Lower half of each curve represents adsorption and upper half desorption. The ordinates have been shifted by 8 units in W for each succeeding temperature (*i.e.*, subtract 8 units from 80° curve, 16 units from 90° curve, etc.). Points are experimental values.

structed with a silicon-oil¹⁴ U-tube manometer as a buffer between the heated protein sample and the mercury manometer. The quartz helix used in these sorption experiments had a sensitivity of 29.8 mg./cm. The joints were sealed with Dow Corning Silicone High Vacuum Grease. Pressure readings and elongation of the quartz helix were determined with a Gaertner cathetometer having a vernier telescope readable to 0.005 cm. Calibration of the quartz helix showed that it obeyed Hooke's law and that the probable error of weighing amounted to ± 0.3 mg. Dry sample weights were about 100 mg. It was shown that even at 100° the buoyancy correction lay within the reading error. The sorption and desorption isotherms at 25 and 40° on native egg albumin agreed closely with previous work on the same system.^{6,8,9} The results of Mellon, *et al.*,⁶ on denatured albumin agree well up to 0.60 relative humidity (RH) with our interpolated data at 30° but fall below ours by about 12% between 0.60 and 0.90 RH where interpolation is less accurate.

Data and Discussion

A. Native Egg Albumin.—Water sorption isotherms on native egg albumin have been obtained at 25, 40, 55 and 70° and these results are presented in Fig. 1 in the same units (g. H₂O/100 g. protein) used by ref. 8. Because it was thought that denaturation of the native protein sample would begin near 70°, measurements were not carried out at higher temperatures.

B. Denatured Egg Albumin.—An egg albumin sample of the same lot number was rendered in-

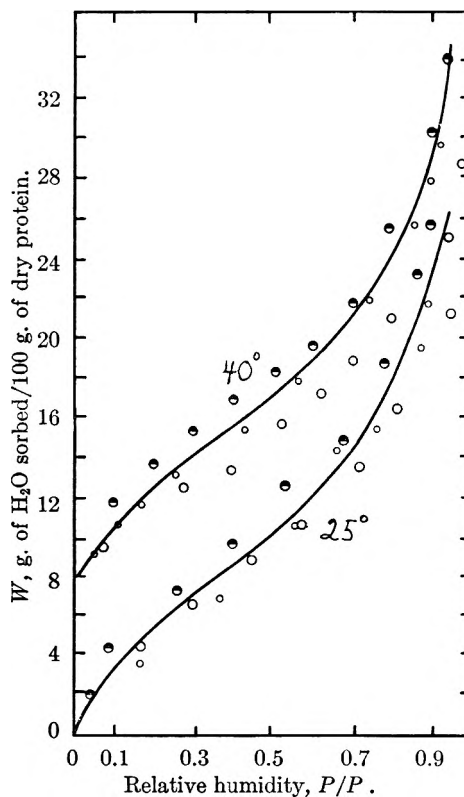


Fig. 4.—Adsorption isotherm of denatured and native egg albumin at 25° (lower curve) and 40° (upper curve). Ordinate for 40° curve has been displaced by 8 units (*i.e.*, subtract 8 units from W for 40° curve). In each case the solid line represents the adsorption isotherm of native egg albumin. The large open circles (O) are experimental points for coagulated egg albumin, the small open circles (o) are for alcohol denatured albumin while the half solid circles (◐) are for steam denatured albumin.

soluble by heating in the presence of water vapor at its saturation vapor pressure. New sorption isotherms then were obtained with this denatured sample at 25, 40, 55, 70, 80, 90 and 100° and these data are plotted in Figs. 3 and 4.

C. Coagulated Egg Albumin.—Some of the same native egg albumin also was rendered insoluble by boiling it in solution. After purifying and drying the coagulate, sorption measurements then were made at 25 and 40° (Fig. 4) on this coagulate to compare this mode of denaturation to that described in B.

D. Alcohol Denatured Egg Albumin.—To explore the uniqueness of the denaturation process still further, another insoluble egg albumin was prepared by the addition of a native egg albumin solution to USP ethyl alcohol. Water sorption isotherms (Fig. 4) then were made with this dried and purified coagulate at 25 and 40°.

The data reported below 70° are those results obtained after no further gain in weight over a 12-hour interval. At the higher temperatures, sorption apparently was completed within an hour for no further weight gain was observed over the next six hours. Because the authors' interest was in the sorption results obtained at high partial pressures, little attention was given to the details of the sorption process below 0.10 relative humidity. Al-

(14) Dow Corning Silicone Fluid 703.

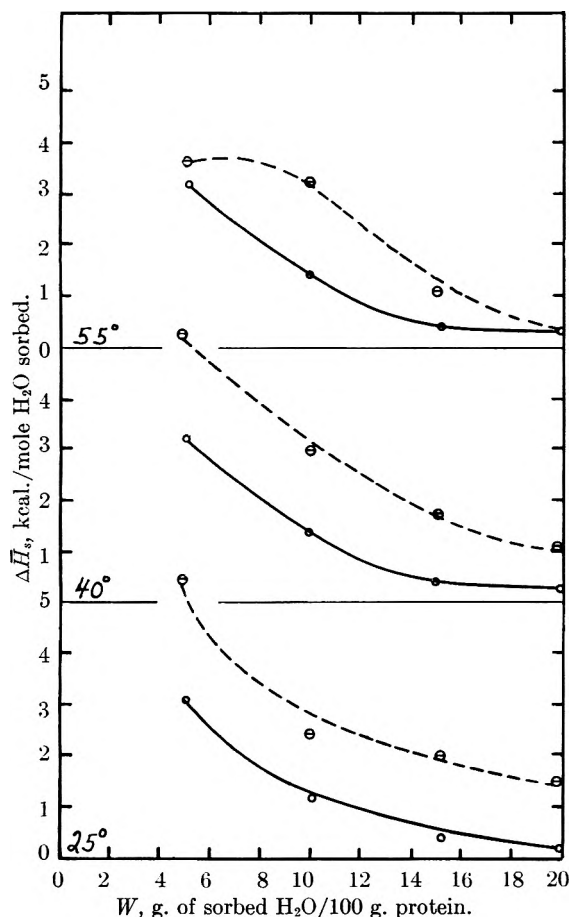


Fig. 5.—Net partial molar heats of sorption on denatured egg albumin at 25°, 40° and 55°. Upper half of each curve is for desorption while lower half represents adsorption.

though the small amount of observed hysteresis may indicate non-equilibrium sorption, the reproducibility of the isotherms both in sorption and in desorption is excellent.

From Figs. 1, 2 and 3 we note that sorption at a given relative humidity (RH) decreases with increasing temperature, the more so the less the RH. These data also indicate that the extent of hysteresis decreases with increasing temperature. And the decrease or disappearance of hysteresis at the higher temperatures always begins at the uppermost end of the humidity range, moving further down the sorption isotherm with increasing temperature.

From Fig. 4, we note that the extent of water sorption on the denatured egg albumin seems to depend on the method of denaturation. If the molecular results of denaturation are independent of the method of denaturation, then isothermal water sorption ought to be the same no matter what process has been employed to denature the native protein. The sorption results suggest that the end product of the denaturation process is not a definite thermodynamic state and that the use of thermodynamic data to characterize the denaturation process is open to question.

Thermodynamics of Sorption

From the Clausius-Clapeyron equation we can

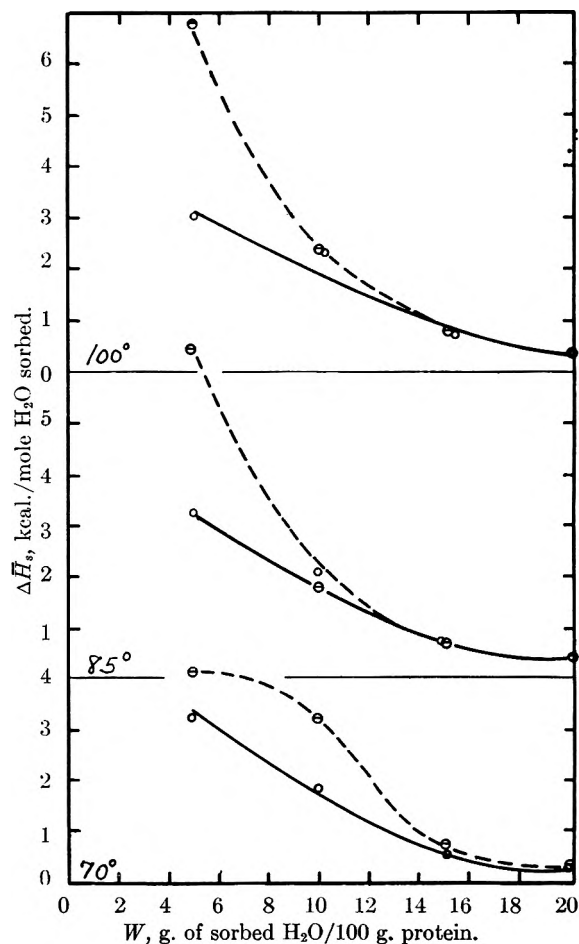


Fig. 6.—Net partial molar heats of sorption on denatured egg albumin at 70°, 85° and 100°. Upper half of each curve is for desorption while lower half represents adsorption.

write for the net partial molar heat of sorption, ΔH_s

$$\Delta H_s = -R \left[\frac{\partial \ln(P/P_0)}{\partial (1/T)} \right]_w$$

where P/P_0 is the ratio of P the vapor pressure of sorbed water (at constant amount sorbed w) to that of pure water P_0 at the temperature in question. In differential form we can write

$$\Delta H_s \sim \frac{RT^2}{P/P_0} \left(\frac{\Delta P/P_0}{\Delta T} \right)_w$$

The slope $(\Delta P/P_0/\Delta T)_w$ was computed numerically from a smoothed table of relative humidities constructed from the sorption values (W) of Figs. 1, 2 and 3. Some of these partial pressures for both *native* and *denatured* egg albumin are presented in Tables I and II.

The results of these *net heat of sorption* calculations for denatured egg albumin at 25, 40, 55, 70, 85 and 100° are presented in Figs. 5 and 6. These calculations show that the enthalpy of desorbed water is less than that of adsorbed water when hysteresis exists. It is also shown in Fig. 7 that the entropy of desorbed water is less than that of the adsorbed. From these data it is concluded that desorbed water is bound more strongly than water adsorbed at the same W and temperature T . This

is, of course, indicated by the lower vapor pressure of the desorption isotherm for any given W and T . But, as shown in Fig. 7, the partial molar entropy of the bound water on desorption is lower than it is upon adsorption indicating that this water is somewhat less free to move than is adsorbed water.

In previous papers^{9,15} we have discussed qualitatively the nature of polar gas sorption on proteins and the present results are in accord with the model presented. The protein is behaving not as a rigid, inert substrate, but rather as a deformable, reactive material. The very unique type of hysteresis displayed by proteins is attributable to the rearrangements of the molecular framework, induced by the water sorption. In this sense the formal thermodynamic quantities, calculated for the sorption process, reflect not only the changes in the H_2O but also the concomitant changes in the protein. Because of this, interpretation of the sorption-desorption cycle in terms only of the physical state of the bound H_2O are necessarily incomplete and we shall not enlarge further upon them here. The greatest difficulty in the way of attempting any molecular interpretation of the "thermodynamic" data lies in the non-equilibrium nature of the hysteresis and the consequent uncertainty thereby introduced into the data. Until this problem has been satisfactorily resolved it is perhaps wisest not to press further the thermodynamic treatments made nor to expand upon the voluminous discussion already present in the literature on the subject.

(15) R. Srinivasan and S. W. Benson, *J. Am. Chem. Soc.*, **78**, 2405 (1956); **78**, 5262 (1956); **77**, 6371 (1955), and earlier papers.

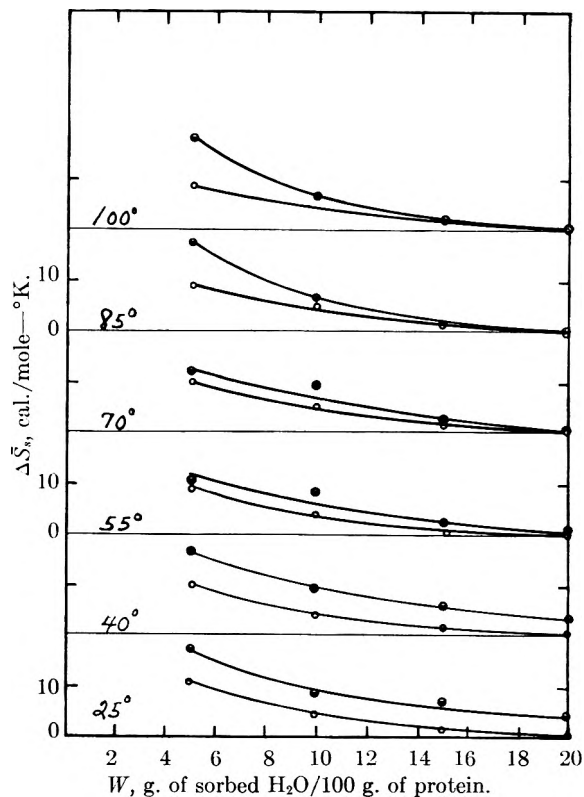


Fig. 7.—Net partial molar entropy of sorption of water on denatured egg albumin as a function of amount sorbed. Upper half of each curve (O) represents desorption and lower half is sorption (●).

THE PHASE RULE: THE SIGNIFICANCE OF NEGATIVE DEGREES OF FREEDOM

BY H. F. HALLIWELL AND S. C. NYBURG

Department of Chemistry, University College of North Staffordshire, Keele, Staffs., England

Received December 7, 1959

It is commonly held that the degrees of freedom (variance) of a system cannot be negative. It is shown that such systems can exist and demand special properties of the components.

The phase rule summarizes the restriction on choice of conditions if a specified number of phases, P , involving a specified number of components, C , are to be in equilibrium. This choice is indicated by F , the number of degrees of freedom (or the variance) of the system. We examine here a particular type of system which might at first sight appear unintelligible, namely, that exhibiting *negative* degrees of freedom. Many authors state categorically that $F \geq 0$ (or give the equivalent result, $P \leq C + 2$) but it is salutary to cite Gibbs' original comments¹ on this problem²: "Hence if $P = C + 2$ no variation in the phases (remaining coexistent) is possible. It does not seem *probable* that P can ever exceed $C + 2$. An example of $C = 1$ and $P = 3$ is seen in the coexistent solid, liquid and gaseous form of any substance of

invariable composition. It seems *not improbable* that in the case of sulfur and some other simple substances there is more than one triad of coexistent phases; but it is *entirely improbable* that there are four coexistent phases of any simple substance."

Gibbs does not here speculate on other systems which would exhibit negative degrees of freedom. It is not easy to see on what grounds he came to conclusion that some kinds of system with negative degrees of freedom are more "probable" than others. Suffice it to say that his improbabilities have been frequently misconstrued as impossibilities.

The phase rule is in essence a mathematical result which follows when a fixed number of variables, pressure P , temperature T , chemical potential μ and, when required, composition x (mole fraction), are related by sets of well-behaved functions. Although, for example, two equations for a single

(1) "Collected works of Willard Gibbs," Vol. 9, Yale, 1948, p. 97.
(2) Our notation and italics.

independent variable are solvable to give one root, this root may be physically unrealizable. Hence the rule cannot predict whether a physical system can exist; if the system exists, then the rule does indicate the manner in which the variables are interconnected. Thus as it happens, one-component systems commonly exhibit triple points. We must not be surprised however that some do not (e.g., He³). We shall examine the problem from three points of view: the functional relationships underlying the phenomena, the P - T - μ diagrams and the phase diagrams.

The Functional Relationships.—In general the chemical potential of the i th component in a phase α is a well-behaved, single-valued function of P , T and x_i

$$\mu_i^\alpha = f_i^\alpha(P_i^\alpha, T_i^\alpha, x_i^\alpha) \dots \quad (1)$$

Only two-component systems will be examined, the treatment for one- or multi-component systems being similar.

For four phases α, β, γ and δ we have two sets of equations which, using $x_2^\alpha = 1 - x_1^\alpha$, etc., are

$$\begin{aligned} \mu_1^\alpha &= f_1^\alpha(P_1^\alpha, T_1^\alpha, x_1^\alpha) & \mu_2^\alpha &= f_2^\alpha(P_2^\alpha, T_2^\alpha, x_1^\alpha) \\ \mu_1^\beta &= \dots \text{etc.} & \mu_2^\beta &= \dots \text{etc.} \end{aligned}$$

At equilibrium these equations resolve to

$$\begin{aligned} f_1^\alpha(P, T, x_1^\alpha) &= f_1^\beta(P, T, x_1^\beta) = f_1^\gamma(P, T, x_1^\gamma) = f_1^\delta(P, T, x_1^\delta) \text{ and} \\ f_2^\alpha(P, T, x_1^\alpha) &= f_2^\beta(P, T, x_1^\beta) = f_2^\gamma(P, T, x_1^\gamma) = f_2^\delta(P, T, x_1^\delta) \end{aligned}$$

These equations allow the six variables (P , T and the x 's) to be uniquely determined (as P_{eq} , T_{eq} , x_{1eq} , x_{2eq}), in accordance with $F = 0$. If now this two-component system has a state in which a fifth phase ϵ is present, then the phase rule gives $F = -1$. In this case an additional function will be added to those above and this negative degree of freedom will mean that not only are P_{eq} , T_{eq} and the x_{eq} 's uniquely determined but that all the functions governing the potentials in terms of P , T and x must be related in a special way; in other words, special physical properties are required of the two components.

The P - T - μ Diagram.—The dependence of μ on P and T is most easily represented graphically by surfaces on P - T - μ diagrams. Where these surfaces intersect stable (or metastable) equilibrium conditions apply.

Figure 1 represents the type of P - T - μ surfaces for the vapor, liquid and solid phases of a single component A. If these surfaces intersect, the intersections projected on the P, T plane give the familiar phase diagram. Now this single component may exhibit a second solid phase (that it might exhibit a second liquid phase is highly unlikely) represented by a fourth P - T - μ surface. However for all four phases to coexist ($F = 1$) all four P - T - μ surfaces must intersect in a point. This implies that there is a restriction on the nature of the $f(P, T)$'s. This is exactly the conclusion we have reached previously; not any second solid phase will suffice, that whose μ has a special $f(P, T)$ is required. The physical situation is rarely met.

Let us now examine the two-component (A,B) case and let Fig. 1 again represent one component,

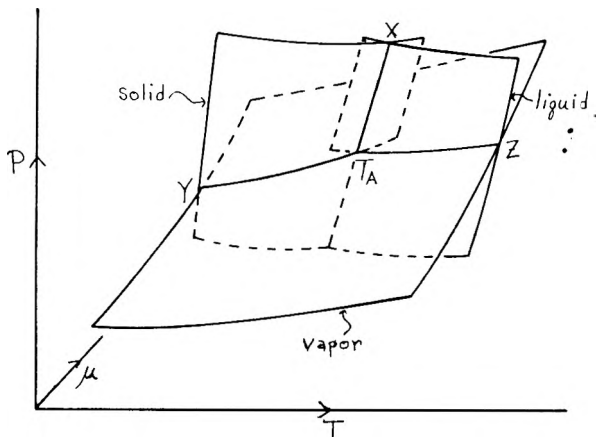


Fig. 1.— P - T - μ diagram for a single component A.

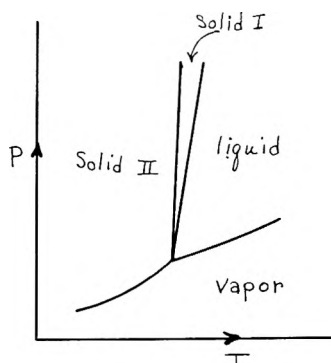


Fig. 2.—Four coexistent phases for a one-component system, $F = -1$.

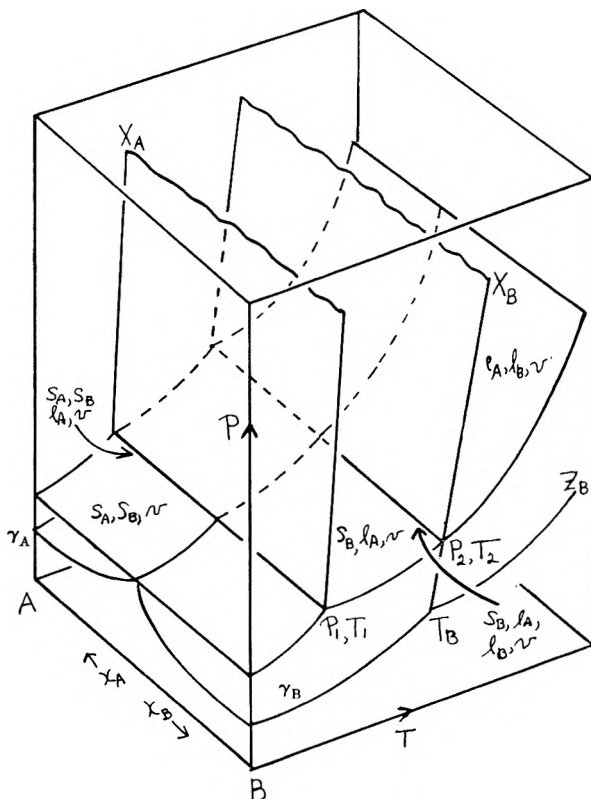


Fig. 3a.—General P - T - x diagram for two immiscible components.

say A. We are interested in the situation where five phases could be in equilibrium: solid A, solid B, A-rich liquid, B-rich liquid (all four of limited mutual miscibility) and A,B vapor.

We now examine the effect on the P - T - μ diagram for A, of adding the vapor of component B to A, assuming initially that such addition does not appreciably affect the P - T - μ surfaces for either solid or liquid A (*i.e.*, negligible miscibility). We find that the P - T - μ surface for component A in the vapor is similar to that given in Fig. 1 but lies above it. These surfaces lie higher, the greater the mole fraction of B present in the vapor, and will cut the line $T_A X$ at new triple points in which solid A, liquid A and mixed vapor are in equilibrium.

Now consider the P - T - μ diagram of component B. This will resemble Fig. 1 but of course, in general, the positions of the intersecting lines will be different. However the addition of the vapor of A to B will raise the latter's μ -vapor surface and give rise in its turn to a new set of triple points for component B. Now it could happen that for a specified composition the two new triple points of A and B had the same P and T values. In this case the five phases could coexist. We thus see that whereas $F = 0$ implies the intersection of P - T -surfaces in a point, $F = -1$ implies the coincidence of two points or, more strictly, since the P - T - μ diagrams for different components cannot be meaningfully superimposed, the coincidence of two projected triple points on the P, T plane.

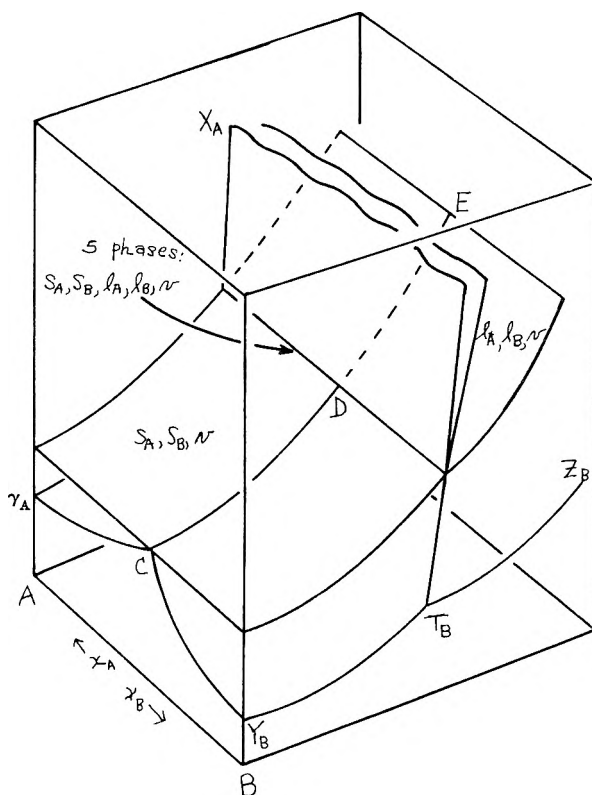


Fig. 4a.—Two-component system with five coexistent phases, $F = -1$.

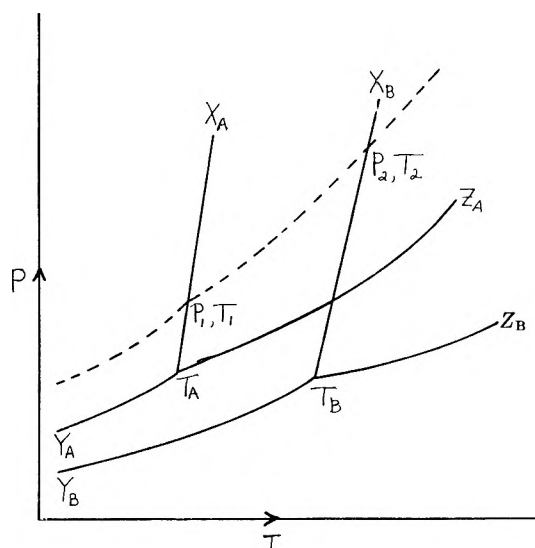


Fig. 3b.—Phase diagram corresponding to Fig. 3a.

The Phase Diagrams.—For the one-component case the P - T - x diagram is simply a P - T diagram and from our previous discussion it is clear that this latter will be of the type shown in Fig. 2, in which the four phase-boundary lines meet in a point.

The nature of the P - T - x diagram for two components depends in the first instance upon the phase diagrams (*i.e.*, P - T diagrams) of the pure components. Initially we will assume the solids and liquids of the components to be immiscible and Figs. 3a and 3b show the P - T - x diagram and corresponding P - T diagram for a general type of

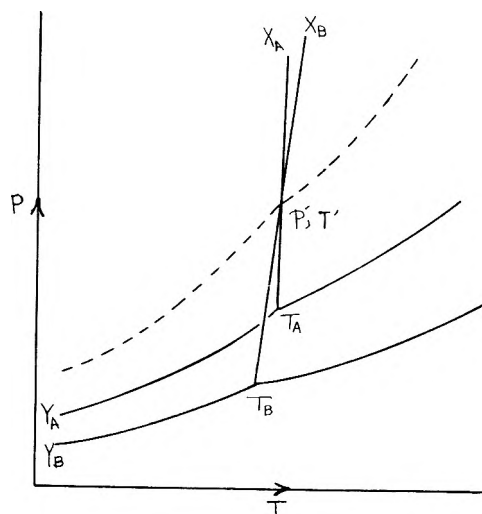


Fig. 4b.—Phase diagram corresponding to Fig. 4a.

behavior. It can be seen from these diagrams that there are two values P_1, T_1 and P_2, T_2 at which four phases can coexist. This is in agreement with the phase rule which gives $F = 0$ and hence fixes both P and T .

Figures 4a and 4b give the P - T - x and individual P, T diagrams for the case where five phases can coexist. For this to be possible P_1, T_1 and P_2, T_2 must coincide. It must be stressed however that although crossing of the corresponding lines $T_A X_A, T_B X_B$ is necessary it is not sufficient since they must coincide at the pressure and temperature which is that of the system. In Fig. 4b it

is not enough for $T_A X_A$ and $T_B X_B$ to intersect; they must intersect at the point P', T' which is also the intersection of the total pressure curve.

Clearly some immiscibility of both solids and liquids is essential for five phases to coexist. If the solids do not have the same mutual miscibility as the liquids, phase diagrams such as Fig. 4a look considerably more complex, the (horizontal) total pressure line no longer stretching across the diagram but confined to limited areas in the center and moreover no longer at a height closely equal to the sum of the vapor pressures of the pure components. Further, the lines CD and DE of Fig. 3b will probably not coincide at D but cut the five phase line at different points. This would mean that there was no composition-temperature condition for the system at which increasing pressure on the vapor would cause all four condensed phases suddenly to appear together. The P - I - μ diagram is less suitable for illustrating this feature of the system.

Conclusions.—Clearly it is not impossible for systems to show negative degrees of freedom. We have seen how such systems would however re-

quire the components to have special properties. In the case of one component we are unable to cite an example. For two-component systems we can utilize the well-known fact that if these components have the same triple point, their melting point curves will be virtually identical and very steep. Thus we merely need immiscibility and identity of normal m.p. for such a five phase system to be a practical possibility. The following two-component systems (the m.p. of each is given in parentheses) will certainly very nearly meet these requirements (exact fulfillment of the conditions could possibly be met by suitable variation of the isotopic composition of the components, hydrogen of course excepted because of its relatively gross difference from deuterium): mercury (-38.9°) + diethylaniline (-38.8°); octafluorocyclobutane (-40°) + 3-bromotoluene (-39.8°); gallium (-29°) + 4-cyanotoluene (-29.5°); phosphorus [yellow] (44.1°) + 1,2-diethoxybenzene (44.0°).

The argument applies to systems of more than two components, but it becomes increasingly difficult to cite examples with the necessary immiscibility and melting point identity.

THE SUBMONOLAYER ADSORPTION OF ARGON AND KRYPTON ON MOLYBDENUM DISULFIDE; PHENOMENOLOGICAL COMPARISON WITH STUDIES ON GRAPHITE

BY PETER CANNON

General Electric Research Laboratory, Schenectady, N. Y.

Received December 10, 1959

The adsorption isotherms of argon and krypton in the submonolayer coverage region on samples of hexagonal molybdenum disulfide are reported. Extensive experimental detail is given, since this constitutes the first such report. Two different temperatures for degassing lead to different results, since oxide contamination is volatile at an intermediate temperature. A comparison of the results with those published for graphitic substrates points out the conditions necessary for MoS_2 to behave as a homogeneous surface.

Introduction

Molybdenum disulfide exists naturally in a highly anisotropic layer structure with trigonal symmetry.¹ In a gross sense, therefore, it is "graphitic," but two important differences exist between it and graphite. The first is that the interlamellar space is much smaller than in graphite, and the second is the aspect of the basal plane, which consists of a hexagonal close-packed array of sulfur, without the periodic variation hole-atom-hole encountered in graphite. The first of these differences is important in that the physical intercalation of gases within the lattice is more difficult to achieve with molybdenum disulfide, thus reducing the possibility of error due to this cause in gas adsorption experiments. The second is important in that the molecular heterogeneity of the basal plane of graphite may reasonably be expected to modify the properties of incomplete monolayers of various gases on these substrates. The fact that molybdenum disulfide possesses neither of these potential disadvantages makes it of some promise as a

homogeneous substrate for studying the thermodynamic properties of dilute sorbed films, particularly those of the rare gases. This paper describes the results of such studies using argon and krypton: it is perhaps worth mentioning that the substrate used here is not the same as that molybdenum disulfide employed as a destructive dehydrogenation catalyst, which has been subjected to much study by petrochemical groups.

There are no data in the literature on the adsorption of the rare gases by hexagonal molybdenum disulfide: in fact, the substance has attracted the attention of the surface chemist but little, apart from its significance as a novel low-friction material.

The first observations of adsorption on hexagonal molybdenum disulfide were those of Kainuma and Uyeda² who observed anomalous diffraction from an oil-pumped electron diffraction set in which they were studying the basal plane of the substance. This result they interpreted in terms of bundles of pump oil molecules lying flat on the basal plane,

(1) (a) R. G. Dickenson and L. Pauling, *J. Am. Chem. Soc.*, **45**, 1466 (1923); (b) P. Hassel, *Z. Krist.*, **61**, 93 (1923).

(2) Y. Kainuma and R. Uyeda, *Proc. Phys. Math. Soc. Japan*, **18**, 563 (1936).

parallel to the α -azimuth. In 1953, Ballou and Ross³ attempted to follow the effects of chemical washings by measuring vapor adsorption on the substance. Their low temperatures of degassing make it appear unlikely that they were dealing with a clean surface, and Ballou⁴ later published a letter in which he disclosed some severe time dependent effects in the adsorption of hydrocarbon vapors on their experimental material. Lyashenko⁵ reported some work function changes as a function of vapor adsorption, also in 1953, and included MoS₂ in the materials he was studying. These studies together with some brief French reports⁶ on stepped isotherms obtained on MoS₂ and other layer solids constitute the apparent extent of knowledge to date.

Experimental

Procedure.—Measurements of adsorption were made on a battery of quartz helix semi-micro balances, and on a capillary volumetric system of the general type described by Corrin,⁷ and commonly used for the precise determination of surface areas by krypton adsorption. The quartz helices were arranged in extra long envelopes so that the samples were at least three feet from the lowest point of the helix proper. This was done to avoid thermal gradients in the helices during outgassing and when the system was cryostatted. The ultimate vacuum in these systems was between 10^{-7} and 10^{-6} mm., and the corrections and precautions commonly taken in accurate adsorption measurements at lower pressures were used.

Pure liquid oxygen and pure liquid nitrogen baths were used to maintain the samples at the experimental temperatures. Pressures were measured with calibrated thermistor and thermocouple gauges, McLeod gauges and with various capillary and normal mercury manometers. The rare gases were reagent grade materials obtained in sealed flasks.

The molybdenum sulfide samples were obtained as fine powders from the Alpha Molykote Corp., Newtown, Conn., and as massive natural crystalline specimens from Ward's Natural Science Establishment, Rochester, N. Y. One of the massive specimens, a magnificent block of almost pure molybdenite from New South Wales, was some $10 \times 5 \times 5$ cm. in size and appeared to be the largest and finest specimen obtainable at the time this work was done. The availability of such large crystals makes the chore of cleavage to produce desired geometries less acute. The chemical analyses of the samples are given below in Table I; the behavior of these materials when they are heated *in vacuo* already has been described.⁸ The sorbent samples in all cases were prepared for the experiments by high temperature evacuation in the measuring systems only; this appeared to be justified since sublimation of oxide contaminants away from the surface is believed to proceed rapidly at ca. 850°, and even the natural material possessed considerable integrity as a pure chemical species. The sorbent samples were held in quartz tube sections on the volumetric lines, and in platinum buckets on the helix balances. Neither of these procedures is completely satisfactory, since there is a slow reaction between molybdenum disulfide and quartz at high temperatures, and the platinum buckets were visibly tarnished after two or three firings. In practice, therefore, new quartz tubulations and new platinum buckets were used in each separate experiment. The powder samples were not subjected to any compression into plug form. The apparatus were equipped with mercury pumps and cutoffs throughout. Oil pumps cannot be used because the hot pump oil probably would react with clean molybdenum sulfide. The effect noted by Kainuma² would also compli-

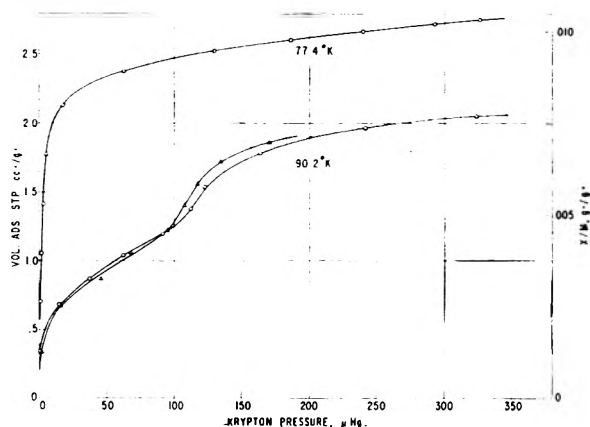


Fig. 1.—Adsorption isotherms of Kr on MoS₂ (degassed at 950°). Available data indicate that the isotherms extend to $\sim 600 \mu$ without change in direction. Monolayer point (BET) for the 77.4°K. isotherm is 2.46 cc.; $\Sigma K_r = 12.90 \text{ m.}^2/\text{g.}$

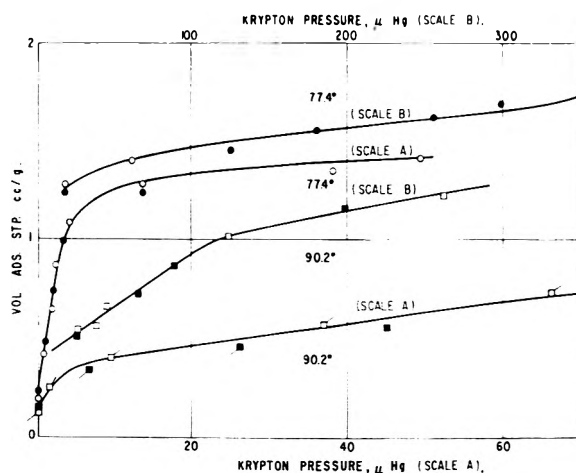


Fig. 2.—Adsorption isotherms of Kr on MoS₂ (degassed at 350°). Available data indicate that the isotherms extend to $\sim 600 \mu$ without change in direction. Different modifications of symbols on the same isotherm indicate results from replicate runs on different equipments. Monolayer point (BET) from the 77.4°K. isotherm is $\sim 1.6 \text{ cc.}$

cate matters. The use of stopcocks was restricted to the pump side of the systems as far as possible.

TABLE I

ANALYSES OF MoS ₂ SAMPLES USED IN SORPTION STUDIES			
	Mo, %	S, %	Other
1 μ Powder (a)	58.89	41.03	0.06% Si, <30 p.p.m. Pb, <0.01% Hg, <10 p.p.m. Ag
1200° Sinter (b)	61.65	38.47	.03% Si, <30 p.p.m. Pb, <0.01% Hg, <10 p.p.m. Ag
Massive natural (Kingsgate, N.S.W.)	58.41	38.70	.09% Si, <0.01% Pb, <0.01% Hg, <50 p.p.m. Ag
Massive natural (Ontario)	59.41	40.34	.06% Si, <30 p.p.m. Pb, <0.01% Hg, <50 p.p.m. Ag
Calcd. for MoS ₂	59.99	40.01	

The use of mercury in this case is also attended with considerable practical difficulties, since though molybdenum disulfide is a refractory material *in vacuo*, it is none the less a sulfide, and any exposure of hot mercury vapor to the clean sorbent results in a rapid reaction yielding a deposit of β -cinnabar throughout the system. It was therefore necessary to provide many traps and baffles in the systems to minimize the consequent rebuilding of our vacuum benches. Most of the reported results in this paper were then obtained from multiply replicated experimental observations. It was found that mercury vapor itself was not noticeably

(3) E. V. Ballou and S. Ross, *THIS JOURNAL*, **57**, 653 (1953).

(4) E. V. Ballou, *J. Am. Chem. Soc.*, **76**, 1199 (1954).

(5) V. A. Lyashenko, *Trudy Inst. Fiz., Akad. Nauk., Ukr. S.S.R.*, **4**, 33 (1953).

(6) L. Bonnetain, X. Duval and M. Letort, *Compt. rend.*, **234**, 1363 (1952).

(7) M. L. Corrin, *THIS JOURNAL*, **59**, 313 (1955).

(8) P. Cannon, *Nature*, **183**, 1636 (1959).

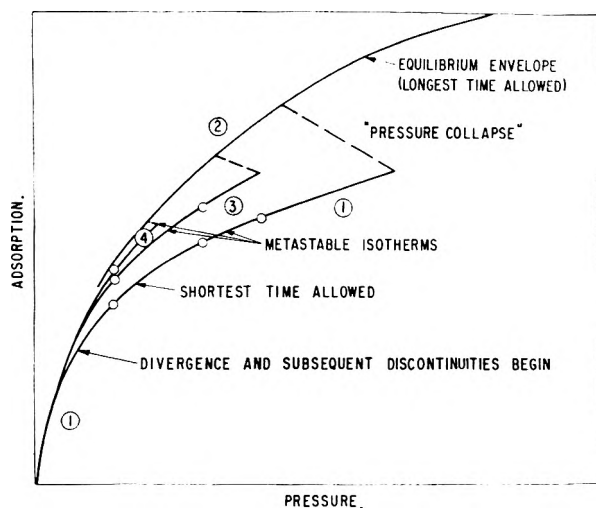


Fig. 3.—Schematic diagram of the time variable pV behavior of argon on MoS_2 , and construction of the equilibrium envelope.

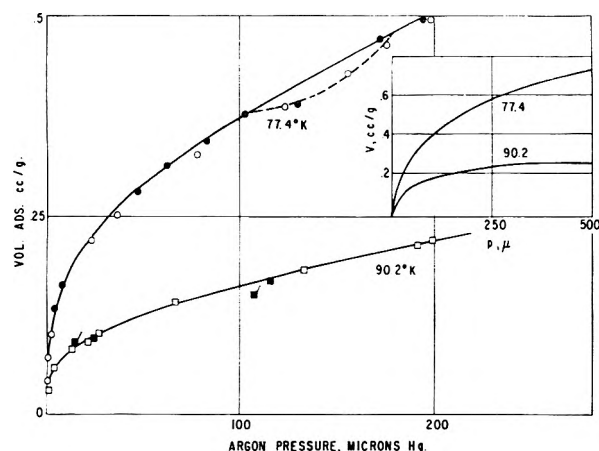


Fig. 4.—Adsorption isotherms of Ar on MoS_2 degassed at 950° . The 77.4°K . isotherm is the equilibrium envelope constructed as described in Fig. 3 and the text. Inset shows the form of the isotherms up to 500μ . Different symbols on the same isotherm indicate replicated data points.

adsorbed by clean cold samples, neither did its presence at this stage affect the adsorption results with the rare gases.

Results.—The adsorption of krypton on MoS_2 proceeds in an orderly manner, the only major problem being that the residual pressures in the early stages of coverage are very small. Consequently, it is difficult to obtain pressure values which are accurate enough to permit thermodynamic calculations to be made in the range $0 < \theta < 0.1$ (77.4°K .), where θ is the fraction of a statistical monolayer of coverage. At 90.2°K ., as will be noted in Fig. 1, there is a strong inflection in the isotherm beginning at $\theta \sim 0.5$, and this gives rise to some variability in the results. Thus, Fig. 1 (90.2°K .) shows the two most divergent sets of data obtained in five separate experiments, performed severally by the author and Miss C. P. Rutkowski. Figure 1 (77.4°K .) shows typical data points obtained from one of four overlapping and coincident experimental plots. The data on both curves extend to terminal pressures of approximately 600μ without change in direction: at pressures in excess of $\sim 1000 \mu$, however, both isotherms swing upwards, presumably due to the onset of multilayer formation on the sample and its container. These various times were found necessary to permit equilibrium to be attained: residual pressures less than 20μ , one day; 20μ – 200μ , 1–4 hr.; 200μ and up, less than 1 hr.

When the adsorption of krypton was measured on samples of MoS_2 which had been degassed at only 350° , some different results were found (Fig. 2). Thus, the 77.4°K ..

isotherm exhibited a weak inflection in the region $p/p_0 \sim 1 \times 10^{-3}$; this detail was found repeatedly and was absent after degassing the solid at temperatures in excess of 950° . In addition, the broad inflection found in the 90.2°K . isotherm on the high-temperature sample was absent from the isotherm measured on the material degassed at 350° : the relative magnitudes of the adsorptions at the same two measuring temperatures were similar at pressures in excess of 100μ , but the 350° sample gave a continuously rising curve to the asymptotic line for pressures less than this, at 90.2°K .

No permanent hysteresis was seen on any of these isotherms, though some slow desorption was measured on the return trip at 90.2°K . on the high-temperature material. Times to equilibrium were otherwise similar for both samples.

The adsorption of argon in the range followed was much more complicated. In general, at amounts adsorbed greater than 0.12 cc./g. , a peculiar time-dependent affect was seen. Since these are fairly frequently encountered on "homogeneous" surfaces and sometimes not identified as spurious effects but as first-order phase changes, it seems worthwhile to describe the manner of approach to equilibrium. On measuring the adsorption at 77.4°K . in a volumetric system, a smooth curve would be obtained up to a coverage in excess of 0.12 cc. , as shown by curve 1 in the schematic Fig. 3. In this region, a trivial mechanical disturbance of the system such as a gentle blow with a pencil on the sample, or a thermal disturbance, such as removal and replacement of the cryostat, would result in a sudden, sharp drop in system pressure with a concomitant increase in the amount adsorbed, giving the curve 2. By allowing progressively longer times for equilibrium than for curve 1, the curves 3 and 4 were obtained. Two hours between points sufficed in general to trace out the general envelope characterized by the lowest part of curve 1 and the maximum values characterized by curve 2. The 77.4°K . curve on Fig. 4 is then a synthesis of nine overlapping runs, in which the maximum values of v observed at given pressures are plotted. The 90.2°K . values are slow to come to equilibrium, possibly because of the very close boiling points of liquid oxygen and liquid argon.

Intercalation and Thermal Effects.—The magnitudes of the observed adsorptions and the absence of permanent hysteresis in this system makes it very unlikely that any intercalation of the inert gases between the lamellae studied did in fact occur. All the figures present data relative to a final BET krypton surface area of $12.90 \text{ m}^2/\text{g.}$: it was found that the high temperature degassing resulted in a net increase in surface area of the sample of about 50%, from ca. $8 \text{ m}^2/\text{g.}$ Electron microscopic examination of the high temperature residue indicated that the samples still possessed morphological integrity as hexagonal or trigonal arrays of platelets. Somewhat higher temperatures (greater than 1100°) have to be employed to obtain any large amount of sintering, which would cause "thermal activation" of the solid and consequently give higher areas: even at these higher temperatures, however, the sublimed MoS_2 is of hexagonal form⁸ and one would see only point or line contact between platelets, with none of the sinter necking and recrystallization observed in other well known cases.⁹ It thus seems likely that the increased area is due to a small degree of thermal splitting of the lamellae, either *via* compressive failure along fault lines or by volatilization of impurities within the lattice. The first is considered more likely from some very high resolution electron microscopic studies.¹⁰

Anomalous results, explicable on the basis that argon enters the entire crystal lattice, were obtained after exposure of the substrate to ammonia vapor. Under no other circumstances were such results obtained, including prior exposure of the substrate to water (the adsorption of ammonia by MoS_2 is unusual and has profound electrical and mechanical effects upon the solid: such results will be presented in a later paper¹¹).

Discussion

The most important comparison to be made

(9) *E.g.*, J. F. Goodman and S. J. Gregg, *J. Chem. Soc.*, 3612 (1956); 694 (1959).

(10) V. A. Phillips and P. Cannon, unpublished results.

(11) P. Cannon, to be submitted to THIS JOURNAL.

using these data is with similar information on graphite and graphitized carbon blacks.

In the many studies of the adsorption of rare gases on graphite accomplished in the past decade, there has been some argument concerning the existence of vertical steps in the isotherms, which have been interpreted in terms of second-order phase changes in the adsorbed film. Thus, Jura and Criddle¹² found some very complex structure at low coverage in their isotherms, but reinvestigation by others failed to give exactly similar results,¹³⁻¹⁷ though large, nearly vertical steps were observed¹⁴⁻¹⁷ frequently at somewhat higher coverages. No equilibrium vertical steps were seen in the present work, though it is conceivable that the inflection in the 77.4°K. isotherm on Fig. 2 could be so described. With argon on the graphitized carbon black P-33, Ross and Winkler¹⁸ found that at the lowest pressures (<30 μ) at 77.8°K., the adsorption followed the Henry law. Careful examination of the present data indicates that here the adsorption of argon does not follow such a law. But the present results for krypton on the 350° degassed material are similar to those observed by the same two workers¹⁹ for this gas on P-33 at 77.4°K., with an inflection at p/p_0 approximately equal to 10^{-3} . However, the present contention is that the 350° MoS₂ sample is oxide contaminated offering substantially different regimes of adsorption sites than the clean and smooth material. The work of Gulbransen and Andrew²⁰ on the adsorption of krypton on artificially smoothed graphite is germane to this point. They regarded a "new" graphite surface as full of irregularities, since they found good linear BET plots for krypton adsorption; however, by controlled oxidation, they rendered the surface topographically more uniform (the adsorption of krypton being but little affected by purely chemical factors). The adsorption isotherms became less well-behaved and the corresponding BET plots had a similar appear-

ance to those found for Kr on the high temperature MoS₂. This behavior was regarded as due to oxygen bridging of the slots and pits in the exposed graphitic surfaces.

McDermot and Lawton²¹ recently have reported data for krypton adsorption on a graphite "known to be heterogeneous" (their sample Acheson GF-3) and found low pressure results similar to those of Ross and Winkler¹⁹ and those reported here on the 350° material. Perhaps the homogeneity of the GF-3 was better than was thought by the above workers: in any event, use of the criterion of vertical discontinuity in the isotherm for homogeneity of substrate surface seems to be justifiable even on the basis of the above conflicting results. However, it is quite apparent that such discussion can only be developed further from considerations of the various partial heats and entropies of the adsorption processes, and that these must be derived from accurate and replicated isotherm points, as has been emphasized by others.²² In addition, Tykodi²³ has advanced thermodynamic considerations which make it seem unlikely that the vertical discontinuities have any permanent significance. Of course, there is a difference in kind between time-dependent and time-independent steps, and the latter appear from the recorded data to be more gradual and continuous.

From the nature of the present argon results, it is apparent (*vide supra*) that as many so-called sharp discontinuities could be observed as experiments run, and that their magnitude varied inversely with one's patience. That they offer an indication of a phase transition in the adsorbed monofilm is hardly disputable, but it seems unlikely that any quantity associated with them, other than the coverage at which they first begin to be observed, has any physical significance. In the present work, they first begin to appear at a co-area of 400 Å.²/Ar atom, which is also the cross-section of an argon gas atom at the temperature of the experiment. The significance of this will be further developed in a later discussion²⁴ of the heats of adsorption in the present systems.

Acknowledgments.—My thanks are due to Miss C. P. Rutkowski, who performed the invaluable service of providing independent checking runs in each of the systems studied.

(12) G. Jura and D. Criddle, *THIS JOURNAL*, **55**, 163 (1951).

(13) A. D. Crowell and D. M. Young, *Trans. Faraday Soc.*, **49**, 1080 (1953).

(14) J. H. Singleton and G. D. Halsey, Jr., *THIS JOURNAL*, **58**, 330 (1954).

(15) H. Clark, *ibid.*, **59**, 1068 (1955).

(16) C. H. Amberg, W. B. Spencer and R. A. Beebe, *Can. J. Chem.*, **33**, 307 (1955).

(17) M. H. Polley, W. D. Schaefer and W. R. Smith, *THIS JOURNAL*, **57**, 409 (1953).

(18) S. Ross and W. Winkler, *J. Colloid Sci.*, **10**, 319 (1955).

(19) S. Ross and W. Winkler, *ibid.*, **10**, 330 (1955).

(20) E. A. Gulbransen and K. F. Andrew, *Ind. Eng. Chem.*, **44**, 1039 (1952).

(21) H. L. McDermot and B. E. Lawton, *Can. J. Chem.*, **37**, 54 (1959).

(22) J. M. Honig, *Ann. N. Y. Acad. Sci.*, **58**, 741 (1954).

(23) R. J. Tykodi, *J. Chem. Phys.*, **22**, 1647 (1954).

(24) P. Cannon, *THIS JOURNAL*, **64**, in press (1960).

THE HEAT OF FUSION OF BISMUTH TRICHLORIDE—A COMPARISON OF CALORIMETRIC AND CRYOSCOPIC DETERMINATIONS¹

BY L. E. TOPOL, S. W. MAYER AND L. D. RANSOM

Atomics International, A Division of North American Aviation, Inc., Canoga Park, California

Received December 17, 1959

The heat of fusion of BiCl_3 was determined to be 5.68 ± 0.08 kcal./mole with a drop calorimeter. With sodium, potassium and barium bromides and sodium iodide as solutes and the assumption of complete ionization, cryoscopic measurements yielded heats of fusion approaching this value at high dilutions, *e.g.*, 4.72 kcal. with solute concentrations less than 4.1 mole % and 5.48 kcal. with concentrations under 1.5 mole %. With sodium and potassium chlorides as solutes much poorer agreement with the calorimetric value was found. The discrepancy in results probably is due to strong interactions among the ions, the interactions between BiCl_3 and the alkali chlorides being somewhat greater than those between BiCl_3 and the bromides. A phase equilibrium study of the KCl-BiCl_3 system showed a glassy region and two solid phases, K_3BiCl_6 and K_2BiCl_6 . The possibility of complex and polymer formation in the melt is considered.

Introduction

Since few calorimetric measurements on inorganic salts have been carried out, most of the values for the heats of fusion in the literature² were derived from phase diagram data. In computing the heat of fusion from such data, ideal behavior of the solvent is assumed. In most phase diagram studies, particularly with systems containing ions of higher valence, the solutions are not sufficiently dilute to permit this assumption. Furthermore, the accuracy of the measurements is often insufficient for the calculation of a satisfactory heat of fusion. With these facts in mind it was decided to determine the heat of fusion of a polyvalent salt, BiCl_3 , calorimetrically. Then, using alkali halides and an alkaline earth bromide as solutes, a cryoscopic determination of this value would provide an interesting comparison of the methods and in turn afford a study of the behavior of molten BiCl_3 .

Experimental

Materials.—The BiCl_3 was purified by distillation under anhydrous conditions as described elsewhere.³ The salt thus prepared had a melting point of 233.5° .

Reagent grade NaCl , NaBr , NaI , KCl , KBr and BaBr_2 were dried by heating slowly *in vacuo* until molten.

Apparatus and Procedure. **A. Calorimetry.**—The drop calorimeter was similar to that described by Goodkin, Solomons and Janz.⁴ A tube furnace manufactured by the Marshall Products Company was kept at constant temperature by a West Gardsman Controller. A uniform temperature zone in the furnace was ensured by employing a heavy-walled tube made from a solid cylinder of nickel. The furnace was secured in a stationary position about 13° above the calorimeter. The path of fall of the sample from the furnace to the calorimeter was through a glass tube, divided into two sections to facilitate insertion and removal of a cork stopper in the calorimeter chamber. The calorimeter, immersed in a water-bath maintained at 25.0° and further shielded from the heat source by two transite plates, consisted of a pint Dewar flask containing a fluid, a copper drop chamber, a motor-driven glass stirrer, and a temperature measuring device. To minimize changes in the heat

equivalent of the calorimeter over long periods of time by evaporation of the calorimeter liquid, Dow-Corning Silicone Fluid #200—viscosity 20 was used. This fluid has a low vapor pressure and a constant specific heat over the temperature range of the measurements. A Fiske precision differential thermistor with an accuracy of $\pm 0.003^\circ$ and manufactured by Advanced Instruments, Inc., was employed as the thermometer; this in turn was calibrated against a standard platinum resistance thermometer. The thermistor probe, stirrer and glass entry tube, extending from the cork-stoppered and paraffin-sealed Dewar flask, were insulated from the water-bath by means of glass tubing. The sample, consisting of about 10 g. of BiCl_3 , was loaded in a 0.010" wall platinum cylinder, $1/2$ " in diameter, in a helium-filled dry box. The capsule then was crimped tight and sealed with molten gold. To calibrate the calorimeter, similar platinum tubes containing platinum or oxide-free copper were used as standards. The temperature of the sample vessel was measured with a Rubicon B potentiometer using a platinum, platinum-10% rhodium thermocouple in contact with the capsule and an ice-bath reference junction.

The procedure was similar to that described by Goodkin, *et al.*,⁴ and by Sturtevant.⁵

B. Cryoscopy.—Each salt mixture (about 10 g. in weight) was weighed out accurately in a dry-box into a 13-mm. Pyrex tube containing a thermocouple well extending about 0.5" into the mixture. The tube was clamped off before removal from the glove box, then evacuated and sealed. Details of the freezing point measurements previously have been given.⁶ Several measurements were made on each sample, and the freezing point was reproducible within an average deviation of 0.1° .

It was found that molten BiCl_3 had a great tendency to supercool. (In fact, violet-colored glasses are formed with concentrations of KCl or KBr greater than 20 mole %.) Accordingly, approximately 0.5 g. of ground Pyrex glass was added to act as a nucleating agent. This reduced the supercooling from several degrees (with no nucleating agent present) to less than one degree.

For the higher temperature studies on the KCl-BiCl_3 system, Vycor capsules and platinum, platinum-10% rhodium thermocouples, standardized against prefused NaCl , were employed. Many of these mixtures formed glasses and thus made temperature-time cooling breaks extremely difficult to detect. In these cases the glasses were allowed to devitrify in an oven at 100° for a week and then heating curves were run.

Results and Discussion

The results of the calorimetry experiments are shown in Table I and Fig. 1. A value of 5.68 ± 0.08 kcal./mole was found for the heat of fusion of BiCl_3 . This result is slightly higher than the value of 5.50 ± 0.15 kcal. reported recently⁷ and is much larger than 2.6 kcal. listed by Kelley.²

(5) J. M. Sturtevant in Weissberger (Ed.), "Physical Methods of Organic Chemistry," Vol. I, Part I, Interscience Publishers, Inc., New York, N. Y., 1949.

(6) S. W. Mayer, S. J. Yosim and L. E. Topol, "Cryoscopic Measurements in the Bi-BiCl_3 System," *THIS JOURNAL*, **64**, 238 (1960).

(7) M. A. Bredig, *ibid.*, **63**, 978 (1959).

(1) This work was supported by the Atomic Energy Commission. It has been presented in part before the Division of Inorganic Chemistry at the National Meeting of the American Chemical Society in Chicago, September, 1958.

(2) K. K. Kelley, U. S. Bur. Mines Bull. 393, 1936; L. Brewer, *et al.*, "The Chemistry and Metallurgy of Miscellaneous Materials: Thermodynamics," ed. by L. L. Quill, McGraw-Hill Book Co., New York, 1950; F. D. Rossini, *et al.*, "Selected Values of Chemical Thermodynamic Properties," National Bureau of Standards Circular 500, 1952.

(3) S. J. Yosim, A. J. Darnell, W. G. Gehman and S. W. Mayer, *THIS JOURNAL*, **63**, 230 (1959).

(4) J. Goodkin, C. Solomons and G. J. Janz, *Rev. Sci. Instr.*, **29**, 105 (1958).

TABLE I
HEAT CONTENT CHANGES OF BiCl₃^{a,b}

Run	Initial temp. of sample, °C.	Temp. rise calorimeter, °C.	Obsd. heat, cal.	Heat of capsule, cal.	Heat of sample, cal./mole	Heat evolved, cor. to 298.16°K. cal./mole
1	178.9	0.981	229.24	69.27	3804	3867
2	190.0	1.003	234.38	73.97	4131	4190
3	200.0	1.055	246.53	78.58	4326	4384
4	204.3	1.155	269.90	81.19	4488	4544
5	206.0	1.070	250.04	81.12	4351	4417
6	210.5	1.130	264.06	83.46	4652	4705
7	220.3	1.191	278.31	87.99	4902	4956
8	225.0	1.289	301.21	90.52	5011	5082
9	225.4	1.200	280.42	89.92	4907	5228
10	225.8	1.320	308.46	91.25	5166	5218
11	231.9	1.255	293.27	93.06	5157	5228
12	239.7	2.400	560.83	96.98	11,032	11,130
13	243.6	2.450	572.52	98.80	11,266	11,361
14	247.2	2.480	579.53	100.76	11,386	11,466
15	249.7	2.490	581.86	102.02	11,412	11,489
16	256.4	2.553	596.58	104.90	11,693	11,783
17	258.7	2.570	600.56	105.93	11,764	11,857
18	272.0	2.659	621.36	112.27	12,108	12,198
19	273.8	2.684	627.20	112.89	12,232	12,333
20	280.3	2.759	644.72	116.32	12,567	12,649
21	285.4	2.780	649.63	118.42	12,634	12,735

^a Runs 2, 3, 5-7, 9, 11: 12.2432 g. BiCl₃ in 13.6197 g. Pt capsule, sealed with 0.4251 g. Au, corrected to 25.0°. Runs 1, 4, 8, 10, 12-21: 13.2605 g. BiCl₃ in 13.5597 g. Pt capsule, sealed with 0.5912 g. Au, corrected to 25.0°. ^b Experimental heat equivalent of calorimeter for above temperature range = 233.68 cal./degree.

With this new heat of fusion and a melting point of 506.7°K., the entropy of fusion of BiCl₃ is calculated to be 11.21 e.u. or about 2.8 e.u. per gram-atom, a value close to 3 found for many salts.⁸ The heat capacity of solid BiCl₃ for the temperature range 180 to 233.5° is 26.1 ± 1.4 cal./deg./mole and that of liquid BiCl₃ is 34.3 ± 1.1 cal./deg./mole for the temperature interval 233.5 to 285°.

The heat of fusion of a substance also can be calculated from the temperature of the solid-liquid phase change by means of the relation

$$\log N_1 = \frac{\Delta H_f}{2.303R} \left(\frac{1}{T_f} - \frac{1}{T} \right) \quad (1)$$

where N_1 , ΔH_f and T_f are the cryoscopic mole fraction, heat of fusion and melting point, respectively, of the solvent and T , the freezing point of the solution. The cryoscopic mole fraction is defined as

$$N_1 = \frac{n_1}{n_1 + \bar{n}n_2} \quad (2)$$

where n_1 and n_2 are the number of moles of solvent and solute, respectively, and \bar{n} is the cryoscopic number of the solute, *i.e.*, the number of foreign particles per molecule of solute. Equation 1 is valid if negligible solid solution and deviation of the solvent from ideality occur and if the heat of fusion is constant over the temperature range of the measurements. The detection of eutectic halts for virtually all samples from 1 to 15 mole % solute served to confirm the lack of solid solution

(8) O. Kubaschewski and E. L. Evans, "Metallurgical Thermodynamics," Pergamon Press, New York, N. Y., 1958, p. 191.

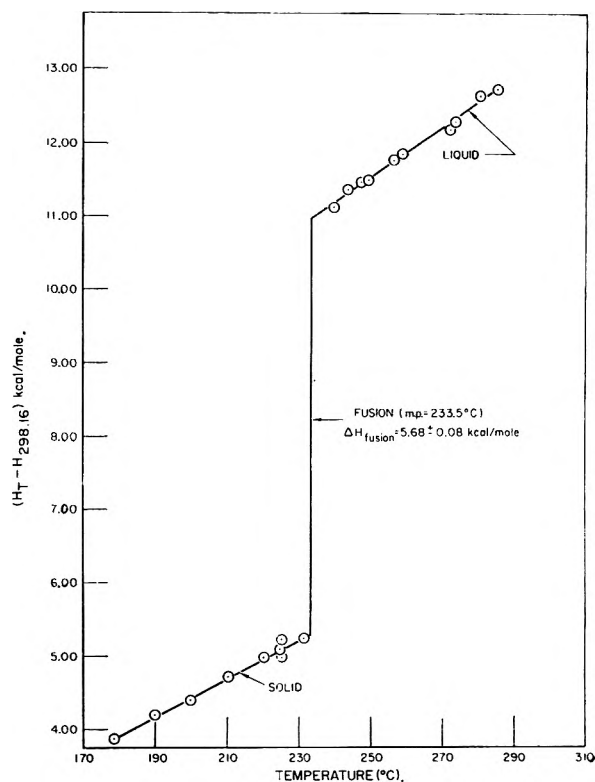


Fig. 1.—Change of heat content of BiCl₃ with temperature.

TABLE II

FREEZING POINT DEPRESSIONS BY NON-CHLORIDE SOLUTES IN BiCl₃

Solute	Solute, mole fraction ^a	ΔT _f , °C.
NaBr	0.00275	0.38
	.00465	0.75
	.00666	1.10
	.00985	1.64
	.01023	2.20
	.01470	2.62
	.01730	3.31
	.01970	3.98
	.0210	4.62
	.0259	4.70
	.0310	5.95
	.0392	8.40
	.0405	8.45
KBr	.00494	0.79
	.00979	1.70
	.01453	2.50
	.01955	3.71
NaI	.0295	5.51
	.0388	8.70
	.00490	0.84
	.01078	2.07
	.01560	3.38
BaBr ₂	.0211	4.50
	.001326	0.51
	.00259	0.59
	.00540	1.32
	.01033	2.66
.01530	3.81	

^a $N_2 = n_2/(n_1 + n_2)$.

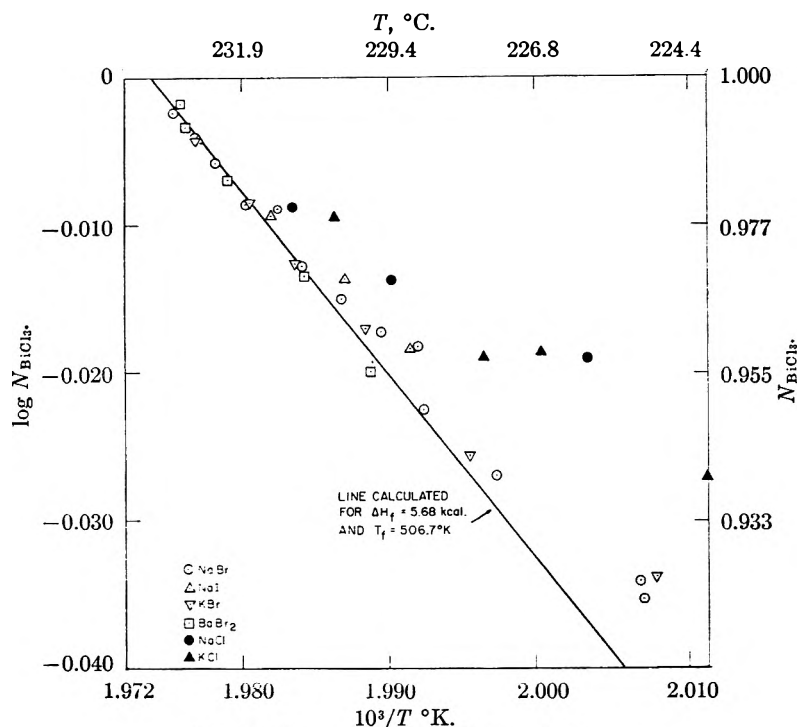
Fig. 2.—Freezing points of BiCl_3 solutions.

TABLE III

FREEZING POINT DEPRESSIONS OF BiCl_3 WITH NaCl AND KCl ADDITIONS

Solute	Solute, mole fraction	ΔT_f , °C.	Cryoscopic no.
NaCl	0.0200	2.52	1.41
	.0311	4.15	1.50
	.0428	7.45	1.99
KCl	.0215	3.16	1.65
	.0418	6.71	1.80
	.0427	5.73	1.51
	.0606	10.0	1.86
	.0969	21.0	2.44

formation of any consequence⁹; corrections in the variation of the heat of fusion with temperature are less than 0.1 kcal.

The experimental results, shown in Tables II and III, are plotted in Fig. 2 assuming complete solute dissociation and a common ion effect for the chloride ion. The calculated freezing point line for BiCl_3 with $T_f = 506.7^\circ\text{K}$. and $\Delta H_f = 5.68$ kcal. is included in Fig. 2 for comparison. It is seen that the data for the chlorides are in much poorer agreement with the calculated line than those for the bromides and iodide. Even in the case of the non-chloride melts, acceptable agreement is not obtained unless solute concentrations below 1.5 mole % are considered. Then a heat of fusion of 5.48 ± 0.25 kcal./mole and a melting point of 233.7° (measured = 233.5°) are found. If the chloride solutions and/or the more concentrated non-chloride solute melts are included in the least squares analysis, the value for ΔH_f is found to be lower. For example, for non-chloride additions of less than 3.1 and 4.1 mole %, heats of fusion of 5.04 and 4.72 kcal., respectively, are obtained.

(9) Further, for the non-chloride solutes there appears to be no trend in the data of Fig. 2 to suggest solid solution formation.

Since no solid solution was found and heat capacity corrections are negligible, it appears that in the case of the more concentrated solutions the discrepancy between the cryoscopic and the calorimetric values for the heat of fusion is due primarily to the deviation of the solvent behavior from Raoult's law. Further, if some solid solution did occur in the more dilute compositions (less than 1% solute) where eutectic halts are difficult to detect, the observed freezing point depressions would be less than the true ones and the ΔH_f 's reported above would in turn be slightly high, *i.e.*, the difference between the calorimetric and the corrected cryoscopic values of the ΔH_f would be still greater. Thus, except for fairly dilute non-chloride solute concentrations (less than 1.5 mole %) and for very dilute chloride mixtures (much less than 1 mole %), the cryoscopic method is not satisfactory

for obtaining a heat of fusion in this system.

In the series of measurements with sodium and potassium chloride solutes, Fig. 2 and Table III, the freezing point of BiCl_3 was lowered to a larger extent than was expected assuming a simple one particle solute effect, *i.e.*, the chloride ion acting as a common ion. The cryoscopic numbers, \bar{n} , for these solutes are given in Table III and are seen to increase with increasing solute concentration. The deviations appear to be larger in the chloride melts than in the bromide-chloride solutions, an effect which may be due to the higher charge density of the chloride ion. As glass formation and some phase transition below the assumed eutectic occur in the KCl-BiCl_3 system (see below) and probably also in the NaCl-BiCl_3 system, the values of the cryoscopic numbers may be in error due to some solid solution formation. However, as can be seen in Fig. 3, eutectic or secondary halts at 168° were noted with samples from 2 to 20 mole % KCl . If some solid solution does occur in these systems below 2% KCl , the true values of \bar{n} would be even greater than those given in Table III.

One interpretation of these strong interactions is that the added halide ion associates with BiCl_3 in the melt to form a complex. Such complexes as BiCl_4^- , BiCl_5^{2-} and BiCl_6^{3-} are known to exist in aqueous solution.¹⁰ A phase diagram study of the KCl-BiCl_3 system (Fig. 3) showed the existence of two solid compounds, congruently melting K_3BiCl_6 and incongruently melting K_2BiCl_5 . The compositions of these compounds as well as the absence of KBiCl_4 were corroborated by X-ray analysis.¹¹ The cryoscopic numbers larger than

(10) D. N. Hume and L. Newman, *J. Am. Chem. Soc.*, **79**, 4576, 4581 (1957).

(11) However, from the phase diagram the possibility of another compound, such as KBiCl_4 , still exists. The halts measured around

unity obtained for the chloride solutes might result from complex formation in the liquid; the existence of solid compounds represents some evidence for this although the presence of a stable compound in the solid state does not necessarily establish its existence in the liquid. Also, the occurrence of color changes (yellow to violet) offers further evidence for the existence of different bismuth species in these melts.

Another mechanism that must be considered is the formation of bismuth chloride polymers. In this case a value of \bar{n} greater than two can be obtained; Table III shows such an \bar{n} at a composition of 9.7% KCl. This result is consistent with the formation of a glass which was found to occur in this system at KCl concentrations greater than 20 mole % (see Fig. 3). This tendency toward glass formation may also have an effect at low solute concentrations. If this is the case, the cryoscopic numbers found for the dilute melts may be the result of several processes: (1) the chloride ion acting as a common ion resulting in an \bar{n} of one, (2) local ordering or the formation of complexes yielding \bar{n} 's of one to two, and (3) polymeric associations producing \bar{n} 's greater than two. The present data do not provide sufficient information to distinguish which one or more of these processes are occurring at a given concentration.

Thus, in the molten BiCl_3 system, freezing point data for the solutes used in this study do not yield a satisfactory heat of fusion except at low solute concentrations. Although these results may not be typical of other molten salt systems, they do suggest that heat of fusion values derived from phase diagrams should be accepted only with great reservations.

135° were smaller than those at 168° and may indicate another eutectic, eutectoid or solid phase change.

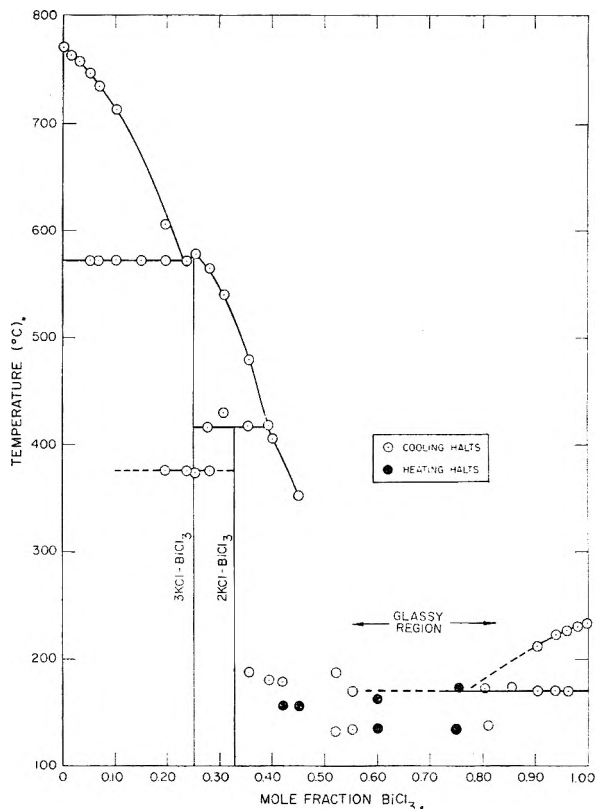


Fig. 3.—The KCl- BiCl_3 system.

Acknowledgments.—The authors wish to acknowledge the assistance of Dr. G. M. Wolten in carrying out the X-ray determinations of the KCl- BiCl_3 mixtures and to thank Drs. S. J. Yosim and D. E. McKenzie for valuable discussions.

PHASE EQUILIBRIA IN THE SYSTEMS $\text{BeF}_2\text{-ThF}_4$ AND $\text{LiF-BeF}_2\text{-ThF}_4$

BY R. E. THOMA, H. INSLEY, H. A. FRIEDMAN AND C. F. WEAVER

Oak Ridge National Laboratory,¹ Reactor Chemistry Division, Oak Ridge, Tennessee

Received December 18, 1969

As a part of a study of materials potentially useful as fluid fuels of high temperature nuclear reactors, equilibrium diagrams for the condensed systems $\text{BeF}_2\text{-ThF}_4$ and $\text{LiF-BeF}_2\text{-ThF}_4$ have been determined. Both thermal analysis and quenching techniques were used with phase identification accomplished by petrographic and X-ray diffraction analysis. The system $\text{BeF}_2\text{-ThF}_4$ contains a single eutectic at 2.0 ThF_4 (mole %), melting point $527 \pm 3^\circ$. In association with primary phase fields of the three components and five binary compounds there occur six ternary invariant points within the system $\text{LiF-BeF}_2\text{-ThF}_4$. Of these, only one invariant point is a eutectic. Unusual solid miscibility occurs in the compound $3\text{LiF} \cdot \text{ThF}_4$, which appears as a single phase solid solution within the area bounded by 75 LiF , 25 ThF_4 –58 LiF , 16 BeF_2 , 26 ThF_4 –59 LiF , 20 BeF_2 , 21 ThF_4 (mole %).

Introduction

Molten fluoride mixtures containing uranium tetrafluoride have been shown to be useful as circulating fuels for high temperature nuclear reactors.^{2a,b} Conversion of thorium to U^{233} can be accomplished in such a reactor if ThF_4 is included in the fuel or if a molten blanket containing ThF_4

surrounds the reactor. Alkali fluorides with beryllium fluoride can serve as solvent mixtures in which moderate concentrations of uranium tetrafluoride and/or thorium tetrafluoride can be maintained in solution at 400–600°. Such mixtures are among the very few fused salt mixtures which exhibit high enough concentrations of thorium to be of interest in high temperature reactor technology. Solutions of UF_4 and ThF_4 in LiF-BeF_2 or in NaF-BeF_2 solvent mixtures have been proposed as fuels for such converters.³

(1) Operated for the United States Atomic Energy Commission by the Union Carbide Corporation.

(2) (a) A. M. Weinberg and R. C. Briant, *Nuclear Sci. and Eng.*, **2**, 797 (1957); (b) E. S. Bettis, J. L. Meem, R. E. Affel, W. B. Cottrell and G. D. Whitman, *ibid.*, **2**, 804 (1957).

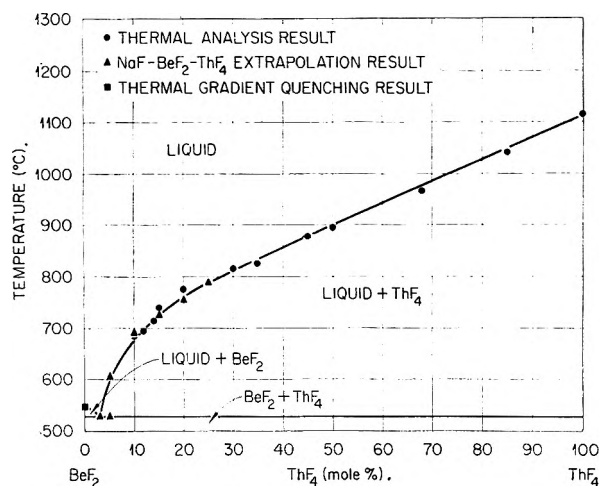


Fig. 1.—The system BeF₂-ThF₄.

As a means of understanding the phase relations existing in LiF-BeF₂-ThF₄-UF₄ nuclear reactor fuel mixtures, a study has been made of the binary and ternary systems limiting the LiF-BeF₂-ThF₄-UF₄ quaternary system. Except for the system BeF₂-ThF₄-UF₄, which is presently under investigation at this Laboratory, phase diagrams of each of the other limiting systems have been reported.^{4a-b} In this paper detailed phase diagrams are presented for the systems BeF₂-ThF₄ and LiF-BeF₂-ThF₄.

Experimental

Materials.—The mixtures used in these phase equilibrium studies were prepared from reagent grade lithium fluoride, beryllium fluoride and thorium fluoride. Lithium fluoride was obtained from Foote Mineral Company and from Maywood Chemical Works, thorium fluoride from Iowa State College and from National Lead Company, and beryllium fluoride from the Brush Beryllium Company. No impurities were found in the thorium tetrafluoride by X-ray diffraction or microscopic analysis. Less than 0.25 weight % impurities were found by spectroscopic analysis of this material.

The phase equilibria data were obtained by thermal analysis of slowly-cooled melts and by identifying the phases present in mixtures which had been equilibrated and quenched. Because thorium fluoride is easily converted to oxyfluorides or oxide at elevated temperatures⁵ it was necessary to remove small amounts of water and oxygen as completely as possible from the starting materials. To facilitate the removal of these substances ammonium bifluoride was added to the mixtures of BeF₂-ThF₄ and LiF-BeF₂-ThF₄ before initial heating in the thermal analysis experiments. As mixtures were heated the water was

evaporated from the system. The oxides were converted by reaction with the ammonium bifluoride to products which have not been identified but which are likely to be ammonium fluorometallates.⁶ Upon further heating the "ammonium fluorometallates" decomposed to form the metal fluorides. These same mixtures were used later in the quenching experiments.

Apparatus and Methods.—The techniques used for measurement of the temperatures which define the phase diagrams as well as the X-ray and microscopic techniques for identifying phases have been discussed previously.^{4a,7,8} The accuracy of the temperature measurements reported in these studies is limited by the characteristics of the chromel-alumel thermocouples used. Manufacturers estimate this accuracy to be within 5° in the temperature range 400–800°. Except in the LiF and ThF₄ apices of the system LiF-BeF₂-ThF₄, so large an amount of reproducible phase data was accumulated that statistically reliable calculations of standard temperature deviations could be made. These deviations in the measurement of invariant temperatures are ±1°. Reproducible phase data were accumulated from experiments performed using six sets of quenching and temperature measurement apparatus, whose design and operation is nearly identical. In each of these is incorporated 18 thermocouples whose independent readings were used to determine a temperature calibration curve of the thermal gradient within the furnace. This arrangement causes error in a single thermocouple to be readily apparent.

Discussion of Results

The System BeF₂-ThF₄.—A preliminary diagram of the system BeF₂-ThF₄ has been reported from this Laboratory.⁹ The phase equilibrium diagram reported here (Fig. 1) represents a synthesis of thermal analysis and thermal gradient quenching data obtained from mixtures of BeF₂-ThF₄, LiF-BeF₂-ThF₄, and NaF-BeF₂-ThF₄. The system contains a single invariant point, the eutectic at 527° and at 2.0 mole % ThF₄. Molten mixtures of BeF₂ and ThF₄ containing more than about 75 mole % BeF₂ are so viscous at temperatures near the liquidus that equilibrium is not reached after heating for as long as three weeks. Rather than employing very long annealing treatments use was made of the fact that small additions of NaF or LiF will so reduce the viscosity of melts that equilibrium can be reached in less than three weeks. Thus, solid-liquid transitions were determined for mixtures having compositions near the BeF₂ apex of the NaF-BeF₂-ThF₄ system and extrapolations based on these data were made to the limiting binary system BeF₂-ThF₄. The results so obtained for the range 0 to 25 mole % ThF₄ in the system BeF₂-ThF₄ are shown in Table I¹⁰ and the data in the system NaF-BeF₂-ThF₄ on which these are based are given in Table II. The eutectic invariant composition and temperature, and the liquidus values from 0 to 25 mole % ThF₄ were determined in this way. The liquidus temperatures for the less viscous region from 25 to 100 mole % ThF₄ were determined by thermal

(6) B. J. Sturm, Oak Ridge National Laboratory, personal communication.

(7) C. J. Barton, W. R. Grimes, H. Insley, R. E. Moore and R. E. Thoma, *THIS JOURNAL*, **62**, 665 (1958).

(8) H. A. Friedman, *J. Am. Ceram. Soc.*, **42**, 284 (1959).

(9) ORNL-2431, p. 36, October 31, 1957.

(10) Tables I, II, III, V and VI have been deposited as Document No. 6241 with the ADI Auxiliary Publications Project, Photoduplication Service, Library of Congress, Washington 25, D. C. A copy may be secured by citing the Document No. and remitting \$2.50 for photoprints or \$1.75 for 35 mm. microfilm, in advance by check or money order payable to: Chief, Photoduplication Service, Library of Congress.

(3) J. A. Lane, H. G. MacPherson and Frank Maslan, editors, "Fluid Fuel Reactors," Addison-Wesley Publishing Co., Inc., Reading, Mass., 1958, Chapters 11 and 12, pp. 567–594.

(4) (a) C. J. Barton, H. A. Friedman, W. R. Grimes, H. Insley, R. E. Moore and R. E. Thoma, *J. Am. Ceram. Soc.*, **41**, 63 (1958); (b) A. V. Novoselova, Yu. P. Simanov and E. I. Yarembash, *Zhur. Fiz. Khim.*, **26**, 1244 (1952); (c) D. M. Roy, R. Roy and E. F. Osborn, *J. Am. Ceram. Soc.*, **37**, [7] 300 (1954); (d) L. J. Wittenberg, *ibid.*, **42**, 209 (1959); (e) R. E. Thoma, H. Insley, B. S. Landau, H. A. Friedman and W. R. Grimes, *THIS JOURNAL*, **63**, 1266 (1959); (f) C. F. Weaver, R. E. Thoma, H. Insley and H. A. Friedman, *J. Am. Ceram. Soc.*, **43**, 213 (1960); (g) L. B. Rinehammer, P. A. Tucker and E. F. Joy, "Phase Equilibria in the System BeF₂-UF₄," in "Phase Diagrams for Ceramists: Part II," by E. M. Levin and H. F. McMurdie, The American Ceramic Society, Columbus, Ohio, 1959, p. 98; (h) L. V. Jones, D. E. Etter, C. R. Hudgens, A. A. Huffman, L. B. Rinehammer, N. E. Rogers, P. A. Tucker and L. J. Wittenberg, "Phase Equilibria in the LiF-BeF₂-UF₄ Ternary Fused Salt System," MLM-1080, Aug. 24, 1959.

(5) R. W. M. D'Eye, *J. Chem. Soc.*, 196 (1958).

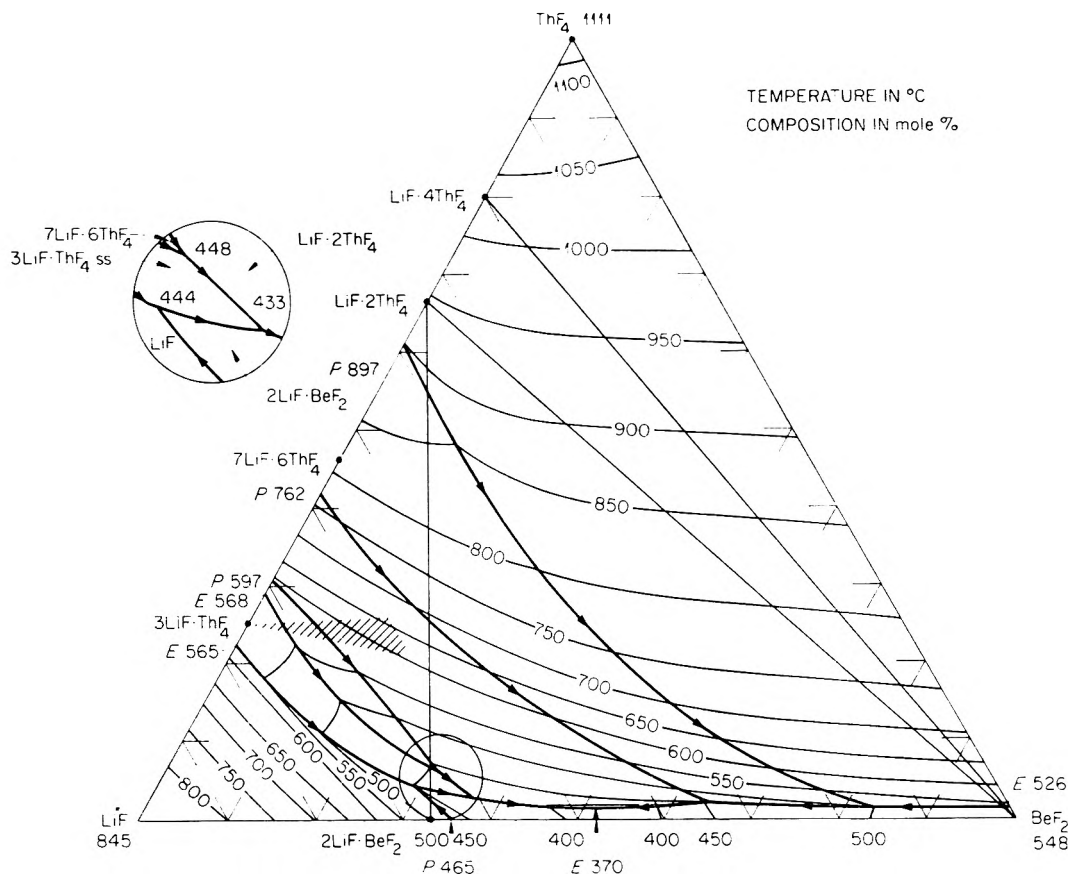


Fig. 2.—The system $\text{LiF-BeF}_2\text{-ThF}_4$.

TABLE IV
INVARIANT EQUILIBRIA IN THE SYSTEMS $\text{BeF}_2\text{-ThF}_4$ AND $\text{LiF-BeF}_2\text{-ThF}_4$

Composition, mole %			Temp., °C.	Type invariant	Phases present
LiF	BeF ₂	ThF ₄			
0	98.0	2.0	526	Eutectic	BeF ₂ , ThF ₄ , liquid
47.0	51.5	1.5	356	Eutectic	2LiF·BeF ₂ , BeF ₂ , LiF·2ThF ₄ , liquid
15	83	2	497	Peritectic	ThF ₄ , LiF·4ThF ₄ , BeF ₂ , liquid
33.5	64	2.5	455	Peritectic	LiF·4ThF ₄ , LiF·2ThF ₄ , BeF ₂ , liquid
60.5	36.5	3	433	Peritectic	2LiF·BeF ₂ , 3LiF·ThF ₄ ss, LiF·2ThF ₄ , liquid
65.5	30.5	4	444	Peritectic	LiF, 2LiF·BeF ₂ , 3LiF·ThF ₄ ss, liquid
63	30.5	6.5	448	Peritectic	3LiF·ThF ₄ ss, 7LiF·6ThF ₄ , LiF·2ThF ₄ , liquid

analysis of $\text{BeF}_2\text{-ThF}_4$ binary mixtures (Table III). Data have been obtained for the region 10–25 mole % ThF_4 by both the extrapolation technique and by thermal analysis. The thermal analysis values are lower by as much as 20°. As mentioned above, equilibrium in the viscous region of the binary system is not attained after annealing for as long as three weeks. Consequently, non-equilibrium effects are pronounced during the cooling of a sample for thermal analysis. For this reason the liquidus values obtained by extrapolating data from thermal gradient quenching experiments in the system $\text{NaF-BeF}_2\text{-ThF}_4$ are much more reliable. Results of examinations of melts from $\text{BeF}_2\text{-ThF}_4$ thermal analysis and thermal gradient experiments showed that the eutectic invariant composition lies between 1 and 3 mole % ThF_4 , that the solidus temperature is between 525 and 530°, and that there are no intermediate compounds in the system. The most precise results for the

determination of the liquidus, eutectic temperature and composition were obtained by the extrapolation technique. A melting point of 548° was obtained for pure BeF_2 by thermal gradient quenching. This value is nearly identical with those reported by most recent investigators.^{11a,b} The existence of pure BeF_2 as a true glass (amorphous, by X-ray diffraction analysis) in samples quenched from temperatures above 548° confirms that this figure is the melting point rather than a solid state transition temperature as has been suggested.^{4b}

The System $\text{LiF-BeF}_2\text{-ThF}_4$.—A diagram of the liquidus temperatures for part of the system $\text{LiF-BeF}_2\text{-ThF}_4$ was constructed at this Laboratory several years ago from cooling curve data,¹²

(11) (a) D. M. Roy, R. Roy and E. F. Osborn, *J. Am. Ceram. Soc.*, **36**, 185 (1953); (b) M. P. Borzenkova, A. V. Novoselova, Yu. P. Simanov, V. I. Chernykh and E. I. Yarembash, *Zhur. Neorg. Khim.*, **1**, [9] 2071 (1956).

(12) C. J. Barton, L. M. Bratcher and W. R. Grimes, Oak Ridge National Laboratory, unpublished work, 1953.

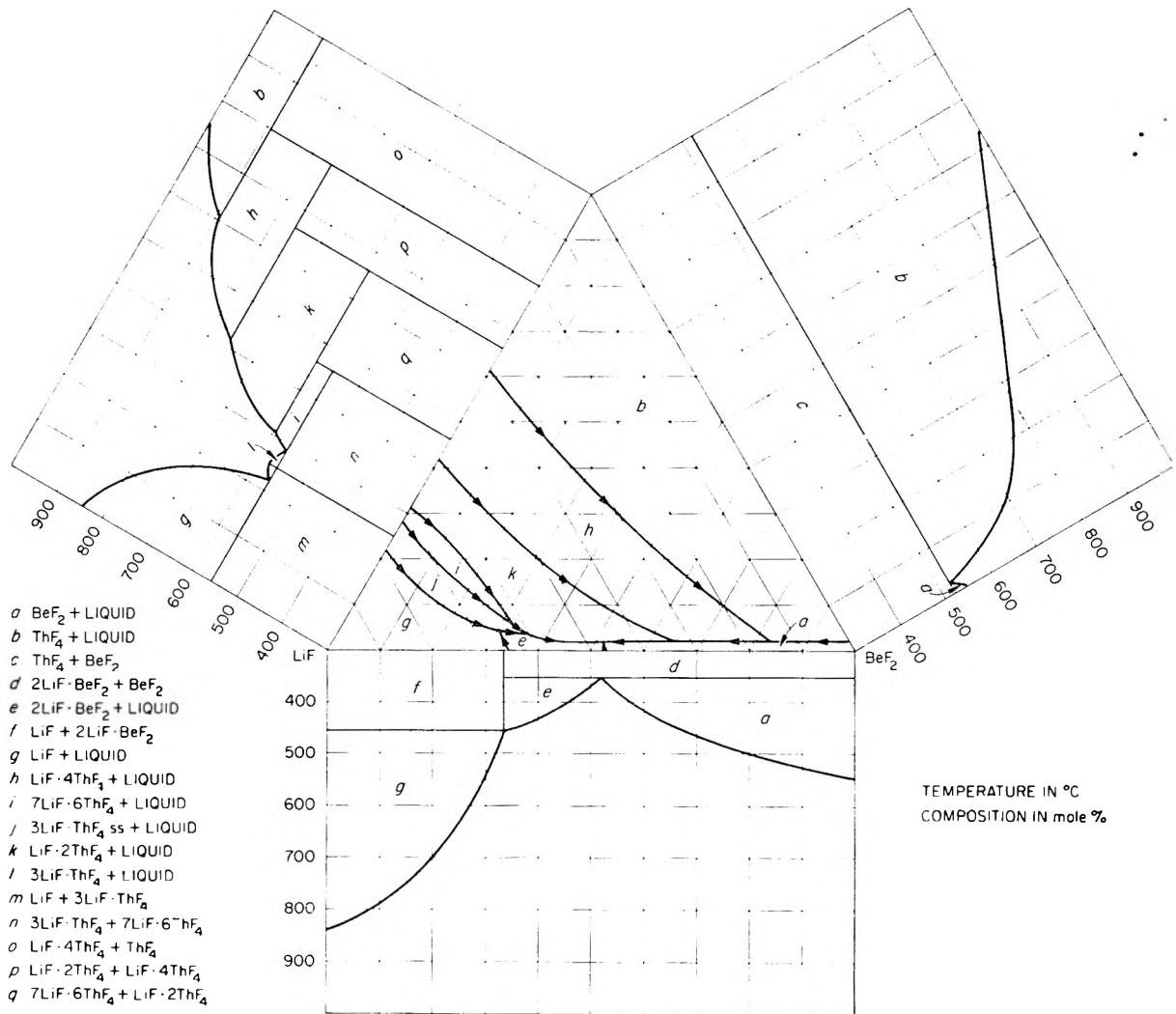


Fig. 3.—The system $\text{LiF}-\text{BeF}_2-\text{ThF}_4$.

and a preliminary phase diagram of the system has been reported by the authors.¹³ The completed polythermal phase equilibrium diagram of the system $\text{LiF}-\text{BeF}_2-\text{ThF}_4$ is shown in Figs. 2 and 3, the invariant equilibria are listed in Table IV, and results of thermal gradient quenching experiments are given in Table V. Supplementary X-ray diffraction and optical phase analysis data to those included in Table IV have been reported elsewhere.¹⁴ Thermal analysis data (Table VI) provided information principally for the construction of the liquidus surfaces in the LiF and ThF_4 apices of the system. Reliance was placed very largely on thermal gradient quenching experiments for the determination of liquidus temperatures, boundary curves and invariant points. Except at compositions higher in ThF_4 concentration than about 40 mole % and higher in LiF concentration than 80 mole %, the temperatures of the inflections in cooling curves were likely to be in error because of the presence of $3\text{LiF}\cdot\text{ThF}_4$ solid

solutions in regions of moderately high LiF concentrations, and because of sluggishness of crystallization in specimens high in BeF_2 . In quenched preparations with compositions higher in BeF_2 than approximately 45 mole %, liquids tended to quench to a glass. In preparations with BeF_2 contents less than this amount, liquids tended to quench to "quench growths," that is, extremely fine-grained aggregates of dendritic or fibrous crystals with glass, which had begun to form during the quenching act. Such "quench growths" could be distinguished easily from equilibrium crystallizations with the polarizing microscope but the distinction could be made with difficulty, if at all, in the X-ray diffraction patterns. In areas where the $3\text{LiF}\cdot\text{ThF}_4$ solid solution was a predominant phase, equilibrium was difficult to attain, and to define the area of a single solid phase it was necessary to hold the samples at the equilibration temperature for as much as three weeks.

In association with primary phase fields of the three components and five binary compounds there occur six ternary invariant points within the system $\text{LiF}-\text{BeF}_2-\text{ThF}_4$. Of these, only one invariant point is a eutectic. Within the tempera-

(13) R. E. Thoma, editor, "Phase Diagrams of Nuclear Reactor Materials," ORNL-2548, Nov. 2, 1959, p. 80.

(14) R. E. Thoma, Oak Ridge National Laboratory Central Files Memoranda Nos. CF-57-2-42, Feb. 5, 1957, CF-58-2-59, Feb. 18, 1958, CF-58-11-40, Nov. 14, 1958 and CF-59-10-18, Oct. 7, 1959.

ture range of the study, that is from the liquidus to approximately 300° , no ternary compounds were observed. Studies of the solid state relationships extended only to temperatures of about 50° below the solidus; consequently the ternary solid state relationships of the compound $\text{LiF}\cdot\text{BeF}_2$, which appears only at sub-solidus temperatures in the binary system, were not defined. Crystal structures have been reported of all the equilibrium compounds in the three limiting binary systems.^{15a-c}

A solid solution region of $3\text{LiF}\cdot\text{ThF}_4$ is of interest because within a roughly triangular area very nearly single phase material occurs at sub-solidus temperatures with crystallographic and optical properties closely related to those of $3\text{LiF}\cdot\text{ThF}_4$. This area is bounded approximately by the compositions (expressed in mole %) 75 LiF , 25 ThF_4 -58 LiF , 16 BeF_2 , 26 ThF_4 -59 LiF , 20 BeF_2 , 21 ThF_4 . The ordinary index of refraction is raised by solid solution from 1.488 for the pure compound to an observed maximum of 1.496 for that with the dissolved material. Besides the increase in refractive indices the presence of solid solution causes a reduction in the unit cell parameters of $3\text{LiF}\cdot\text{ThF}_4$. Both tetragonal unit cell parameters are reduced equally by approximately 0.003 Å./mole % BeF_2 substituted in $3\text{LiF}\cdot\text{ThF}_4$. The roughly triangular area of homogeneous single phase solid solution immediately below the solidus in the ternary system at first suggests that $3\text{LiF}\cdot\text{ThF}_4$ simultaneously dissolves both BeF_2 and ThF_4 of a gradient concentration ratio. T. Fjørland¹⁶ has suggested that two substitution models may provide an explanation for the single phase solid-solid solution area in the system $\text{LiF-BeF}_2\text{-ThF}_4$: (1) a substitution of one Be^{++} ion for a Li^+ ion with the formation of a Th^{+4} vacancy for every four Be^{++} ions substituted for Li^+ ions to provide electroneutrality and (2) substitution of a single Be^{++} ion for a Li^+ ion with the simultaneous formation of a Li^+ vacancy. Model (1) would afford a solid solution limit in good agreement with the leg of the triangular area with the lesser ThF_4 content whereas model (2) would give a line extending from 75 LiF -25 ThF_4 (mole %) toward 60 BeF_2 -40 ThF_4 (mole %). This is a limiting line which has considerably higher ThF_4 content than that found experimentally. Accordingly, it appears that $3\text{LiF}\cdot\text{ThF}_4$ solid solutions are constituted of $3\text{LiF}\cdot\text{ThF}_4$ in which BeF_2 has simultaneously substituted for Li^+ ions as described by the two models proposed by Fjørland.

As previously noted, samples of compositions in the solid solution composition triangle can be quenched to single phase $3\text{LiF}\cdot\text{ThF}_4$ ss. Minor variations in the unit cell parameters of $3\text{LiF}\cdot\text{ThF}_4$ ss produced from samples quenched to this single

phase indicate that further reduction of the unit cell parameters occurs with the formation of Li^+ vacancies. In these samples unit cell reductions are greater along the high ThF_4 leg of the $3\text{LiF}\cdot\text{ThF}_4$ solid solution composition triangle than those along the lower leg. The existence of this area of single phase solid makes necessary four sub-solidus two-phase regions. Three such regions have been observed, the region containing $7\text{LiF}\cdot 6\text{ThF}_4$ and $3\text{LiF}\cdot\text{ThF}_4$ ss, the region containing $\text{LiF}\cdot 2\text{ThF}_4$ and solid solution, and the region containing $2\text{LiF}\cdot\text{BeF}_2$ and solid solution. The fourth region, that of LiF and $3\text{LiF}\cdot\text{ThF}_4$ ss, is so small that it has escaped detection. The occurrence of this solid solution also accounts for the fact that $7\text{LiF}\cdot 6\text{ThF}_4$ disappears in a peritectic reaction which does not involve a binary phase of LiF and BeF_2 .

Single phase regions of homogeneous ternary solid solutions are not unknown in fluoride salt systems. These exist, however, as the result of interaction of two solid solutions formed along joins of one compound with two different compounds. This case is unique in salt systems because no compounds are known which could provide the solid solutions with $3\text{LiF}\cdot\text{ThF}_4$. Comparable solutions have been reported in the oxide systems $\text{PbO-B}_2\text{O}_3\text{-SiO}_2$,¹⁷ $\text{CaO-B}_2\text{O}_3\text{-SiO}_2$,¹⁸ and $\text{CaO-SnO}_2\text{-TiO}_2$.¹⁹ Many $3\text{MF}\cdot\text{XF}_4$ compounds (where M is an alkali metal ion and X is Zr, Hf, Th or U) form tetragonal crystals where the coordination number of the heavy metal cation is probably the same as that of Th in $3\text{LiF}\cdot\text{ThF}_4$. It would be expected that future studies will show that Be^{++} substitutions will occur in these 3:1 compounds as in $3\text{LiF}\cdot\text{ThF}_4$. Preliminary investigations of the system $\text{NaF-BeF}_2\text{-ZrF}_4$ suggest that this kind of substitution occurs in the tetragonal²⁰ compound $3\text{NaF}\cdot\text{ZrF}_4$.

Thermal effects on cooling $\text{LiF-BeF}_2\text{-ThF}_4$ mixtures containing 0 to 45 mole % LiF and more than approximately 5 mole % BeF_2 indicate that BeF_2 reacts slowly in these mixtures. The thermal effect associated with the apparent liquidus, on the first cooling cycle, often occurred at an unrealistically high temperature. Second heats using the same charge material generally produced a liquidus break somewhat lower than occurred during the first cooling. These and undercooling effects made these data unreliable for definition of the isotherms. Accordingly, isotherms in this composition region were derived from the results of thermal gradient quenching experiments and measurements of liquid-solid transitions in and near the limiting binary systems. Erratic thermal effects were noted in approximately the same LiF and BeF_2 compositions in the investigation of the phase equilibria in the system $\text{LiF-BeF}_2\text{-UF}_4$.^{4b}

No systematic study of the structures in $\text{LiF-BeF}_2\text{-ThF}_4$ liquids has been made, except to ensure that no two liquid region exists in the low melting

(15) (a) K. Spangenberg, *Z. Krist.*, **57**, 494 (1923); (b) W. H. Zachariassen (1947b) Manhattan District Declassified Documents, 1552; (c) V. M. Goldschmidt, "Geochemische Verteilungsgesetze der Elemente: VIII, Untersuchungen über Bau und Eigenschaften von Kristallen," *Skrifter Norske Videnskaps-Akad. Oslo, I. Mat. Naturv. Klasse*, 1926, No. 8, pp. 7-156 (1927); (d) Erich Thilo and H. A. Lehmann, *Z. anorg. Chem.*, **258**, [3-5] 332 (1949); (e) L. A. Harris, G. D. White and R. E. Thoma, *THIS JOURNAL*, **63**, 1974 (1959).

(16) Tormod Fjørland, Norwegian Institute of Technology, Trondheim, Norway, personal communication.

(17) R. F. Geller and E. N. Bunting, *J. Research Natl. Bur. Standards*, **23** [8], 279 (1939), RP 1231.

(18) F. P. Flint and L. S. Wells, *ibid.*, **17** [5], 745 (1936) RP 941.

(19) L. W. Coughanour, R. S. Roth and S. Marzullo, *ibid.*, **54** [3], 155 (1955) RP 2576.

(20) L. A. Harris, *Acta Cryst.*, **12**, 179 (1959).

temperature-composition regions. The sharp change of slope of the ThF_4 liquidus in the system $\text{BeF}_2\text{-ThF}_4$ at compositions approaching that of the eutectic occurs similarly in the primary phase fields of both $\text{LiF}\cdot 4\text{ThF}_4$ and $\text{LiF}\cdot 2\text{ThF}_4$ for compositions in those primary phase fields near the $\text{LiF}\text{-BeF}_2$ limiting system.

The notable features of the systems $\text{BeF}_2\text{-ThF}_4$ and $\text{LiF}\text{-BeF}_2\text{-ThF}_4$ are (1) the large primary phase field of ThF_4 , (2) the proximity of the eutectic to BeF_2 in the case of $\text{BeF}_2\text{-ThF}_4$ and of the low temperature even reaction boundary curves to the $\text{LiF}\text{-BeF}_2$ border of the diagram in the case of

$\text{LiF}\text{-BeF}_2\text{-ThF}_4$. The large primary phase field is undoubtedly the result of the relatively high melting point of ThF_4 as compared with that of BeF_2 , and the proximity of the low temperature boundary curves to the $\text{LiF}\text{-BeF}_2$ border is part of the same result.

Acknowledgments.—It is a pleasure to acknowledge the assistance of T. N. McVay who assisted in some of the phase identification by optical microscopy. We are also grateful to W. R. Grimes for his support and encouragement, and to T. Førlund and J. E. Ricci for their advice concerning several aspects of the phase studies.

A SPECTROPHOTOMETRIC STUDY OF THE COMPLEXES FORMED BETWEEN URANYL AND CHLORIDE IONS IN WATER AND WATER-ETHANOL SOLVENTS

BY JACK D. HEFLEY AND EDWARD S. AMIS

Chemistry Department of the University of Arkansas, Fayetteville, Arkansas

Received December 28, 1959

Using the method of continuous variations at 25° , the complex ion UO_2Cl^+ was proved to exist in dilute aqueous solutions. In more concentrated aqueous solutions, 0.237 to 1.58 *M* in uranyl ion, the complexes UO_2Cl^+ , UO_2Cl_2 and UO_2Cl_3^- were found. With 30 and 60 volume % ethanol in the solvent, the complex ion UO_2Cl^+ exists. All these complexes were found using a tungsten lamp on the Beckman DU spectrophotometer. In 90 volume % ethanol using a hydrogen discharge lamp on the Beckman DU spectrophotometer and a wave length of 288 $\text{m}\mu$ the existence of the UO_2Cl^+ ion was proved. The equilibrium constant for the dissociation of the complex ion UO_2Cl^+ in water and in 30, 60 and 90 volume % ethanol was found to be 2.28×10^{-2} , 1.65×10^{-1} , 5.10×10^{-1} and 1.47×10^{-3} , respectively.

Introduction

Several investigators¹⁻⁴ have reported uranyl complexes of the type UO_2X^+ , where X is an anionic complexing group. Mathews, Hefley and Amis⁵ explained the orders with respect to U(IV) and U(VI) found in the U(IV)-U(VI) electron exchange reaction in water, ethanol and water-ethanol solvents by postulating the existence of the UO_2OH^+ and UOH^{+++} ions. Mathews, Wear and Amis⁶ have explained transference number data on uranyl chloride by assuming the existence of UO_2Cl^+ and UO_2Cl_3^- ions.

Since the uranyl ion-chloride ion complexes mentioned above were strongly indicated by the transference number data on uranyl chloride, it seemed desirable to confirm their existence.

A spectrophotometric approach using the method of continuous variations discussed by Vosburgh and Cooper⁷ was selected for the study. This method is more generally applicable when more than one complex is formed in solution.

The dissociation constant for the UO_2Cl^+ ion was found by the procedure of Foley and Anderson.¹

(1) R. T. Foley and R. C. Anderson, *J. Am. Chem. Soc.*, **71**, 909 (1949).

(2) C. F. Baes, Jr., *This Journal*, **60**, 878 (1956).

(3) F. Nelson and K. A. Kraus, *J. Am. Chem. Soc.*, **73**, 2157 (1951).

(4) J. Sutton, *J. Chem. Soc.*, S275 (1949).

(5) D. M. Mathews, J. D. Hefley and E. S. Amis, *This Journal*, **63**, 1236 (1959).

(6) D. M. Mathews, J. O. Wear and E. S. Amis, *J. Inorg. Nuclear Chem.*, in press.

(7) Vosburgh and Cooper, *J. Am. Chem. Soc.*, **63**, 437 (1941).

Experimental

Wave lengths which gave maxima in absorption values were determined with a Beckman Model DK-1 Recording Spectrophotometer using a tungsten or hydrogen lamp as required and quartz cells of 10.00 ± 0.01 mm. light path. Absorption values were measured with a Beckman DU quartz spectrophotometer using a tungsten or hydrogen lamp as required and quartz cells of 10.00 ± 0.01 mm. light path.

A Beckman Model G pH meter was used to measure the pH of the water solutions.

The uranium trioxide obtained from Mackay Chemical Company analyzed 99.8% pure. Uranyl perchlorate was prepared from the trioxide by treating with perchloric acid (Baker Analytical Reagent) with the method described by Sutton.⁴ The concentrations of the uranyl perchlorate solutions were determined by a procedure similar to that given by Hefley, Mathews and Amis⁵ for uranyl chloride. A measured volume of $\text{UO}_2(\text{ClO}_4)_2$ solution was evaporated, and the $\text{UO}_2(\text{ClO}_4)_2$ dried and burned to U_3O_8 which was weighed. The heating of the $\text{UO}_2(\text{ClO}_4)_2$ can be safely done.

The NaCl and NaClO_4 were Mallinckrodt Analytical Reagents which were dried and used without further purification. The sodium perchlorate was used to adjust the ionic strength of the solutions to a constant value.

Solutions were prepared with distilled water at 25° . The equilibrium constants for the dissociation of $[\text{UO}_2\text{Cl}]^+$ in dilute aqueous and alcohol solutions were determined by the method described by Foley and Anderson.¹

The detailed procedure in the determination of the empirical formulas of the complexes was as follows. A series of solutions was prepared in which the concentrations of the uranyl and chloride ion were varied but the sum of the concentrations was constant. The acid concentration and the ionic strength in each sample was constant.

(8) J. D. Hefley, D. M. Mathews and E. S. Amis, *J. Inorg. Nuclear Chem.*, **12**, 84 (1959).

The blank used for each sample contained uranyl perchlorate of the same concentration as in the sample. In alcohol containing solvents, the blank contained the same amount of alcohol as the sample. Perchlorate ions were found by Sutton⁴ not to form complexes with uranyl ion.

Optical densities of the various solutions were first measured at various wave lengths with a Beckman DK-1 recording spectrophotometer and in this way the wave lengths of maximum optical densities corresponding to the various complexes were determined.

Then careful continuous variation measurements were made at these wave lengths with the more accurate Beckman DU spectrophotometer.

The equilibrium constants were determined making use of the Beckman DU spectrophotometer for measuring the optical densities of the sample containing the uranyl and chloride ions in a 1:1 ratio diluted at constant ionic strength with a solution of NaClO₄.

The accuracy of the absorption values was found to be ±0.2% by using the same volumetric delivery and dilution techniques as in the experimental runs on a solution of potassium chromate as described by the National Bureau of Standards.⁹ The precision was found to be ±0.2% by repeating the preparation and also by repeated measurements on the same sample.

Data and Discussion

The results of the spectrophotometric investigations of the uranyl ion-chloride ion complexes are represented in graphical form in which the optical density is plotted against the mole fraction of chloride ion in the complexing components.

In dilute aqueous solution, 0.0200 to 0.1800 M, maxima were observed to occur at 424, 450 and 466 mμ as is shown in Fig. 1. At each of these wave lengths a 1:1 ratio of complexing components, corresponding to an empirical formula UO₂Cl⁺, exist at the maxima of the curves.

When the same measurements were made on more concentrated aqueous solutions, 0.237 to 1.58 M, four maxima and one minimum corresponding to three complexes were obtained as shown in Fig. 2. The maxima and minima at X = 0.5, 0.67 and 0.75 in Figs. 1 and 2 indicate the existence of three complexes, UO₂Cl⁺, UO₂Cl₂ and UO₂Cl₃⁻, respectively.

In 30 and 60 volume % ethanol runs, the maxima at 424, 450 and 466 mμ occur at 1:1 ratio of complexing components corresponding to an empirical formula of UO₂Cl⁺.

In the 90 volume % ethanol no maximum was found in the visible region of the spectrum, however a maximum was found in the ultraviolet at a wave length of 288 mμ. At the maximum the ratio of complexing components was 1:1 and the empirical formula of the complex was UO₂Cl⁺.

In Table I are given the data at 25° on the equilibrium constant and the free energy for the dissociation of the UO₂Cl⁺ complex in the various solvents. The small equilibrium constants and the resulting positive free energy of dissociation show that the UO₂Cl⁺ complex is dissociated only to a small extent and that the complex is stable. The data in this table also give an idea of the drastic effect of solvent on the equilibrium. The free energy was calculated using the equation

$$\Delta F^{\circ} = -RT \ln K \quad (1)$$

Mathews, Hefley and Amis found a similar de-

(9) Letter circular LC929 from the U. S. Dept. of Comm., National Bureau of Standards, Wash., D. C., Nov. 26, 1948.

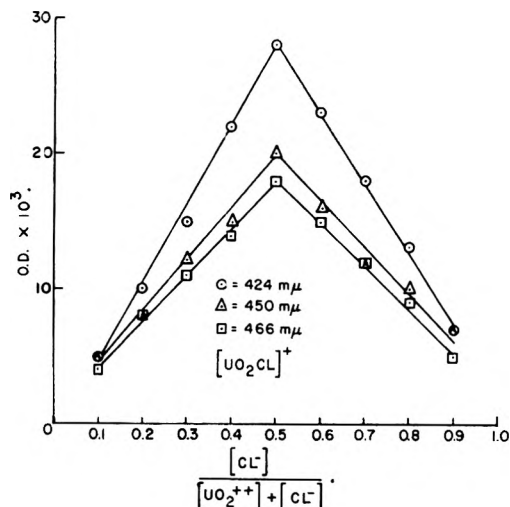


Fig. 1.—Ionic species in dilute solutions.

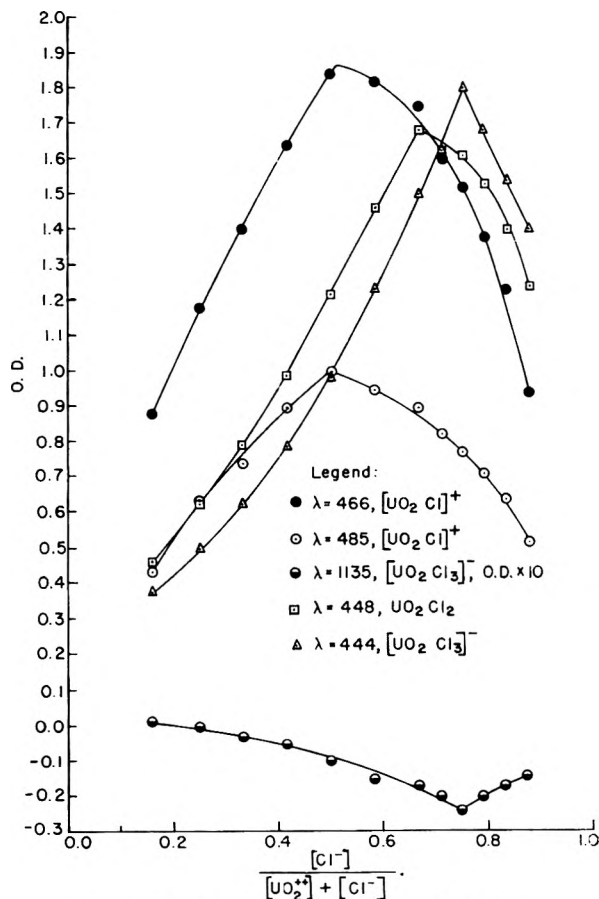


Fig. 2.—Ionic species in concentrated solution.

pendence of the logarithm of the specific velocity constant on the mole per cent. ethanol in the solvent for the electron exchange reaction between the U(IV) and U(VI) ions as is found here for the logarithm of the equilibrium constant as a function of the mole per cent. ethanol. The maxima in the two curves fall at almost the same volume per cents. of ethanol in the solvent. These authors assumed the existence of UO₂OH⁺ and UOH⁺³ ions to explain the orders of the reaction with respect to U(IV), U(VI) and H₃O⁺ ions. If we can extrapolate

the data on the UO_2Cl^+ complex to the UO_2OH^+ ion in the kinetic situation, it would appear that the effect of the solvent on the stability of the UO_2X^+ ion is a principal factor in the influence of the solvent on the rate of the electron exchange reaction between U(IV) and U(VI) ions.

The data for the equilibrium constants were neither as precise nor as accurate as those for the empirical formulas as is illustrated for 60 volume % ethanol solvent in Table II. The values of the constants given in Table I are average values for all the wave lengths used in the case of a particular solvent.

TABLE I

EQUILIBRIUM CONSTANTS AND FREE ENERGY OF DISSOCIATION AT 25° OF THE UO_2Cl^+ COMPLEX IN VARIOUS SOLVENTS

Vol. % ethanol	pH	HClO_4 , M^a	Ionic strength	$K \times 10^{-1}$	ΔF° , cal./mole
0	0.50		1.238	22.8	2240
30		0.1411	1.238	165	1070
60		.1411	1.238	510	400
90		.0088	0.078	1.47	3880

^a In alcohol containing solvents the molarity of the acid rather than the pH of the solution is given.

TABLE II

EQUILIBRIUM DATA FOR THE UO_2Cl^+ COMPLEX IN 60 VOLUME % ETHANOL SOLVENT

λ	a_1	b_1	a_2	b_2	$K \times 10^{-1}$
424	0.040	0.040	0.0085	0.1915	5.36
450	.040	.040	.0085	.1915	5.36
466	.040	.040	.0087	.1915	4.57

Av. 5.10

The lack of relatively high accuracy and precision in the case of the equilibrium data arose perhaps from the fact that dilutions of the solutions had to be made and optical densities read from graphs prepared originally for obtaining empirical formulas of the UO_2Cl^+ complex.

The data for the UO_2Cl^+ and UO_2Cl_3^- complexes substantiate the assumption of their existence made by Mathews, Wear and Amis⁶ based on transference data.

Acknowledgment.—The authors are indebted to the United States Atomic Energy Commission for a grant under Contract AT-(40-1)-2069, which made this research possible. J.D.H. is also indebted to the National Science Foundation for a Cooperative Fellowship which gave him financial support.

SELF-DIFFUSION IN MOLTEN NITRATES¹

BY A. S. DWORKIN, R. B. ESCUE AND E. R. VAN ARTSDALEN

Contribution from the Chemistry Division, Oak Ridge National Laboratory, Oak Ridge, Tennessee

Received January 2, 1960

The self-diffusion coefficients D for the ions in molten LiNO_3 , NaNO_3 , KNO_3 , CsNO_3 , and AgNO_3 have been measured as a function of temperature by the capillary method. The results are expressed in the form of the equation $D = A \exp(-\Delta H^\ddagger/RT)$. The values for the energy of activation for diffusion, ΔH^\ddagger , for the cation and anion, respectively, in kcal. are: LiNO_3 , 5.49 and 6.34; NaNO_3 , 4.97 and 5.08; KNO_3 , 5.53 and 5.76; CsNO_3 , 5.61 and 6.28; and AgNO_3 , 3.73 and 3.84. The values for the diffusion coefficients, ($D \times 10^5$), for the cation and anion, respectively, in $\text{cm}^2 \text{sec}^{-1}$ at 350° are: LiNO_3 , (2.93) and (1.15); NaNO_3 , 2.33 and 1.48; KNO_3 , 1.52 and 1.35; CsNO_3 , (1.22) and (1.11); and AgNO_3 , (2.40) and (1.40). The results indicate that the diffusion coefficients of the cation vary inversely with ion size. The Nernst-Einstein relationship is shown not to hold for molten nitrates. Values for phenomenological friction coefficients as proposed by Laity are all positive and all but those for LiNO_3 are of the same order of magnitude. The friction coefficients for the relative motion of anion and cation and for cation and cation increase with increasing cation size while those for anion-anion motion decrease with increasing cation size.

As part of our program to elucidate the mechanism of transport in molten salts, we have measured the self-diffusion coefficients of the individual ions in molten LiNO_3 , NaNO_3 , KNO_3 , CsNO_3 and AgNO_3 as a function of temperature. The method employed involved a determination of the rate at which a tracer ion diffused from a capillary tube into a stirred bath of pure untagged nitrate. The method was originally used by Anderson and Saddington² in aqueous solution and has since been employed by many others.^{3,4} We have reported previously the results of our measurements in NaNO_3 .⁵ The only other published work on self-diffusion in

molten salts appears to be that of measurements in TlCl ,⁶ NaCl ⁷ and ZnBr_2 ,⁸ and only for NaCl are data available for both cation and anion diffusion.

The nitrates were chosen for study because their relatively low melting temperatures made it experimentally feasible to study the self-diffusion in a group of compounds thereby permitting one to note the effect of change in cation size and mass on the diffusion process. The nitrates also lend themselves to the use of a combination of readily available stable and radioactive isotopes as tracers, enabling one to follow both the cation and anion diffusion in one experiment.

The equation used to calculate the self-diffusion coefficient D of a tracer in a pure salt

$$\ln \frac{\pi^2}{8} \left[\frac{C_{\text{ave}}}{C_0} \right] = - \frac{\pi^2 D t}{4l^2} \quad (1)$$

(1) Work performed for the U. S. Atomic Energy Commission at the Oak Ridge National Laboratory, operated by the Union Carbide Corporation, Oak Ridge, Tennessee.

(2) J. S. Anderson and K. Saddington, *J. Chem. Soc.*, S381 (1949).

(3) J. H. Wang and J. W. Kennedy, *J. Am. Chem. Soc.*, **72**, 2080 (1950); J. H. Wang, *ibid.*, **74**, 1182 (1952).

(4) R. Mills, *ibid.*, **77**, 6116 (1955), and previous papers.

(5) E. R. Van Artsdalen, D. Brown, A. S. Dworkin and F. J. Miller, *ibid.*, **78**, 1772 (1956).

(6) E. Berne and A. Klemm, *Z. Naturforsch.*, **8A**, 400 (1953).

(7) A. Z. Bornicka, J. O'M. Bockris and J. A. Kitchener, *Proc. Roy. Soc. (London)*, **A241**, 554 (1957).

(8) L. Wallin and A. Lunden, *Z. Naturforsch.*, **14A**, 262 (1959).

has been derived⁹ from a solution of Fick's law of diffusion of a tracer from a uniform tube of length l , closed at one end, into a bath containing zero concentration of tracer. C_0 is the initial concentration of tracer in the tube and C_{ave} is the average concentration of tracer in the tube after time t . This simplified form of the equation is good to better than 0.2% under the conditions of our experiment.

Experimental

Apparatus.—The capillary tubes which contained the tagged salt were of transparent fused silica and were specially selected for uniformity of bore. They ranged in length from 3–5 cm. (measured on a micrometer stage to ± 0.02 mm.) and had an external diameter of about 5 mm. with an internal diameter of less than 0.7 mm. They were closed at one end with a flat seal. The extremely small bore tubes made the filling operation more difficult. Nevertheless, it was considered desirable to use them in order to eliminate uncertainties due to convection which would have been encountered with larger bore tubes.

The capillaries were filled in the apparatus shown in Fig. 1 in the following manner. Molten salt from the reservoir G was drawn into the filling tube E by means of a screw syringe. The filling tube then was maneuvered into the silica capillary D. The salt was forced into the capillary, filling it from the bottom as the filling tube was raised, thereby preventing the trapping of gas bubbles. Some insulation around the Pyrex tube A was necessary to attain the somewhat higher temperature necessary for the $CsNO_3$ experiment, but not enough to obscure the view of the filling operation. Pyrex capillary holders were used in many of the experiments as well as the platinum capillary holder, C. It was possible to fill as many as three capillaries to be used concurrently in the same bath. When the salts used were more dense than fused silica, the capillaries were secured in the holder to prevent their floating to the surface of the bath.

The diffusion experiments were carried out in a 3.5 in. bore Marshall tube furnace 16 in. long, having ten external taps for the attachment of shunt resistors to reduce the temperature gradient. A heavy-walled Inconel liner was placed in the furnace and an aluminum shield was used as a cover. The furnace was controlled by a chromel–alumel thermocouple which operated a Leeds and Northrup recorder-controller in conjunction with a Leeds and Northrup "DAT" controller. The temperature of the salt bath remained constant to $\pm 0.3^\circ$ during the course of the diffusion period. The baths, made up of from 400 to 800 g. of salt, were contained in either Pyrex tubes or platinum crucibles depending upon which salt was being measured. The baths were stirred with Pyrex or silica spiral stirrers powered by 100 r.p.m. constant speed motors. The temperature of the bath was measured with a platinum, 90% platinum–10% rhodium thermocouple by means of a Rubicon precision potentiometer. The thermocouple was placed in a silica tube which in turn was inserted in the salt bath close to the diffusion capillaries.

Materials.—The nitrates used were reagent grade materials which were dried in an oven at 120° . They were heated slowly *in situ* under dry argon to the temperatures at which the measurements were made. The radioactive and stable isotopes used as tracers were obtained from the Oak Ridge National Laboratory. The radioactive isotopes used were Na^{22} , Cs^{134} and Ag^{110} . The stable isotopes were Li^6 , K^{41} , N^{15} and O^{18} .

Experimental Procedure.—The capillaries were filled with tagged salt in the manner described above. The molten salt was allowed to overflow slightly and cover the top of the capillary tube to allow for contraction during the transfer operation. The capillaries were transferred from the filling apparatus to the furnace containing the untagged salt bath without allowing the salt to freeze. This prevented the formation of gas bubbles in the capillary. The capillaries were partially submerged in the salt-bath until temperature equilibrium was reached at which time they were completely submerged and the diffusion period was begun.

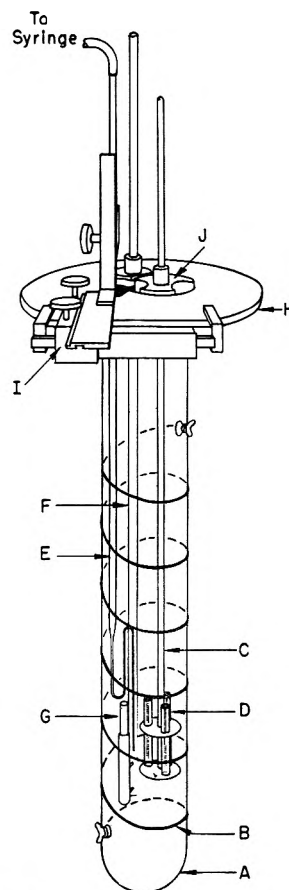


Fig. 1.—Capillary filling device: A, Pyrex tube; B, nichrome heating ribbon; C, platinum capillary holder; D, silica capillaries; E, silica filling tube drawn to fine capillary at end; F, Pyrex tube-cup holder and thermocouple tube; G, platinum cup-salt reservoir; H, aluminum top; I, tridimensional control for filling tube; J, three-position plug for capillary holder.

When sufficient time was allowed for about 60–70% of the tracer to diffuse out of the capillary (about two to five days), the diffusion period was ended by removing the capillaries from the bath. The capillaries then were cleaned on the outside and dried. If they contained radioactive tracer, they were weighed and then placed in a 4π high pressure ion chamber and counted. The activities were obtained in terms of a reading on a Brown chart. Since a ratio was all that was required, (C_{ave}/C_t in eq. 1) no conversion to actual counts was made. When the capillaries contained stable isotope tracers, the salt was washed into a small beaker by a stream of distilled water from a fine silica capillary, transferred to the silica tubes in which the analysis was to be made, and evaporated to dryness. The salt then was analyzed for isotopic abundance with a G.E. mass spectrometer.

The initial isotopic concentration of the salt could not be measured during an actual diffusion run, thereby necessitating separate calibration determinations. These were made in the same manner as were the diffusion runs except that the capillaries were held under the surface of the salt-bath only momentarily. By determining C_0 in this manner, any errors incurred by the entry of the capillaries into and their removal from the bath should be cancelled. When stable isotopes were employed, the concentration of isotope in the "normal" salt bath, C_N , as well as the initial concentration of isotope in the capillary was obtained. It was necessary to subtract C_N from both the numerator and denominator in the term (C_{ave}/C_0) in equation 1 to account for back diffusion of the stable isotope from the normal bath into the capillary. Ten to fifteen calibration runs were made for each salt which gave values for C_0 good to ± 0.5 –1.0%.

(9) A. C. Wahl and N. A. Bonnar, "Radioactivity Applied to Chemistry," John Wiley and Sons, Inc., New York, N. Y., 77, 1951, p. 507.

Results

The effect of a number of variables on the self-diffusion coefficient D was studied during the course of the measurements in NaNO_3 . It was found that D did not change, within experimental error, with a change in the length of capillaries (from 3–5 cm.) or duration of the diffusion period (from 2–4 days). This indicated that the stirring rate was sufficient to prevent accumulation of tracer at the mouth of the capillary but slow enough to prevent an appreciable amount of liquid from being dragged out of the capillary due to stirring. The rate was somewhat lower than that used by Klemm.⁶ It was approximately the same as that discussed by Mills⁴ and found to be satisfactory within the experimental error of our measurements. Borucka, Bockris, and Kitchener⁷ used a much slower rate and also applied a correction for the stirring effect. Their larger bore and rather short capillaries may have led to the more serious stirring problem which they encountered. A series of twenty diffusion runs made with larger bore silica capillaries (approximately 1 mm. bore) led to values of D for Na^+ NaNO_3 approximately 3% higher than those obtained from forty runs made with the smaller bore capillaries. A very definite loss in precision was also noted. This certainly can be ascribed to a greater influence of convection currents with larger-bore capillaries in which case the stirring rate has greater effect than with the smaller bore capillaries.

NaNO_3 was the only salt for which a separate series of runs was made for the cation and anion. O^{18} was used initially to follow the nitrate diffusion. However, it was shown that the self-diffusion coefficients of the nitrate ion as determined with N^{15} as the tracer agreed very well with those determined using O^{18} (Table I). Since N^{15} could be obtained at a much higher enrichment than O^{18} and could be incorporated in the salts more easily, it was used in all subsequent measurements.

The self-diffusion coefficients D may be expressed by an equation of the form

$$D = A \exp(-\Delta H^\ddagger/RT) \quad (2)$$

where A is a constant, ΔH^\ddagger is a temperature coefficient factor generally considered to represent the energy of activation for the diffusion, R is the molar gas constant, and T is absolute temperature. The parameters of this equation for the ions in the five nitrates measured, as derived by the method of least squares, are given in Table II. Table II also includes the applicable temperature ranges for each equation (60–70° above the melting points of the salts) and the probable errors in D and ΔH^\ddagger . The experimental values of D are given in Table I.

TABLE I

SELF-DIFFUSION COEFFICIENTS FOR MOLTEN NITRATES

t , °C.	$D \times 10^5$, cm. ² sec. ⁻¹	t , °C.	$D \times 10^5$, cm. ² sec. ⁻¹	t , °C.	$D \times 10^5$, cm. ² sec. ⁻¹
Li^+ in LiNO_3		Na^+ in NaNO_3	(cont'd.)	NO_3^- in NaNO_3^a	
264.0	1.46	324.6	1.97	332.5	1.30
	1.43		1.98		1.33
271.3	1.59	330.0	2.04	343.4	1.40
	1.53	334.6	2.16		1.43
279.0	1.66		2.10	364.3	1.67

	1.66		2.13		
288.5	1.72	344.8	2.18	K^+ in KNO_3	
	1.78		2.16		
296.3	1.92		2.26	344.8	1.51
	1.93	349.1	2.32		1.51
309.7	2.16		2.30		1.44
	2.16		2.22	345.5	1.49
320.5	2.39		2.38		1.48
		357.6	2.46	352.9	1.53
NO_3^- in LiNO_3^a			2.43		1.54
			2.42	359.0	1.57
264.0	0.510	360.0	2.52		1.67
	.52		2.54	363.3	1.66
271.3	.60	368.4	2.65		1.66
	.53		2.66	367.3	1.70
279.0	.59		2.60		1.74
	.60		2.61	368.7	1.71
288.5	.60		2.70		1.70
	.65	375.3	2.60	375.0	1.78
296.3	.70		2.76		1.75
	.72		2.70	381.2	1.88
309.7	.81	375.8	2.70		1.90
	.82		2.75	389.0	2.06
320.5	.94		2.64		2.01
Na^+ in NaNO_3		NO_3^- in NaNO_3^b		NO_3^- in KNO_3^a	
313.5	1.79	320.6	1.21	345.5	1.33
	1.77		1.21		1.29
314.5	1.82		1.25	352.9	1.32
	1.73		1.21		1.35
315.5	1.93	328.7	1.27	359.0	1.53
	1.83		1.27		1.49
	1.81		1.27	367.3	1.54
	1.85	350.9	1.48		1.49
320.5	1.91		1.49	375.0	1.61
	1.97		1.51		1.58
	1.94	359.4	1.56	389.0	1.80
			1.57		1.77
			1.59		
Cs^+ in CsNO_3			1.54		
		366.2	1.32		
428.7	2.02		1.53		
443.8	2.18	377.4	1.78		
456.5	2.40		1.80		
	2.36				
477.9	2.70	Ag^+ in AgNO_3		NO_3^- in AgNO_3^a	
	2.55	219.5	1.39	219.5	0.64
			1.37		.59
NO_3^- in CsNO_3^a		233.0	1.19	233.0	.62
			1.23		.73
428.7	1.90	244.0	1.30	244.0	.72
443.8	2.21	255.3	1.40	255.3	.82
456.5	2.37	274.5	1.58	274.5	.90
	2.35				.86
477.9	2.67			288.5	1.08
	2.54				1.08

^a N^{15} used as tracer. ^b O^{18} used as tracer.

The probable error in D as derived from the deviations from the calculated least squares $\log D$ vs. $1/T$ lines is in general about $\pm 1.5\%$. The uncertainty in ΔH^\ddagger (the slope of the lines) is in general $\pm 2-4\%$ although it is somewhat higher for the ions in CsNO_3 and the nitrate in AgNO_3 .

Discussion

It appears that the energy of activation for diffusion, ΔH^\ddagger , for each of the ions measured is tem-

TABLE II
SELF-DIFFUSION COEFFICIENT EQUATIONS FOR MOLTEN
NITRATES

$$D = A \exp(-\Delta H^\ddagger / RT) \text{ cm.}^2 \text{ sec.}^{-1}$$

	$A \times 10^3$	ΔH^\ddagger (cal. mole ⁻¹)	Probable error in D , %	Applicable temp. range, °C.
LiNO ₃				
Li	2.47	5490 ± 110	1.5	264-320
NO ₃	1.95	6340 ± 270	2.5	
NaNO ₃ ^a				
Na	1.29	4970 ± 80	1.5	313-376
NO ₃	0.90	5080 ± 80	1.0	
KNO ₃				
K	1.32	5530 ± 200	1.5	344-389
NO ₃	1.42	5760 ± 260	1.5	
CsNO ₃				
Cs	1.13	5610 ± 270	1.5	428-478
NO ₃	1.78	6280 ± 380	1.5	
AgNO ₃				
Ag	0.49	3730 ± 80	1.0	219-289
NO ₃	0.31	3840 ± 370	4.0	

^a Reported previously; cf. ref. 5.

perature independent over the rather short temperature range of these investigations. The energy of activation for cation and anion in each salt is approximately equal within experimental error (Table II). LiNO₃ is the exception, in which case ΔH^\ddagger for the nitrate is somewhat larger. (Although CsNO₃ appears to be an exception, it should be noted that the experimental errors involved in the CsNO₃ measurements were somewhat larger than those with the other nitrates.) It may also be noted that ΔH^\ddagger for both of the ions in AgNO₃ is significantly lower than those found for the alkali-metal nitrates.

The observation was made at the conclusion of the discussion of the NaNO₃ measurements,⁵ that the ratio of the self-diffusion coefficients of the two ions is approximately proportional to the inverse square roots of their masses. The data for the five nitrates reported in this work, however, show that the above relationship is not a general one. On the other hand, a relationship between the diffusion coefficients and ion size does appear to exist. Table III lists self-diffusion coefficients for the nitrates at 350°. To compare the results at this temperature, it was necessary to extrapolate the LiNO₃ and AgNO₃ values above the actual measured temperature range and the CsNO₃ below its melting point. The CsNO₃ values, therefore, are hypothetical and are included merely for the purpose of comparison. Since the ΔH^\ddagger values are all approximately equal, a comparison at any reasonable temperature would lead to approximately the same relative cation to anion values for each salt and the same relative cation to cation values among the alkali-metal nitrates as those shown in Table III. As can be seen from Table III, the self-diffusion coefficient of the cation is larger than that for the anion in each salt. The self-diffusion coefficient of the cation is highest for the Li⁺ in LiNO₃ and decreases with increasing cation size. The product of the cation diffusion coefficient and cation radius ($D_+ r_+$) is given for each salt in Table III. The constancy of this quantity suggests that the cation diffusion coefficients

vary inversely with the cation radius. AgNO₃ does not fit in this order. However, since ΔH^\ddagger for the ions in AgNO₃ is significantly different from that for the alkali-metal nitrates, the extrapolated diffusion coefficients in AgNO₃ at 350° are not indicative of the relative values at all temperatures. The data for the anion diffusion coefficients indicate that the D_- for the NO₃⁻ in LiNO₃ is somewhat lower than would be expected. The above considerations seem to indicate that the migration of the ions is affected more by the ion size or core repulsions than by the attractive forces which are mainly coulombic. If the latter were the most important factor, one would expect Li⁺ in LiNO₃ to have the smallest diffusion coefficient. One must be careful not to ascribe too much importance to any correlations of radius with diffusion coefficients, such as the relative constancy of $D_+ r_+$, or to any speculation which follows from such correlations. The effective radii of the ions in the melt may very well differ from the crystal radii used in the above correlations. In this connection, it may be significant to note that at 350°, the molar volume of AgNO₃ is

TABLE III
SELF-DIFFUSION COEFFICIENTS AT 350°

	$D_+ \times 10^6$, cm. ² sec. ⁻¹	$D_- \times 10^6$, cm. ² sec. ⁻¹	$D_+ r_+$ ^a
LiNO ₃	2.93 ^b	1.15 ^b	1.99
NaNO ₃	2.33	1.48	2.21
KNO ₃	1.52	1.35	2.02
CsNO ₃	1.22 ^b	1.11 ^b	2.04
AgNO ₃	2.40 ^b	1.40 ^b	3.02

^a The following ionic radii (in Å.) were used to calculate $D_+ r_+$: Li⁺, 0.68; Na⁺, 0.95; Ag⁺, 1.26; K⁺, 1.33; Cs⁺, 1.67. ^b Extrapolated.

less than that of NaNO₃ although the radius of the silver ion as given by Pauling is considerably larger than that of the sodium ion.

There has been some discussion^{7,10} concerning the applicability of the Nernst-Einstein relationship in molten salts. This relation between the equivalent conductance (Λ) of the medium and the self-diffusion coefficients of the cation and anion (D_+ and D_-) for a uni-univalent electrolyte is given by the equation

$$\Lambda = \frac{F^2}{RT} (D_+ + D_-) \quad (3)$$

where F is faraday's constant, R is the gas constant, and T is the absolute temperature. Although this relation is valid for electrolyte solutions at infinite dilution and in some cases for ionic crystals, the equivalent conductance of molten salts as calculated from equation 3 is always higher than the experimental value. Λ (calculated) is higher than Λ (exp.) for NaCl⁷ by about 40% and, for the nitrates, by about 30% for LiNO₃ to about 65% for CsNO₃. Borucka, Bockris and Kitchener⁷ apparently have assumed that the Nernst-Einstein relation is applicable in molten salts and that discrepancies are due entirely to "molecule" or "vacancy-pair" diffusion. On this basis, they have calculated self-diffusion coefficients for the ions and "molecule" in molten NaCl which agree very well with those calculated from the Stokes-Einstein relationship. Yang¹⁰ has

(10) L. Yang, *J. Chem. Phys.*, **27**, 601 (1957).

also done this using our previously published values for NaNO_3 and again obtained good agreement for the ions (although not for the molecule). When this treatment is applied to the remaining nitrates the agreement is in general poor. However, the calculations from which the three "true" self-diffusion coefficients (*i.e.*, cation, anion and molecule) are derived are based on a fallacy. As Laity¹¹ has pointed out, "... in the calculations from the conductance and self-diffusion data no account has been taken of the relative concentrations of ions and molecules, a factor which has a controlling effect on the values calculated for the three 'true' self-diffusion coefficients." In light of the above, the apparent corroboration of the hypothesis of Borucka, Bockris and Kitchener when applied to NaCl and NaNO_3 must be considered fortuitous.

Laity¹¹ has proposed a method of writing phenomenological equations for the description of electrical and mass transport which give rise to a set of friction coefficients. These quantities relate the results of such measurements as electrical conductance, transference numbers and diffusion coefficients in such a way that a single type of physical concept can be applied in interpreting the results of all three. For a pure molten salt, equations (4), (5) and (6) can be derived¹¹ (assuming only two ionic species).

$$\frac{\Lambda}{F^2} = [(z_+ + z_-)/r_{+-}] \quad (4)$$

and

$$\frac{D_{++}}{RT} = (z_+ + z_-)/(z_+r_{+-} + z_-r_{++}) \quad (5)$$

and

$$\frac{D_{--}}{RT} = (z_+ + z_-)/(z_-r_{+-} + z_+r_{--}) \quad (6)$$

where r_{+-} , r_{++} and r_{--} represent the friction coefficients for the relative motion of unlike and like ions, respectively, and z is the ionic charge. (The symbols D_{++} and D_{--} are used by Laity in the same sense as D_+ and D_- are used in this work.) It can be shown that the Nernst-Einstein relationship (equation 3) is a very special case of equations 4, 5 and 6.¹¹ The friction coefficients for the nitrates were calculated using equations 4, 5 and 6 from values of D_+ and D_- (some of which are extrapolated) and from the equivalent conduct-

ance measurements given with the friction coefficients in Table IV. All of the friction coefficients are positive and except for LiNO_3 , r_{+-} , r_{++} , and r_{--} for each salt are of the same order of magnitude indicating, according to Laity, that a high degree of association need not be postulated in the melt and that the choice of the ions as the mobile species is probably a proper one. It can be noted that for the alkali-metal nitrates the r_{+-} and r_{++} values increase with increasing cation size while the r_{--} value decreases with increasing cation size. For each salt, r_{++} is always less than r_{+-} and r_{--} . For the alkali-metal nitrates, the friction coefficient for the relative motion of unlike ions is always larger than that for like ions except in the case of LiNO_3 where r_{--} is larger. LiNO_3 is also the only salt in which ΔH^\ddagger for the nitrate is larger than that for the cation, the others all showing approximately equal values of ΔH^\ddagger for cation and anion. This seems to indicate that in the latter cases, migrations of both anion and cation are complementary interactions while for the nitrate in LiNO_3 , the anion-anion interaction is the important factor.

TABLE IV
FRICTION COEFFICIENTS FOR MOLTEN NITRATES

	Λ , ohms ⁻¹ cm. ²	t_+ °C.	r_{+-} $\times 10^{-8}$	$r_{++} \times 10^{-8}$ (joules/ cm. ² /sec.)	$r_{--} \times 10^{-8}$
LiNO_3	53.0 ¹²	350	3.51	0.03	5.50
NaNO_3	52.7 ¹³	350	3.53	.92	3.47
	72.3	450	2.57	.39	2.03
KNO_3	35.9 ¹⁴	350	5.19	1.63	2.48
	54.8	450	3.39	0.78	1.28
CsNO_3	42.4 ¹⁴	450	4.39	.87	0.99
AgNO_3	55.7 ¹³	350	3.34	.98	4.06

As is the case with the diffusion coefficients, other correlations of radius with friction coefficients are obvious, but are too speculative to make at the present stage of development of the theory of transport processes. Further application of the apparently useful hypothesis advocated by Laity toward the derivation of a quantitative theory to explain transport properties in molten salts awaits the availability of more experimental data (*e.g.*, inter-diffusion coefficients in mixtures).

(12) F. M. Jaeger and B. Kapma, *Z. anorg. Chem.*, **113**, 27 (1920).

(13) J. Byrne, H. Fleming and F. E. W. Wetmore, *Can. J. Chem.*, **30**, 922 (1952).

(14) D. F. Smith and E. R. Van Artsdalen, unpublished data.

(11) R. W. Laity, *J. Chem. Phys.*, **30**, 682 (1955)

ANOMALOUS SOLVENT EXTRACTION EQUILIBRIA DUE TO VIOLENCE OF AGITATION

BY KENNETH A. ALLEN AND W. J. McDOWELL

Oak Ridge National Laboratory, Oak Ridge, Tennessee¹

Received January 7, 1960

It is shown that previously anomalous dependences of uranium extraction coefficients on tri-*n*-octylamine sulfate and di-*n*-decylamine sulfate concentrations in benzene are due to metastable conditions induced by the vigorous agitation customarily employed in separatory funnel equilibrations. Nearly theoretically ideal results are obtained on slow equilibration in special cells which limit the liquid-liquid interfacial area markedly, and prevent interfacial turbulence completely. An explanation is proposed, based on adsorption of the critical components at the much larger interfacial area generated during vigorous agitation, which accounts for the long-term persistence of the anomalous effects after phase clarification. It is believed that this is the first observation of such effects in liquid-liquid extraction systems.

Introduction

It has been pointed out in previous papers that in the extraction of uranyl sulfate from acidic aqueous sulfate solutions by benzene solutions of tri-*n*-octylamine sulfate (TOAS) and di-*n*-decylamine sulfate (DDAS), anomalies appeared when attempts were made to reconcile the uranium extraction coefficient dependences on extractant concentration with other measured parameters.²⁻⁴ For example, while the reagent dependences were apparently nearly first power for both amines, consistent evidence from quite independent experiments indicated from two to three amine sulfates per uranium in a mononuclear complex. For a monomeric extractant such as TOAS, the corresponding reagent dependence should be second or third power, while for the large DDAS particle the reagent dependence should be nearly zero power, as predicted previously from particle size determinations⁴ (*i.e.*, the extraction coefficients should have been nearly independent of the DDAS concentration⁵).

One of us (McD) had suggested several years ago that spurious distributions could result from metastable conditions induced by the vigorous agitation customarily used in liquid-liquid equilibrations (*e.g.*, organic droplets small enough so that a significant portion of the extractant could be adsorbed at the liquid-liquid interface). The present paper describes the results of experiments designed to test this hypothesis.

Experimental

The amines and the pertinent analytical methods have been described elsewhere.^{2,3} The other materials were of the usual reagent grade. In a typical run benzene solutions

(1) Operated for the U.S.A.E.C. by Union Carbide Nuclear Company.

(2) K. A. Allen, *J. Am. Chem. Soc.*, **80**, 4133 (1958).

(3) W. J. McDowell and C. F. Baes, Jr., *THIS JOURNAL*, **62**, 777 (1958).

(4) K. A. Allen, *ibid.*, **62**, 1119 (1958).

(5) Light scattering and viscosity measurements have shown that each DDAS micelle contains *ca.* 40 monomers, while the DDAS-uranyl sulfate complex is a monomer.⁴ Thus, for $\text{UO}_2\text{SO}_4 + 3/40(\text{DDAS})_{40} = \text{UO}_2\text{SO}_4 \cdot 3\text{DDAS}$,

$$K = \frac{[\text{UO}_2\text{SO}_4 \cdot 3\text{DDAS}]_{\text{org}}}{[\text{UO}_2\text{SO}_4]_{\text{aq}} [\text{DDAS}]_{\text{org}}^{3/40}}$$

and since

$$E = \frac{[\text{U}]_{\text{org}}}{[\text{U}]_{\text{aq}}}$$

we have $E = K[\text{DDAS}]^\nu$, where $\nu < 0.1$, and wide variation in $[\text{DDAS}]$ should affect E only slightly.

of the amines, ranging from 0.2 down to 0.006 *N*, pre-equilibrated with an aqueous solution of a given sulfuric acid activity, were pipetted into separatory funnels with aqueous phases of the same acid activity, but containing 0.05 mole of uranyl sulfate per equivalent of amine present in the corresponding organic layer. The funnels were shaken in a 25.00 ± 0.01° bath at a fixed amplitude and frequency (*ca.* 100 strokes per min.) by a motor driven assembly. This degree of agitation was sufficient in all cases to produce droplets small enough so that the dispersions acquired the visible texture of a reasonably well homogenized emulsion. After shaking for a given length of time (well in excess of the few minutes known from previous work to be sufficient for the establishment of equilibrium²), the funnels were allowed to stand until the phases became clear enough for sampling. The primary phase separation usually was complete within a few minutes; 30 minutes to an hour was allowed for coalescence of the very fine droplets sometimes present, and filtration was used as a further precaution against entrainment. Small samples of the aqueous layers were taken for uranium analysis (since the extraction coefficients were large, analyzing the aqueous phases allowed accurate calculation of the organic uranium concentrations from material balances), and 50-ml. portions of both phases were transferred to cells in which the phases could be stirred by paddles while maintaining an almost quiescent interface, with the same liquids in contact as before. The cells were immersed in the 25° bath, and the paddles were run at 10, 25 and sometimes 60 r.p.m. by synchronous motors.⁶ In no case were the interfaces broken, and in all cases the aqueous layers were sampled at intervals (*e.g.*, daily) until constant uranium analyses indicated the attainment of equilibrium. At this point 25-ml. portions of each phase were transferred back to separatory funnels, again with the same liquids in contact, and the vigorous agitation step was repeated, followed, of course, by another aqueous uranium analysis.

The extraction coefficients ($E = [\text{U}]_{\text{org}}/[\text{U}]_{\text{aq}}$) were sufficiently high in these runs so that depleting the aqueous volumes by removal of the 1-ml. samples required for fluorimetric uranium analysis made only negligible changes in the over-all uranium material balances. Likewise, the shaft seals were of sufficient integrity so that evaporative depletion of the organic volumes was also negligible.

Results and Discussion

The extractant concentration dependences obtained by the two methods of equilibration with the normal sulfate forms of TOAS and DDAS are shown in Figs. 1 and 2 respectively.⁷ It is

(6) In the early runs extreme caution with the new technique led to the choice of 10 r.p.m. Later, with an improved cell design, it was found possible to drive the paddles at 25 and even 60 r.p.m. without disrupting the interfaces. Incidentally, the latter were not planar; shallow undulations slowly followed the paddle rotation. However, the interfacial area during the runs was at most only a few per cent. larger than the corresponding internal cross section of a cell. The times required for equilibrium were about one week at 10 r.p.m., a few days at 25 r.p.m., and less than 12 hours at 60 r.p.m.

(7) The reagent concentrations plotted here are the total equivalents of amine per liter. It is realized that at 20:1 loading between a quarter and a third of the extractant is tied up with uranium in the complex, and also that at these acid activities neither amine is completely in

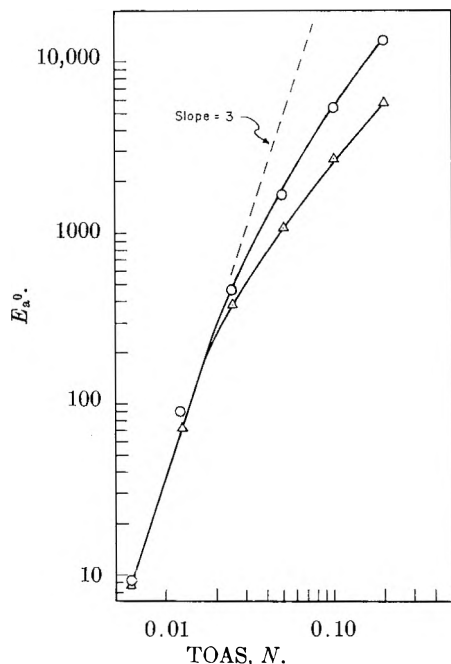


Fig. 1.—Uranium extraction coefficient dependence on TOAS concentration in benzene, with loading constant at 0.05 mole U per equivalent of amine, and aqueous phases containing 0.005 M H_2SO_4 only; Δ , vigorous agitation in separatory funnels; O , slow equilibration in limited interface contacting cells.

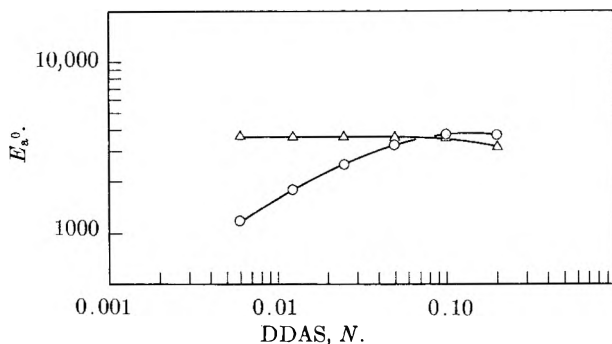


Fig. 2.—Uranium extracting coefficient dependence on DDAS concentration under the same conditions as those for TOAS, Fig. 2; O , vigorous agitation; Δ , slow equilibration.

obvious that with both amines there are startling differences between the vigorous agitation results and those of the limited interface equilibrations.

Consider first the TOAS results. Below *ca.* 0.025 N the two equilibrations agree both with each other and with theory.⁸ Above this concentration level the two methods diverge both from each other and from the line of slope three, but the limited interface results diverge from the line less than the

normal sulfate form (K. A. Allen, *THIS JOURNAL*, **60**, 239, 943 (1956)). However, since the extractions were run at constant uranium loading and at constant acid activity the fraction of free amine sulfate in equilibrium with the other components was the same over the whole concentration range and for both types of agitation. Thus, the experimental conditions permit the use of the total amine concentration as a valid representation of the behavior of the actual extractant molarity without the necessity of making questionable corrections for differences in loading and/or acid activity.

(8) At the low loadings used here it is assumed that the major complex species contains three amine sulfates per uranium. Numbers between two and three were reported in ref. 2, but these were based largely on much higher equilibrium aqueous uranium levels.

others. Thus, while the behavior is still by no means ideal, the departures from ideality are considerably smaller, and will therefore probably lend themselves more readily to further investigation.

The results with DDAS were even more striking. Here, the vigorous agitation dependence was in good agreement with the previously published curve,³ showing a slope of nearly unity at low concentration, and becoming fractional ($1/2$ to $2/3$) at 0.02 to 0.05 M DDAS. Considerable effort had been expended in attempts to fit this behavior with stoichiometric models, without success. The fact that the complex is a monomer, separate from the large DDAS micelle, as shown by particle size determinations,⁴ made the situation even more difficult (see footnote 5). However, the limited interface equilibrations have now provided confirmation of the behavior predicted from the particle size determinations. The line shown in Fig. 2 is actually horizontal; in other runs slopes as high as 0.1 to 0.2 have been observed. Since the ideal slope would be *ca.* $3/40$ or 0.075, the scatter around this value is not considered unreasonable.

Since the initial experiments numerous confirmatory runs have been made over a period of more than two years. In each case, using TOA and DDA in the normal sulfate forms in benzene *vs.* an aqueous phase containing only sulfuric acid and uranyl sulfate, the extractant concentration dependences showed the differences seen in Figs. 1 and 2. Other parameters in the amine extraction systems (*e.g.*, sulfate ion dependence, acid activity dependence, etc.) have not shown such differences. In fact, even the reagent concentration dependence differences with TOA and DDA disappear under certain conditions: with TOA in the bisulfate form, for example, the two equilibrations both give the same curve as the one already published,² and in this range of high sulfuric acid activity, therefore, the TOA behavior still lacks satisfactory theoretical interpretation. Similarly, when the ionic strength of the aqueous phase is increased markedly, the DDA differences disappear also: with 1 M Na_2SO_4 + 0.005 M H_2SO_4 (again keeping the DDA in the normal sulfate form in benzene) the two equilibrations agree with each other in giving a straight line of slope between 0.1 and 0.2 (Fig. 3). Thus, while fortunately this effect is apparently not widespread, the fact that it has been observed at all calls for some attempt at an interpretation.

The most reasonable explanation considered so far involves interfacial adsorption. It is proposed that sufficient interfacial area is generated during the vigorous agitation so that most of the amine sulfate is adsorbed at the liquid-liquid interface. The uranyl sulfate adsorbs there too, forming an interfacial complex with the amine salt which may and probably does have, not only a different free energy of formation, but also even a different composition from the one which finally appears in stable solution in the benzene. On coalescence, which occurs in a few minutes, these interfacial complexes might do any of four things: (1) simply remain at the new, much smaller interface, (2) dissociate, (3) go into the aqueous phase, or (4)

go into the organic phase. The first is ruled out by the experimental procedure: since the same liquids were used for the gentle equilibration as for the initial vigorous equilibration, then at least some of the interfacial complexes must have been homogeneously dispersed in the organic phase; otherwise, the slow equilibration would have resulted in the same final aqueous uranium analysis as the vigorous one. The second possibility indubitably occurs to some extent; the third probably not at all (even if each uranyl sulfate in an interfacial complex is bonded to only one amine sulfate, it is unlikely that the large alkyl chains are thereby sufficiently solubilized to remain in stable aqueous dispersion even temporarily). Therefore, during the rapid coalescence most of the interfacial complexes which remain undissociated would be forced to dissolve in the organic phase because of their predominantly organic nature. If indeed they were of different composition (presumably, they would involve fewer amines per uranium because of steric effects at the interface), they would soon encounter additional amine sulfates for the formation of the stable benzene-soluble species.

The clear phase analyses obtained immediately after phase clarification would therefore reflect an interfacial adsorption distribution, temporarily frozen into place, as it were, by the extreme comparative slowness with which the true equilibrium would become established in the unagitated bulk phases. The apparent uranium extraction coefficients observed initially could be either higher or lower than those characteristic of true equilibrium, depending, of course, on the number of uranyl sulfates which formed interfacial complexes in the first place, and then, during coalescence, on the relative importance of dissociation and solution in the organic phase.

An important question which has been raised concerning these results is whether a very fine suspension in one phase or the other might not lead to apparent differences of the type observed. The presence of such a suspension in the aqueous phase can be ruled out at once: as is pointed out in the Experimental section, enough coalescence time was allowed for visible clarity, and then the aqueous phases were filtered as an additional precaution. The organic phases were visibly clear also: if the data are the result of a sufficiently invisible suspension in the organic phase, then it is not that we are not still faced with anomalous behavior, it is simply that an alternative explanation has been proposed which depends on determining the average molecular weight of the uranium-bearing particles in the organic phase. This has been done, both by light scattering and by isopiestic measurements.⁴ For the two extractant systems of interest here, the amine sulfate-uranyl sulfate complexes were monomeric with respect to uranium. However, time is required for such measurements, and even though the light scattering and isopiestic solutions were indeed prepared by vigorous equilibration, it is possible that changes in the average molecular weight could have occurred after the equilibrations but before the molecular weight measurements. This would be akin to what is put

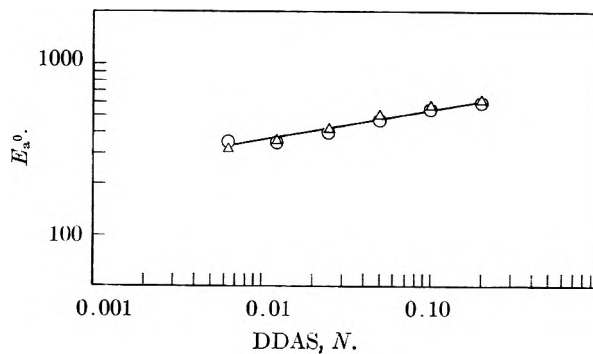


Fig. 3.—Uranium extraction coefficient dependence on DDAS concentration under the same conditions as those for Figs. 1 and 2, except that 1 *M* Na₂SO₄ was added to the aqueous phases; O, vigorous agitation, Δ, slow equilibration.

forward in the foregoing, anyway, and at this point, while it must be conceded that there may be still other mechanisms which could account for the data, it would seem that further experimental evidence, of a type far different from that leading to the present results, will be required before any such alternative mechanism can be shown to be more realistic than the one proposed.

As far as can be determined from a reasonably thorough search of the literature, the results reported in this paper represent the first observation of anomalous equilibria in solvent extraction systems due to violence of agitation during equilibration. A related effect has long been known in the case of dilute solutions of indicator dyes, where the critical component was soluble in only one phase. Changes in the colors of indicators in 0.01% aqueous solutions on shaking with inert liquids such as benzene, or even with air, were observed by Deutsch over 30 years ago.⁹ Various explanations have appeared and some of the experiments have been repeated.¹⁰ The proposed mechanisms involve adsorption of the indicators at the greatly increased liquid-liquid (or liquid-gas) interface, with consequent changes in their dissociations. However, in all these cases one had the benefit of instantaneous reversibility; on coalescence the true colors always reappeared immediately. In the present systems the long term persistence of the anomalous effects presents an entirely different problem.

In conclusion, while it is worth re-emphasizing that this effect apparently is restricted to only certain conditions involving one parameter in the amine sulfate extraction systems, it is also strongly recommended, in any careful investigation of solvent extraction equilibria involving ordinary concentrations (0.1 *M* or less), that at least a few slow equilibrations through limited interfaces be performed in order to make certain that such effects are indeed absent. Such equilibrations have become standard practice in this Laboratory. With the improved equipment and techniques they are

(9) D. Deutsch, *Ber.*, **60B**, 1036 (1927); *Z. physik. Chem.*, **136**, 353 (1928).

(10) I. M. Kolthoff, *Kolloid-Z.*, **43**, 51 (1927); H. Freundlich, *J. Chem. Soc.*, 164 (1930); G. J. Szasz, *J. Am. Chem. Soc.*, **62**, 3520 (1940).

no more time consuming than the usual shakeouts (e.g., the cells can be run overnight and sampled in the morning), and in addition they even have some positive advantages. For example, they have never given phase disengagement difficulties, they

seldom become cloudy, and entrainment troubles are simply non-existent.

Acknowledgments.—The authors are indebted to G. N. Case for technical assistance, and to Barbara S. Carmack for numerous carefully performed fluorimetric uranium analyses.

MICROWAVE ABSORPTION AND MOLECULAR STRUCTURE IN LIQUIDS. XXXII. ANALYSIS OF THE RELAXATION TIMES OF *n*-ALKYL BROMIDES IN TERMS OF A DISTRIBUTION BETWEEN LIMITING VALUES¹

BY KENITI HIGASI, KLAUS BERGMANN AND CHARLES P. SMYTH

Frick Chemical Laboratory, Princeton University, Princeton, N. J.

Received January 11, 1960

The previously measured dielectric constants and losses of the *n*-alkyl bromides may be represented in terms of a distribution of relaxation times between two limiting values, which may be calculated from the relaxation time and the distribution parameter α obtained previously from the Cole-Cole arc plot. The lower limit is taken as the relaxation time of the rotational orientation of the CH₂Br group about its bond to the rest of the molecule, while the upper limit is the relaxation time of the largest orienting unit, usually the molecule as a whole. The numerical values obtained for the two limits, one small and increasing slowly with molecular size, and the other large and increasing rapidly with molecular size, are consistent with this physical picture of the relaxation process, indicating the approximate correctness of this distribution function.

Dielectric constant and loss measurements at 1.27, 3.22 and 10.0 cm. wave lengths carried out in this Laboratory²⁻⁴ on eleven *n*-alkyl bromides were examined^{5,6} on the basis of the arc plots of Cole and Cole.⁷ The present paper describes a new analysis and interpretation of the same experimental data by the use of a function for the distribution of relaxation times similar to that discussed by Fröhlich.⁸

Because of the existence of internal rotation an alkyl halide molecule should have more than one relaxation time and the number of relaxation times should increase with increase in chain length. It is natural to assume that the relaxation times of a straight-chain alkyl bromide are distributed between two extreme values. The lower limit, τ_1 , is the relaxation time for the rotation of the smallest polar unit, the CH₂Br group, situated at the end of the molecule. The upper limit, τ_2 , which is the relaxation time of the largest unit, corresponds roughly to the end-over-end rotation of the whole molecule in the extended form. The probabilities of occurrence of τ_1 and τ_2 in the actual relaxation mechanism are not equal since the former should greatly exceed the latter. Increase in the number of carbon atoms in the molecule increases

the length and variety of the molecular segments which may rotate with the C-Br dipole, but the probability of occurrence of such rotation decreases with increase in the size of the rotating unit, hence with increase in the magnitude of the corresponding relaxation time itself. This picture is in qualitative agreement with a distribution function $y(\tau)$ defined⁹ by

$$y(\tau) = \frac{1}{A\tau}, \text{ if } \tau_1 < \tau < \tau_2 \quad (1)$$

$$y(\tau) = 0, \text{ if } \tau < \tau_1 \text{ and } \tau > \tau_2$$

where A is a parameter which is associated with the distribution of relaxation times.

Although the observed dielectric constants and losses of the alkyl halides have been treated by the Cole-Cole method with fair success, their examination in terms of $y(\tau)$, which is based on an entirely different mechanism, is revealing. As will be seen, the two very different methods may be equally effective in an empirical representation of the same experimental results. In certain cases we can transform with fair precision the two limiting relaxation times, τ_1 and τ_2 , into the relaxation time τ_0 and the distribution parameter α of the Cole-Cole method and *vice versa*. τ_0 is the reciprocal of the angular frequency at which the observed dielectric loss has its maximum value ϵ''_m .

When the values of ϵ'' at different frequencies are plotted as ordinates against the corresponding values of ϵ' as abscissas, the arc of a circle is obtained for a substance which obeys the Cole-Cole relation. In contrast to this, it has been shown by Bergmann¹⁰ that, for a material obeying eq. 1, when ϵ'' is plotted against ϵ' the curve obtained is very close to a half-ellipse with the axes $b = (\epsilon_0 - \epsilon_\infty)/2$ and $a = \epsilon''_m$, if the parameter A is not

(1) This research was supported in part by the National Science Foundation, in part by the Office of Ordnance Research and in part by the United States Air Force through the Office of Scientific Research of the Air Research and Development Command. Reproduction, translation, publication, use or disposal in whole or in part by or for the United States Government is permitted.

(2) W. M. Heston, Jr., E. J. Hennelly and C. P. Smyth, *J. Am. Chem. Soc.*, **70**, 4093 (1948).

(3) H. L. Laquer and C. P. Smyth, *ibid.*, **70**, 4097 (1948).

(4) F. H. Branin, Jr., and C. P. Smyth, *J. Chem. Phys.*, **20**, 1121 (1952).

(5) E. J. Hennelly, W. M. Heston, Jr., and C. P. Smyth, *J. Am. Chem. Soc.*, **70**, 4102 (1948).

(6) C. P. Smyth, "Dielectric Behavior and Structure," McGraw-Hill Book Co., New York, N. Y., 1955, pp. 114-127.

(7) K. S. Cole and R. H. Cole, *J. Chem. Phys.*, **9**, 341 (1941).

(8) H. Fröhlich, "Theory of Dielectrics," Oxford University Press, London, 1949, pp. 93-95.

(9) Compare ref. 8.

(10) K. Bergmann, Thesis, Freiburg/Breisg., West Germany, 1957.

very large, that is, if $A < 4$. By comparing the arc of the circle with the curve of the ellipse, one is able to find relationships connecting the three parameters A , τ_1 and τ_2 with the Cole parameters α and τ_0 . The simplest method of finding this desired relationship is to set the ϵ''_m values equal for the two curves, so that the ellipse is tangent to the arc at its top. This approximation would appear to be justified only when both curves are close to a semicircle, or when the observed points are only in the vicinity of ϵ''_m . If the experimental accuracy of the dielectric constant and loss values were high, one should be able to determine which of the two functions should be more nearly correct. In the majority of cases, however, the precision of the measurements is not great enough to distinguish between the two functions, and both the Cole-Cole and the function of eq. 1 usually fit the same experimental data within the limit of error.

For the sake of illustration, we shall assume an extreme case, where all the experimental values lie on an ellipse (Fig. 1) with $A = 4.5$. If the range of experimental error is $\pm 2\%$ in the dielectric constant and $\pm 5\%$ in the loss values, it will be seen from Fig. 1 that a Cole-Cole arc with $\alpha = 0.305$ can also be drawn through the same points. The smaller arc represented by the broken line is concentric with the Cole-Cole arc and passes through the end points of the ellipse axis.

For the Cole-Cole arc there is a relation⁷

$$\tan \frac{(1-\alpha)\pi}{4} = \frac{2\epsilon''_m}{(\epsilon_0 - \epsilon_\infty)} = \frac{a}{b} \quad (2)$$

For the ellipse there is a relation⁸ between the ratio of the ellipse axes, a/b , and the parameter A

$$a/b = (2/A)(\tan^{-1} e^{A/2} - \tan^{-1} e^{-A/2}) = \frac{2}{A} \tan^{-1} \sinh \frac{A}{2} \quad (3)$$

By substituting eq. 3 into eq. 2 one gets the desired relation between A and α

$$\alpha = 1 - \frac{4}{\pi} \tan^{-1} \left[\frac{2}{A} \tan^{-1} \sinh \frac{A}{2} \right]; \quad 0 \leq \alpha < 1 \quad (4)$$

Equation 4 is plotted in Fig. 2, which shows the dependence of A and $e^{A/2}$ upon α . By use of eq. 4 or Fig. 2, τ_1 and τ_2 can be obtained from τ_0 and α , for τ_1 and τ_2 are⁸

$$\begin{aligned} \tau_1 &= \tau_0 e^{-A/2} \\ \tau_2 &= \tau_0 e^{A/2} \end{aligned} \quad (5)$$

There are other methods of obtaining τ_1 and τ_2 from τ_0 and α , but this method seems to be the most practical. τ_1 and τ_2 are very sensitive to the selection of the value of A , which is most accurately determined by the points close to ϵ''_m . The transformation described above is permissible in the first approximation only in the range of $1 > a/b > 0.6$, i.e., $\alpha < 0.30$.

Table I shows the results of the application of the method to the data for the *n*-alkyl bromides.⁵ The values of $e^{A/2}$ are obtained from those of the Cole-Cole distribution parameter⁶ α by means of the curve in Fig. 2. The two relaxation times, τ_1 and τ_2 , then are obtained from τ_0 and $e^{A/2}$ by means of eq. 5.

The experimental values²⁻⁴ of ϵ' and ϵ'' for each compound in Table I were plotted in the complex

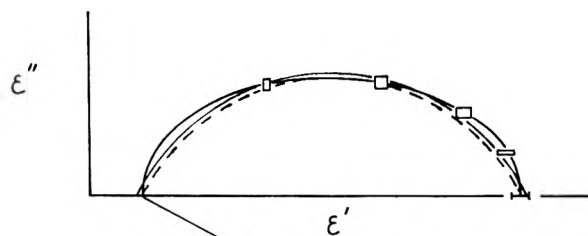


Fig. 1.—Plots of ϵ'' and ϵ' in a complex plane.

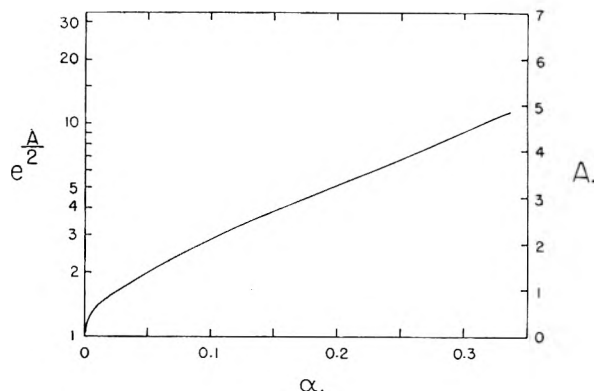


Fig. 2.—Correlation of distribution parameters A and $e^{A/2}$ with the Cole-Cole parameter α .

plane, and the best fitting ellipse was drawn through these points. From the ratio of the ellipse axes, a/b , A was found by means of eq. 3. The left-hand intersection of the ellipse with the abscissa axis gave the value of the optical dielectric constant ϵ_∞ . For each angular frequency ω used in measurement, it was possible to calculate τ_0 from the equation

$$\omega \tau_0 = \frac{\sinh \frac{A}{2} \pm \left(\sinh^2 \frac{A}{2} - \tan^2 A z \right)^{1/2}}{\tan A z} \quad (6)$$

Equation 6 follows from the equation⁸

$$z = \frac{\epsilon''}{\epsilon_0 - \epsilon_\infty} = \frac{1}{A} \left\{ \tan^{-1} (e^{A/2} \omega \tau_0) - \tan^{-1} (e^{-A/2} \omega \tau_0) \right\} \quad (7)$$

The + sign of eq. 6 is to be taken for points lying to the left of ϵ''_m , the - sign for those lying to the right of ϵ''_m . The mean of the values of τ_0 thus obtained for each substance at 25° is given in Table II, together with the resultant values of $e^{A/2}$, τ_1 and τ_2 calculated as before.

The third decimal place in the values of α and the second decimal place in those of τ in Tables I and II are significant only in showing trends in the series. The values for τ_0 and τ_2 in Table II do not differ greatly from those in Table I. The much smaller values for τ_1 show relatively greater differences. It seems probable that only orders of magnitude and major trends are of significance.

The excellent representation of the data for *n*-propyl bromide by the elliptical plot is shown in Fig. 3, where the experimental points lie on the solid line of the ellipse rather than on the dashed line of the arc. The difference between the two is, however, within the probable experimental error,

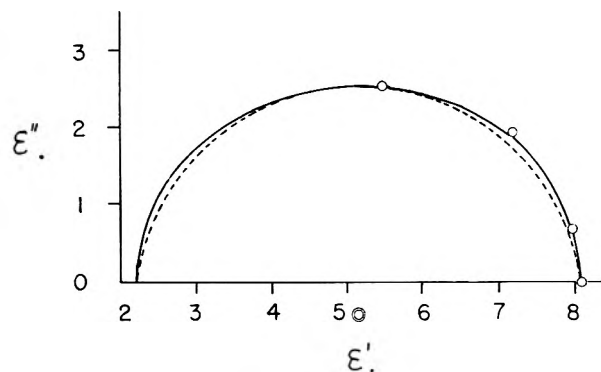


Fig. 3.—Plots of ϵ'' and ϵ' in a complex plane for *n*-propyl bromide.

TABLE I

VALUES OF LIMITING RELAXATION TIMES (10^{-11} SEC.) FOR THE *n*-ALKYL BROMIDES, $C_nH_{2n+1}Br$, CALCULATED FROM THE COLE-COLE PARAMETERS

<i>n</i>	α	$c^{A/2}$	τ_0	τ_1	τ_2
1.0°					
2	0.064	2.24	0.52	0.22	1.16
3	.087	2.64	0.82	.31	2.16
4	.119	3.21	1.12	.35	3.60
5	.177	4.45	1.77	.40	7.88
6	.189	4.75	2.31	.49	11.0
7	.220	5.68	3.05	.54	17.3
8	.248	6.76	3.60	.53	24.3
9	.246	6.68	4.84	.72	32.3
10	.273	7.80	6.92	.89	54.0
12	.293	8.92	10.20	1.14	91.0
14	.299	9.20	12.40	1.35	114.1
25.0°					
2	0.055	2.11	0.38	0.18	0.80
3	.087	2.63	.58	.22	1.52
4	.098	2.83	.87	.31	2.46
5	.143	3.68	1.21	.33	4.45
6	.172	4.32	1.57	.36	6.78
7	.204	5.20	1.92	.37	9.98
8	.226	5.88	2.18	.37	12.8
9	.243	6.57	2.85	.43	18.7
10	.251	6.85	3.37	.49	23.1
12	.259	7.12	4.89	.69	34.8
14	.270	7.68	5.38	.70	41.3
16	.287	8.58	6.96	.81	59.7
55.0°					
3	0.033	1.78	0.47	0.26	0.84
4	.078	2.48	.64	.26	1.59
5	.118	3.20	.87	.27	2.78
6	.148	3.79	1.06	.28	4.02
7	.180	4.51	1.25	.28	5.64
8	.220	5.69	1.37	.24	7.80
9	.227	5.94	1.58	.27	9.39
10	.229	6.00	1.91	.32	11.5
12	.232	6.10	2.44	.40	14.9
14	.235	6.19	2.81	.45	17.4
16	.248	6.77	3.07	.45	20.8

and the data for the alkyl bromides, in general, fail to distinguish directly between the two methods of analysis.

Since τ_1 is the relaxation time for the rotational orientation of the CH_2Br group around its C-C bond, it should increase with molecular chain length

TABLE II
RESULTS OF THE ELLIPTICAL ANALYSIS OF THE *n*-ALKYL BROMIDES AT 25°

<i>n</i>	$c^{A/2}$	τ_0	τ_1	τ_2
2	2.51	0.36	0.14	0.90
3	2.51	.63	.25	1.58
4	2.51	.89	.35	2.23
5	3.97	1.28	.32	5.1
6	5.00	1.62	.32	8.1
7	5.75	2.09	.36	12.0
8	6.68	2.56	.38	17.2
9	7.38	3.17	.43	23.5
10	8.75	3.71	.42	32.5
12	9.68	4.38	.45	43
14	9.68	4.59	.47	45
16	15.1	5.06	.34	76

only insofar as it is affected by increasing viscosity of the liquid or by steric hindrance within the molecule. Since small, nearly spherical molecules have been found^{11,12} to show but slight increase in relaxation time with increase in the viscosity of the medium, the relatively small increase apparent in τ_1 with increasing molecular size is consistent with the picture which has been proposed. The great increase in τ_2 with increasing chain length, much greater than that in τ_0 , is consistent, at least qualitatively, with its association with the orientation of the extended molecule as a whole.

In the first analysis⁵ of the data, a hypothetical volume V_D of the *N* molecules in a mole was calculated from the equation

$$V_D = \tau_0 RT / 3\eta$$

The fact that the values of V_D rose to a maximum for the six-carbon chain instead of increasing continuously with increasing chain length was regarded as indicating that increasing possibility of internal orientation caused the increase in relaxation time to fall farther and farther behind the increase in viscosity, η . Use of the values of τ_2 from Table II leads to much larger values for V_D , reaching a maximum at the ten-carbon chain, but still smaller than the values of the molar volume, M/d .

It may be shown easily that the ratio of the molar volume M/d to V_D is equal to the ratio of the relaxation time calculated by the Debye theory⁵ to the observed value. The observed relaxation time has, in general, been much smaller than the calculated, particularly for small molecules, that is, the ratio of M/d to V_D is generally much larger than 1. It has recently been observed¹³ that, for solutions, the ratio of the calculated to the observed relaxation times decreases from values as high as 20 or more and approaches 1 as the size of the solute molecule begins to exceed that of the solvent. The ratio of M/d to V_D calculated from τ_2 for these pure alkyl bromides decreases from 3.85 for ethyl bromide to 1.72 for nonyl and 1.76 for decyl and then increases to 3.26 for hexadecyl. The ratios are much larger if V_D is calculated from

(11) A. J. Curtis, P. L. McGeer, G. B. Rathmann and C. P. Smyth, *J. Am. Chem. Soc.*, **74**, 645 (1952).

(12) C. P. Smyth, *Proc. Natl. Acad. Sci.*, **42**, 234 (1956).

(13) (a) E. J. Meakins, *Trans. Faraday Soc.*, **54**, 1160 (1958); (b) D. A. Pitt and C. P. Smyth, *THIS JOURNAL*, **63**, 582 (1959).

τ_0 . It is logical to conclude either that the probability of orientation of the longest molecular segments is less than that assumed in eq. 1, or that increased coiling with increased chain length shortens the relaxation time, or both.

It is evident that the arc plots and the elliptical plots differ too little from one another to make

possible a direct distinction between them by means of the data for the alkyl bromides. However, the magnitudes of the relaxation times calculated from the elliptical distribution favor the latter through their consistency with the most reasonable physical picture of the relaxation process in the alkyl bromides.

BLOCK-POLYMERS OF STYRENE AND ISOPRENE WITH VARIABLE DISTRIBUTION OF MONOMERS ALONG THE POLYMERIC CHAIN. SYNTHESIS AND PROPERTIES¹

BY S. SCHLICK AND M. LEVY

Chemistry Department, Israel Institute of Technology, Haifa, Israel

Received January 14, 1960

A number of block-polymers of styrene and isoprene were prepared by applying the technique of "living" polymers: I₃₄₀₀-S₉₀₀₀-I₃₄₀₀; I₃₄₀₀₀-S₉₀₀₀₀-I₃₄₀₀₀; I₁₇₀₀-S₄₅₀₀-I₃₄₀₀-S₄₅₀₀-I₁₇₀₀; I₁₇₀₀₀-S₄₅₀₀₀-I₃₄₀₀₀-S₄₅₀₀₀-I₁₇₀₀₀; I₁₇₀₀-S₂₂₅₀-I₁₇₀₀-S₄₅₀₀-I₁₇₀₀-S₂₂₅₀-I₁₇₀₀; I₁₇₀₀₀-S₂₂₅₀₀-I₁₇₀₀₀-S₄₅₀₀₀-I₁₇₀₀₀-S₂₂₅₀₀-I₁₇₀₀₀; I₁₁₃₀-S₂₂₅₀-I₁₁₃₀-S₂₂₅₀-I₂₂₆₀-S₂₂₅₀-I₁₁₃₀-S₂₂₅₀-I₁₁₃₀; and I₁₁₃₀₀-S₂₂₅₀₀-I₁₁₃₀₀-S₂₂₅₀₀-I₂₂₆₀₀-S₂₂₅₀₀-I₁₁₃₀₀-S₂₂₅₀₀-I₁₁₃₀₀ I and S denoting the blocks of isoprene and styrene and the subscripts their respective molecular weights. All these polymers have the same composition and form two series of total mol. wt. 15,800 and 158,000, respectively. In addition random copolymers of the same composition and the same molecular weights were prepared. These polymers were characterized and their properties were investigated. The latter show systematic changes with changes in the block's size. The dependence of these properties on the block's size is discussed.

Many methods for preparing block-polymers have been described in the literature, and a comprehensive review of this subject was published in 1956 by Immergut and Mark.² Most of the known techniques yield a mixture of block-polymers and homo-polymers, and the two components have to be separated before a sample of pure block-polymer is obtained. Furthermore, even a purified product is very heterogeneous, being composed of molecules of variable composition and variable molecular weight.

A new method of preparation of block-polymers has been described recently by Szwarc, Levy and Milkovich.³ It was demonstrated that this method yields a pure block-polymer, not contaminated by homo-polymer,³ and, moreover, it permits the experimenter to vary at will the distribution of the monomers along the chain of the polymer.⁴ A further advantage of the method arises from the fact that under proper experimental conditions a narrow molecular weight distribution product is formed,^{5,6} hence block-polymers of uniform architecture can be synthesized.

By applying this technique we succeeded in preparing samples of block-polymers of styrene and isoprene which have the same composition and molecular weight and differ only in the distribution of the two monomers along the chain of the

polymer. This is, to the best of our knowledge, the first time when such material became available and its study permits us to investigate the effect of distribution upon properties of the respective block-polymers. In this publication we report the details of preparation of such samples, their characterization and some of their properties which vary with the degree of distribution of the monomers along the chain.

Preparation of Block-polymers.—Anionic polymerization carried out in non-protonating solvents and in absence of impurities acting as "killing" agent yields "living" polymers,³ *i.e.*, polymeric molecules possessing active ends capable of further growth. If the active end of a monomer A initiates polymerization of a monomer B, and *vice versa*, if the active end of B initiates polymerization of A, then block-polymers of the type



can be prepared readily. The procedure is simplified further if both ends of the polymeric molecule are active, and it was shown that this is the case if the polymerization is initiated by electron-transfer mechanism, *e.g.*, when sodium naphthalene is used as an initiator.

Poly-styryl anion initiates polymerization of isoprene and polyisoprene anion initiates polymerization of styrene, hence this pair of monomers suits our purpose. Polymerization was initiated by sodium naphthalene, and the reaction was carried out in a stirred reactor *in vacuo* at 0° by adding successively the required amounts of monomers to the initiator. The molecular weight of the obtained polymer is given by $2M_T/I$, where M_T denotes the total number of moles of added monomers and I the amount of initiator in moles. The molecular weight of each block is given by $M_j/I_j M_j$

(1) Taken from a thesis submitted by S. Schlick in partial fulfillment of the requirements for the M.S. degree at the Israel Institute of Technology.

(2) E. H. Immergut and H. Mark, *Makromolekular Chem.*, **18/19**, 322 (1956).

(3) M. Szwarc, M. Levy and R. Milkovich, *J. Am. Chem. Soc.*, **78**, 2656 (1956).

(4) (a) M. Szwarc, *Nature*, **178**, 1168 (1956); (b) *Advances in Chem. Physics*, **2**, 147 (1959); *Makromolekular Chem.*, in press (1959).

(5) R. Waack, A. Rembaum, J. D. Coombes and M. Szwarc, *J. Am. Chem. Soc.*, **79**, 2026 (1957).

(6) H. W. McCormick, *J. Polymer Sci.*, **36**, 341 (1959).

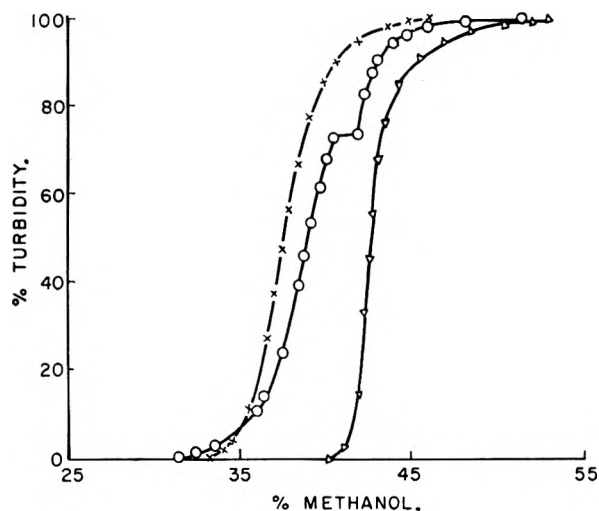


Fig. 1.

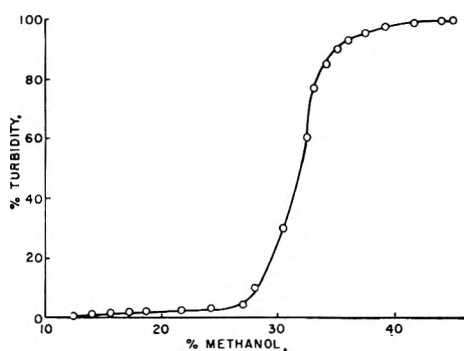


Fig. 2.

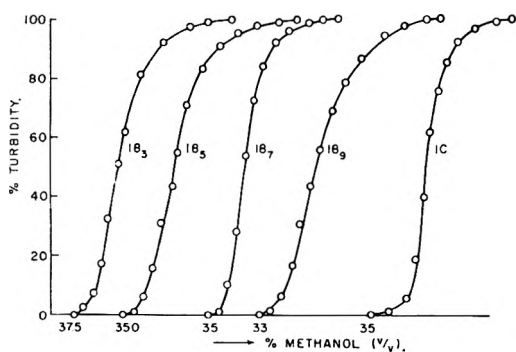
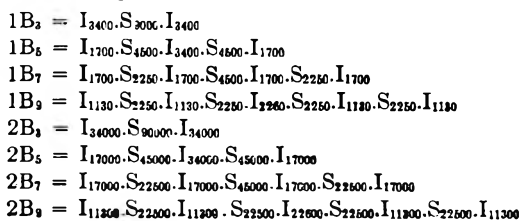


Fig. 3.

denoting the number of moles of the monomer added in the j -th portion, the middle block being an exception since its weight is doubled. The samples prepared were



I and S denote the blocks of isoprene and styrene, respectively, the subscripts being the molecular weights of the respective blocks. One notices that the compositions of all these polymers are identical,

the molar ratio of S/I being 0.865, but the molecular weight of the 2B series is ten times greater than that of 1B series (molecular weights of 1B = 15,800 and of 2B = 158,000). In addition two samples of "copolymers" were prepared. These samples result from a very slow addition of a mixture of styrene and isoprene (S/I = 0.865) to the initiator, the rate of addition being such that each drop of mixture essentially polymerizes completely before the next is added. The "copolymer" is therefore a material composed of very small and irregular blocks of styrene and isoprene. These samples are denoted by 1C and 2C, the former having molecular weight of the 1B series, the latter that of the 2B series.

Each polymerization was terminated by addition of a drop of water to the solution, then the polymer was precipitated in methanol and dried *in vacuo* at 60°. Polymers 2B₃ and 1C were prepared in duplicate. The reproducibility of those samples was satisfactory.

Each experiment involved 114 cc. of tetrahydrofuran, and 5 cc. each of styrene and isoprene. The monomers were carefully purified, dried with CaH₂ and distilled in high vacuum. The yield was quantitative.

Characterization of the Block-polymers.—The mol. wt. distribution and homogeneity of each sample was checked by the turbidimetric technique described by Melville, *et al.*⁷ The reliability of the turbidimetric method was checked by precipitating a mixture of polystyrene and polyisoprene (Fig. 1) and by precipitating polystyrene prepared by benzoyl peroxide as initiator (Fig. 2). Turbidimetric titrations were carried out at 30°. The initial concentration of polymer was 5 mg. in 100 cc. toluene. Toluene was used as solvent and methanol as precipitant. The turbidimetric curves are shown in Figs. 3 and 4 for the low and high mol. wts., respectively. The curves demonstrate clearly the homogeneity and sharp mol. wt. distribution of samples obtained by this method. It is interesting to note the sharp rise in turbidity in the higher mol. wt. samples up to approximately 90% precipitation and then the gradual bending of the curve. This corresponds to the shape of distribution predicted by Szwarc and Litt⁸ from theoretical considerations.

Attention is drawn to the fact that curves 2B₃ and 2B₇ are steeper than curves 2B₅ and 2B₉. The former samples were initiated by styrene and the latter by isoprene. Apparently the initiation of isoprene is slower than that of styrene and therefore a wider distribution is obtained. This difference in behavior of styrene and isoprene was confirmed by independent observations, using a method described previously.⁹

Viscosity measurements were carried out in a modified Ubbelohde viscometer at 30 ± 0.03° using toluene, toluene-methanol, and toluene-isoctane mixtures as solvents. The solvent flow time was always over 100 sec.

(7) A. S. Dunn, B. P. Stead and H. W. Melville, *Trans. Faraday Soc.*, **50**, 279 (1954).

(8) M. Szwarc and M. Litt, *This Journal*, **62**, 568 (1958).

(9) M. Levy and M. Szwarc, *J. Am. Chem. Soc.*, **82**, 521 (1960).

Properties of Block-polymers.—Two properties of the block-polymers were studied in the course of this investigation: their precipitation by addition of non-solvents and their viscosities in toluene, toluene-methanol and toluene-isoöctane mixtures. It was shown previously³ that a block-polymer of styrene and isoprene is not precipitated from toluene solution by addition of isoöctane. This phenomenon now was studied quantitatively using a turbidimetric titration.

When methanol is used as a precipitant and toluene as a solvent the onset of precipitation seems to be independent of the block's size. The critical concentration of methanol was found to be 35% \pm 2 for the 1B series and 1C (mol. wt. 15,800) and 28% \pm 0.5 for the 2B series and 2C (mol. wt. 158,000). On the other hand, the size of the blocks affected markedly the critical concentration of isoöctane when this hydrocarbon was used as non-solvent in the turbidimetric titration. The results are given in Table I. As the size of the blocks decreased, their solubility increased so much that it was necessary to work with more and more concentrated solutions since no precipitation did take place in the dilute solutions. The effect of the block's size on the solubility of the respective polymer casts doubts on Kilb and Bueche¹⁰ calculations of the free energy of mixing of block-polymers.

The viscosity measurements in toluene solution are summarized in Table II. The results show clearly that the intrinsic viscosity increases with decreasing block's size. This behavior might be accounted for by the incompatibility of polystyrene and polyisoprene—the respective blocks avoid each other and as a result the polymer molecule expands as the number of blocks increases and their size decreases. The same trend is seen in mixed solvents: toluene and methanol and toluene and isoöctane (see Tables II and III).

TABLE I

Type of blocks	% isoöctane	Concn. of polymer, mg./100 cc.
2B ₃	55	2.5
2B ₅	57	10
2B ₇	62	15
2B ₉	68	25
2C	No pptn. even at the highest concn. of isoöctane	

TABLE II

Type of block-polymer	% methanol			
	0	10	20	24
1B ₃	0.220	0.210	0.195	...
1B ₅	.232	.212	.180	...
1B ₇	.250	.220	.200	...
1B ₉	.255	.224	.190	...
1C	.190	.185	.155	0.148
2B ₃	.810	.695	.530	...
2B ₅	.878	.735	.545	...
2B ₇	.890	.780	.545	...
2B ₉	.980	.864	.650	...
2C	1.075	.970	.680	0.550

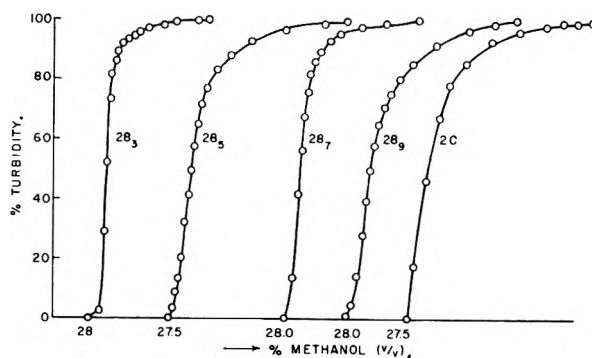
(10) R. W. Kilb and A. M. Bueche, *J. Polymer Sci.*, **28**, 285 (1958).

Fig. 4.

TABLE III

INTRINSIC VISCOSITIES IN G./100 CC. OF BLOCK-POLYMERS IN TOLUENE-ISOÖCTANE MIXTURES

Type of block-polymer	% of Isoöctane					
	0	20	40	50	60	70
1B ₃	0.220	0.200	0.185
1B ₅	.232	.215	.194	0.188	0.170	...
1B ₇	.250	.233	.220	.210	.190	...
1B ₉	.255	.233	.220200	...
1C	.190185165	0.150
2B ₃	.810	.690	.515
2B ₅	.878	.810	.670	.520
2B ₇	.890	.840	.710	.580
2B ₉	.980	.908	.805580	...
2C	1.075980725	0.530

Rossi, *et al.*,¹¹ described a method of determining $[\eta]_{\theta}$ at constant temperature by varying the composition of the solvent. Plotting $\log [\eta]$ versus $\log (M)$ at each composition one determines the exponent a of the $[\eta] = KM^a$ relation as a function of the solvent composition, and by extrapolation (or interpolation) the composition for which $a = 0.5$ could be found. Solvent of this particular composition is assumed to be the θ solvent.

It remains to be shown that for a series of block-polymers characterized by the same distribution of monomers along the chain but of varying molecular weights, the log of intrinsic viscosity is linear with log of mol. wt. However, if such a relation is assumed then our data permit to find a for each type of block-polymers and for each composition of the mixed solvent. Figure 5 illustrates this method. Here a plot of a as a function of % of methanol in the solvent is given for the copolymer, and determination of the composition of the θ solvent from this graph is self-evident. In this way the data listed in Table IV have been obtained. These data show a definite trend in the composition of the " θ solvent" with the decreasing block's size, and they are therefore interesting whatever is their meaning. Since the polymer seems to expand as the block's size decreases it is natural to expect that the proportion of the precipitant in the " θ solvent" should increase accordingly.

Table IV lists also the intrinsic viscosities of the respective polymers in their " θ solvents." Although considerable experimental uncertainties are involved in the interpolation (or extrapolation)

(11) C. Rossi, U. Bianchi and V. Magnasco, *ibid.*, **30**, 175 (1958).

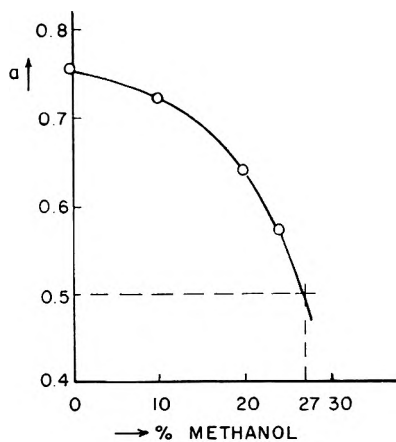


Fig. 5.

method applied in their derivation, it is interesting to notice that the corresponding $[\eta]_{\theta}$ obtained in the toluene-methanol and toluene-isoöctane mixtures are similar in spite of the great difference in the composition of these solvents. This is surprising since different configurations of the polymer coil are expected in each case. While methanol causes a contraction of both polystyrene and polyisoprene chains, isoöctane contracts the former but expands the latter. However, the contracted polystyrene blocks would act as pseudo crosslinks for polyisoprene blocks, and therefore a similar $[\eta]_{\theta}$ might be expected after all. In any

case, although the similarities of the respective $[\eta]_{\theta}$ add weight to the assumption that one deals here indeed with θ solvents, the difficulties of application of a θ solvent concept to solutions of block-polymers should be clearly recognized.

TABLE IV

Type of block-polymer	% in " θ solvent"	$[\eta]_{\theta}$		% Isoöctane in " θ solvent"	$[\eta]_{\theta}$	
		Mol. wt. 158,000	Mol. wt. 15,800		Mol. wt. 158,000	Mol. wt. 15,800
B ₃	12.5	0.65	0.205	31.0	0.61	0.190
B ₅	17.0	.60	.190	47.0	.59	.185
B ₇	17.0	.63	.205	42.0	.69	.220
B ₉	24.0	.55	.170	56.0	.64	.205
C	27.0	.45	.135	73.0	.44	.145

In conclusion it is desirable to emphasize that this work demonstrates the practicality of the synthesis of block-polymers with desirable and predetermined patterns. It shows that there are polymer properties which vary systematically with the distribution of monomers along the polymer chain and it demonstrates, therefore, that one deals here with a new problem in polymer chemistry which calls for further experimental and theoretical studies.

Acknowledgment.—We are grateful to Prof. M. Szwarc for very helpful discussions. This work was partially supported by a grant from Quartermaster Corps No. DA-19-129-QM-1297.

NUCLEAR MAGNETIC RESONANCE STUDIES OF HYDROGEN BONDING. I. CARBOXYLIC ACIDS¹

BY JEFF C. DAVIS, JR., AND KENNETH S. PITZER

Department of Chemistry and Lawrence Radiation Laboratory, University of California, Berkeley, California

Received January 14, 1960

The proton magnetic resonance spectra of solutions of formic, acetic and benzoic acids in benzene have been studied in the temperature range 20–100°. Previously reported equilibrium constants and heats of dimerization are employed to calculate the chemical shifts of the monomer and dimer species of the acids. Exceptionally high shieldings are found for the monomers at room temperature which shift to lower applied fields at higher temperatures. Association of the acid monomers with the aromatic solvent is a possible explanation of these results. The nature of the higher acid polymers is also discussed.

The association of carboxylic acids has been the subject of extensive investigation by a variety of methods.² In the vapor phase, equilibrium constants and enthalpies of dimerization have been determined for a number of the lower acids.³ Electron diffraction studies have shown these dimers to be cyclic in the gas phase with each of the carboxyl protons hydrogen bonded.⁴ X-Ray studies of crystalline acids have shown structures varying from a symmetric array of cyclic dimers, as in

solid benzoic acid,^{5,6} to long chain polymers, as in formic and acetic acids.⁷ Evidence has been given that long polymers are also present in pure liquid formic acid.⁸ Although carboxylic acids in non-hydrogen bonding solvents have been studied by several techniques, there has been little agreement in those cases in which the same system has been studied by two methods.²

Nuclear magnetic resonance (n.m.r.) techniques have been applied successfully in the investigation

(1) Based in part on a thesis by JGD in partial fulfillment of the requirements for the Ph.D. degree, University of California, 1959.

(2) G. Allen and M. A. Caldin, *Quart. Revs.*, **7**, 255 (1953).

(3) A. S. Coolidge, *J. Am. Chem. Soc.*, **50**, 2166 (1928); H. L. Ritter and J. H. Simons, *ibid.*, **67**, 757 (1945); M. D. Taylor, *ibid.*, **73**, 315 (1951); E. W. Johnson and L. K. Nash, *ibid.*, **72**, 547 (1950); and others.

(4) J. Karle and L. O. Brockway, *ibid.*, **66**, 574 (1944).

(5) A. Ahmed and M. Cruickshank, *Acta Cryst.*, **6**, 385 (1955).

(6) R. W. G. Wyckoff, "Crystal Structures," Interscience Publishers, New York, N. Y., 1948, Chap. 14, p. 58b.

(7) F. Holtzberg, B. Post and I. Fankuchen, *Acta Cryst.*, **6**, 127 (1953); R. E. Jones and D. H. Templeton, *ibid.*, **11**, 484 (1958).

(8) D. Chapman, *J. Chem. Soc.*, 225 (1956); J. F. Johnson and R. H. Cole, *J. Am. Chem. Soc.*, **73**, 4536 (1951).

of hydrogen bonding systems in solution.⁹ In general it has been observed that upon formation of a hydrogen bond, the proton resonance is shifted to a lower applied magnetic field. In such systems a single "average" resonance is observed, the position of this resonance depending on the relative amounts of the various species in equilibrium.

In the present investigation, the proton magnetic resonance spectra of solutions of formic, acetic and benzoic acid in benzene have been studied in an attempt to obtain more specific information about the equilibria involved and the nature of the monomer and polymer species. These spectra were observed over a temperature range of 20–100° with the aid of specially constructed temperature control equipment.

Experimental

Chemicals.—The removal of traces of water from the reagents was of primary interest in this investigation. The materials were purified in the following manner.

Benzene.—Matheson C.P. benzene was twice distilled from anhydrous calcium sulfate; b.p. 80.0–80.1°.

CCl₄.—Bakers C.P. CCl₄ was twice distilled from anhydrous calcium sulfate and stored in a desiccator with P₂O₅; b.p. 76.7–76.8°.

Benzoic Acid.—Fisher C.P. benzoic acid was recrystallized from benzene and dried ten hours at 80° in a vacuum oven; m.p. 122.3°.

Formic Acid.—Baker and Adamson 98–100% formic acid was distilled from anhydrous calcium sulfate and then twice vacuum distilled from anhydrous sodium sulfate. The dried product was stored as a solid at 0° to avoid decomposition.

Acetic Acid.—J. T. Baker C.P. glacial acetic acid was distilled from anhydrous calcium sulfate and vacuum distilled from anhydrous sodium sulfate.

All materials were stored in a water-free atmosphere and samples were prepared in a dry box. The solutions were all made up by weight. The concentrations of the solutions are given in mole fraction units which avoids temperature dependence.

Measurement of Chemical Shifts.—All of the spectra were obtained on a Varian Associates Model V-4300B High Resolution NMR Spectrometer operating at 60 Mcps. and equipped with a Model V-K3506 Super Stabilizer. A number of solutions also were observed at 40 Mcps., the measured shifts agreeing within experimental error with those obtained at 60 Mcps.

Chemical shifts were measured by the side-band technique¹⁰ using a Hewlett-Packard Model 200J Audio Oscillator which was calibrated with a Hewlett-Packard Model 524B Electronic Counter. All shifts are reported in cycles per second, measured at 60 Mcps.

In the more concentrated solutions the shifts were measured directly on the oscilloscope by superimposing the audio sidebands of the reference peak directly on the peaks of interest. In the very dilute solutions the peaks were recorded with the sidebands of the reference peak placed on either side of the measured peak during recording, the actual position of the peak then being obtained by graphical interpolation between the sidebands. Shifts were measured to an accuracy of ± 0.5 c.p.s., and each reported shift is the result of at least six separate measurements.

Variable Temperature Apparatus.—For the purpose of maintaining the spinning samples at the desired temperatures, a special receiving coil insert for use in the Varian V-4331A probe was constructed. This insert and associated apparatus is shown in Fig. 1. Teflon plugs in the bottom of the insert provided a convenient arrangement for changing and adjusting the receiver coil in the apparatus, gave mechanical strength to the insert, and were an effective insulating barrier to heat flow to the rest of the probe.

(9) J. A. Pople, W. G. Schneider and H. J. Bernstein, "High Resolution Nuclear Magnetic Resonance," McGraw-Hill Book Co., Inc., New York, N. Y., 1959, pp. 400–421.

(10) J. T. Arnold and M. E. Packard, *J. Chem. Phys.*, **19**, 1608 (1951).

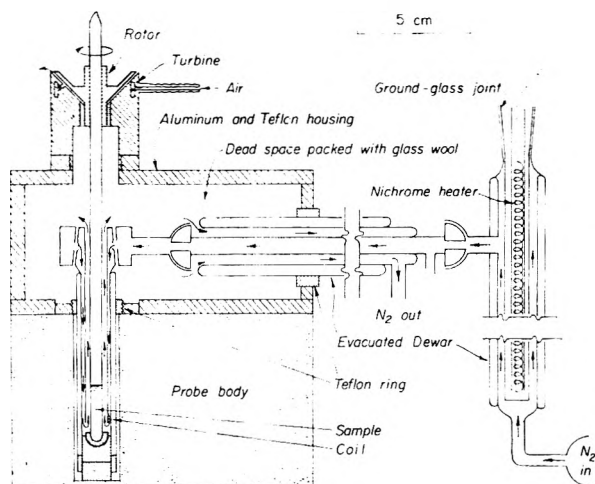


Fig. 1.—Variable temperature apparatus for high resolution n.m.r. studies.

The temperature of the nitrogen stream was monitored continuously to within $\pm 0.05^\circ$, and it was determined that the sample temperature could be determined to within $\pm 1.0^\circ$. The signal to noise ratio of the variable temperature insert was slightly less than that of the standard Varian insert. However, the resolution obtainable was comparable to normal operation.

Experimental Results

The shifts observed for the carboxyl protons of formic, acetic and benzoic acids in benzene solutions at several temperatures are listed in Tables I–III. The symbol α designates the total apparent mole fraction of acid in the solution assuming no association. The shifts are given in cycles per second measured at 60 Mcps., a negative shift indicating that the measured peak lies at a lower applied magnetic field than the reference peak from which the shift is measured.

The peak of the benzene solvent was used as a reference because of its convenient position and to avoid bulk susceptibility corrections. It was assumed that any changes in the bulk susceptibility of the solution would be experienced equally by the solvent and acid molecules. This was verified in two cases. Solutions of acetic acid in benzene showed no shift of the acid CH₃ protons more than 2 c.p.s. relative to the benzene. In addition, solutions of cyclohexane in benzene showed a similar constancy in the relative shifts. The use of an external standard would have required bulk susceptibility corrections which would very likely be in error due to the unknown effect of association on the susceptibility of the acid and the anomalous effects observed in aromatic solvents.¹¹ Also, accurate susceptibility data are lacking at the higher temperatures of this investigation.

The effect of temperature on the carboxyl protons of the benzoic acid solutions is illustrated in Fig. 2. The behavior of formic acid and acetic acid solutions was similar.

Several solutions of benzoic acid in CCl₄ were also studied at 25°. The carboxyl proton shifts measured relative to the largest peak displayed by the benzoic acid ring protons are given in Table IV.

(11) A. A. Bothner-By and R. E. Glick, *ibid.*, **26**, 1651 (1957).

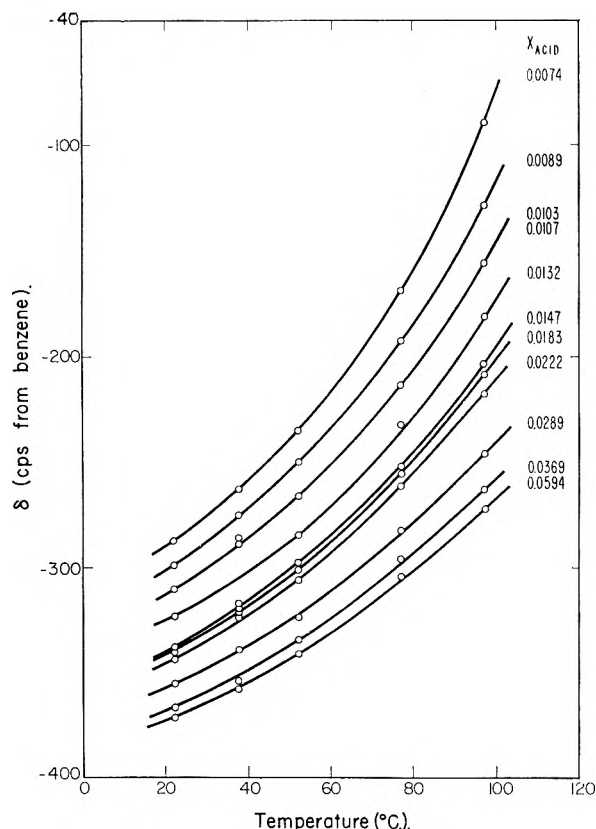


Fig. 2.—Effect of temperature on the carboxyl proton resonance of benzoic acid in benzene solutions of different concentrations.

TABLE I

CHEMICAL SHIFTS OF FORMIC ACID IN BENZENE SOLUTIONS

x_{acid}	δ (c.p.s. from benzene) ^a				
	23°	40°	53°	71°	110°
0.0088	-120	-87.3	-66.0	-37.5	Obscured by benzene peak
.0115	-147.3	-117.0	-75.0	-45.0	Obscured by benzene peak
.0136	-163.8	-134.1	-112.5	-75.0	Obscured by benzene peak
.0159	-173.1	-142.8	-116.7	-75.0	Obscured by benzene peak
.0171	-177.3	-147.6	-117.0	-82.5	-22.5
.0227	-209.1	-177.3	-150.3	-112.5	-55.8
.0268	-215.7	-187.5	-157.8	-123.0	-61.2
.0304	-219.0	-190.0	-165.3	-129.6	-64.8
.0354	-229.8	-200.7	-172.5	-130.5	-68.7
.0395	-235.2	-208.5	-183.6	-146.7	-85.5
.0464	-236.7	-211.2	-184.5	-153.0	-90.3
.0555	-241.5	-216.6	-192.0	-157.2	-97.8
.0660	-249.6	-225.3	-201.8	-157.8	-112.5
.0752	-250.5	-229.8	-210.3	-181.5	-127.8
.0854	-250.5	-226.8	-211.5	-183.5	-131.7
.0977	-250.8	-232.5	-213.9	-184.8	-130.8
.1225	-247.5	-231.3	-217.8	-198.0	-151.0
.1416	-242.4	-223.5	-209.4	-190.8	-140.7
.1587	-238.5	-225.0	-208.5	-190.5	-129.3

^a The shifts were measured at 60 Mc.; a negative value corresponds to a downfield shift from the internal reference, benzene.

Discussion

The Monomer-Dimer Equilibrium.—The carboxylic acids presumably associate to form a cyclic dimer in solution similar to that observed in the vapor phase.² It is not definitely known what form the higher polymers assume although infrared and dielectric measurements⁸ indicate that they are similar to those found in the crystalline acids in which each acid molecule is hydrogen bonded to two different acid molecules to form infinitely long

TABLE II

CHEMICAL SHIFTS OF ACETIC ACID IN BENZENE SOLUTIONS

x_{acid}	δ (c.p.s. from benzene) ^a			
	23°	49°	53°	77°
0.0100	-196.0	-152.0	-88.0
.0144	-197.0	-155.0	-92.2
.0131	-204.1	-163.1	-101.5
.0151	-232.3	-194.3	-135.1
.0223	-246.0	-209.1	-156.3
.0271	-262.1	-231.0	-187.1
.0360	-272.8	-242.8	-200.2
.0429	-278.0	-250.0	-244.0	-208.0
.0580	-284.1	-256.0	-252.2	-217.8
.0705	-291.2	-267.1	-260.9	-229.1
.0870	-298.0	-272.5	-267.1	-236.0

^a The shifts were measured at 60 Mc.; a negative value corresponds to a downfield shift from the internal reference, benzene.

TABLE III

CHEMICAL SHIFTS OF BENZOIC ACID IN BENZENE SOLUTIONS

x_{acid}	δ (c.p.s. from benzene) ^a				
	22°	37.5°	52°	77°	98°
0.0074	-287.0	-262.3	-235.0	-168.2	-88.1
.0087	-298.9	-275.0	-250.0	-192.2	-127.5
.0103	-310.2	-288.7	-266.0	-212.5	-154.8
.0107	-310.2	-288.7	-266.0	-212.5	-154.8
.0132	-323.0	-317.2	-284.1	-232.2	-180.9
.0147	-338.0	-319.1	-298.4	-252.0	-202.5
.0183	-339.0	-320.1	-301.0	-255.4	-208.1
.0222	-343.4	-323.7	-306.1	-261.5	-218.0
.0289	-355.1	-339.3	-323.0	-282.1	-245.9
.0369	-366.0	-354.0	-334.1	-296.0	-263.4
.0594	-371.0	-357.2	-340.9	-304.0	-271.1

^a The shifts were measured at 60 Mc.; a negative value corresponds to a downfield shift from the internal reference, benzene.

TABLE IV

CHEMICAL SHIFTS OF BENZOIC ACID IN CCl₄ SOLUTIONS AT 25°

x_{acid}	δ (c.p.s. from ring protons) ^a
0.0067	-274.0
.0074	-284.0
.0122	-305.1
.0154	-312.0
.0192	-318.0

^a The shifts were measured at 60 Mc.; a negative value corresponds to a downfield shift.

chains.⁷ Matrix isolation studies of solid formic acid have elucidated the variety of polymers that are formed as the concentration of acid in the inert matrix is varied.¹²

In dilute solution the monomer-cyclic dimer equilibrium is the most important. Huggins, Pimentel and Shoolery¹³ have shown that such a system can be studied advantageously by n.m.r. techniques. In the case where monomer and dimer species are in equilibrium, the observed shift δ of the carboxyl protons is given by the expression

$$\delta = \frac{m}{a} \delta_M + \frac{(a-m)}{a} \delta_D \quad (1)$$

where δ_M and δ_D are the characteristic monomer and

(12) R. Millikan and K. S. Pitzer, *J. Am. Chem. Soc.*, **80**, 3515 (1958); T. Miyazawa and K. S. Pitzer, *J. Chem. Phys.*, **30**, 1076 (1959).

(13) C. M. Huggins, G. C. Pimentel and J. N. Shoolery, *THIS JOURNAL*, **60**, 1311 (1956).

dimer shifts, m the moles of acid in the monomer form at equilibrium, and a the total moles of acid used to make up the solution. Letting s designate the total moles of solvent and x_M and x_D the mole fractions of monomer and dimer in solution, the equilibrium constant for the dimerization is

$$K_2 = \frac{x_D}{x_M^2} = \frac{(a-m)(2s+a+m)}{4m^2} \quad (2)$$

Huggins, *et al.*, have shown that at infinite dilution the slope of the δ vs. x curve is given by the expression

$$\left(\frac{\partial\delta}{\partial x}\right)_{x=0} = 2K_2(\delta_M - \delta_D) \quad (3)$$

It is thus possible to evaluate the equilibrium constant if δ_M , δ_D and the slope at infinite dilution are known. The former is the limiting value of δ at infinite dilution and δ_D may be evaluated, in the absence of higher polymers, from the extrapolation to a solution containing all dimer species.

The behavior of δ as a function of the mole fraction of benzoic acid in benzene at 30° is shown in Fig. 3a. The lower concentration region at the highest measured temperature where the most monomer is present is shown in Fig. 3b. It can be seen that for this system $d\delta/dx$ is still changing rapidly, even at conditions most suitable to monomer, and it is not possible to extrapolate to a limiting value for infinite dilution. This indicates that substantial association remains at $x = 0.01$. The association constant for benzoic acid is, in fact, of the order of 10^3 so that at $x = 0.01$ the degree of association is still rather large.

Although it is not possible to determine K_2 in such strongly associating systems by this method, it is still possible to obtain information about the monomer and dimer shifts δ_M and δ_D . A rearrangement of equation 2 leads to an expression for m/a

$$\frac{m}{a} = \frac{-s + [s + a(4K_2 + 1)(a + 2s)]^{1/2}}{a(4K_2 + 1)} \quad (4)$$

and that for $(a-m)/a$ follows directly. If then K_2 is known from some other source it is possible to determine m/a and $(a-m)/a$ for any solution prepared with s moles of solvent and a moles of acid. For a given solution, these calculated values can be substituted in equation 1 along with the measured δ for that solution. The unknown quantities δ_M and δ_D may then be obtained by solving any two such equations for two different acid solutions simultaneously.

Benzoic Acid.—The equilibrium constant for dimer formation in the benzoic acid-benzene system has been determined at several temperatures by a number of investigators.¹⁴ All of the results except the dielectric constant measurements are in excellent agreement with a ΔH of -8.4 ± 0.5 kcal. mole⁻¹. This value of ΔH , the value of K_2 at 30° of 5.25×10^3 , and equation 4 have been used to calculate m/a and $(a-m)/a$ for each solution at ten degree intervals to 100°. The monomer and dimer shifts then have been calculated

(14) H. A. Pohl, M. E. Hobbs and P. M. Gross, *J. Chem. Phys.*, **9**, 408 (1941); B. C. Barton and C. A. Krauss, *J. Am. Chem. Soc.*, **73**, 4561 (1951); G. Allen and E. F. Caldin, *Trans. Faraday Soc.*, **49**, 895 (1953); F. T. Wall and F. W. Banes, *J. Am. Chem. Soc.*, **67**, 848 (1945).

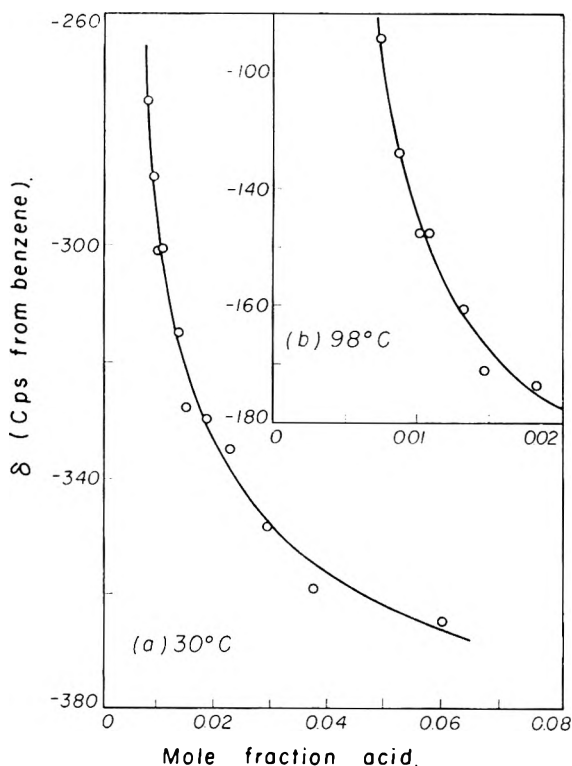


Fig. 3.—(a) Effect of concentration in benzene on the carboxyl proton resonance of benzoic acid at 30°; (b) effect of concentration at 98°.

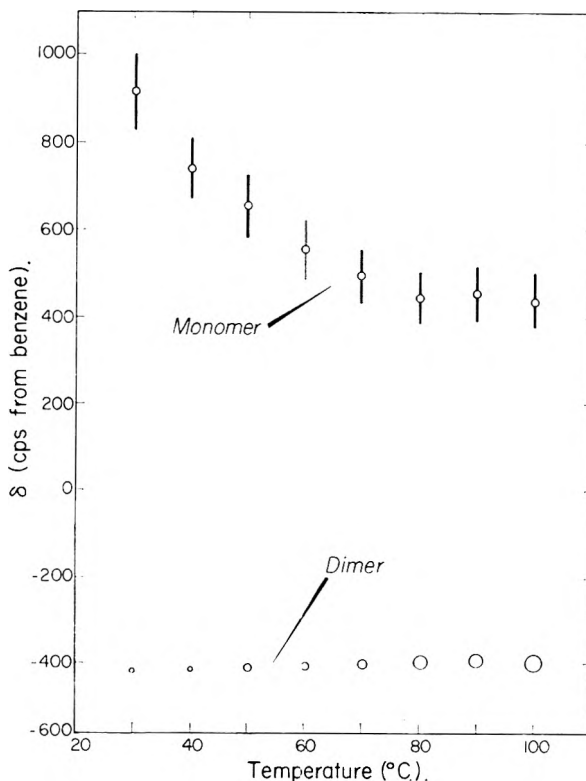


Fig. 4.—Calculated monomer and dimer shifts for benzoic acid in benzene at several temperatures.

with equation 1 by solving for every pair of benzoic acid solutions except those of nearly equal concentration. This was done independently at each

ten degree interval using the same pairs of solutions at each temperature.

The average values of δ_M and δ_D calculated at each temperature are in Table V. The errors given for each are average deviations of the calculated values from the means. These averages and their deviations are also illustrated in Fig. 4. It is seen that the calculated δ_D lies in the region usually measured for pure carboxylic acid shifts, and there is a slight shift to higher field with temperature which might be expected if the hydrogen bond were being weakened. The values for δ_M , however, are quite high. At 30° δ_M is at a higher field than has ever been reported previously for protons. The calculated δ_M drops rapidly with increasing temperature and approaches the region in which alcohol monomers also are found.

This behavior of the monomer shifts is strongly suggestive of an interaction of the monomer with the benzene solvent. It is recognized that molecules with acidic protons associate with benzene, and n.m.r. studies indicate in such an association the proton is drawn into the face of the benzene molecule rather than around the edge.¹⁵ It has been shown that the benzene molecule exhibits an anisotropic diamagnetic susceptibility which can be viewed as arising from a circulation of the mobile π electrons around the ring induced by the external magnetic field.¹⁶ These circulating electrons give rise to a secondary magnetic field around the benzene molecule. The magnitude of this field averaged over all orientations of the benzene molecule with time has been calculated by various means.¹⁷

TABLE V
CALCULATED MONOMER AND DIMER SHIFTS FOR BENZOIC ACID IN BENZENE
($\Delta H = -8.4$ kcal. mole⁻¹)

T, °C.	K_2	δ_M (c.p.s. from benzene)	δ_D (c.p.s. from benzene)
30	5250	915 ± 90	-423 ± 7
40	3390	740 ± 70	-416 ± 7
50	2290	655 ± 70	-413 ± 9
60	1510	556 ± 70	-407 ± 11
70	1050	498 ± 60	-402 ± 11
80	676	448 ± 60	-400 ± 14
90	525	460 ± 60	-398 ± 15
100	380	442 ± 60	-400 ± 18

If the carboxyl proton of an acid molecule is drawn into the face of the benzene ring near the symmetry axis, then it will experience a secondary field from the benzene molecule which opposes the external magnetic field, and a larger external field will be required for resonance. If the association is weakened at higher temperatures and the proton withdraws from the benzene ring, then the secondary field in the vicinity of the proton will be less and δ_M correspondingly will shift to lower field. This is the behavior observed for δ_M in Fig. 4.

(15) L. W. Reeves and W. G. Schneider, *Can. J. Chem.*, **35**, 251 (1957); D. Cook, Y. Lupien and W. G. Schneider, *ibid.*, **34**, 957, 964 (1956); C. M. Huggins, G. C. Pimentel and J. N. Shoolery, *J. Chem. Phys.*, **23**, 896 (1955).

(16) L. Pauling, *ibid.*, **4**, 673 (1936); J. A. Pople, *ibid.*, **24**, 1111 (1956).

(17) J. S. Waugh and R. W. Fessenden, *J. Am. Chem. Soc.*, **79**, 846 (1957); C. E. Johnson, Jr., and F. A. Bovey, *J. Chem. Phys.*, **29**, 1012 (1958).

When one attempts to make a quantitative treatment of the monomer-benzene interaction, serious difficulties arise. The benzoic acid dimerization enthalpy¹⁴ in the vapor exceeds that in benzene by approximately 3 kcal. per mole of monomer. This difference, which may be taken as a rough estimate of the energy of monomer-benzene association, will shift the logarithm of the ratio of associated to non-associated molecules by only 0.4 over the range 30 to 100°. This yields only a moderate change in the fraction associated with the benzene. The calculations of Johnson and Bovey require the proton to approach on the sixfold axis within 1.6 Å. of the face of the benzene ring, in order to experience a 450 c.p.s. shift from the ring current effect. This is as close an approach as is reasonable. But a 450 c.p.s. shift is observed over the experimental range 30-100° in Table V, and the total difference between associated and non-associated monomers must be considerably larger. A model with the acid proton sandwiched between two benzenes would yield a larger shift and might just barely fit the observation. These models are grossly over-simplified and it is not clear whether their refinement might yield quantitative agreement or not. Experiments are planned for other solutes in benzene where the results may be easier to interpret.

Other possible temperature effects on the acid proton are an increase in proportion of a *trans* isomer¹⁸ and an increase in the amplitude of torsional oscillation, but neither of these effects seems likely to account for the large change in δ_M in Table V.

Because the calculated δ_M depends on the assumed values of K_2 it is desirable to see whether large changes in K_2 are necessary in order to maintain δ_M at approximately 450 c.p.s. at all temperatures. Assuming the K_2 at 100° to remain unchanged and setting K_2 at 30° at a value which also gives a δ_M of 450 c.p.s. at 30° a new ΔH of -5.62 kcal. mole⁻¹ is obtained. The average values of δ_M and δ_D calculated from these new equilibrium constants are given in Table VI. The deviations are about the same as in Table V. It is seen that δ_M now decreases about 70 c.p.s. and then increases again, although the total fluctuation is of the order of the deviations in the calculated values. Apparently a set of equilibrium constants which would make δ_M exactly the same at all temperatures would not fall on a straight-line $\log K$ vs. $1/T$ plot. Although this adjusted value of K_2 at 30° is in closer agreement with the dielectric measurements (1.41×10^3), the disagreement with the freezing point, isopiestic, and boiling point studies both in K_2 and ΔH make it rather unlikely that this alternate interpretation is the correct one.

If the behavior of δ_M , as illustrated in Fig. 4, is caused by association of the acid with the aromatic solvent, then it should not be observed in more inert solvents such as CCl₄. An infrared determination of the dimerization of benzoic acid in CCl₄ has been

(18) See T. Miyazawa and K. S. Pitzer, *ibid.*, **30**, 1076 (1959), for information on the *trans* isomer of formic acid.

TABLE VI

CALCULATED MONOMER AND DIMER SHIFTS OF BENZOIC ACID IN BENZENE AFTER ADJUSTMENT OF EQUILIBRIUM CONSTANTS

$T, ^\circ\text{C.}$	K_2	$(\Delta H = -5.62 \text{ kcal. mole}^{-1})$	
		δ_M (c.p.s. from benzene)	δ_D (c.p.s. from benzene)
30	2200	450	-425
40	1622	413	-419
50	1230	388	-415
60	955	381	-410
70	741	380	-407
80	589	398	-405
90	468	424	-403
100	380	442	-400

reported.¹⁹ The K_2 at 25° converted to mole fraction units was calculated to be 4.56×10^4 . Unfortunately, the concentration range of our n.m.r. data, which are given in Table IV, was severely limited by the solubility of the acid in CCl_4 and the signal to noise ratio of the spectrometer. On the basis of these limited measurements δ_M and δ_D were calculated to be $2,267 \pm 302$ and -399 ± 9 c.p.s. from benzene after correcting for the bulk susceptibility differences in benzene and CCl_4 . This monomer shift is even higher than that calculated for the benzene solutions, suggesting some cause other than solvent association. On the other hand, the concentrations of the solutions were limited to a very small range and, in addition, the reliability of the infrared equilibrium constant is unknown. There are no other measurements of the benzoic acid- CCl_4 system, but comparison of the distribution and infrared studies of acetic acid in CCl_4 shows the infrared K_2 to be about ten times that obtained from the distribution measurements.^{3,18} A K_2 of 4.2×10^3 would bring the calculated δ_M to about 440 c.p.s. and δ_D to -396 c.p.s.

It is possible that the very high δ_M values may be spurious and may have arisen from these calculations because of the very small amounts of monomer as compared to dimer. However, the average deviations from the means are relatively consistent throughout the temperature range in Table V, and it is not clear that such an error should be predominantly in one direction rather than random.

Formic and Acetic Acid.—Only one investigation of the monomer-dimer equilibrium for formic acid in benzene has been reported.¹⁴ A K_2 of 1.41×10^3 was calculated from dielectric constant data at 30°. Since no values of ΔH have been reported it was only possible to calculate the monomer and dimer shifts for one temperature. The average values at 30° are 908 ± 141 and -333 ± 19 c.p.s., respectively.

The acetic acid-benzene system has been investigated by study of the distribution of acetic acid between benzene and water and by measurement of the dielectric constant.^{14,20} The calculations by Davies appear to be the most reliable, having taken into account the solubility of water in the solvent,

association in the aqueous phase, and possible higher polymers. The equilibrium constants obtained by Davies were used to calculate the monomer and dimer shifts for acetic acid in benzene at several temperatures. Davies' values of $\Delta H = -8.89 \text{ kcal. mole}^{-1}$ and $\Delta S = 19.82 \text{ cal. deg.}^{-1} \text{ mole}^{-1}$ were used to calculate K_2 at higher temperatures. The resulting constants and shifts are listed in Table VII.

TABLE VII

CALCULATED MONOMER AND DIMER SHIFTS FOR ACETIC ACID IN BENZENE

$T, ^\circ\text{C.}$	K_2	$(\Delta H = -8.2 \text{ kcal. mole}^{-1})$	
		δ_M (c.p.s. from benzene)	δ_D (c.p.s. from benzene)
30	1360	547 ± 122	-348 ± 16
40	831	421 ± 107	-341 ± 15
50	536	293 ± 95	-332 ± 12
60	371	199 ± 92	-320 ± 14
70	235	122 ± 94	-308 ± 11
80	161	102 ± 101	-310 ± 13

The behavior of δ_M is similar to that observed for benzoic acid in benzene but the shifts are at much lower field than calculated for the latter system. The change of δ_M with temperature is approximately the same as for benzoic acid. This offers support for the postulated complexing with the solvent. The K_2 calculated from dielectric studies is much higher than Davies' value and yields considerably larger monomer shifts.

The average δ_D for the three acids shifts to lower applied magnetic fields in the order formic, acetic, benzoic. Since a shift to lower field is characteristic of the formation of a hydrogen bond, this trend may indicate increasing strength of hydrogen bonding in the three acids in that order. The magnitudes of the shift of the hydroxyl stretching frequency in the infrared are also observed to increase in this order.²¹

High Polymers.—It has not been possible to determine the nature or amount of higher polymers in these dilute solutions. The larger deviations of the calculated monomer and dimer shifts for formic acid and acetic acid might indicate interference by higher polymers, but no particular trends were observed to be dependent on whether pairs of solutions in the low or high concentration regions were used in the calculations. The behavior of the observed shifts at higher concentrations is interesting, however. None of the observed shifts reached the calculated dimer values in the concentration ranges studied. The aliphatic acids, in fact, show a shift of the resonance back toward higher field at greater concentrations. This behavior was first observed by Reeves and Schneider²² for acetic acid in several solvents and was again observed in this study. The shift of δ for pure acetic acid toward higher field amounts to about 60 c.p.s. from the lowest observed shift, or about 110 c.p.s. from the calculated dimer frequency. A similar shift was observed for formic

(21) L. J. Bellamy, "Infrared Spectra of Complex Molecules," John Wiley and Sons, Inc., New York, N. Y., 1958.

(22) L. W. Reeves and W. G. Schneider, *Trans. Faraday Soc.*, **54**, 314 (1958); L. W. Reeves, *ibid.*, **55**, 1684 (1959).

(19) J. Wenograd and R. A. Spurr, *J. Am. Chem. Soc.*, **79**, 5844 (1957).

(20) M. Davies, *Z. physik. Chem. (Frankfurt) N.F.*, **2**, 353 (1954).

acid, and the pure acid resonance is about 100 c.p.s. to higher field from the calculated δ_D .

In the formation of hydrogen-bonded polymers larger than the dimer it generally has been observed that the OH stretching frequency in the infrared is shifted a larger amount than in the dimer, indicating a stronger hydrogen bond in the higher polymers.²¹ On this basis it would be expected that the stronger hydrogen bonds in the higher polymers would also cause a corresponding shift of the n.m.r. resonance to lower field than in the dimer. This has been observed in the alcohols and phenols.⁹ Reeves and Schneider²² have suggested that the hydrogen bonds in the higher polymers of the acids are not as strong as in the dimer, but such an argument does not seem reasonable since the polymers presumably have lower entropy per monomer unit but are formed preferentially at higher concentrations in competition with the dimer. Also it is known that the hydrogen bonds in the polymer in crystals are shorter than the bonds in cyclic dimer.⁶

It seems to us much more likely that the n.m.r. shift is not a reliable indicator of hydrogen bond strength because this shift is influenced by factors which have no effect (or may even have a reverse effect) on the bond strength. Thus in the higher polymers the O—O distance may be small enough for the unbonded oxygen electrons to contribute significantly to a diamagnetic shielding of the carboxyl

proton. The O—O distance in formic acid dimer is 2.75 Å.; while that in the polymer present in the solid is reduced to 2.58 Å. The actual O—O distance in the polymers in solution may also be of this magnitude. Several molecules are known in which this distance is extremely short because of steric reasons. Examples are maleic acid (2.46 Å.) and Ni-dimethylglyoxime (2.44 Å.). It has not been possible to observe the n.m.r. shift of these compounds in non-hydrogen-bonding solvents because of their limited solubilities. It would be desirable to do so, since then only the hydrogen bonds of the molecule of interest would be observed. Several solutions of maleic acid in acetone have been measured, and an extrapolation of the shifts toward pure maleic acid indicates that the shift in the absence of bonding with acetone is about 250 c.p.s. below benzene. This is a little higher than that usually observed for hydrogen-bonded acids (300–400 c.p.s. below benzene), but not appreciably so. Since this average shift includes the internally bound hydrogen as well as the hydrogen bond in the dimer, the higher observed shielding may reflect a higher shielding in the internal bond.

Acknowledgment.—The authors wish to express their appreciation to Dr. George C. Pimentel for many helpful discussions and to Dr. Power Sogo for aid with electronic problems. A portion of this work was supported by the Atomic Energy Commission.

KINETICS OF *n*-PENTANE ISOMERIZATION OVER Pt-Al₂O₃ CATALYST

BY J. H. SINFELT, H. HURWITZ AND J. C. ROHRER

Esso Research and Engineering Company, Linden, N. J.

Received January 16, 1960

The kinetics of *n*-pentane isomerization over a Pt-Al₂O₃ catalyst were investigated at 372°. The reaction was carried out in a flow reactor in the presence of added hydrogen at pressures ranging from 7.7 to 27.7 atm. and hydrogen to *n*-pentane ratios ranging from 1.4 to 18. The rate of isomerization was found to correlate with the *n*-pentane to hydrogen mole ratio and to be independent of total reactor pressure at a fixed *n*-pentane to hydrogen ratio. These results can be explained in terms of the postulated mechanism by which isomerization proceeds *via* an olefin intermediate present in equilibrium concentration. According to this mechanism *n*-pentane dehydrogenates on platinum sites to *n*-pentene, which in turn migrates to acidic sites to isomerize, presumably by a carbonium ion mechanism. The rate-controlling step is the isomerization of the intermediate olefin on acidic sites.

Introduction

Isomerization of *n*-paraffins over dual-function catalysts is becoming increasingly important in the petroleum industry. The dual-function catalysts consist of an active hydrogenation-dehydrogenation component such as platinum supported on an acidic oxide such as alumina or silica-alumina. A mechanism involving olefin intermediates has been proposed by several investigators for isomerization of paraffins over these catalysts.^{1–3} According to this mechanism the dehydrogenation component of the catalyst generates the intermediate olefin which migrates to acidic sites to isomerize, presumably *via* a carbonium ion mechanism. In general, either the dehydrogenation or acidic func-

tion may be rate controlling, depending on catalyst and reaction conditions. With these thoughts in mind it was decided to investigate the kinetics of *n*-pentane isomerization over a Pt-Al₂O₃ catalyst to check the proposed mechanism.

Experimental

Materials.—Phillips pure grade *n*-pentane (>99 mole % purity) was used in these experiments. The *n*-pentane was dried with Drierite (CaSO₄) to less than 5 p.p.m. H₂O before using. The hydrogen used was passed through a Deoxo cylinder containing palladium catalyst to convert trace amounts of oxygen to water, and then dried over Linde 5A molecular sieves. The catalyst contained 0.3% platinum supported on alumina and was prepared by impregnation of alumina with aqueous chloroplatinic acid. The surface area of the catalyst was 155 m.²/g. The catalyst was used in the form of pellets with an equivalent spherical diameter of about 1/8 inch.

Procedure.—The reaction studies were carried out in the presence of added hydrogen in a flow system using a 1/2 inch i.d. stainless steel reactor containing 15 g. of catalyst. The

(1) G. A. Mills, H. Heinemann, T. H. Milliken and A. G. Oblad, *Ind. Eng. Chem.*, **45**, No. 1, 134 (1953).

(2) F. G. Ciapetta and J. B. Hunter, *ibid.*, **45**, 147 (1953).

(3) P. B. Weisz and E. W. Swegler, *Science*, **126**, 31 (1957).

TABLE I
n-PENTANE ISOMERIZATION AT 372°—PRODUCT COMPOSITION DATA

Period no.	5	6	7	8	9	10	11	12	13
Pressure, atm.	27.7	27.7	7.7	7.7	24.4	24.4	11.0	21.0	11.0
H ₂ / <i>n</i> -C ₅	5.0	5.0	5.0	5.0	18.0	18.0	1.4	5.0	1.4
LHSV ^a	26.4	9.3	26.7	9.1	23.4	9.1	26.6	26.5	9.4
Composition, mole % ^b									
C ₁	0.1	0.1		0.1		0.1			0.2
C ₂	.2	.3	0.1	.2	0.2	.3	0.1	0.1	.1
C ₃	.2	.3		.2	0.1	.2	0.1	0.1	.2
<i>n</i> -C ₄	.1	.1		.1		.1			.1
<i>i</i> -C ₄									.1
<i>n</i> -C ₅	94.0	85.8	95.1	87.4	95.9	92.2	90.7	95.1	82.1
<i>i</i> -C ₅	5.5	13.4	4.7	12.0	3.4	7.1	8.8	4.5	17.5
Cyclo-C ₅	0.2	0.2		0.2	0.2	0.1	0.2	0.2	0.2

^a Liquid hourly space velocity, g. *n*-pentane/hr./g. catalyst. ^b Where blank spaces occur the amount present is less than 0.1%.

reactor was surrounded by an electrically heated aluminum block to maintain isothermal operation. The catalyst was pretreated with hydrogen for three hours at 527° prior to introducing the *n*-pentane feed. Reaction products were analyzed by a chromatographic column coupled directly to the outlet of the reactor.

Reaction periods of 30 minutes were employed throughout this work. This was found to be more than adequate for attainment of steady-state conditions prior to sampling. Reaction temperature was maintained at 372° for all the *n*-pentane runs. Total pressure was varied from 7.7 to 27.7 atm., and the hydrogen to *n*-pentane mole ratio from 1.4 to 18. Liquid hourly space velocities ranged from 9.1 to 26.7 g./hr./g. catalyst. The *n*-pentane conversion levels ranged from 4.1 to 17.9%.

Results

The *n*-pentane isomerization experiments were made at low conversion levels to minimize the effects of secondary reactions. The reaction rate r is defined by the expression

$$r = \frac{F dx}{dW} \quad (1)$$

where F is the *n*-pentane feed rate in g. mole/hr. and dx is the fractional conversion obtained in an element of catalyst dW . Thus, the slope at the origin of a plot of fractional conversion vs. W/F is the initial reaction rate. The quantity W/F is the reciprocal of the space velocity. By making the experiments at low conversion levels the initial rates can be determined satisfactorily.

The reaction kinetics were investigated by varying the *n*-pentane and hydrogen partial pressures individually and noting the effects on initial isomerization rates. Detailed product composition data from which the rates were calculated are shown in Table I. Small amounts of hydrocracking and cyclization were noted in addition to isomerization, but the selectivity to isomerization was 90–95%. Isomerization rates are summarized in Table II. The rate was found to increase with increasing *n*-pentane partial pressure but to decrease with increasing hydrogen partial pressure. At a constant *n*-pentane to hydrogen mole ratio, the rate was found to be independent of total pressure. The reaction rates can be correlated with the *n*-pentane to hydrogen mole ratio. The rate data are fitted satisfactorily by an equation of the form

$$r = k \left(\frac{p_{nC_5}}{p_{H_2}} \right)^n \quad (2)$$

where the constants k and n at 372° take the values 0.040 and 0.5, respectively, when the rates are expressed in g. moles/hr./g. catalyst.

TABLE II

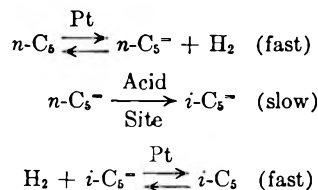
 SUMMARY OF *n*-PENTANE ISOMERIZATION RATES AT 372°

Pressure, atm.	24.4	7.7	21.0	27.7	11.0
Total	24.4	7.7	21.0	27.7	11.0
<i>n</i> -C ₅	1.3	1.3	3.5	4.6	4.6
H ₂	23.1	6.4	17.5	23.1	6.4
Reaction rate ^a	0.011	0.018	0.017	0.020	0.034

^a Initial rate (zero conversion), g. mole/hr./g. catalyst.

Discussion

These results support the postulated mechanism by which paraffin isomerization proceeds via an olefin intermediate, with the rate-controlling step being the reaction of the olefin on acidic sites.



The *n*-pentene which is formed on the platinum is in equilibrium with *n*-pentane and hydrogen in the gas phase, so that the partial pressure of the *n*-pentene is given by

$$p_{nC_5^-} = K \frac{p_{nC_5}}{p_{H_2}} \quad (3)$$

where K is the thermodynamic equilibrium constant and $p_{nC_5^-}$, p_{nC_5} , and p_{H_2} are the partial pressures of *n*-pentene, *n*-pentane and hydrogen, respectively. The *n*-pentene migrates to an acidic site where it is adsorbed. The adsorbed *n*-pentene then isomerizes, presumably by a carbonium ion mechanism. The rate of this step is controlling and therefore the over-all rate is given by

$$r = k' [n\text{-C}_5^-]_a \quad (4)$$

where k' is the rate constant and $[n\text{-C}_5^-]_a$ is the concentration of adsorbed *n*-pentene. The concentration of adsorbed *n*-pentene may be related to the *n*-pentene partial pressure in the gas phase by a Freundlich type relation

$$[n\text{-C}_5^-]_a = b p_{nC_5^-}^n \quad (5)$$

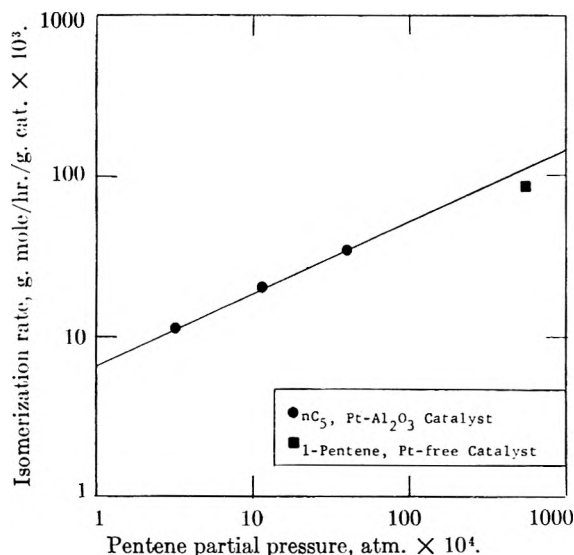


Fig. 1.—Isomerization rate *vs.* pentene partial pressure.

where b and n are constants. Substituting equations 3 and 5 into 4 the rate expression becomes

$$\begin{aligned} r &= k' b K^n \left(\frac{p_{nC_5}}{p_{H_2}} \right)^n \\ &= k \left(\frac{p_{nC_5}}{p_{H_2}} \right)^n \end{aligned} \quad (6)$$

which is identical with the form of equation 2 found by experiment.

The rate equation could also be expressed in the form

$$r = \frac{k'' p_{nC_5} / p_{H_2}}{1 + m p_{nC_5} / p_{H_2}} \quad (7)$$

which follows from the assumption that the Langmuir adsorption isotherm applies in relating the concentration of adsorbed n -pentene to its partial pressure in the gas phase. However, the simple Langmuir equation is strictly applicable to a homogeneous surface, which is very likely not the case for the type of catalyst used here. To apply the Langmuir equation rigorously it is necessary to account for differences in activity of the various sites. If it is assumed that the active sites are distributed exponentially with respect to the energy of adsorption, it has been shown that the Freundlich type isotherm is a reasonable approximation.⁴

The assumption of olefin intermediates in isomerization is supported by the observation of olefins in the reaction products. However, at 372° and at the hydrogen pressures used in this work the equilibrium concentration of olefins is very low (<0.1%), and the accuracy of the analyses at these low concentrations was not good enough to establish that equilibrium concentrations of olefins were attained.

The results of an experiment in which 1-pentene was passed over a sample of the catalyst containing no platinum lend additional strong support to the proposed mechanism. In this case the catalyst possesses only the acid function, and if the proposed mechanism is correct, it should be possible to

predict the rate of pentene isomerization to methylbutenes over this catalyst from the results on n -pentane isomerization over the Pt-Al₂O₃ catalyst. Figure 1 is a plot of the rate of n -pentane isomerization over the Pt-Al₂O₃ catalyst *vs.* the calculated equilibrium partial pressure of n -pentenes at the conditions of the experiments. The equilibrium partial pressures were calculated from free energy data compiled in API Project 44.⁵ Also included in the plot is a point showing the rate of 1-pentene isomerization over the Pt-free catalyst. This point is found to agree with the rate predicted from n -pentane data within about 25%, which is considered to be strong evidence that the rate-controlling step in n -pentane isomerization is the isomerization of the pentene intermediate on acidic sites.

That the rate-controlling step in paraffin isomerization is the isomerization of the olefin intermediate is also supported by results on n -heptane at 471°, 21 atmospheres total pressure, and 5:1 hydrogen to n -heptane mole ratio. In these experiments the dehydrogenation activity of the catalyst was varied by changing the platinum content, while the acid function of the catalyst remained unchanged. Increasing platinum content from 0.1 to 0.6 wt. % had essentially no effect on the rate of isomerization, the rate increasing only from 0.11 to 0.12 g. mole/hr./g. catalyst. Thus, even at the lowest platinum content the dehydrogenation activity of the catalyst was sufficient to maintain an equilibrium between paraffin and olefin in the gas phase. The isomerization rate is therefore controlled by the acid activity of the catalyst.

As mentioned previously the reaction of the olefin intermediate on acidic sites can be pictured in terms of a carbonium ion mechanism. The adsorption of the olefin results in the formation of a carbonium ion by addition of a proton from the catalyst surface. The carbonium ion then rearranges on the surface according to the rules for carbonium ion reactions.⁶ The isomerized carbonium ions can revert to isoolefins by elimination of a proton. The isoolefins then migrate to platinum sites where they are hydrogenated to the corresponding isoparaffins, thus completing the reaction.

Conclusion

Kinetic data on n -pentane isomerization over Pt-Al₂O₃ catalyst support the postulated mechanism by which paraffin isomerization proceeds *via* an olefin intermediate. At the conditions used in this work the rate-controlling step is the isomerization of the intermediate olefin.

Acknowledgment.—The authors wish to express their appreciation to the Esso Research and Engineering Company for permission to publish the results of this work. The authors also wish to thank Professor M. Boudart for helpful discussions and encouragement in this work.

(5) "Selected Values of Physical and Thermodynamic Properties of Hydrocarbons and Related Compounds," API Research Project 44, Carnegie Press, Inc., New York, N. Y., 1953.

(6) F. C. Whitmore, *J. Am. Chem. Soc.*, **54**, 3274 (1932).

(4) J. Zeldowitch, *Acta physicochim. U.S.S.R.*, **1**, 961 (1935).

KINETICS OF HYDROLYSIS OF POLYETHYLENE TEREPHTHALATE FILMS

BY R. C. GOLIKE AND S. W. LASOSKI, JR.

Film Department, Yerkes Research Laboratory, E. I. du Pont de Nemours & Co., Inc., Buffalo, New York

Received January 21, 1960

The hydrolytic degradation of polyethylene terephthalate films as measured by molecular weight change has been shown to be a second-order reaction limited by diffusion of water into the film. The theoretical equations defining such a reaction were developed. Through application of these equations, it was possible to define accurately the rate of degradation of ethylene terephthalate film over the temperature range of 60 to 175° over water activities of essentially zero to one, and over four orders of magnitude in rate.

Introduction

Several works dealing with the degradation of polyethylene terephthalate have been reported; however, thus far, only a semi-quantitative definition of the kinetics of hydrolytic degradation has evolved.¹⁻³ From work on the kinetics and mechanisms of thermal degradation^{1,2} in the molten state and on photolysis³ it may be estimated that at moderate temperatures, e.g., below 150°, the only appreciable degradation will occur by hydrolysis of the ester linkages. A rigorous description of hydrolysis kinetics would seem to require that consideration be given to the fact that the reaction takes place in the solid state. This would require such factors as the degree of water sorption and the rate of water diffusion be taken into account since they will vary with the physical structures of the solid. The main objective of this work was to isolate the specific rate constant for the hydrolysis reaction of polyethylene terephthalate in film form, to define its dependence upon temperature, and to account for its dependence upon the factors mentioned above.

Experimental

Samples of films 0.0025, 0.0075, 0.0125 and 0.0187 cm. in thickness were exposed at various water activities in the temperature range of 60 to 175°. At temperatures of 60, 80 and 100° samples were exposed in containers placed in ovens at constant temperatures; water activities of 1.0, 0.51 and 0.23 were maintained by placing water, saturated sodium bromide and saturated sodium iodide solutions, respectively, in these containers. At temperatures of 125, 150 and 175° samples were exposed in an air-tight oven with an internal circulating system. In these cases, air containing 18 mm. partial pressure of water vapor was continuously introduced; the water content of the discharge air stream was continuously monitored to ensure that the correct water concentration was maintained in the oven. A set of samples also was exposed by sealing films in "Citrate of Magnesia" bottles containing enough water to provide saturated conditions and placing the bottles in an oven at 136°.

Since polyethylene terephthalate crystallizes at temperatures above the glass transition temperature of about 70°, it was not possible to carry out most of the above on amorphous films.⁹ Therefore, a set of oriented semicrystalline films was used. These were specially selected to have the

same initial intrinsic viscosities and levels of orientation and crystallinity. (These were selected Types C and D "Mylar" polyester films.) Exposure of one amorphous film at 60° was carried out in order to compare data on comparable amorphous and oriented crystalline films.

In all the above exposures, samples were removed after the desired times and their intrinsic viscosity measured in tetrachloroethane-phenol solution.⁸ From the decrease in viscosity the number of moles of ester linkages hydrolyzed per mole of polymer was calculated; the details of this calculation are given in Appendix A.

Simple Kinetic Analysis

In order to show the basis for presenting the experimental results it is desirable to present a simple picture of the hydrolysis kinetics. If the reaction obeys second-order kinetics then it will be defined by

$$\frac{dn}{dt} = k(A - n)(B - n) \quad (1)$$

where

k = specific reaction rate constant

n = moles of ester linkages hydrolyzed per mole of polymer

A = moles of ester linkages initially present per mole of polymer

B = moles of water initially present per mole of polymer

t = time

If it is assumed that maintaining samples at constant humidity maintains constant water concentration in the film then $(B - n)$ may be replaced by C , which is the effective water concentration and which has the same units as B . Therefore, the reaction may be described as a pseudo first-order reaction, and equation 2 becomes

$$\frac{dn}{dt} = kC(A - n) \quad (2)$$

which integrates simply to

$$\ln(1 - n/A) = -kCt \quad (3)$$

The value of A , which is the average number of ester linkages per mole of polymer, is calculated from the initial number average molecular weight. The intrinsic viscosity of all samples studied was 0.58 ± 0.01 which corresponds to a number average molecular weight of 13,800.⁸ For this polymer, A equals 144. Since the diffusion and sorption of water in these films has been shown to be limited to the amorphous portion,¹⁰ it was assumed that hydrolysis occurred only in the amorphous fraction of the film. Therefore, the value of A was corrected in proportion. The density of the films was 1.389 which corresponds to an amorphous fraction of 0.53.¹⁰ Hence, the corrected value of A is

(10) S. W. Lasoski, Jr., and W. H. Cobbs, Jr., *J. Polymer Sci.*, **36**, 21 (1959).

- (1) H. A. Pohl, *J. Am. Chem. Soc.*, **73**, 5660 (1951).
- (2) I. Marshall and A. Todd, *Trans. Faraday Soc.*, **49**, 67 (1953).
- (3) J. R. Whinfield, *Endeavor XI*, **41**, 29 (1952).
- (4) R. A. Hudson, *British Plastics*, **26**, 6 (1953).
- (5) D. G. Bannerman and E. E. Magat in "Polymer Processes," C. E. Schildknecht, editor, Interscience Pub., New York, N. Y., 1956.
- (6) H. A. McMahon, et al., *Chemical and Engineering Data Series*, **4**, 57 (1959).
- (7) J. P. Harrington and R. J. Ward, Hermetic Motor Systems Insulated with "Mylar" (Du Pont registered trademark) Polyester Film: ASRE Meeting, New Orleans, December, 1958.
- (8) K. R. Osborn, *J. Polymer Sci.*, **38**, 357 (1959).
- (9) H. J. Kolb and E. F. Izard, *J. Appl. Phys.*, **20**, 564, 571 (1950).

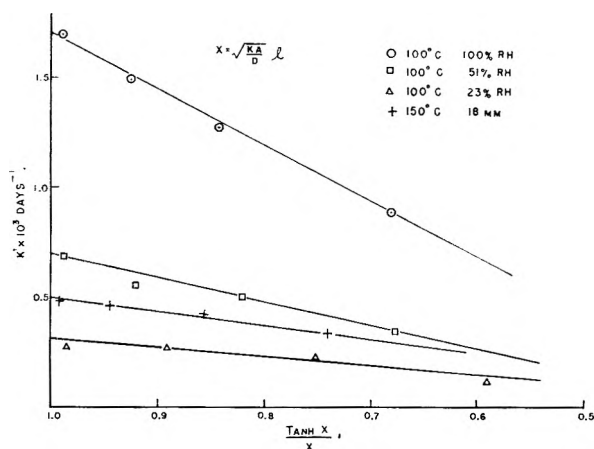


Fig. 1.

$144 \times 0.53 = 76$. It should be noted that, since all these films had the same initial molecular weight and degree of crystallinity, any error in the above value of A would be important only in comparison of these data with those on other films and would have no effect on the conclusions reached here. From the above value of A and the values of n shown in Table I, it can be seen that n/A will be less than about 0.02; this maximum value corresponds to a reduction in the number average molecular weight by a factor of 2.5. For these small values of n/A , equation 4 reduces to

$$\frac{n}{A} = kCt = k't \quad (5)$$

From values of n and t obtained in the manner noted, values of kC , denoted k' , were calculated by the least-squares method for the various exposure conditions. In Table I an example of the data and calculation for one exposure are shown.

TABLE I

EXAMPLE OF CALCULATION OF k'
100°, 51% RH, 0.0125 cm. film

$$kC = \frac{\sum \frac{n_i t_i}{A}}{\sum t_i^2} = \frac{1.945}{3576} = 5.44 \times 10^{-4} \text{ days}^{-1}$$

t , days	$[\eta]t$	$\frac{n_i}{A}$ (mole/mole of polymer)	$\frac{n_i t_i}{A}$	t_i^2
0	0.58	0	0	0
7	.55	0.11	0.010	49
10	.49	.38	.051	100
17	.43	.77	.174	289
20	.33	.77	.203	400
27	.40	1.03	.367	729
28	.38	1.24	.457	784
35	.36	1.48	.683	1225
$\sum \frac{n_i t_i}{A} = 1.945$			$\sum t_i^2 = 3576$	

In Table II values of k' for the films studied at various exposure conditions are summarized. Examination of these data reveals large variations in k' with film thickness at many exposure conditions. This behavior indicated the reaction was limited by the diffusion of water molecules into the film. In order to carry out a rigorous analysis, it will therefore be necessary to analyze the data in terms of a diffusion limited reaction.

Theory of Diffusion Limited Hydrolysis.—If the hydrolysis is limited by diffusion of water into the film the value of C in equation 2 is not a simple function of water activity but should also be a function of both the rate of chemical reaction and the rate of water diffusion. In order to develop the expression for k' under such conditions, the equations for the diffusion process and the chemical reaction were set up as they apply to a thin film. These were solved for steady-state conditions to yield an equation defining the reaction under such conditions. The details of this development are given in Appendix B. The end result is that, for the diffusion limited reaction, equation 5 must be replaced by

$$\frac{n}{A} = \left[kC_0 \frac{\tanh \sqrt{\frac{kA}{D}} l}{\sqrt{\frac{kA}{D}} l} \right] t = k't \quad (6)$$

where

C_0 is the water concn. at the film surface

D is the diffusion coefficient

l is one-half the film thickness

To apply this equation it is necessary to know kA/D to a reasonable approximation or to calculate families of curves for various values. It will be convenient to use the approximation $\tanh x/x = 1 - x^2/3$ which is valid for small values of x ; use of this gives

$$k' \cong kC_0 - \frac{kC_0}{3} \left(\frac{kA}{D} \right) l^2 \quad (7)$$

If $\sqrt{(kA/D)l}$ is small enough that the above approximation is valid, equation 7 can be used; if not, equation 7 may be used as a means of approximating $\sqrt{kA/D}$ for use in equation 6.

Discussion of Results

Figure 1 shows values of k' at 100 and 150° plotted vs. $\tanh \sqrt{(kA/D)l} / \sqrt{(kA/D)l}$. Values of k' were first plotted vs. l^2 and values of $\sqrt{kA/D}$ were calculated from the slopes and intercepts of these plots according to equation 7. These values were then used in obtaining the abscissa of Fig. 1. The excellent agreement between experimental data and the theoretical equations is felt to confirm both the equations which were developed and that the reaction is limited by diffusion. Table III summarizes values of kC_0 , the rate constant at zero thickness, and $\sqrt{kA/D}$, which were obtained from Fig. 1 and similar plots of data at other temperatures.

Having removed the dependence of rate of hydrolysis on the diffusion of water into the film, it is possible to define more accurately the dependence of rate upon water concentration. The concentration of water is best expressed in terms of activity, the quantity p/p_0 , where p is the partial pressure and p_0 the vapor pressure at that temperature. Upon examination of values of kC_0 at 100 and 80° at various relative humidities shown in Table III, it may be seen that there will be no large error introduced if it is assumed that kC_0 and, since k is independent of concentration, C_0 are linear

TABLE II

VALUE OF k' IN DAYS⁻¹

Exposure conditions		0.0025 cm. film	0.0075 cm. film	0.0125 cm. film	0.0187 cm. film
175°	18 mm.	6.19×10^{-4}	9.08×10^{-4}	9.08×10^{-4}	8.42×10^{-4}
150	18 mm.	4.74×10^{-4}	4.61×10^{-4}	4.21×10^{-4}	3.29×10^{-4}
125	18 mm.	2.00×10^{-4}	1.82×10^{-4}	1.91×10^{-4}	1.24×10^{-4}
136	100% RH	3.7×10^{-2}	3.90×10^{-2}	4.47×10^{-2}	3.17×10^{-2}
100	100% RH	1.70×10^{-3}	1.50×10^{-3}	1.28×10^{-3}	8.90×10^{-4}
100	51% RH	6.83×10^{-4}	5.44×10^{-4}	5.00×10^{-4}	3.42×10^{-4}
100	23% RH	2.76×10^{-4}	2.63×10^{-4}	2.24×10^{-4}	1.16×10^{-4}
80	100% RH	2.97×10^{-4}	2.74×10^{-4}	2.28×10^{-4}	1.53×10^{-4}
80	51% RH	1.34×10^{-4}	9.87×10^{-5}	1.03×10^{-4}	4.61×10^{-5}
80	23% RH	6.71×10^{-5}	3.42×10^{-5}	4.34×10^{-5}	1.58×10^{-5}
60	100% RH	3.37×10^{-5}	1.82×10^{-5}	1.93×10^{-5}	8.95×10^{-6}
60	51% RH	2.55×10^{-5}	1.27×10^{-5}	2.41×10^{-5}	6.71×10^{-6}

TABLE III

Conditions	p/p_0	kC_0 (days ⁻¹)	$\sqrt{kA/D}$
175°, 18 mm.	0.0026	8.15×10^{-4}	..
150, 18 mm.	0.0049	4.97×10^{-4}	112
136, 100% RH	1.00	3.80×10^{-2}	..
125, 18 mm.	0.010	2.03×10^{-4}	119
100, 100%	1.00	1.72×10^{-3}	131
100, 51	0.51	6.91×10^{-4}	132
100, 23	0.23	3.16×10^{-4}	162
80, 100	1.00	3.05×10^{-4}	131
80, 51	0.51	1.37×10^{-4}	155
80, 23	0.23	6.71×10^{-5}	171
60, 100	1.00	4.64×10^{-5}	625
60, 51	0.51	4.01×10^{-5}	740

^a These are the average values of kC_0 ; too much scatter to determine kC_0 and $\sqrt{kA/D}$.

functions of water activity. This approximation is especially good at values of p/p_0 less than about 0.7. If the units on C_0 are chosen as activity then k may be calculated directly by dividing kC_0 by the corresponding value of p/p_0 . In Fig. 2 the values of k calculated from the data of Table II are plotted as a function of reciprocal of the absolute temperature. The equation of the line shown, determined by least-squares, is

$$\log k = 10.546 - 4936/T \quad (8)$$

The activation energy of the reaction is 22.6 kcal./mole: the probable error is 0.5 kcal. It should be noted that this function extends over 60 to 175°, over water activities from 0.003 to 1.0, and over four orders of magnitude in rate.

As noted previously, a sample of amorphous film, comparable to the oriented crystalline films, was exposed below the glass transition temperature; this was to check both the assumption that degradation takes place only in the amorphous phase and the resulting correction of the value of A . This sample was 0.012 cm. in thickness and was exposed at 60° and 100% RH; the value of kC was 2.10×10^{-5} days⁻¹. This value must be compared with that for the oriented crystalline film of the same thickness and exposed at the same conditions given in Table II; this latter value is 1.93×10^{-5} days⁻¹. The agreement within 8% is considered quite good, and is felt to confirm the above assumption and correction of A .

Appendix A

Calculation of Moles of Polymer Hydrolyzed from Intrinsic Viscosity Data.—If the undegraded poly-

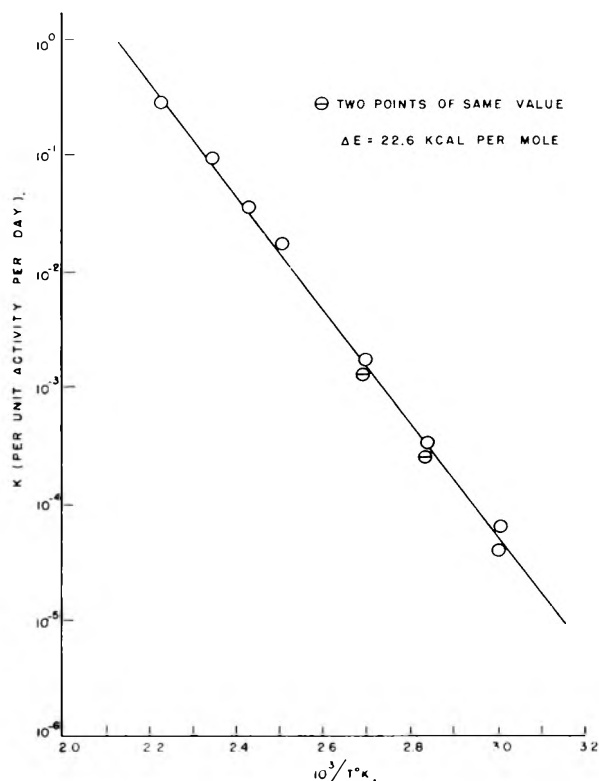


Fig. 2.

mer molecule is made up, on the average, of m repeat units the number average molecular weight, M_0 , will equal $192m$, since the formula weight of a repeat unit is 192. Reaction of a polymer molecule with n molecules of water yields $n + 1$ new polymer molecules. If after time t a polymer system with an average chain length m has reacted with n_t moles of water per mole of polymer the new average chain length will be $m/(n_t + 1)$. M_t , the number average molecular weight after time t , will be $192m/(n_t + 1)$. Therefore

$$\frac{M_0}{M_t} = \frac{192m(n_t + 1)}{192m} \quad (A1)$$

OR

$$n = \frac{M_0}{M_t} - 1 \quad (A2)$$

The number average molecular weight is related to the intrinsic viscosity by⁸

$$M = K[\eta]^{1.9}$$

Therefore

$$n_t = \frac{[\eta]_0^{1.9}}{[\eta]_t^{1.9}} - 1 \quad (\text{A3})$$

Appendix B

Derivation of Equations Defining the Diffusion Limited Hydrolysis of a Film.—Consider a film of thickness $2l$, whose other dimensions are large by comparison, exposed to a humid atmosphere such that the concentration of water vapor at the film surface is constant. Set up a coordinate system such that the origin is at the center of the film. The diffusion processes will be defined by

$$D \frac{\partial^2 C}{\partial x^2} = \frac{\partial C}{\partial t} \quad (\text{B1})$$

where

C is the concentration of water in the volume element dx at x (a rectangle of sides one cm. by one cm. by dx cm.)

D is the diffusion coefficient which is assumed to be constant

t is the time

The hydrolysis reaction will be defined by

$$\frac{dn}{dt} = k(A - n)C \quad (\text{B2})$$

where

n is the no. of moles of water or ester linkages per mole of polymer which have reacted after time t

A is the initial concn. of ester linkages per mole of polymer

k is the rate constant

The total change in water concentration with time, $\partial C/\partial t$, will be the difference between the amount diffusing in and that reacting; for steady-state conditions this must equal zero. Therefore

$$\frac{\partial C}{\partial t} = 0 = D \frac{\partial^2 C}{\partial x^2} - k(A - n)C \quad (\text{B3})$$

The procedure is to solve the steady-state equation, put these solutions into the kinetics equation, and solve the kinetics equation. The boundary conditions imposed upon equation B3 may be expressed

$$\left(\frac{\partial C}{\partial x}\right) = 0, x = 0$$

and

$$C = C_0, x = \pm l$$

Specifically n is a function of x since more reaction will take place at the surface; however, since n is much less than A the quantity $(A - n)$ may be considered constant for this integration. Carrying out

solution of equation B3 and imposing the boundary conditions yields

$$C(x) = C_0 \frac{\text{Cosh} \sqrt{\frac{k(A-n)}{D}} x}{\text{Cosh} \sqrt{\frac{k(A-n)}{D}} l} \quad (\text{B4})$$

It should be noted this equation has no meaning for $|x| > l$ and that it is finite and non-zero for all allowed values of x and l . Substitution of this relation into equation B2 yields

$$\frac{dn}{dt} = k(A - n)C_0 \frac{\text{Cosh} \sqrt{\frac{k(A-n)}{D}} x}{\text{Cosh} \sqrt{\frac{k(A-n)}{D}} l} \quad (\text{B5})$$

This equation defines the rate of reaction, under the conditions stated above, in the region between x and $x+dx$ in the film. In order to obtain an equation defining n as a function of time, film thickness, and k/D , it is necessary to carry out two integrations. First, the average rate must be obtained by integration in the usual manner over the range of $x = -l$ to $x = +l$; second, the rate equation is then integrated over the limits of 0 to n and 0 to t . The result is

$$\log_e \frac{\sinh^2 \sqrt{\frac{kA}{D}} l}{\sinh^2 \sqrt{\frac{k(A-n)}{D}} l} = kC_0 t \quad (\text{B6})$$

Values of the logarithm term were calculated on a Bendix G-15 computer for $n = 0$ to 2.0, $k/D = 10$ to 1280, and $2l = 0.0025$ to 0.0187, which cover the entire range of values encountered in this work. It was found: (1) the maximum value of the ratio $\sinh^2 \sqrt{(kA/D)} l / \sinh^2 \sqrt{(k(A-n)/D)} l$ is 1.017 and (2) the logarithm term is a linear function of n to within 1.1% or less. On the basis of these facts, equation B6 may be simplified. The approximation $\log_e x \cong (1 - x)$ may be made and shown to introduce a maximum error of 0.85%. By expansion of the terms into series, neglecting the higher powers of n , and rearranging we obtain the approximate equation

$$\frac{n}{A} \cong \left[kC_0 \frac{\text{tanh} \sqrt{\frac{kA}{D}} l}{\sqrt{\frac{kA}{D}} l} \right] t \quad (\text{B7})$$

The maximum error in rate involved in using this equation rather than equation B6 will be the accumulation of errors discussed above or about 2%.

ANALYSIS OF ABSORPTION SPECTRA OF MULTICOMPONENT SYSTEMS¹

BY RICHARD M. WALLACE

E. I. du Pont de Nemours & Company, Savannah River Laboratory, Aiken, South Carolina

Received January 28, 1960

A method was developed to find the number of components that contribute to the absorption spectrum of a multicomponent system. A complementary procedure was also developed to test for the presence of a non-absorbing species. The only assumption involved is that Beer's law is valid for each component.

Introduction

Absorption spectra have been used to study a number of systems in which several components exist in solution simultaneously. The stepwise formation of inorganic complexes and the formation of different species of organic dyes are examples. The analysis of the data in such studies usually involves two assumptions: (1) that Beer's law is valid for all components independently; and (2) that a relation is known, from equilibrium considerations, between the concentrations of the various components and some other parameter, such as the ligand concentration or the pH. The most complete analysis of this sort has been given by Newman and Hume² for the formation of inorganic complexes. The number of components, as well as information concerning their nature and the equilibrium constants for reactions between them, can be obtained from such an analysis.

Frequently, the conditions required for the validity of the second assumption are difficult to achieve experimentally. It is possible, however, to find the number of components from the first assumption alone.

Theoretical

Beer's law for a multicomponent system may be expressed as

$$a_{\lambda} = \sum_{k=1}^m \epsilon_{\lambda k} c_k \quad (1)$$

where a_{λ} is the absorbance at wave length λ , $\epsilon_{\lambda k}$ is the extinction coefficient of the k th component at wave length λ , c_k is the concentration of the k th component, and m is the total number of components.

If n experiments are performed in which the relative values of the c_k 's are caused to change, equation 1 becomes

$$a_{\lambda_j} = \sum_{k=1}^m \epsilon_{\lambda k} c_{kj} \quad (2)$$

where a_{λ_j} is the absorbance at wave length λ in the j th experiment, and c_{kj} is the concentration of component k in the j th experiment. These changes in the c_k 's may be accomplished, for example, by changing the ligand concentration in the formation of inorganic complexes or the pH of solutions containing organic indicators.

Equation 2 is the definition of matrix multiplication and may be written in the more compact form

(1) The information contained in this article was developed during the course of work under contract AT(07-2)-1 with the U. S. Atomic Energy Commission.

(2) L. Newman and D. N. Hume, *J. Am. Chem. Soc.* **79**, 4571 (1957).

$$A = EC \quad (3)$$

where A is a $p \times n$ matrix, E is a $p \times m$ matrix, and C a $m \times n$ matrix. p is the number of different wave lengths at which one chooses to measure the absorbance.

Since the rank of A is equal to the rank of E or C , whichever is smaller, and since the rank of both E and C can be no larger than m , the rank of A can be no larger than m . The rank of both E and C will usually be m , provided p and n are equal to or greater than m , and it will only be necessary to determine the rank of A to find the number of components in the system.

The only conditions that could cause the rank of C to be less than m are: (1) the concentration of one component is zero in all experiments, (2) the concentrations of all components are zero in more than m experiments, and (3) the concentration of one or more components can be expressed as a linear combination of the other components in all experiments. The first of these conditions violates the hypothesis of m components, the second is trivial, and the third is so unlikely it need not be given serious consideration. The rank of C will therefore always be m .

The rank of E will be less than m only if (1) the extinction coefficients of all components are zero at more than m different wave lengths, (2) the extinction coefficients of one or more components are zero at all wave lengths, or (3) the spectra of one or more of the components can be expressed as a linear combination of the spectra of the other components. The first of these can be eliminated by the proper choice of wave lengths. The second implies the existence of a non-absorbing component, and together with the third (which is possible although unlikely) constitutes a limitation on the method.

It is possible under certain circumstances to determine if the rank of E is equal to or less than m and consequently to demonstrate the presence of a non-absorbing species or one whose spectrum is a linear combination of the spectra of the other components.

Let the sum of the concentrations of the components be constant in all experiments.

$$\sum_{k=1}^m c_{kj} = C \text{ for all } j \quad (4)$$

This condition can be arranged, for example, by holding the concentration of the central ion constant and varying the ligand concentrations in the formation of inorganic complexes.

Let a new matrix A^* be formed by subtracting one of the columns in A , say the i th, from every column

$$A^* = A - A^{(i)} \quad (5)$$

A^* can then be represented as the product

$$A^* = EC^* \quad (6)$$

where C^* is formed by subtracting the i th column of C from every column of C . Due to the restriction imposed by equation 4 the rank of C^* and therefore A^* can be no greater than $m - 1$.

If the rank of A is equal to m , the actual number of components, the rank of A^* will be $m - 1$; while if the rank of A is less than m , the rank of A and A^* will be the same. This procedure is not applicable where two of the components have identical spectra. In that case the rank of A^* will be one less than that of A , even though the rank of A is less than the number of components.

Statistical Criterion for Determining Rank.—

Since the elements of both A and A^* are experimental quantities, it is highly unlikely that any square submatrix in A or A^* will be singular in a strictly mathematical sense. A statistical criterion is therefore necessary to find when the determinant of one of these submatrices may be considered to have vanished, in order to determine the rank by finding the largest non-singular submatrix.

The standard deviation $\sigma_{|A|}$ of a determinant $|A|$ can be expressed in terms of the standard deviations of the individual measurements $\sigma_{a_{\lambda j}}$ and the cofactors of the elements $a^{\lambda j}$.

$$\sigma_{|A|} = \left[\sum_{\lambda, j} \sigma_{a_{\lambda j}}^2 (a^{\lambda j})^2 \right]^{1/2} \quad (7)$$

The summation is carried out over all elements of the matrix. Equation 7 follows from the general equation for the propagation of errors and the fact that the partial derivative of a determinant with respect to an element is equal to the cofactor of that element.

If the errors of the individual measurements are known, the probability that a matrix is singular can be determined from the ratio of the absolute value of its determinant to its deviation $|A|/\sigma_{|A|}$ by referring to a statistical table such as the one found in the "Handbook of Chemistry and Physics."³

It is generally more convenient, however, to determine the quantity

$$d = \frac{|A|}{\left[\sum_{\lambda, j} (a^{\lambda j})^2 \right]^{1/2}} \quad (8)$$

Since the determinant of a singular matrix will be equal to its own standard deviation, it follows from equation 7 that d will be equal to the standard deviation, σ , of the individual elements if the errors are assumed to be constant in all measurements. A reliable estimate of σ can be obtained by examination of enough singular matrices. If a matrix is non-singular d will be larger than σ , and the probability that it is singular can be estimated from the ratio d/σ .

For purposes of calculations in which computers are used, it is preferable to put equation 8 in its equivalent form

$$d = \frac{1}{\left[\sum_{\lambda, j} (a_{j\lambda}^{-1})^2 \right]^{1/2}} \quad (9)$$

where $a_{j\lambda}^{-1}$ is an element of the inverse A^{-1} of A . The summation is now carried out over the square of all elements in A^{-1} .

While these procedures are applicable to A^* as well as A , it must be remembered that the errors in the elements of A^* are larger than those in A , since $\sigma_{|A^*|}$ will be sensitive not only to errors in the absorbance measurements but also to those in the concentration. If errors in the absorbances and concentrations are known, the errors in the elements of A^* can be estimated from the equation

$$\sigma_{a^*_{\lambda j}} = \left[\sigma_{a_{\lambda j}}^2 + \sigma_{a_{\lambda i}}^2 + \frac{\sigma_c^2}{C_2} a^2_{\lambda j} + a^2_{\lambda i} \right]^{1/2}$$

where C and σ_c are the concentration and its standard error, respectively.

Experimental

All absorption measurements were made in the visible region with a Cary Model 11M recording spectrophotometer with a tungsten lamp as a light source. The spectra were first scanned rapidly to determine the region in which absorption occurred. More precise absorption measurements were then made at 25-m μ intervals over this region by measuring the absorbance for about 15 seconds at each of these points. This procedure was necessary in order to obtain accurate values in the region where the absorbance was changing rapidly with wave length.

The individual methyl orange and methyl red solutions were prepared by adding 100 microliters of a 0.1% solution of the indicator to 10 ml. of a Clark and Lubs buffer solution of the appropriate pH.

Mixed solutions of the indicators were prepared by adding 100 microliters of each of the 0.1% indicators to 10 ml. of the appropriate buffer solution.

Application.—Methyl orange and methyl red were chosen to test the method. Both of these compounds exhibit spectra in the visible region that change as the pH is varied between 2.0 and 7.0. It seemed probable that each of these compounds existed in two forms and that the rank of each of their A matrices would be two. The method was also applied to a mixture of methyl orange and methyl red whose A matrix should then have the rank of four. The concentrations of the dyes were kept constant in each solution so that the condition expressed by equation 4 was valid and the ranks of the A^* matrices should be 1 and 3 for each of the dyes and their mixture, respectively.

The following procedure was used in applying the method. The spectra of a number of different solutions were measured in which the same amount of dye was present but in which the pH was varied between 2.0 and 7.0. The A matrix was constructed by sampling the spectrum of each of these solutions at a number of different wave lengths and placing the absorbance measured for the same solutions in the same columns and those at the same wave lengths in the same rows of the matrix. The A^* matrices were constructed by subtracting the elements in the last column in each A matrix from the corresponding element in every column.

The rank of each matrix was determined by first choosing a 2×2 submatrix and calculating d . If the value of d was close to the standard deviation, σ , the submatrix was considered to be singular. All 2×2 submatrices that could be constructed from an element of the first and one additional row or column from the original matrix were examined similarly. If the d value of each of these was close to σ , the rank of the matrix was taken to be one. If one of the 2×2 submatrices was found to be non-singular, all 3×3 submatrices that could be formed from that 2×2 submatrix and one additional row and column were examined until a non-singular 3×3 was found or all of them were shown to be singular. This procedure was continued until the largest non-singular submatrix was found.

The results of the measurements and calculations are shown in Tables I through III. The A matrices are shown at the top of each of these tables, while sections A and B

(3) "Handbook of Chemistry and Physics," Thirty-fourth Edition, C. D. Hodgman, Editor, Chemical Rubber Publishing Co., Cleveland 7, Ohio, p. 228.

contain the d values of the submatrices of A and A^* , respectively, necessary to establish their rank. The first column in each table gives the order of the submatrix, the second and third the rows and columns, respectively, of the original matrix from which they were taken, while the last column contains the values of d . Since the A^* matrices were formed by a simple subtraction they are not shown. Their indexing however is the same as that for the corresponding A matrix. Values of d were calculated using equation 8 in Tables I and II while equation 9 was used with the larger submatrices in Table III. An IBM 650 computer was used to invert the matrices when equation 9 was employed.

The values of d for all the 3×3 submatrices in Tables IA and IIA are very close to the smallest value of the absorbance that can be estimated, which is 0.001 absorbance unit. These matrices can then be assumed to be singular, and with this assumption the standard deviation, σ , of the individual measurements can be calculated from the values of d to be ± 0.003 . None of the values of d for the 3×3 submatrices is as large as 2σ while the values of d for the 2×2 submatrices are about 45σ . The rank of each A matrix is therefore two.

Similarly the rank of each of the A^* matrices may be taken to be one since the largest value of d for any of the 2×2 submatrices in Tables IB and IIB is only slightly larger than 2σ with σ equal to ± 0.004 . The larger value of σ arises from the necessity of holding the concentrations constant.

TABLE I
A MATRIX FOR METHYL RED

$\lambda, m\mu$	pH			
	3.4	4.6	5.4	6.2
575	0.460	0.342	0.108	0.018
525	.993	.742	.282	.077
475	.400	.365	.310	.288
425	.060	.152	.320	.400

A. Evaluation of the rank of the A matrix

Order of determinant	Rows	Columns	d
2	2, 3	2, 3	0.145
3	1, 2, 3	1, 2, 3	.0041
3	1, 2, 3	2, 3, 4	.0029
3	2, 3, 4	1, 2, 3	.0020
3	2, 3, 4	2, 3, 4	.0003

B. Evaluation of the rank of the A^* matrix

Order of determinant	Rows	Columns	d
2	4, 3	1, 2	0.0036
2	4, 2	1, 2	.0008
2	4, 1	1, 2	.0012
2	4, 3	1, 3	.0040
2	4, 2	1, 3	.0036
2	4, 1	1, 3	.0084

It may be concluded from these results that both these systems contain but two components that contribute to the absorption, and no non-absorbing components.

The largest value of d for a 4×4 submatrix in Table IIIA is 5.5σ . The probability of this having occurred by chance is about 1×10^{-6} . This 4×4 submatrix must therefore be non-singular. The 5×5 matrix itself is singular with a d value less than σ . Its rank is therefore four.

One would have predicted the rank of the A^* matrix for the mixture of dyes to be three. Actually the value of d for the 3×3 submatrix is larger than those for the two 4×4 submatrices. The difference, however, is not large enough to state with a great deal of assurance that the rank is three. The small value of d in the 3×3 submatrix

TABLE II
A MATRIX FOR METHYL ORANGE

$\lambda, m\mu$	pH			
	2.2	3.0	3.8	6.2
550	0.825	0.670	0.315	0.050
500	1.250	1.100	.770	.515
475	0.810	0.790	.770	.745
425	0.150	0.250	.460	.620

A. Evaluation of the rank of the A matrix

Order of determinant	Rows	Columns	d
2	2, 3	2, 3	0.137
3	1, 2, 3	1, 2, 3	.0007
3	1, 2, 3	2, 3, 4	.0007
3	2, 3, 4	1, 2, 3	.0054
3	2, 3, 4	2, 3, 4	.0026

B. Evaluation of the rank of the A^* matrix

Order of determinant	Rows	Columns	d
2	1, 2	1, 2	0.0017
2	1, 3	1, 2	.0054
2	1, 4	1, 2	.0041
2	1, 2	1, 3	.0025
2	1, 3	1, 3	.0027
2	1, 4	1, 3	.0006

TABLE III
THE A MATRIX FOR A MIXTURE OF METHYL ORANGE AND METHYL RED

$\lambda, m\mu$	pH				
	2.2	3.4	4.6	5.4	6.6
575	0.430	0.540	0.390	0.137	0.022
525	2.325	1.835	1.070	0.508	0.262
475	1.395	1.245	1.155	1.075	1.060
425	0.223	0.427	0.742	0.938	1.055
375	0.052	0.159	0.319	0.438	0.512

A. Evaluation of the rank of the A matrix

Order of determinant	Rows	Columns	d
2	1, 5	1, 5	0.326
3	1, 3, 5	1, 3, 5	.136
4	1, 2, 3, 5	1, 3, 4, 5	.0051
4	1, 3, 4, 5	1, 2, 3, 5	.0077
4	1, 2, 3, 5	1, 2, 3, 5	.0164
4	1, 3, 4, 5	1, 3, 4, 5	.0031
50009

B. Evaluation of the rank of the A^* matrix

Order of determinant	Rows	Columns	d
2	1, 2	1, 2	0.159
3	1, 2, 3	1, 2, 3	.0225
4	1, 2, 3, 4	1, 2, 3, 4	.0125
4	1, 2, 3, 5	1, 2, 3, 4	.0139

probably arises from the similarity in the spectra of the two dyes, while the comparatively large values of d for the two 4×4 submatrices were due to the failure to hold the concentration of the two dyes sufficiently constant in all the experiments.

Acknowledgments.—I wish to acknowledge the helpful suggestions and criticisms of W. E. Shuler and also the assistance of J. C. English in inverting the matrices.

OSCILLATING TEMPERATURES IN REACTION KINETICS. I. ACTIVATION ENERGY FROM STEADY STATE CONCENTRATION

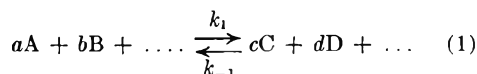
BY THOMAS I. CROWELL

Cobb Chemical Laboratory, University of Virginia, Charlottesville, Va.

Received February 4, 1960

A simple, reversible reaction with forward and reverse rate constants k_1 and k_{-1} is maintained alternately at temperatures T' and T'' . If the alternation frequency is rapid, a steady state is reached. The apparent equilibrium constant for these conditions, K_s , is then equal to $(nk_1' + k_1'')/(nk_{-1}' + k_{-1}'')$ where n is the ratio of the times spent at T' and T'' . By observing K_s as a function of n , the activation energies of the forward and reverse reactions can be evaluated.

Consider a chemical equilibrium



with forward and reverse rate constants k_1' and k_{-1}' at the temperature T' , and k_1'' and k_{-1}'' at T'' . The equilibrium constants at T' and T'' are given by $K' = k_1'/k_{-1}'$ and $K'' = k_1''/k_{-1}''$. If the temperature is maintained alternately at T' and T'' for times which are long compared with the time required to approach chemical equilibrium and if $K' \neq K''$, the concentrations $[A]$, $[B]$, . . . $[C]$, $[D]$, . . . will change so that the system will be at equilibrium practically all the time.

If, however, the fluctuation in temperature is more rapid, the system will be more sluggish in responding to the change. A very rapid fluctuation will lead to constant concentrations of reactants and products (Fig. 1A). These steady-state concentrations are easily calculated without considering the course of the reaction. Suppose for simplicity that the rate equations correspond to the terms in the stoichiometric equation 1, so that $dx/dt = k_1'[A]^a[B]^b \dots - k_{-1}'[C]^c[D]^d \dots$ at T' and similarly at T'' . Here the reaction variable x has the usual meaning.¹ Let the system be at T' for the time interval $n\Delta t/(1+n)$ and at T'' for the interval $\Delta t/(1+n)$, where Δt is the time of one complete heating and cooling cycle and n is the ratio of the times spent at T' and T'' (Fig. 1B).

For a steady state, Δx , the change in x during Δt , must be zero

$$(n+1)\Delta x = nk_1'\Delta t[A]^a[B]^b \dots - nk_{-1}'\Delta t[C]^c[D]^d \dots + k_1''\Delta t[A]^a[B]^b \dots - k_{-1}''\Delta t[C]^c[D]^d \dots = 0 \quad (2)$$

$$\frac{[C]^c[D]^d \dots}{[A]^a[B]^b \dots} = \frac{nk_1' + k_1''}{nk_{-1}' + k_{-1}''} = K_s \quad (3)$$

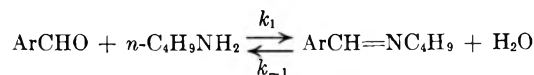
K_s is an apparent equilibrium constant for the steady state. It should be noted that the system is never at or near equilibrium except momentarily during the rise and fall of temperature.

Equation 3 shows that a determination of K_s for a certain n , together with K' and K'' , is sufficient for the calculation of k_1'/k_1'' . Paradoxically, the activation energy, a quantity pertaining to rates, can thus be obtained from data which are not a function of time, though time is involved in fixing the value of n .

More experimental data can be utilized if K_s is measured as a function of n . The expected form of the function is seen from 3 to be $(K_s - q)(n + r) =$

s . Equating coefficients gives $q = k_1'/k_{-1}' = K'$, $r = k_{-1}''/k_{-1}'$ and $s = (k_1''k_{-1}' - k_1'k_{-1}'')/(k_{-1}')^2 = (K'' - K')$. Thus $n + k_{-1}''/k_{-1}' = (k_{-1}''/k_{-1}')(K'' - K')/(K_s - K')$, and a plot of n vs. $1/(K_s - K')$ has an intercept on the $1/(K_s - K')$ axis of k_{-1}''/k_{-1}' , the temperature coefficient of reaction rate for the reverse reaction. The ratio k_1''/k_1' is then evaluated from k_{-1}''/k_{-1}' , K' and K'' .

These relationships have been verified by actual measurements on a system previously studied in this Laboratory, the reaction of piperonal and *n*-butylamine to form piperonylidene-*n*-butylamine and water²



Experimental

Apparatus.—The reaction vessel was a 10" × 1/4" o.d. stainless steel tube fitted with a screw cap and Teflon gasket. It was situated inside a larger glass tube through which water was circulated from either of two large thermostat baths at 25 and 50°. The circulating pumps in the respective baths were alternately actuated by a simple timer and two-way relay, to give the desired temperature cycle. The response inside the reaction vessel was checked with a thermocouple attached to a Sargent recorder, and is shown (for $n = 5$ and $\Delta t = 1$ hour) in Fig. 1C and 1D. A special plunger valve ensured the return of the water to the proper bath.

Procedure.—A solution of *n*-butylamine ($\sim 10^{-3} M$), piperonal ($\sim 10^{-4} M$) and water (5.0 *M*) was prepared in a 100-ml. volumetric flask at 25°, using reagent grade methanol as the solvent. About 3 ml. of this solution was placed in each of four reaction tubes, which were capped and placed in the oscillating temperature apparatus for two days. A 2-ml. sample was then withdrawn from each tube at the mid-point of a 25° interval, diluted to 10 ml. with methanolic hydrochloric acid, and analyzed spectrophotometrically at 348 μ for Schiff base.^{3,4} Because 1 *M* H₂O was present in the diluted sample, conversion of piperonal to the acetal was incomplete and necessitated a small correction for absorption of piperonal at this wave length.

Results

Equilibrium constants for Schiff base formation were determined at the two temperatures used. Although the water concentration was practically constant at 5 *M*, it was included in the expression $K = [\text{ArCH}=\text{NBu}][\text{H}_2\text{O}]/[\text{ArCHO}][\text{BuNH}_2]$ to conform with our preceding work.^{2,4} The value obtained at 25°, $K' = 3.10 \times 10^3$, is in fair agreement with that found by titration (3.18×10^3). At 50°, $K = 0.95 \times 10^3$, though the value used in the calculations was obtained differently as explained below.

(2) R. L. Hill and T. I. Crowell, *J. Am. Chem. Soc.*, **78**, 2284 (1956)

(3) T. I. Crowell and D. W. Paok, *ibid.*, **75**, 1075 (1953).

(4) C. E. Bell and T. I. Crowell, *J. Org. Chem.*, **24**, 1159 (1959).

(1) A. A. Frost and R. G. Pearson, "Kinetics and Mechanism," John Wiley and Sons, Inc., New York, N. Y., 1953, p. 9.

The reaction was then studied with oscillating temperatures as described in the experimental section. The reaction and the oscillation rate were both quite slow; n ranged from 0 (temperature constant at 50°) to 7.09 (7.42 minutes at 50°, 52.58 minutes at 25°). The time for one complete temperature cycle, Δt , was one hour in every case. The maximum permissible Δt for a given variation from steady-state concentrations can be calculated from equation 2 if the rate constants are known.

A plot of $1/(K' - K_s)$ is shown in Fig. 2. The straight line through the experimental points follows the equation $1/(K' - K_s) = 0.478 + 0.0078n$. The n -intercept of -6.14 is multiplied by 1.026 to correct for the change in concentrations when the methanol expands at 50°, so that $k_{-1}''/k_{-1}' = 6.30$. The ratio of the forward rate constants, k_1''/k_1' , is then $6.30 K''/K'$; the value 1.15 for K'' taken from the intercept at $n = 0$ in Fig. 2, was used rather than the experimentally determined value. From k_1''/k_1' , the activation energy for the forward reaction is 6.2 kcal./mole.

By conventional measurement of rate constants at 0, 25 and 45°, Hill and Crowell found an activation energy of 6.7 kcal./mole in pure methanol.² In the present work, a determination of the rate in methanol containing 5 *M* H₂O, at 0.1°, gave $k_1 = 0.85$ l./mole min. This together with the 25° value² yields an activation energy of 6.1 kcal./mole, in accord with the known accelerating effect of water and with the results of the oscillating temperature method set forth in this paper.

Discussion

Non-square Temperature Oscillations.—The above treatment has been based on "square" time-temperature functions, where the temperature changes from one fixed value to the other instantaneously, as in Fig. 1B. The experimental work was made to approach these conditions as closely as possible. It is also instructive, however, to calculate K_s for cases in which the temperature varies continually. While it is sufficient in the particular case of a square oscillation to know the extreme values of the rate constants as in equation 3, in general the forward and reverse rate constants must be known as a function of temperature. Then

$$K_s = \int_C k_1(T)dt / \int_C k_{-1}(T)dt$$

where the integration is carried out over the complete temperature cycle or a suitable portion C of a symmetrical time-temperature function.

For example, if $\log k_1 = 4.806 - 1334/T$ and $\log k_{-1} = 6.231 - 2799/T$, approximating the reaction studied in this work, the calculated values of K_s are 1.56×10^3 for the square relation E, 1.74×10^3 for the sine curve F and 1.80×10^3 for the saw tooth G (Fig. 1).

A Dual Temperature Flow Analog.—Equation 3 also applies to a system of two connected reaction vessels where the first, of volume V_1 , is maintained at temperature T_1 , and the second volume V_2 at T_2 . The definition of n is now V_1/V_2 . A pump and stirrers ensure constant concentration of all components throughout the system (neglecting concentration changes due to thermal expansion).

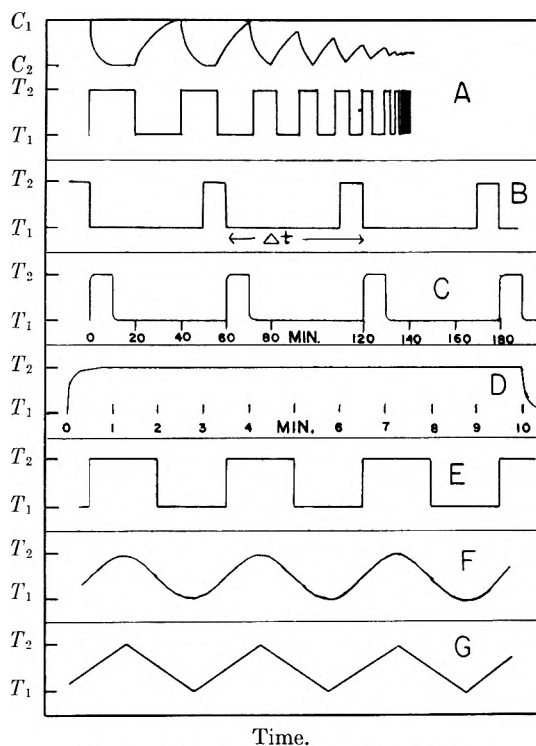


Fig. 1.—Time-temperature relationships.

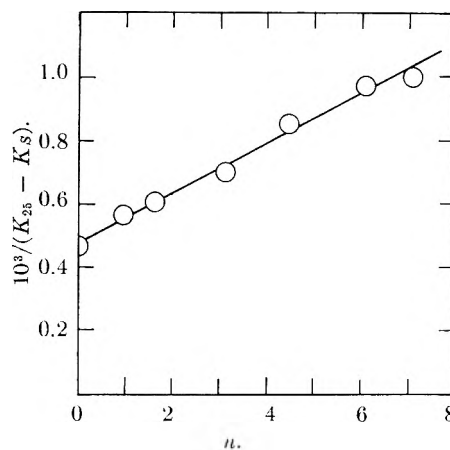
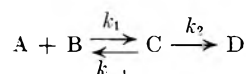


Fig. 2.—Plot of $10^3/(K_{25} - K_s)$ as a function of n .

Applications.—The oscillating temperature method will not supplant conventional rate studies, for it is less direct and yields heats but not entropies of activation. Possibly it would be useful in certain systems for which steady-state measurements are much easier than rate measurements.

The most interesting application, however, seems to be the detection of equilibria in complex reactions, such as



In the commonly encountered case where $k_2 \ll k_1 < k_{-1}$, the reaction rate is

$$dx/dt = (k_1 k_2 / k_{-1})(a - x)(b - x) \quad (4)$$

Carried out at a temperature which varies but not rapidly enough to preclude virtual equilibrium between A, B and C, the rate would still be given

by equation 4, where the k 's are functions of T . With not too rapid an oscillating temperature cycle (Fig. 1B), equation 4 reduces to

$$\frac{dx}{dt} = \left[\left(\frac{n}{n+1} \right) \frac{k_1'k_2'}{k_{-1}'} + \left(\frac{1}{n+1} \right) \frac{k_1''k_2''}{k_{-1}''} \right] (a-x)(b-x) \quad (5)$$

However, if the oscillation frequency is so high that a steady state is reached in the concentrations of A, B and C with respect to the changing temperature, the rate will be $dx/dt = K_3k_2(T)(a-x)(b-x)$ at all times, and over the period Δt will be

$$\frac{dx}{dt} = K_3 \left(\frac{nk_2'}{1+n} + \frac{k_2''}{1+n} \right) (a-x)(b-x) \quad (6)$$

Since in general, (5) is not equal to (6), a complex reaction would show a different rate at oscillating temperatures than calculated from the isothermal rates at T' and T'' . Whether the difference is experimentally detectable remains to be seen.

The method would be somewhat similar in principle to the rotating sector method for photochemical chain reactions⁵ in that a periodic impulse—here a thermal one—is given to the reaction. The use of varying temperatures also bears some similarity to existing methods for the calculation of activation energies from non-isothermal rates⁶ and of integrated rates from experiments made under non-isothermal conditions.⁷

Acknowledgment.—I am indebted to the National Science Foundation for support of this work.

(5) H. W. Melville and G. M. Burnett, "Technique of Organic Chemistry," (A. Weissberger, Ed.), Interscience Publishers, Inc., New York, N. Y., 1953, Vol. VIII, p. 138.

(6) H. J. Borchardt and F. Daniels, *J. Am. Chem. Soc.*, **79**, 41 (1957); K. S. Vorres and L. Eyring, Abstracts of Papers, 136th A.C.S. Meeting, Atlantic City, p. 45S.

(7) J. B. Malloy and H. S. Seelig, *A.I.Ch.E. Jour.*, **528** (1955); E. Baum, *This Journal*, **63**, 1704 (1959).

THE HEAT CAPACITY AND THERMODYNAMIC FUNCTIONS OF URANIUM FROM 5 TO 350°K.¹

By HOWARD E. FLOTOW AND HAROLD R. LOHR

Contribution from the Chemistry Division, Argonne National Laboratory, Lemont, Illinois

Received February 8, 1960

The heat capacity of uranium metal containing less than 0.01% impurities was measured from 5 to 350°K. From these data the entropy, enthalpy and free energy function were calculated. The values of C_p , S° , $(H^\circ - H_0^\circ)$ and $(F^\circ - H_0^\circ)/T$ at 298.15°K. are 6.612 ± 0.013 cal. deg.⁻¹ mole⁻¹, 12.00 ± 0.02 cal. deg.⁻¹ mole⁻¹, 1521 ± 3 cal. mole⁻¹ and -6.893 ± 0.014 cal. deg.⁻¹ mole⁻¹, respectively. The results are compared with previously published data.

Introduction

The heat capacity of α -uranium has been previously reported by Smith and Wolcott² in the range 1 to 20°K., by Jones, Gordon and Long³ in the range 15 to 300°K., by Clusius and Piesbergen⁴ in the range 10°K. to room temperature, by Moore and Kelley⁵ and by Ginnings and Corruccini⁶ in the range 298 to 935°K. Recently, uranium metal which contained substantially lesser amounts of impurities than the metal used in previous investigations became available at this Laboratory. This paper reports a determination of the heat capacity of this high purity α -uranium from 5 to 350°K. and a calculation of the entropy, enthalpy and free energy function. Also, these results are compared with those of Smith and Wolcott and with those of Jones, Gordon and Long.

Experimental

Uranium Sample.—The uranium metal used for this experiment was prepared by the Metallurgical Division of

this Laboratory⁷ by the electrolysis of UF_4 in a fused mixture of KCl and LiCl. The crystals obtained in this process were vacuum cast into billets which were then swaged into rods 0.3 cm. in diameter. This uranium metal was later converted to the uranium hydride sample for which heat capacity measurements already have been published.⁸ Spectroscopic analyses of the billet from which the sample was taken showed the presence of the following impurities in parts per million: Al, 5; Cr, 2; Cu, 1; Fe, 2; Mg, 1; Si, 12; all other elements were below the limits of spectroscopic detection. Chemical analyses detected the following elements in parts per million: C, 18; N, 5; O, 15. On the basis of the analyses it was concluded that the sample contained less than 0.01% impurities. Prior to loading the sample into the calorimeter the uranium was annealed at 600–650° for 0.5 hour *in vacuo* and then cooled slowly to room temperature. The mass of the sample was 106.3102 g. The calorimeter contained 1.20×10^{-3} mole of helium to facilitate the establishment of temperature equilibrium.

Apparatus and Technique.—The calorimetric measurements were made using the apparatus and adiabatic method which already have been described in detail.^{8,9} A capsule type platinum resistance thermometer (Laboratory designation A-1) was used to determine the temperature of the calorimeter. The thermometer was calibrated on the temperature scale of the National Bureau of Standards¹⁰ from 14 to 373°K. Below 14°K., the scale was obtained by fitting the equation $R = A + BT^2 + CT^6$ to the resistance at the boiling point of helium, at 4°K. and to dR/dT

(1) Based on work performed under the auspices of the U. S. Atomic Energy Commission.

(2) P. L. Smith and N. M. Wolcott, "Conference de Physique des Basses Temperatures," Paris, 2–8 Sept., 1955, Annexe 1955–3, Supplément au Bulletin de l'Institut International du Froid, pp. 283–286.

(3) W. M. Jones, J. Gordon and E. A. Long, *J. Chem. Phys.*, **20**, 695 (1952).

(4) K. Clusius and U. Piesbergen, *Helv. Phys. Acta*, **31**, 302 (1958).

(5) G. E. Moore and K. K. Kelley, *J. Am. Chem. Soc.*, **69**, 2105 (1947).

(6) O. C. Ginnings and R. J. Corruccini, *J. Research Natl. Bur. Standards*, **39**, 309 (1947).

(7) B. Blumenthal and R. A. Noland, "Progress in Nuclear Energy," Vol. I, Pergamon Press, New York, N. Y., 1956, Series V, pp. 62–80.

(8) H. E. Flotow, H. R. Lohr, B. M. Abraham and D. W. Osborne, *J. Am. Chem. Soc.*, **81**, 3529 (1959).

(9) E. F. Westrum, Jr., J. B. Hatcher and D. W. Osborne, *J. Chem. Phys.*, **21**, 419 (1953).

(10) H. J. Hoge and F. G. Brickwedde, *J. Research Natl. Bur. Standards*, **22**, 351 (1939).

at 14°K. A slight correction was applied to the calibration to make the ice point equal to 273.15°K. It is estimated that the scale agrees with the thermodynamic scale within 0.1° from 4–14°K., within 0.03° from 14–90°K. and within 0.05° from 90–373°K.

Results and Discussion

Heat Capacity Results.—The experimental values of the heat capacity are presented in chronological sequence in Table I. The data are expressed in terms of the defined thermochemical calorie equal to 4.1840 absolute joules. A small correction for the finite temperature interval was made by adding $-(d^2C_p/dT^2)(\Delta T)^2/24$ to the measured heat capacity. Approximate temperature increments of the individual measurements can be calculated from the differences between the successive mean temperatures within a series. The heat capacities at selected temperatures given in Table II were read from a large scale smooth curve through the experimental points. It is estimated that the heat capacity values given in Tables I and II have a probable error of 5% at 5°K., 1% at 14°K., and 0.2% above 30°K.

TABLE I
HEAT CAPACITY OF URANIUM METAL IN CAL. DEG.⁻¹
MOLE⁻¹

Mol. wt. = 238.07; 0° = 273.15°K.			
T, °K.	C _p	T, °K.	C _p
Series I		Series III	
300.104	6.614	49.520	3.727
307.465	6.648	54.470	3.963
317.478	6.700	59.986	4.209
327.514	6.745	66.134	4.463
337.489	6.790	73.049	4.691
347.549	6.827	80.640	4.916
Series II		88.873	5.118
		98.141	5.281
5.703	0.027	108.041	5.428
7.204	.038	118.131	5.561
8.906	.060	128.225	5.675
10.784	.105	138.123	5.772
12.644	.176	147.980	5.856
14.648	.287	157.765	5.925
16.653	.426	167.755	5.994
18.645	.597	177.804	6.056
20.662	.799	186.311	6.101
22.632	1.029	196.331	6.155
24.927	1.304	206.324	6.202
27.490	1.624	216.322	6.250
30.297	1.972	226.307	6.309
33.432	2.360	236.222	6.342
36.911	2.762	246.154	6.389
40.832	3.154	256.120	6.429
45.148	3.486	266.096	6.467
49.741	3.744	278.483	6.529
		285.104	6.556
		294.998	6.611
		304.950	6.639
		314.904	6.678

A comparison of these heat capacities with those previously reported by Jones, Gordon and Long³ show that between 15 and 50°K. the heat capacity values of the two investigations agree within ± 0.13 cal. deg.⁻¹ mole⁻¹ and that between 50 and 300°K. the values of Jones, Gordon and Long are on the

TABLE II
THERMODYNAMIC PROPERTIES OF URANIUM METAL AT SELECTED TEMPERATURES

T, °K.	C _p , cal. deg. ⁻¹ mole ⁻¹	S°, cal. deg. ⁻¹ mole ⁻¹	H° - H ₀ °, cal. mole ⁻¹	$-\left(\frac{F^\circ - H_0^\circ}{T}\right)$, cal. deg. ⁻¹ mole ⁻¹
5	0.020	0.015	0.042	0.007
10	.084	.044	0.26	.018
15	.308	.113	1.16	.035
20	.727	.255	3.67	.071
25	1.312	.478	8.73	.128
30	1.934	.772	16.84	.210
35	2.546	1.117	28.06	.315
40	3.078	1.492	42.16	.437
45	3.476	1.879	58.59	.576
50	3.754	2.261	76.70	.726
60	4.212	2.986	116.58	1.042
70	4.593	3.666	160.69	1.370
80	4.899	4.299	208.18	1.696
90	5.138	4.891	258.44	2.019
100	5.315	5.442	310.74	2.334
110	5.458	5.955	364.61	2.639
120	5.583	6.436	419.82	2.937
130	5.694	6.887	476.21	3.223
140	5.789	7.313	533.63	3.500
150	5.871	7.715	591.94	3.768
160	5.942	8.096	651.01	4.026
170	6.009	8.458	710.77	4.276
180	6.067	8.803	771.15	4.518
190	6.121	9.133	832.10	4.753
200	6.173	9.448	893.57	4.979
210	6.222	9.751	955.54	5.200
220	6.270	10.041	1018.0	5.413
230	6.316	10.321	1080.9	5.620
240	6.360	10.591	1144.3	5.822
250	6.404	10.851	1208.1	6.017
260	6.445	11.103	1272.4	6.208
270	6.486	11.347	1337.0	6.394
280	6.530	11.584	1402.1	6.575
290	6.574	11.814	1467.6	6.752
300	6.619	12.037	1533.6	6.924
310	6.664	12.247	1600.0	7.093
320	6.709	12.459	1666.9	7.257
330	6.754	12.666	1734.2	7.418
340	6.799	12.869	1801.9	7.576
350	6.842	13.066	1870.2	7.730
273.15	6.499	11.42	1358	6.452
298.15	6.612	12.00	1521	6.893
	± 0.013	± 0.02	± 3	± 0.014

average 0.032 cal. deg.⁻¹ mole⁻¹ higher than those of the present investigation. Since the uranium specimen used by Jones, Gordon and Long³ was reported to be only 99.7% uranium, it is likely that a significant fraction of this disparity is due to chemical and physical differences in the samples.

Clusius and Piesbergen report in a brief paper⁴ that they have measured the heat capacity of uranium between 10°K. and room temperature. A comparison with their results cannot be made until a more detailed publication of their data is available.

In the region 5 to 20°K. a comparison can be made with the data of Smith and Wolcott.^{2,11} From a smooth curve drawn through one of their

(11) W. M. Wolcott, private communication.

most reliable runs the values of the heat capacities at 5, 10, 15 and 20°K. were found to be 0.020, 0.100, 0.328 and 0.760 cal. deg.⁻¹ mole⁻¹, respectively. A comparison of these values with those in Table II shows that the values of the heat capacities are identical at 5°K. but that the values diverge at higher temperatures, the results of Smith and Wolcott² being substantially higher than those of this investigation. The reason for the disagreement is not known.

Thermodynamic Functions.—The thermodynamic functions derived from the heat capacity are shown in Table II at selected temperatures. The heat capacity values reported by Smith and Wolcott² were used to evaluate the entropy and en-

thalpy from 0 to 5°K. The value of the entropy at 298.15°K. reported in Table II, 12.00 ± 0.02 cal. deg.⁻¹ mole⁻¹, agrees within experimental error with the value published by Jones, Gordon and Long,³ 12.03 ± 0.03 cal. deg.⁻¹ mole⁻¹. Jones, Gordon and Long did not report a value of the enthalpy of uranium at 298.15°K. However, using their heat capacity data we calculate that $H_{298.15} - H_0^0$ is 1526 ± 3 cal. mole⁻¹ which agrees well with the value 1521 ± 3 cal. mole⁻¹ given in Table II.

Acknowledgments.—We thank Dr. D. W. Osborne and Dr. B. M. Abraham for their guidance and helpful discussions.

CHEMICAL THERMODYNAMIC PROPERTIES OF METHYLCYCLOPENTANE AND 1-*cis*-3-DIMETHYLCYCLOPENTANE

BY D. W. SCOTT, W. T. BERG AND J. P. McCULLOUGH

Contribution No. 86 from the Thermodynamics Laboratory, Bartlesville Petroleum Research Center, Bureau of Mines, U. S. Department of the Interior, Bartlesville, Okla.

Received February 8, 1960

Thermodynamic functions were calculated for methylcyclopentane by methods of statistical mechanics and for 1-*cis*-3-dimethylcyclopentane by a refined method of increments. Values of the heat, free energy and equilibrium constant of formation also were calculated for both substances.

Thermodynamic functions of methylcyclopentane and the isomeric dimethylcyclopentanes were calculated previously by approximate incremental methods by staff members of American Petroleum Institute Research Project 44.^{1,2} More recently the vapor capacities of methylcyclopentane and 1-*cis*-3-dimethylcyclopentane³ were determined in this Laboratory.⁴ The experimental values of vapor heat capacity, in addition to the experimental values of entropy (ref. 4) that were available to the earlier workers, made possible more accurate calculations of the thermodynamic functions of methylcyclopentane by methods of statistical mechanics and of 1-*cis*-3-dimethylcyclopentane by a refined method of increments. These calculations are described herein.

Thermodynamic Functions of Methylcyclopentane.⁵—The 54 degrees of freedom of the methylcyclopentane molecule may be classified as 3 translations, 3 over-all rotations, 46 vibrations, one internal rotation of the methyl group, and one pseudo-rotation of the 5-membered ring. The contributions of translation and over-all rotation to the thermodynamic functions were calculated by standard formulas. In the simplified model

used for calculating moments of inertia, the ring was planar, and the bond distances and angles were: C-C, 1.54 Å.; C-H, 1.09 Å.; C-C-C (ring), 108°; H-C-H (methylene), H-C (ring)-C (methyl) and all methyl group angles, 109° 28'. For this model, the product of principal moments of inertia is 1.438 × 10⁻¹¹³ g.³ cm.⁶, and the reduced moment of inertia for internal rotation of the methyl group is 5.155 × 10⁻⁴⁰ g. cm.². Corresponding values for the actual molecule with a slightly puckered ring cannot differ much from the foregoing values.

The set of fundamental vibrational frequencies listed in Table I was selected after consideration of all available Raman and infrared spectral data⁶ and comparison with the frequencies of cyclopentane, other monosubstituted cyclopentanes and related heterocyclic compounds. The descriptive names for the modes of vibration are somewhat schematic and are intended merely to show that the expected number of frequencies are assigned in the several regions of the spectrum. The two lowest frequencies, for ring puckering and a CH₃-C-C bending mode, are assigned to the doublet 307-320 cm.⁻¹ reported in the Raman spectrum by Bazhu-

(1) J. E. Kilpatrick, H. G. Werner, C. W. Beckett, K. S. Pitzer and F. D. Rossini, *J. Research Natl. Bur. Standards*, **39**, 523 (1947).

(2) M. B. Epstein, G. M. Barrow, K. S. Pitzer and F. D. Rossini, *ibid.*, **43**, 245 (1949).

(3) 1-*cis*-3-Dimethylcyclopentane is the lower boiling (90.77°) isomer of 1,3-dimethylcyclopentane. This isomer was incorrectly labeled 1-*trans*-3-dimethylcyclopentane in literature before 1955. See F. D. Rossini and Kun Li, *Science*, **122**, 513 (1955).

(4) J. P. McCullough, R. E. Pennington, J. C. Smith, I. A. Hosselopp and Guy Waddington, *J. Am. Chem. Soc.*, **81**, 5880 (1959).

(5) The gas constant is taken to be 1.98719 cal. deg.⁻¹ mole⁻¹ and the atomic weights of carbon and hydrogen are taken to be 12.010 and 1.0080.

(6) Raman: K. W. F. Kohlrausch, A. W. Reitz and W. Stockmair, *Z. physik. Chem.*, **B32**, 229 (1936); E. J. Rosenbaum and H. F. Jacobson, *J. Am. Chem. Soc.*, **63**, 2841 (1941); P. A. Bazhulin, Kh. E. Sterin, T. F. Bulanova, O. P. Solovava, M. B. Turova-Pollak and B. A. Kazanskiĭ, *Izvest. Akad. Nauk S. S. R. Otdel. Khim. Nauk*, **7** (1946); APIRP 44 at the Carnegie Inst. of Tech., Catalog of Raman Spectral Data, Serial No. 159. Infrared: P. Lambert and J. Lecomte, *Ann. phys.*, **10**, 503 (1938); D. Bărcă-Gălăteanu, *Bull. soc. roumaine phys.*, **36**, 109 (1938); E. K. Plyler, *J. Optical Soc. Am.*, **37**, 746 (1947); E. K. Plyler, R. Stair and C. J. Humphreys, *J. Research Natl. Bur. Standards*, **38**, 211 (1947); APIRP 44 at the Carnegie Inst. of Tech., Catalog of Infrared Spectral Data, Serial Nos. 14, 15, 255, 344, 510, 511, 597, 616, and 1556; F. F. Bentley and E. F. Wolforth, WADC TR 58-198, May 1958; A. Cornu, *Bull. soc. chim. France*, 721 (1959).

lin, *et al.* However, other Raman investigations, as well as the infrared spectrum, indicate only a single frequency in that range. If there is only a single frequency at about 315 cm.^{-1} , another frequency, unobserved in the Raman spectrum, could occur in the range below 285 cm.^{-1} , where the infrared spectrum has not been observed.

TABLE I

FUNDAMENTAL VIBRATIONAL FREQUENCIES OF METHYLCYCLOPENTANE, CM.^{-1} ^a

Skeletal bending	307, 320, 429, 534, 593
C-C stretching	891, 901, 979(2), 1000, 1134
CH ₂ rocking	780, 845, 1012, 1195
CH ₂ wagging	1024(2), 1225, 1305
CH ₂ twisting	1087, 1140, 1276, 1317
CH wagging	1294, 1352
CH ₂ rocking	(891), (1087)
CH ₃ and CH ₂ bending	1380, 1436(2), 1453(2), 1477(2)
C-H stretching	2930(12)

^a Parentheses indicate multiple weights or frequencies used a second time.

methyl rotation is somewhat smaller than expected from the value in the related molecule 2-methylpropane ($3600 \text{ cal. mole}^{-1}$)⁸; differences in molecular geometry may account for this difference, if real.

The calculated values of the thermodynamic functions of methylcyclopentane are listed in columns 2-6 of Table II.⁹ Comparison with experimental results is shown in Table IV.

Thermodynamic Functions of 1-cis-3-Dimethylcyclopentane.—Thermodynamic functions of 1-cis-3-dimethylcyclopentane were calculated by a refined method of increments.¹⁰ The formulas used were

$$C_p^\circ = C_p^\circ(\text{methylcyclopentane}) + C_p^\circ(\text{CH}_2) + 0.81$$

$$S^\circ = S^\circ(\text{methylcyclopentane}) + S^\circ(\text{CH}_2) + 0.81 \ln T - 7.60$$

$$(H^\circ - H^\circ_0) = (H^\circ - H^\circ_0)(\text{methylcyclopentane}) + (H^\circ - H^\circ_0)(\text{CH}_2) + 0.81T$$

In these formulas, $C_p^\circ(\text{CH}_2)$, $S^\circ(\text{CH}_2)$ and $(H^\circ - H^\circ_0)(\text{CH}_2)$ are the methylene increments of Person and Pimentel¹¹ for the indicated functions. These

TABLE II

THE MOLAL THERMODYNAMIC PROPERTIES OF METHYLCYCLOPENTANE^a

T, °K.	$(F^\circ - H^\circ_0)/T$, cal. deg. ⁻¹	$(H^\circ - H^\circ_0)/T$, cal. deg. ⁻¹	$H^\circ - H^\circ_0$, kcal.	S° , cal. deg. ⁻¹	C_p° , cal. deg. ⁻¹	ΔH_f° , ^b kcal.	ΔF_f° , ^b kcal.	log K_f^b
0	0	0	0	0	0	-16.52	-16.52	Infinite
273.15	-64.23	14.80	4.044	79.03	23.87	-24.81	+5.73	-4.59
298.15	-65.56	15.66	4.670	81.22	26.24	-25.50	8.55	-6.27
300	-65.65	15.73	4.719	81.38	26.42	-25.55	8.76	-6.38
400	-70.70	19.62	7.850	90.32	36.16	-28.07	20.59	-11.25
500	-75.53	23.83	11.92	99.36	44.96	-30.10	33.01	-14.43
600	-80.24	27.99	16.80	108.23	52.36	-31.69	45.78	-16.68
700	-84.85	31.93	22.35	116.78	58.56	-32.89	58.80	-18.36
800	-89.36	35.59	28.48	124.95	63.80	-33.76	71.95	-19.66
900	-93.75	38.98	35.08	132.73	68.27	-34.34	85.21	-20.69
1000	-98.02	42.11	42.11	140.13	72.10	-34.66	98.51	-21.53
1100	-102.18	44.98	49.48	147.16	75.39	-34.76	111.82	-22.22
1200	-106.21	47.64	57.17	153.85	78.23	-34.70	125.13	-22.79
1300	-110.12	50.09	65.12	160.21	80.67	-34.52	138.44	-23.27
1400	-113.91	52.35	73.29	166.26	82.79	-34.25	151.74	-23.69
1500	-117.60	54.44	81.66	172.04	84.63	-33.90	165.02	-24.04

^a To retain internal consistency, some values are given to one more decimal place than is justified by the absolute accuracy. For the reaction $6\text{C}(\text{s, graphite}) + 6\text{H}_2(\text{g}) = \text{C}_6\text{H}_{12}(\text{g})$.

Values of three molecular-structure parameters were selected to fit the experimental calorimetric data: the height of the potential barrier restricting internal rotation of the methyl group, $3000 \text{ cal. mole}^{-1}$; the height of the potential barrier restricting pseudo-rotation of the 5-membered ring, $750 \text{ cal. mole}^{-1}$; and the effective moment of inertia for pseudo-rotation, $18.0 \times 10^{-40} \text{ g. cm.}^2$. Effects of vibrational anharmonicity were neglected. The values given for the three molecular-structure parameters are somewhat uncertain because of neglect of anharmonicity as well as uncertainties in the moments of inertia and vibrational frequencies. Nevertheless, these values are reasonable in terms of present knowledge of the structure of related molecules. In particular, the height of the potential barrier to pseudo-rotation agrees well with the value, $900 \text{ cal. mole}^{-1}$, calculated by Pitzer and Donath⁷ from considerations of differences in torsional strain energy. The barrier height for the

increments are strictly for normal paraffins above *n*-heptane; their use in the foregoing formulas is justified only by the good empirical fit to the experimental calorimetric data over a wide range of temperatures. [No advantage could be gained by use of less empirical but more complicated formulas like

$$C_p^\circ = 2C_p^\circ(\text{methylcyclopentane}) - C_p^\circ(\text{cyclopentane}) + [\text{corn. for restricted pseudorotation}] + [\text{constant}]$$

where the term "correction for restricted pseudorotation" is necessary because pseudorotation is restricted in the substituted compounds but not in cy-

(8) K. S. Pitzer and J. E. Kilpatrick, *Chem. Revs.*, **39**, 435 (1946).

(9) The vibrational contributions were computed at the Bureau of Mines Computation Laboratory, Pittsburgh, Pa.; the contributions of internal rotation and restricted pseudo-rotation were computed at Southwestern Computing Service, Denver, Colo., by two-way curvilinear interpolation in the tables of K. S. Pitzer and W. D. Gwinn, *J. Chem. Phys.*, **10**, 428 (1942).

(10) D. W. Scott, H. L. Finke, J. P. McCullough, J. F. Messerly, R. E. Pennington, I. A. Hossenlopp and G. Waddington, *J. Am. Chem. Soc.*, **79**, 1062 (1957).

(11) W. B. Person and G. C. Pimentel, *ibid.*, **75**, 532 (1953).

(7) K. S. Pitzer and W. E. Donath, *J. Am. Chem. Soc.*, **81**, 3213 (1959).

TABLE III

THE MOLAL THERMODYNAMIC PROPERTIES OF 1-*cis*-3-DIMETHYLCYCLOPENTANE^a

$T, ^\circ\text{K.}$	$(F^\circ - H^\circ_0)/T,$ cal. deg. ⁻¹	$(H^\circ - H^\circ_0)/T,$ cal. deg. ⁻¹	$H^\circ - H^\circ_0,$ kcal.	$S^\circ,$ cal. deg. ⁻¹	$C_p^\circ,$ cal. deg. ⁻¹	$\Delta Hf^\circ, b$ kcal.	$\Delta Ff^\circ, b$ kcal.	$\log Kf^b$
0	0	0	0	0	0	-22.48	-22.48	Infinite
273.15	-66.05	18.77	5.126	84.82	29.79	-31.75	+ 5.90	- 4.72
298.15	-67.74	19.80	5.904	87.54	32.52	-32.50	9.38	- 6.87
300	-67.86	19.88	5.965	87.74	32.72	-32.56	9.64	- 7.02
400	-74.20	24.50	9.799	98.70	43.91	-35.32	24.13	-13.18
500	-80.19	29.42	14.71	109.61	54.01	-37.52	39.26	-17.16
600	-85.98	34.24	20.54	120.22	62.51	-39.23	54.79	-19.96
700	-91.61	38.81	27.16	130.41	69.65	-40.49	70.56	-22.03
800	-97.07	43.05	34.44	140.12	75.68	-41.38	86.48	-23.62
900	-102.37	46.97	42.27	149.34	80.83	-41.93	102.51	-24.89
1000	-107.51	50.58	50.58	158.09	85.24	-42.18	118.58	-25.91
1100	-112.49	53.91	59.30	166.40	89.04	-42.20	134.64	-26.75
1200	-117.32	56.98	68.37	174.30	92.31	-42.01	150.69	-27.44
1300	-121.99	59.81	77.75	181.80	95.14	-41.70	166.73	-28.03
1400	-126.52	62.42	87.39	188.94	97.58	-41.28	182.76	-28.53
1500	-130.92	64.83	97.25	195.75	99.71	-40.78	198.75	-28.96

^a To retain internal consistency, some values are given to one more decimal place than is justified by the absolute accuracy. ^b For the reaction $7\text{C}(\text{c, graphite}) + 7\text{H}_2(\text{g}) = \text{C}_7\text{H}_{14}(\text{g})$.

TABLE IV

OBSERVED AND CALCULATED VALUES OF ENTROPY AND HEAT CAPACITY FOR THE VAPOR STATE^a

$T, ^\circ\text{K.}$	Entropy, cal. deg. ⁻¹ mole ⁻¹		Heat capacity, cal. deg. ⁻¹ mole ⁻¹		
	Obsd.	Calcd.	$T, ^\circ\text{K.}$	Obsd.	Calcd.
Methylcyclopentane					
304.09	81.76	81.74	333.20	29.70	29.66
325.98	83.69	83.69	362.55	32.55	32.55
344.97	85.36	85.38	402.35	36.36	36.39
			436.25	39.49	39.52
			471.05	42.58	42.57
1- <i>cis</i> -3-Dimethylcyclopentane					
322.62	90.20	90.21	352.20	38.63	38.63
341.82	92.31	92.31	375.20	41.16	41.20
363.93	94.76	94.74	415.20	45.54	45.54
			455.20	49.65	49.67
			500.20	54.04	54.03

^a See ref. 4 for the source of the observed values.

lopentane itself.] The constants, 0.81 and -7.60 cal. deg.⁻¹ mole⁻¹, in the formulas actually used, were selected to fit the experimental values of heat capacity and entropy, respectively. Omission of an integration constant in the expression for $(H^\circ - H^\circ_0)$ is justified in ref. 10. The calculated values

are listed in columns 2-6 of Table III. Comparison with experimental results is shown in Table IV.

Heat, Free Energy and Equilibrium Constant of Formation.—Values reported for the standard heat of formation of liquid methylcyclopentane and 1-*cis*-3-dimethylcyclopentane at 25° are -33.08 and -40.68 kcal. mole⁻¹.^{12,13}

From the data of ref. 4, values of the standard heat of vaporization at 25° are calculated to be 7.58 and 8.18 kcal. mole⁻¹. Values of the standard heat of formation of the gaseous substances at 25° are then -25.50 and -32.50 kcal. mole⁻¹. These results and the thermodynamic functions of the two compounds, C(c, graphite)¹⁴ and H₂(g)¹⁴ were used to calculate the values of ΔHf° , ΔFf° and $\log Kf$ in columns 7-9 of Tables II and III.

The values of thermodynamic properties in Tables II and III do not differ seriously from those of ref. 1 and 2; however, they are more reliable because they are based on accurate experimental values of the vapor heat capacity.

(12) E. J. Prosen, W. H. Johnson and F. D. Rossini, *J. Research Natl. Bur. Standards*, **37**, 51 (1946).

(13) W. H. Johnson, E. J. Prosen and F. D. Rossini, *ibid.*, **42**, 251 (1949).

(14) D. D. Wagman, J. E. Kilpatrick, W. J. Taylor, K. S. Pitzer and F. D. Rossini, *ibid.*, **34**, 143 (1945).

THE MERCURY-MERCURIC CHLORIDE SYSTEM¹

By S. J. YOSIM AND S. W. MAYER

Atomics International, A Division of North American Aviation, Inc., Canoga Park, California

Received February 8, 1960

A phase equilibrium study of the mercury-mercuric chloride system has been carried out by thermal analysis and by the visual method. The salt-rich eutectic composition is 4.9 mole % Hg and occurs at 273°. The syntectic line at 525° extends from 48 to 94 mole % Hg. The solubility of HgCl₂ in Hg increases to 6.8 mole % at 560°. Freezing point depression measurements for HgCl₂ suggest that Hg dissolves either as atoms or as Hg₂Cl₂ molecules formed by reaction of Hg with HgCl₂. A thermodynamic analysis of the liquid-solid equilibrium curve between the salt-rich eutectic and the base of the miscibility gap suggests that solution of Hg as atoms is not likely in this region.

Introduction

Although there have been many investigations of the interaction of mercury with HgCl₂ and of the properties of the reaction product Hg₂Cl₂, relatively little research has been carried out to determine the phase diagram of the Hg-HgCl₂ system. The freezing point depression of HgCl₂ by calomel, up to 1.2 mole %, was determined by Beckmann.² Ruff and Schneider,³ in a series of exploratory experiments, determined approximate melting temperatures of Hg₂Cl₂-HgCl₂ mixtures equivalent in composition to 25-45 mole % mercury dissolved in HgCl₂. Smith and Menzies,⁴ in their studies of the constitution of calomel vapor, measured the solubility of Hg₂Cl₂ in mercury from 250 to 400°. In order to obtain a more extensive phase diagram of this system, a series of phase equilibria measurements therefore was carried out.

Experimental

A. Materials.—Reagent grade HgCl₂ and Hg₂Cl₂, dried under vacuum at 110° for 24 hours, and triple-distilled mercury were used.

B. Apparatus and Procedure.—Two techniques were used in this work, thermal analysis and the visual method. For freezing point determinations by thermal analysis, the salts were contained in a sealed 18 mm. Pyrex or Vycor tube which had a thin-walled thermocouple well sealed into the bottom of the tube. Temperatures were measured with a calibrated chromel-alumel thermocouple, using a Rubicon B potentiometer. The cold junction of the thermocouple was maintained in an oil-filled tube, placed in a distilled water-ice-bath. The sample was heated in a furnace which was automatically controlled by a regulator-pyrometer operating through a variable transformer.

Because the high vapor pressures of HgCl₂ and Hg above 390° could lead to explosions of the tubes containing the samples, a stainless steel pressure vessel was used to hold the quartz tubes for thermal arrest measurements on samples in the 15.9-85.0 mole % Hg range. In the pressure vessel, external pressures as high as 50 atmospheres of nitrogen were applied to the sample tubes. Thermal arrest measurements were not made above 600° since that was considered to be the safety limit of the pressure vessel.

For solubility determinations by the visual method, the mixture of salt and metal was placed in a thick-walled quartz tube and sealed under vacuum. The tube then was fastened to a nickel rod and suspended in a Marshall furnace, equipped with two sight windows opposite one another. The tube was illuminated from the rear and from a third window at one side. A chromel-alumel thermocouple fastened to the tube was employed for measurement of temperature. The furnace was mounted on a metal base which was provided with a rocking mechanism. In this way the entire system could be inverted frequently to en-

sure adequate surface contact of the two phases. The sample was heated until the second condensed phase completely disappeared. The solution process was found in all cases to be reversible with temperature.

Results

Figure 1 shows the phase diagram of the Hg-HgCl₂ system under its own pressure. Mercuric chloride was found to freeze at 279.5° compared with the literature value of 277°. The salt-rich eutectic temperature was 273° and the eutectic composition was 4.9 mole % Hg. The curve between the salt-rich eutectic and the base of the miscibility gap is in sharp disagreement with that of Ruff and Schneider.³ However, in their admittedly exploratory work, the liquidus temperatures were determined by heating and were defined as temperatures at which mixtures formed droplets. These temperatures are therefore likely to be considerably lower than those reported here. The syntectic temperature, or that temperature at which Hg₂Cl₂ forms two liquid phases, was found to be 525°, in good agreement with Ruff and Schneider's value of 522°. The fact that the syntectic line extends to compositions less than 50 mole % Hg suggests that some disproportionation of Hg₂Cl₂ takes place on liquefying at the syntectic temperature.

Visual observations of the salt-rich region showed an interesting behavior. As mercury or Hg₂Cl₂ is added in increasing concentrations to HgCl₂ which is almost colorless, the solution becomes yellow, red and eventually black. As a given solution containing Hg or Hg₂Cl₂ is heated the same darkening in color, which is reversible, takes place.⁶

The solubility of the salt in the metal rises from 0.2 mole % HgCl₂ (or Hg₂Cl₂) at 280° to 6.8 mole % HgCl₂ (7.13 mole % Hg₂Cl₂) at 555°. The solubilities measured by Smith and Menzies⁴ are in good agreement with these values.

Discussion

The HgCl₂ liquidus and the liquid-solid equilibrium curve between the salt-rich eutectic and the base of the miscibility gap were examined in order to see whether information on the mechanism of solution of Hg in HgCl₂ could be obtained. The mechanisms which can be considered for the solution of Hg in HgCl₂ fall into two classes. The

(5) L. Brewer, "The Chemistry and Metallurgy of Miscellaneous Materials—Thermodynamics," L. L. Quill, Ed., NNE IV-19B, McGraw-Hill Book Co., New York, N. Y., 1950.

(6) For example, an HgCl₂ solution containing 10% Hg was yellow at 415°, orange at 465°, red at 510° and dark transparent red at 535° while a more concentrated solution, 25 mole % Hg, was very dark red and barely transparent at 415° and black at 467°.

(1) This work was supported by the Research Division of the Atomic Energy Commission.

(2) E. Beckmann, *Z. anorg. Chem.*, **55**, 175 (1907).

(3) O. Ruff and R. Schneider, *Z. anorg. allgem. Chem.*, **170**, 42 (1928).

(4) A. Smith and A. Menzies, *J. Am. Chem. Soc.*, **32**, 1541 (1910).

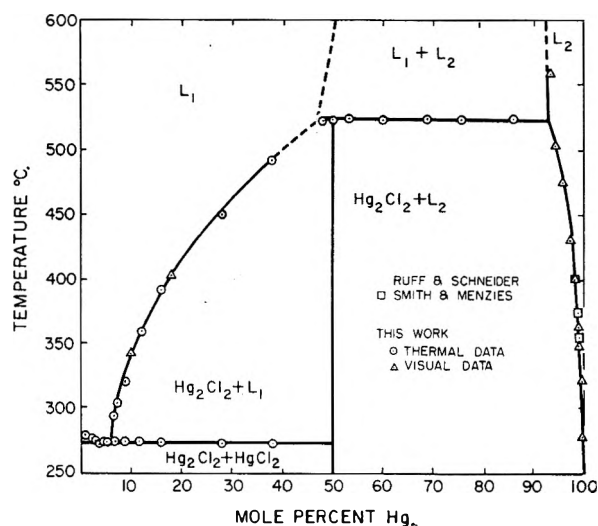


Fig. 1.—The mercury-mercuric chloride system. Circles denote the results obtained by thermal analysis. Data obtained by the visual technique are represented by the triangles. Smith and Menzies' results⁴ are denoted by the squares, and the cross-hatched line summarizes the work of Ruff and Schneider.³

first is solution as Hg atoms, dimers or higher polymers and the second is solution by reaction of Hg with HgCl₂ to form the lower-valent compound, mercurous chloride. (The fact that solid Hg₂Cl₂ is stable with respect to its disproportionation products in the pure state does not prove its existence in the liquid solution).

In the case of the HgCl₂ liquidus the cryoscopic number, the apparent number of particles formed in molten HgCl₂ per molecule of solute, was calculated from the Raoult-van't Hoff equation.⁷ The calorimetric value of the heat of fusion of HgCl₂, 4640 ± 50 cal./mole,⁸ was used for this calculation. The cryoscopic number was found to be 1.17 ± 0.03 (Table I). The discrepancy between this value and unity may be due to deviations of the solvent from ideality or to the fact that two or more processes of solution are taking place. The cryoscopic number of about unity indicates that Hg

TABLE I
FREEZING POINT DEPRESSIONS IN MOLTEN MERCURIC CHLORIDE

Solute	Solute, mole %	ΔT _f , °C.	Cryoscopic no.
Hg	0.69	1.05	1.16
Hg	1.09	1.73	1.21
Hg	2.15	3.31	1.17
Hg	3.16	5.04	1.22
Hg	4.27	6.34	1.13
Hg	4.85	7.04	1.11
Hg ₂ Cl ₂	0.87	1.32	1.16
Hg ₂ Cl ₂	1.37	2.14	1.19
Hg ₂ Cl ₂	2.50	3.90	1.19
Hg ₂ Cl ₂	3.41	4.99	1.12
Hg ₂ Cl ₂	4.76	6.78	1.09

does not dissolve in molten HgCl₂ predominantly as a metal polymer or as HgCl. There are two

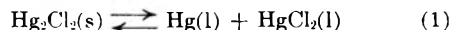
(7) S. W. Mayer, S. J. Yosim and L. E. Topol, *THIS JOURNAL*, **64**, 238 (1960).

(8) L. E. Topol and L. D. Ransoin, *ibid.*, in press.

mechanisms of solution which yield a cryoscopic number of unity. These are solution of mercury as atoms or solution by reaction to form Hg₂Cl₂. If the latter mechanism takes place, the Hg₂Cl₂ is presumably un-ionized since the addition of small amounts of Hg₂Cl₂ to HgCl₂ does not increase the electrical conductivity of the latter.⁹ Molten HgCl₂ has the relatively low specific conductance¹⁰ of 8 × 10⁻⁵ ohms⁻¹ cm.⁻¹ which suggests that its chloride ion concentration is correspondingly low.

It can be seen from Table I that mercurous chloride solute also has a cryoscopic number of about unity. As in the case of Hg, solution of mercurous chloride as the un-ionized Hg₂Cl₂ or by disproportionation to form Hg plus HgCl₂ are mechanisms which are consistent with a cryoscopic number of one. The above evidence plus the visual observations of similar color changes suggest that the resulting solutions formed by dissolving Hg or Hg₂Cl₂ are identical, but the data of the HgCl₂ liquidus curve do not distinguish whether these solutions contain Hg atoms or Hg₂Cl₂ molecules.

The liquid-solid equilibrium curve between the salt-rich eutectic and the base of the miscibility gap (5-47 mole % Hg) cannot be examined on the basis of freezing point depressions since the heat of fusion of Hg₂Cl₂ is not known. However, the possibility that this curve can be interpreted in terms of a molten solution containing only Hg and HgCl₂ can be examined. If one assumes that solid Hg₂Cl₂ is in equilibrium only with its disproportionation products, *i.e.*



then the variation of the Hg concentration with temperature is given by

$$\frac{d \log N_{\text{Hg}}}{dT} = \left(\frac{1 - N_{\text{Hg}}}{1 - 2N_{\text{Hg}}} \right) \left[\frac{-\Delta H^0 - \Delta \bar{H}_{\text{Hg}} - \Delta \bar{H}_{\text{HgCl}_2}}{4.57} \right] + N_{\text{Hg}} \left(\frac{\partial \ln \gamma_{\text{Hg}}}{\partial N_{\text{Hg}}} \right)_T \quad (2)$$

where N_{Hg} is the mole fraction of Hg, ΔH^0 is the standard heat of reaction 1, $\Delta \bar{H}$ is the relative partial molal heat of solution and γ is the activity coefficient, the standard state being the pure liquid.¹¹

(9) H. Foote and N. Martin, *Am. Chem. J.*, **41**, 451 (1908).

(10) W. Klemm and W. Biltz, *Z. anorg. allgem. Chemie*, **152**, 225 (1926).

(11) The derivation of equation 2 is as follows: the equilibrium constant K for reaction 1 is given by

$$K = a_{\text{Hg}} a_{\text{HgCl}_2} \quad (a)$$

where "a" is the activity, the standard states being the pure liquids. Then

$$\frac{d \ln K}{dT} = \frac{\Delta H^0}{RT^2} = \left(\frac{1 - 2N_{\text{Hg}}}{1 - N_{\text{Hg}}} \right) \left(\frac{\partial \ln N_{\text{Hg}}}{\partial T} \right)_{\text{sat}} + \left(\frac{\partial \ln \gamma_{\text{Hg}} \gamma_{\text{HgCl}_2}}{\partial T} \right)_{\text{sat}} \quad (b)$$

where the subscript "sat" refers to the saturation curve. Since, at the saturation curve, both temperature and composition are varying, it is necessary to evaluate the effect of each on the activity coefficient. Applying a treatment similar to that of Williamson (*Trans. Faraday Soc.*, **40**, 421 (1944)), it can be shown that

$$\left(\frac{\partial \ln \gamma_{\text{Hg}}}{\partial T} \right)_{\text{sat}} = - \frac{\Delta \bar{H}_{\text{Hg}}}{RT^2} + \left(\frac{\partial \ln \gamma_{\text{Hg}}}{\partial N_{\text{Hg}}} \right)_T \left(\frac{\partial N_{\text{Hg}}}{\partial T} \right)_{\text{sat}} \quad (c)$$

Using a similar expression for $(\partial \ln \gamma_{\text{HgCl}_2} / \partial T)_{\text{sat}}$ and substituting into (b)

To illustrate the magnitude of the terms of equation 2, two temperature regions will be considered, one near the syntectic temperature at a composition of 38 mole % Hg where $d \log N_{\text{Hg}}/d(1/T) = -1600$ and one near the eutectic region at a composition of 7 mole % Hg where the slope = -1500 . Substituting these values and the value $13,000^5$ for ΔH^0 of reaction 2 into equation 2, one obtains for the high temperature and low temperature, respectively

$$\left(\frac{\partial \ln \gamma_{\text{Hg}}}{\partial N_{\text{Hg}}}\right)_T - \frac{\Delta \bar{H}_{\text{Hg}} + \Delta \bar{H}_{\text{HgCl}_2}}{1060} = 10 \quad (3)$$

$$\left(\frac{\partial \ln \gamma_{\text{Hg}}}{\partial N_{\text{Hg}}}\right)_T - \frac{\Delta \bar{H}_{\text{Hg}} + \Delta \bar{H}_{\text{HgCl}_2}}{382} = 19 \quad (4)$$

In the usual binary system in which a miscibility gap exists, the $\Delta \bar{H}$ terms and therefore their sum are positive. Also the term $(\partial \ln \gamma_i / \partial N_i)_T$ is negative, *i.e.*, at small values of N_i , γ_i is greater than unity due to positive deviations from ideality while, at values of N_i close to unity, γ_i approaches one. Between these two limits, γ_i decreases continuously with increasing concentration in the single phase region and is of course constant in the two

$$\left(\frac{d \log N_{\text{Hg}}}{d 1/T}\right)_{\text{sat}} \left[\left(\frac{1 - 2N_{\text{Hg}}}{1 - N_{\text{Hg}}} \right) + N_{\text{Hg}} \left(\frac{\partial \ln \gamma_{\text{Hg}} \gamma_{\text{HgCl}_2}}{\partial N_{\text{Hg}}} \right)_T \right] = - \frac{(\Delta H^0 + \Delta \bar{H}_{\text{Hg}} + \Delta \bar{H}_{\text{HgCl}_2})}{4.57} \quad (d)$$

Applying the Gibbs-Duhem relation, one then obtains equations 2.

liquid phase region. Thus in the usual binary system in which a miscibility gap exists the difference between the term $(\partial \ln \gamma_i / \partial N_i)_T$ and the term consisting of the partial molal heats of solution would be negative. However the initial assumption that Hg_2Cl_2 disproportionates on dissolving in HgCl_2 leads to positive values for this difference—a fact which suggests that the initial assumption is incorrect.

While the activity coefficients and the relative partial molal heats of solution of the HgCl_2 - Hg_2Cl_2 system are not known, it is not anticipated that such apparent inconsistencies arise if this model is assumed for the solutions discussed above. The fact that the melt obtained when Hg_2Cl_2 is heated to 580° is diamagnetic¹² is consistent with this mechanism. As stated earlier the heat of fusion of Hg_2Cl_2 is not known. However, if one assumes that Hg_2Cl_2 rather than Hg exists in the salt melt, and calculates the heat of fusion from the slope of a $\log N_{\text{Hg}_2\text{Cl}_2}$ vs. $1/T$ plot near the miscibility gap, a value of 11 kcal./mole ($\Delta S_{\text{fus}} = 14$ e.u.) is obtained. Such a value is not unreasonable. Therefore, the above arguments suggest that Hg dissolves in HgCl_2 as Hg_2Cl_2 rather than as Hg atoms.

Acknowledgment.—The authors are grateful to Dr. D. E. McKenzie and to Professor H. Flood for many helpful discussions.

(12) J. Farquharson and E. Heyman, *Trans. Faraday Soc.*, **31**, (2) 1004 (1935).

HIGH-TEMPERATURE FREE ENERGY, ENTROPY, ENTHALPY AND HEAT CAPACITY OF THORIUM SULFATE¹

BY S. W. MAYER, B. B. OWENS, T. H. RUTHERFORD AND R. B. SERRINS

Research Department, Atomics International, A Division of North American Aviation, Canoga Park, California

Received February 15, 1960

Decomposition pressures of $\text{Th}(\text{SO}_4)_2$ have been measured from 908 to 1057°K. The results show that the decomposition reaction is: $\text{Th}(\text{SO}_4)_2(\text{s}) = \text{ThO}_2(\text{s}) + 2\text{SO}_2(\text{g}) + \text{O}_2(\text{g})$. The heat capacity of $\text{Th}(\text{SO}_4)_2$ has been determined from 623 to 897°K. by a drop calorimeter technique and the results are given by: $C_p = 25.0 + 55.2 \times 10^{-3}T$ cal. mole⁻¹ deg.⁻¹ Least squares treatments of the decomposition pressure and heat capacity data have been used to obtain equations for the thermodynamic functions of the decomposition reaction. Equations have also been calculated for the absolute entropy of $\text{Th}(\text{SO}_4)_2$ and for the standard free energy and enthalpy of formation of $\text{Th}(\text{SO}_4)_2$ from its elements.

Introduction

A series of measurements of the decomposition pressures of $\text{Th}(\text{SO}_4)_2$ has been made as part of a program for determining the high-temperature thermodynamic functions for thorium and uranium compounds. Heat capacities at elevated temperatures have also been determined in this study to obtain free energy, enthalpy and entropy equations for $\text{Th}(\text{SO}_4)_2$ applicable from 298 to 1057°K.

$\text{Th}(\text{SO}_4)_2$ is of particular interest because of its possible use as the fertile material in reactor fuels based on a molten alkali metaphosphate-sulfate system.² The only previous reported thermochemical values for this compound are a heat of

formation³⁻⁵ at 298°K. and a heat capacity^{6,7} at 298°K. No thermochemical values have hitherto been reported for $\text{Th}(\text{SO}_4)_2$ at elevated temperatures.

Experimental

Materials.—Thorium sulfate, prepared by the S. W. Shattuck Chemical Company, was dried in a vacuum system for nine days; the temperature of the sample was increased by fifty degrees each day until it had been dried at 375° for 24 hours. Chemical analysis of the product showed that the water content was less than 0.01%, and that the sulfate content corresponded to $99.9 \pm 0.1\%$ $\text{Th}(\text{SO}_4)_2$. The powder X-ray diffraction pattern showed only $\text{Th}(\text{SO}_4)_2$ lines, with no evidence of a hydrate or oxy-sulfate.

(3) F. D. Rossini, *et al.*, Circular 500, National Bureau of Standards, 1952.

(4) J. J. Katz and G. T. Seaborg, "The Chemistry of the Actinide Elements," John Wiley and Sons, Inc., New York, N. Y., 1957.

(5) G. Beck, *Z. anorg. Chem.*, **174**, 31 (1928).

(6) L. F. Nilson and O. Peterson, *Ber.*, **13**, 1459 (1880).

(7) K. K. Kelley, Bulletin 476, U. S. Bureau of Mines, 1949.

(1) This research was performed under the auspices of the U. S. Atomic Energy Commission.

(2) S. W. Mayer, W. S. Ginell and D. E. McKenzie, *Trans. Am. Nuclear Soc.*, **2**, 126 (1959).

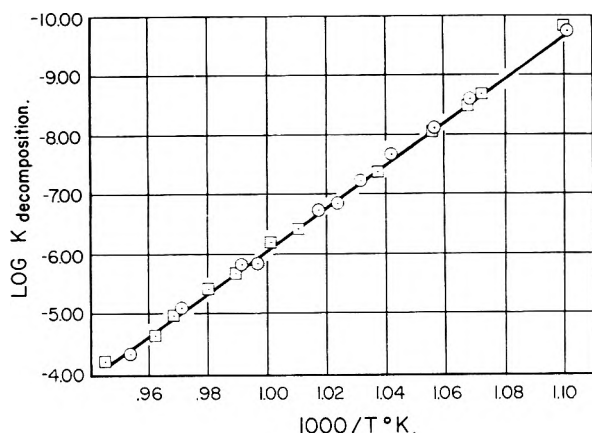


Fig. 1.—Equilibrium constants for the decomposition of $\text{Th}(\text{SO}_4)_2$. The circles denote the results for $\text{Th}(\text{SO}_4)_2$ powder, and the squares denote the results for the $\text{Th}(\text{SO}_4)_2$ - ThO_2 pellets.

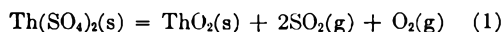
Procedure. (a) **Vapor Pressure Measurements.**—One hundred grams of the dried thorium sulfate was placed in the bottom of a 20-inch long, 33-mm. diameter silica tube which had a thin-walled thermocouple well sealed in the bottom. A platinum-foil helix having an area of 150 cm.² was placed above the sulfate to catalyze the sulfur dioxide, oxygen equilibrium. The silica tube was heated in a temperature-controlled Marshall furnace adjusted to maintain uniform temperature over the region containing the sample. The temperature of the sample was measured with a chromel-alumel thermocouple standardized against a Bureau of Standards resistance thermometer. Pressures were measured manometrically and were read with a precision of 2×10^{-6} atmosphere using a cathetometer. Preliminary tests had shown that sulfur trioxide vapor could attack hydrocarbon types of vacuum greases and mercury manometric fluid. Consequently, fluorocarbon vacuum grease was used for the joints of the vacuum system, and silicone diffusion pump fluid in the manometer.

Before pressure measurements were begun the sample was dried again *in vacuo* for two days at 375°, and then for one hour at 800°, which was higher than any temperature at which the vapor pressure was determined. For a given temperature, three to four hours were required to attain constancy of pressure; the temperature was kept constant for an additional 20 hours to ascertain that no drift in pressure occurred. After several pressure measurements had been made, temperatures were raised and then lowered to the original temperatures and the pressures were found to be reproducible.

(b) **Heat Capacity Determination.**—The drop calorimeter and procedure were similar to those of Goodkin, Solomons and Janz.⁸ The dried $\text{Th}(\text{SO}_4)_2$ was held in an unsealed platinum vessel. Four or more drops were made at each of a series of temperatures: 350, 400, 450, 551 and 624°. The average deviation in the temperature rise of the calorimeter was less than 2%. No significant weight loss of $\text{Th}(\text{SO}_4)_2$ was observed throughout the foregoing measurements, but the sample did lose weight when heated at 675°. The occurrence of weight loss corresponded to the appearance of detectable vapor pressures in the manometric measurements. Consequently, heat capacity measurements were discontinued above 624°. The calorimeter constant was obtained at each of the temperatures from 350 to 624° by similar drops made with NaCl in the same platinum vessel. The use of Kelley's equation⁹ for the heat capacity of NaCl gave calorimeter constants which had an average deviation of less than 0.6% over the 350 to 624° range.

Results

Decomposition Equilibrium for $\text{Th}(\text{SO}_4)_2$.—The results are summarized in Fig. 1 and Table I. In Fig. 1 the circled points denote the experimental results for the decomposition reaction of $\text{Th}(\text{SO}_4)_2$



The ordinate of each point in Fig. 1 is the logarithm of the equilibrium constant

$$K_{\text{dec}} = P_{\text{SO}_2}^2 \times P_{\text{O}_2} \text{ atm.}^3 \quad (2)$$

TABLE I
THERMAL DECOMPOSITION OF $\text{Th}(\text{SO}_4)_2$

Temp., °K.	Dec. pressure, atm. $\times 10^2$	SO_2 Partial pressure, atm. $\times 10^2$	O_2 Partial pressure, atm. $\times 10^2$	K_{dec} , atm. ³
(a) $\text{Th}(\text{SO}_4)_2$ Powder				
907.2	1.14	0.66	0.36	1.87×10^{-10}
935.2	2.89	.18	0.90	2.94×10^{-9}
946.3	4.11	.28	1.28	8.40×10^{-9}
959.0	5.94	.41	1.84	2.49×10^{-8}
968.9	8.24	.62	2.54	6.56×10^{-8}
977.2	10.68	.83	3.28	1.41×10^{-7}
982.4	11.91	.90	3.67	1.98×10^{-7}
1004.5	22.81	1.96	6.95	1.34×10^{-6}
1008.1	24.31	2.09	7.41	1.63×10^{-6}
1029.2	42.92	3.91	13.00	8.80×10^{-6}
1049.2	73.81	6.97	22.28	4.41×10^{-5}
(b) $\text{Th}(\text{SO}_4)_2$ - ThO_2 Pellets				
907.7	1.10	0.06	0.35	1.68×10^{-10}
932.4	2.62	.16	.82	2.20×10^{-9}
936.5	3.08	.18	.97	3.60×10^{-9}
947.8	4.36	.30	1.35	9.84×10^{-9}
964.0	7.11	.51	2.20	4.24×10^{-8}
989.6	14.92	1.22	4.57	3.82×10^{-7}
997.8	18.45	1.55	5.63	7.12×10^{-7}
1010.5	26.76	2.34	8.14	2.16×10^{-6}
1020.1	33.39	3.00	10.13	4.16×10^{-6}
1032.7	47.29	4.40	14.30	1.17×10^{-5}
1040.0	57.58	5.38	17.40	2.11×10^{-5}
1057.2	85.74	7.85	25.96	7.00×10^{-5}

Since some SO_3 is formed as a result of the equilibrium



corresponding corrections (ranging from 5 to 9%) have been made to the observed pressures. Coughlin's high temperature free energy data¹⁰ were used to make the corrections.

It can be seen in Fig. 1 that the circled points show a relationship between $\log K_{\text{dec}}$ and reciprocal absolute temperature which is linear within experimental error. This suggests that no side reactions occurred to a significant extent. Powder X-ray diffraction patterns of the residue left after the completion of this set of vapor pressure measurements supported that deduction since every line in the pattern was identified as belonging to $\text{Th}(\text{SO}_4)_2$ or ThO_2 , and there was no evidence of solid solution or oxysulfate formation. Chemical analysis of the residue showed a sulfate and thorium content corresponding to a mixture of 48 mole % $\text{Th}(\text{SO}_4)_2$ and 52 mole % ThO_2 . In order to determine whether ThO_2 was the final solid decomposition product, a 20-g. sample of the dry $\text{Th}(\text{SO}_4)_2$ was heated *in vacuo* for 10 days at 1053°K. No sulfate could be detected by chemical analysis of the solid product, and the X-ray powder diffraction pattern showed that the solid residue was ThO_2 .

(8) J. Goodkin, C. Solomons and G. J. Janz, *Rev. Sci. Instr.*, **29**, 105 (1958).

(9) W. A. Roth and W. W. Bertram, *Z. Elektrochem.*, **35**, 297 (1929).

(10) J. P. Coughlin, Bulletin 542, U. S. Bureau of Mines, 1954.

It is possible, however, that decomposition of solids can occur in such a way that a solid product can be formed as an extremely finely divided powder having different thermochemical properties from the bulk solid.¹¹ Because of this possibility, a set of vapor pressure measurements was carried out on 70 g. of pellets formed by pressing an equimolar mixture of $\text{Th}(\text{SO}_4)_2$ and ThO_2 . The pellets were cylinders, three-eighths inch in diameter and about three-eighths inch long; they were pressed at 2000 lb./in.² The squares in Fig. 1 denote the results obtained with the $\text{Th}(\text{SO}_4)_2$ - ThO_2 pellets. It can be seen that they were concordant with the results obtained from $\text{Th}(\text{SO}_4)_2$ powder alone.

Heat Capacity of $\text{Th}(\text{SO}_4)_2$.—In Fig. 2, the circled points denote the results of drop calorimeter measurements of the heat evolved when one mole of $\text{Th}(\text{SO}_4)_2$ was cooled from the indicated temperatures to 24°. The solid curve was fitted to these data by the least squares method to give an equation for the heat capacity

$$C_p = -\frac{d\Delta H}{dT} = 25.0 + 55.2 \times 10^{-3}T \text{ cal. mole}^{-1} \text{ deg.}^{-1} \quad (4)$$

where T is the absolute temperature, and $-\Delta H$ is the heat evolved on cooling one mole of $\text{Th}(\text{SO}_4)_2$ from T to 297°K. The standard deviation for C_p was 1.5%. At 298°K., equation 4 gives a calculated heat capacity of 41.4 cal. mole⁻¹deg.⁻¹ compared to the value of 41 cal. mole⁻¹deg.⁻¹ reported in the literature.⁷ This suggests that equation 4 is applicable to 298°K. The absence of solid state transformations for $\text{Th}(\text{SO}_4)_2$ was confirmed, in the 297 to 910°K. range, by direct thermal analysis of a 25-g. sample of the $\text{Th}(\text{SO}_4)_2$ powder.

Thermodynamic Data for the Decomposition of $\text{Th}(\text{SO}_4)_2$.—The heat capacity equations for the products of $\text{Th}(\text{SO}_4)_2$ decomposition (equation 1) have been reported.¹²

$$\text{ThO}_2: C_p = 15.84 + 2.88 \times 10^{-3}T - 1.60 \times 10^5 T^{-2} \quad (5)$$

$$2\text{SO}_2: C_p = 20.76 + 5.08 \times 10^{-3}T - 2.84 \times 10^5 T^{-2} \quad (6)$$

$$\text{O}_2: C_p = 7.16 + 1.00 \times 10^{-3}T - 0.40 \times 10^5 T^{-2} \quad (7)$$

Equations 5, 6 and 7 are applicable from 298 to 1800°K.

Using the heat capacity equation 4 for $\text{Th}(\text{SO}_4)_2$, ΔC_p for reaction 1 is

$$\Delta C_p = 18.76 - 46.24 \times 10^{-3}T + 4.84 \times 10^5 T^{-2} \text{ cal. mole}^{-1} \text{ deg.}^{-1} \quad (8)$$

The sigma function method¹³ for calculating thermodynamic data was applied by using equation 8 in conjunction with the 23 experimentally determined equilibrium constants of Fig. 1. The sigma function, Σ , follows these relationships¹³

$$\Sigma = -R \ln K + \Delta a \ln T + \frac{\Delta b T}{2} + \frac{\Delta c T^{-2}}{2} = \frac{\Delta H_0}{T} + I \quad (9)$$

(11) H. Flood and O. J. Kleppa, *J. Am. Chem. Soc.*, **69**, 998 (1947).

(12) O. Kubaschewski and E. L. Evans, "Metallurgical Thermochemistry," Third Edition, Pergamon Press, London, 1958.

(13) L. S. Darken and R. W. Gurry, "Physical Chemistry of Metals," McGraw-Hill Book Co., New York, N. Y., 1953.

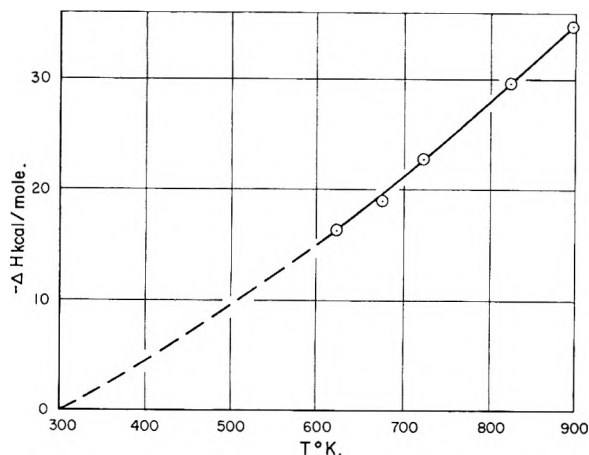


Fig. 2.—Heat evolved in drop calorimeter per mole of $\text{Th}(\text{SO}_4)_2$ cooled from T to 297°K.

where Δa , Δb and Δc are the constants in equation 8.

ΔH_0 and I were calculated by least squares treatment of the data and were found to be 167.23 kcal./mole and $-33.12 \text{ cal. mole}^{-1} \text{ deg.}^{-1}$, respectively. The standard deviations were 0.55 kcal. mole for ΔH_0 and 0.09 cal. mole⁻¹deg.⁻¹ for I . Using these results for ΔH_0 and I , the following thermodynamic equations can be written¹³ for the decomposition of $\text{Th}(\text{SO}_4)_2$ (equation 1)

$$\Delta F_{\text{dec}}^0 = 167,230 - 33.12T - 18.76 T \ln T + 23.12 \times 10^{-3}T^2 + 2.42 \times 10^5 T^{-1} \text{ cal./mole} \quad (10)$$

$$\Delta S_{\text{dec}}^0 = 51.88 + 18.76 \ln T - 46.24 \times 10^{-3}T + 2.42 \times 10^5 T^{-2} \text{ cal. mole}^{-1} \text{ deg.}^{-1} \quad (11)$$

$$\Delta H_{\text{dec}}^0 = 167,230 + 18.76T - 23.12 \times 10^{-3}T^2 + 4.84 \times 10^5 T^{-1} \text{ cal./mole} \quad (12)$$

The curve shown in Fig. 1 corresponds to an equation (derived from equation 10) for $\log K_{\text{dec}}$

$$\log K_{\text{dec}} = -36.553T^{-1} + 7.244 + 9.444 \log T - 5.05 \times 10^{-3}T - 0.529 \times 10^5 T^{-2} \quad (13)$$

The slope of the higher temperature section of the curve differs by only 2% from that of the lower temperature section. Equations 10-13 were derived in part from $\text{Th}(\text{SO}_4)_2$ heat capacity data based on measurements at temperatures up to 897°K., and consequently involve the assumption that equation 4 is applicable to 1057°K. If melting or a solid state transformation occurred in the 897 to 1057°K. range, that assumption would be invalid. The absence of melting or transformation of $\text{Th}(\text{SO}_4)_2$ was indicated by visual and X-ray examination of the powder remaining from the decomposition pressure measurements and by the absence of discontinuities in the equilibrium constant data (Fig. 1). Consequently, the use of equation 4 in deriving equations 10-13 for the 908 to 1057°K. range probably did not introduce large errors.

Discussion

Formation of $\text{Th}(\text{SO}_4)_2$ from its Elements.—Equations 10-12 have been combined with the thermochemical data¹² for $\text{Th}(s)$, $\text{O}_2(g)$, S , $\text{ThO}_2(s)$ and $\text{SO}_2(g)$ to obtain equations for the free energy and enthalpy of formation of $\text{Th}(\text{SO}_4)_2$ from its elements and the absolute entropy of $\text{Th}(\text{SO}_4)_2$.

For the formation of $\text{Th}(\text{SO}_4)_2$ from Th , O_2 and orthorhombic sulfur (298 to 368.6°K.)

$$\Delta F^\circ_f = -603,540 + 83.40T + 17.20T \ln T - 17.83 \times 10^{-3}T^2 - 0.62 \times 10^5T^{-1} \text{ cal./mole} \quad (14)$$

$$\Delta H^\circ_f = -603,540 - 17.20T + 17.83 \times 10^{-3}T^2 - 1.24 \times 10^5T^{-1} \text{ cal./mole} \quad (15)$$

At 298.15°K., $\Delta F^\circ_f = -551.2$ kcal./mole, $\Delta H^\circ_f = -607.4$ kcal./mole and $S^\circ = 35.4$ e.u./mole.

Equations 16–18 are applicable from 298 to 1057°K.

$$S^\circ = -123.47 + 25.0 \ln T + 55.2 \times 10^{-3}T \text{ e.u./mole} \quad (16)$$

For the formation of $\text{Th}(\text{SO}_4)_2$ from Th , O_2 and $\text{S}_2(\text{g})$

$$\Delta F^\circ_f = -634,400 + 116.50T + 18.58T \ln T - 23.93 \times 10^{-3}T^2 - 1.02 \times 10^5T^{-1} \text{ cal./mole} \quad (17)$$

$$\Delta H^\circ_f = -634,400 - 18.58T + 23.93 \times 10^{-3}T^2 - 2.04 \times 10^5T^{-1} \text{ cal./mole} \quad (18)$$

Since equations 10–12 were based largely on decomposition pressure measurements made from 907 to 1057°K., their extrapolation to 298°K. to obtain equations 14–18 increased the standard deviations of values calculated from those equations. For example, the standard deviation for equation 10 was 1.1 kcal. at 298°K. compared to 0.6 kcal. at 1000°K. Furthermore, because of the estimated errors in the thermochemical data¹² for ThO_2 , SO_2 and their elements, combining them with the errors of equations 10–12 led to estimated standard deviations from 298 to 1057°K. of 1.5 kcal./mole for ΔF°_f and for ΔH°_f and 0.5 e.u./mole for S° values calculated from the corresponding equations.

Comparison with Older Data.—It has been pointed out that the only thermochemical data previously reported for $\text{Th}(\text{SO}_4)_2$ were the heat capacity⁶ and enthalpy⁵ at 298°K. The heat capacity results obtained in this work at elevated temperatures have been shown to extrapolate to ± 1.4 cal. mole⁻¹deg.⁻¹ at 298°K., in accord with the reported value⁶ of 41 cal. mole⁻¹deg.⁻¹.

From equation 15, the heat of formation of $\text{Th}(\text{SO}_4)_2$ at 298.15°K. was calculated to be -607.4 kcal./mole. The literature⁴ value of -603 kcal./mole was based on a heat of solution reported by Beck,⁵ in a table involving ten heavy metal sulfates. Beck gave the result of only one measurement of the heat evolved when $\text{Th}(\text{SO}_4)_2$ (preparation and water content not given) was added to aqueous NaOH (concentration not specified). He assumed that the precipitate formed in the calorimeter was pure $\text{Th}(\text{OH})_4$, but precipitates formed by adding aqueous NaOH to a solution of heavy metal sulfate usually contain significant quantities of the NaOH reactant and the Na_2SO_4 product.⁴ In view of that uncertainty, the degree of agreement of his result with that obtained in this work is perhaps only fortuitous.

Wohler, *et al.*,¹⁴ have reported decomposition pressure measurements above thorium sulfate and several other polyvalent metal sulfates. However, no linear relationship was found between their log K data and reciprocal absolute temperature. Kelley¹⁵ deemed it inadvisable to calculate thermochemical data for $\text{Th}(\text{SO}_4)_2$ from their work. Their decomposition pressure results are considerably higher than those found in this study and suggest that their material may have contained water, H_2SO_4 or other volatile impurities.

Entropy.—Equation 16 was used to calculate a value of 35.4 e.u. for the entropy of $\text{Th}(\text{SO}_4)_2$ at 298.15°K. That value can be compared with one obtained by using Latimer's additive method for estimating the entropy of solid compounds.¹⁶ Latimer has attempted to estimate the effect of tetravalent cations on the entropy contribution of sulfate ion by extrapolating the effect of divalent cations *via* one trivalent cation (Al^{+3}) to the tetravalent cations. His estimated values add up to an entropy of 39.9 e.u. for $\text{Th}(\text{SO}_4)_2$. Since the average deviation per ion in Latimer's estimates (Table 89,¹⁶ column 6) is about 10%, this deviation of 12% for a compound involving three ions does not appear to be excessive for such a method of estimating the entropy.¹⁷

The entropy of decomposition of $\text{Th}(\text{SO}_4)_2$ (equation 1) was computed from equation 11 to be 135.5 e.u. at 1000°K. The dependence of the free energy of decomposition on temperature is known for other sulfates^{15,18}; accordingly, the entropy of decomposition of these sulfates has been calculated at 1000°K. in order to compare them with $\text{Th}(\text{SO}_4)_2$. Calculated entropies of decomposition, per two SO_2 molecules formed, are: $\text{Al}_2(\text{SO}_4)_3$, 138; BaSO_4 , 136; MgSO_4 , 132; PbSO_4 , 132; CdSO_4 , 122; CoSO_4 , 122; MnSO_4 , 132; Na_2SO_4 , 138; CaSO_4 , 134; and CuSO_4 , 140 e.u. The entropy of decomposition for $\text{Th}(\text{SO}_4)_2$ is within the range observed for the other sulfates, and is somewhat greater than the median value of 132 e.u.

Acknowledgments.—The authors wish to express their gratitude for valuable discussions with Professor Håkon Flood and Dr. S. J. Yosim.

(14) L. Wohler, W. Pluddemann and P. Wohler, *Ber.*, **41**, 703 (1908).

(15) K. K. Kelley, Bulletin 406, U. S. Bureau of Mines, 1937.

(16) W. M. Latimer, "Oxidation Potentials," Second Ed., Prentice-Hall, New York, N. Y., 1952, p. 359 ff.

(17) The only oxygenated anion for which the entropy-reducing effect of a tetravalent cation is known is the tetrahedral SiO_4^{-4} anion (ref. 16, p. 363). The effect of divalent cations is known for both SiO_4^{-4} and SO_4^{-2} . In a solid containing a divalent cation, the entropy contribution is 13.8 e.u. for SiO_4^{-4} and 17.2 for SO_4^{-2} ; for a solid with a tetravalent cation the entropy contribution of SiO_4^{-4} is 7.9 e.u. Maintaining this ratio leads to a calculated value of 9.8 e.u. for the entropy contribution of SO_4^{-2} in a solid having a tetravalent cation. The estimated entropy of $\text{Th}(\text{SO}_4)_2$ then becomes 35.5 e.u. compared with 35.4 e.u. obtained in this study.

(18) C. J. Osborn, *J. Metals*, **188**, 600 (1950).

THE HEAT CONTENT OF BORON AT HIGH TEMPERATURES

BY STEPHEN S. WISE, JOHN L. MARGRAVE AND

Department of Chemistry, University of Wisconsin, Madison, Wisconsin

ROBERT L. ALTMAN

Department of Mineral Technology, University of California, Berkeley, California

Received February 17, 1960

The heat contents of commercially available "crystalline" and "amorphous" borons have been measured from 500 to 1200°K. in a copper block-type drop calorimeter. Equations have been derived for both forms, and heat capacities, free-energy functions and entropies have been calculated. A Debye-Einstein heat capacity equation has been derived for both amorphous and crystalline boron and used for calculation of thermodynamic functions over the range 0–2400°K.

Reliable heat content data on crystalline and amorphous boron at high temperatures are not available in the literature. Johnston, Hersh and Kerr¹ have measured the low temperature heat capacity of both forms of boron. Evans, Wagman and Prosen² have made corrections to their data and calculated the thermodynamic functions to 300°K. Various workers have reported high temperature heat content data for "amorphous" boron, the most complete work being by Magnus and Danz³; but in all cases there is question as to the purity of the boron. No high temperature data (above 100°) are available for crystalline boron. In this work studies of "amorphous" and "crystalline" borons from 500 to 1200°K. are reported.

Experimental

Grimley and Margrave^{4,5} have described in detail the construction and arrangement of the high temperature copper block-type drop calorimeter and the resistance thermometer circuit used in this Laboratory.

The calorimeter was recalibrated electrically in terms of the number of calories required to raise the resistance of the copper-manganin resistance thermometer one ohm. The platinum vs. platinum-10% rhodium thermocouple, which was suspended just above the sample capsule in the furnace, was recalibrated against an N. B. S. calibrated thermocouple.

The boron samples were contained in sealed gold capsules. Several preliminary experiments in which boron was heated in gold to 800° gave no indication of reaction. However, the capsules were observed to gain in weight after runs above 700°, and it is believed that small leaks developed. A small amount of boric oxide was probably formed. The weight gains amounted at the most to 1.0% of the starting weight of boron. The heat content data were corrected for this weight gain by the assumption that glassy B₂O₃ was formed.

Materials.—The analysis of a sample of -100 mesh "crystalline" boron (I) supplied by the American Potash and Chemical Corporation was as follows: B 99.6%, Si 0.017%, Fe 0.074%, Ti 0.28%, Mg 0.0011% and Cu 0.074%.

A sample of "crystalline" boron (II) from the U. S. Borax and Chemical Corporation also was studied. Analysis showed Mn, 0.2%; Si, 0.2%; Fe, 0.05% as the major impurities.

Pure "amorphous" electrolytic boron (III) was obtained from the Fairmount Chemical Company and by spectrographic analysis contained major impurities of Fe, 0.04%; Na, 0.06%; Si, 0.08%; Ni, 0.02%.

X-Ray powder patterns of all the samples indicated the

presence of some of the high temperature β -rhombohedral form.⁶ I was more crystalline than II, and III was only slightly crystalline.

Results

The high temperature heat content data for "crystalline" borons I and II and "amorphous" boron III are presented in Tables I, II, and III.

TABLE I

MEASURED HEAT CONTENT OF BORON I

<i>T</i> , °K.	$H^{\circ}_T - H^{\circ}_{298}$, cal. mole ⁻¹	<i>T</i> , °K.	$H^{\circ}_T - H^{\circ}_{298}$, cal. mole ⁻¹
530.7	879	843.1	2504
589.2	1145	922.3	2928
654.8	1473	985.7	3307
720.1	1806	1038.5	3603
779.6	2125	1102.9	3985

TABLE II

MEASURED HEAT CONTENT OF BORON II

<i>T</i> , °K.	$H^{\circ}_T - H^{\circ}_{298}$, cal. mole ⁻¹	<i>T</i> , °K.	$H^{\circ}_T - H^{\circ}_{298}$, cal. mole ⁻¹
516.1	821	791.7	2244
596.5	1204	839.9	2515
658.6	1531	908.1	2912
729.8	1909	975.4	3310

TABLE III

MEASURED HEAT CONTENT OF BORON III

<i>T</i> , °K.	$H^{\circ}_T - H^{\circ}_{298}$, cal. mole ⁻¹	<i>T</i> , °K.	$H^{\circ}_T - H^{\circ}_{298}$, cal. mole ⁻¹
509.6	784	926.0	2984
614.0	1283	1025.3	3586
695.3	1706	1097.8	4049
776.7	2138	1173.9	4510
861.3	2617	1233.7	4886

Using Johnston's¹ data, as corrected by Prosen, *et al.*,² for the heat capacity, enthalpy and entropy at 298.16°K. of both forms of boron, one may derive these equations according to the methods of Shomate⁷ with the atomic weight of boron = 10.82.⁸

Boron I:

$$H^{\circ}_T - H^{\circ}_{298} = 4.0130T + 1.0822 \times 10^{-3}T^2 + \frac{1.7867 \times 10^5}{T} - 1892.3 \text{ cal. mole}^{-1}$$

$$C^{\circ}_p = 4.0130T + 2.1645 \times 10^{-3}T^2 - \frac{1.7867 \times 10^5}{T^2} \text{ cal. mole}^{-1} \text{ deg.}^{-1}$$

(1) H. L. Johnston, H. N. Hersh and E. C. Kerr, *J. Am. Chem. Soc.*, **73**, 1112 (1951).

(2) W. H. Evans, D. D. Wagman and E. J. Prosen, N. B. S. Report No. 6252, December 15, 1958.

(3) A. Magnus and H. Danz, *Ann. Physik*, **81**, 407 (1926).

(4) R. T. Grimley and J. L. Margrave, *This Journal*, **62**, 1436 (1958).

(5) R. T. Grimley, Ph.D. thesis, University of Wisconsin, 1958.

(6) T. N. Godfrey and B. E. Warren, *J. Chem. Phys.*, **18**, 1121 (1950); D. E. Sands and J. L. Hoard, *J. Am. Chem. Soc.*, **79**, 5582 (1957); and J. L. Hoard and A. E. Newkirk, *ibid.*, **82**, 70 (1960).

(7) C. H. Shomate, *This Journal*, **58**, 368 (1954).

(8) E. Wichers, *J. Am. Chem. Soc.*, **80**, 4121 (1958).

Boron II:

$$H^{\circ}_T - H^{\circ}_{298} = 4.3810T + 9.4938 \times 10^{-4}T^2 + \frac{2.0426 \times 10^5}{T} - 2075.8 \text{ cal. mole}^{-1}$$

$$C^{\circ}_p = 4.3810 + 1.8988 \times 10^{-3}T - \frac{2.0426 \times 10^5}{T^2} \text{ cal. deg.}^{-1} \text{ mole}^{-1}$$

Boron III:

$$H^{\circ}_T - H^{\circ}_{298} = 3.836T + 1.1966 \times 10^{-3}T^2 + \frac{1.5048 \times 10^5}{T^2} - 1755.1 \text{ cal. mole}^{-1}$$

$$C^{\circ}_p = 3.836 + 2.3932 \times 10^{-3}T - \frac{1.5048 \times 10^5}{T^2} \text{ cal. mole}^{-1} \text{ deg.}^{-1}$$

Values of heat contents, entropies and free energy functions are presented in Tables IV, V and VI from 298 to 1200°K.

TABLE IV
CALCULATED THERMODYNAMIC FUNCTIONS OF
"CRYSTALLINE" BORON I

$T, ^{\circ}\text{K.}$	$H^{\circ}_T - H^{\circ}_0$, cal. mole ⁻¹	C°_p , cal. deg. ⁻¹ mole ⁻¹	S°_T , cal. deg. ⁻¹ mole ⁻¹	$\frac{F^{\circ}_T - H^{\circ}_0}{T}$, cal. deg. ⁻¹ mole ⁻¹
298	290.4	2.650	1.402	-0.428
400	623	3.762	2.355	-0.797
500	1032	4.381	3.266	-1.201
600	1493	4.815	4.105	-1.616
700	1993	5.164	4.874	-2.047
800	2524	5.465	5.584	-2.428
900	3085	5.741	6.244	-2.816
1000	3672	5.999	6.862	-3.190
1100	4284	6.246	7.445	-3.551
1200	(4922)	(6.486)	(7.999)	(-3.898)

TABLE V

CALCULATED THERMODYNAMIC FUNCTIONS OF
"CRYSTALLINE" BORON II

$T, ^{\circ}\text{K.}$	$H^{\circ}_T - H^{\circ}_0$, cal. mole ⁻¹	C°_p , cal. deg. ⁻¹ mole ⁻¹	S°_T , cal. deg. ⁻¹ mole ⁻¹	$\frac{F^{\circ}_T - H^{\circ}_0}{T}$, cal. deg. ⁻¹ mole ⁻¹
298	290.4	2.650	1.402	-0.428
400	630	3.864	2.372	-0.798
500	1051	4.513	3.310	-1.208
600	1525	4.953	4.174	-1.632
700	2037	5.293	4.964	-2.053
800	2582	5.581	5.690	-2.462
900	3154	5.838	6.362	-2.858
1000	3749	6.076	6.990	-3.240
1100	(4368)	(6.301)	(7.579)	(-3.608)
1200	(5009)	(6.518)	(8.137)	(-3.963)

TABLE VI

CALCULATED THERMODYNAMIC FUNCTIONS OF
"AMORPHOUS" BORON III

$T, ^{\circ}\text{K.}$	$H^{\circ}_T - H^{\circ}_0$, cal. mole ⁻¹	C°_p , cal. deg. ⁻¹ mole ⁻¹	S°_T , cal. deg. ⁻¹ mole ⁻¹	$\frac{F^{\circ}_T - H^{\circ}_0}{T}$, cal. deg. ⁻¹ mole ⁻¹
298	314.3	2.858	1.564	-0.510
400	661	3.851	2.560	-0.907
500	1077	4.431	3.485	-1.330
600	1542	4.854	4.331	-1.761
700	2046	5.204	5.107	-2.184
800	2582	5.516	5.822	-2.595
900	3148	5.804	6.489	-2.991
1000	3742	6.079	7.115	-3.372
1100	4364	6.344	7.706	-3.740
1200	5011	6.603	8.270	-4.094

Discussion

The X-ray patterns of both "crystalline" samples of boron were practically identical.

TABLE VII

THERMODYNAMIC PROPERTIES OF CRYSTALLINE BORON
CALCULATED FROM DEBYE-EINSTEIN EQUATION

$T, ^{\circ}\text{K.}$	C_p , cal. mole ⁻¹ deg. ⁻¹	$(H^{\circ}_T - H^{\circ}_0)$, kcal./mole	$\frac{T}{-(F^{\circ}_T - H^{\circ}_0)}$, cal. mole ⁻¹ deg. ⁻¹	$\frac{S^{\circ}_T}{\text{cal. mole}^{-1} \text{ deg.}^{-1}}$
100	0.227	0.006	0.019	0.077
200	1.429	0.081	0.146	0.551
298.15	2.823	0.292	0.411	1.392
300	2.845	0.298	0.418	1.409
400	3.841	0.635	0.786	2.374
500	4.498	1.054	1.198	3.307
600	4.966	1.529	1.622	4.170
700	5.333	2.044	2.044	4.964
800	5.639	2.593	2.455	5.697
900	5.902	3.171	2.854	6.377
1000	6.130	3.773	3.238	7.011
1100	6.329	4.396	3.608	7.605
1200	6.502	5.038	3.965	8.163
1300	6.652	5.695	4.308	8.689
1400	6.783	6.367	4.639	9.187
1500	6.897	7.051	4.958	9.659
1600	6.996	7.746	5.266	10.107
1700	7.083	8.450	5.563	10.534
1800	7.160	9.162	5.851	10.941
1900	7.228	9.882	6.129	11.330
2000	7.288	10.608	6.399	11.703
2100	7.341	11.339	6.660	12.059
2200	7.388	12.076	6.913	12.402
2300	7.430	12.817	7.159	12.731
2400	7.468	13.561	7.398	13.048

TABLE VIII

THERMODYNAMIC PROPERTIES OF AMORPHOUS BORON CAL-
CULATED FROM DEBYE-EINSTEIN EQUATION

$T, ^{\circ}\text{K.}$	C_p , cal. mole ⁻¹ deg. ⁻¹	$(H^{\circ}_T - H^{\circ}_0)$, kcal./mole	$\frac{T}{-(F^{\circ}_T - H^{\circ}_0)}$, cal. mole ⁻¹ deg. ⁻¹	$\frac{S^{\circ}_T}{\text{cal. mole}^{-1} \text{ deg.}^{-1}}$
100	0.328	0.009	0.030	0.117
200	1.496	0.095	0.194	0.671
298.15	2.781	0.307	0.485	1.515
300	2.803	0.312	0.492	1.532
400	3.767	0.644	0.870	2.480
500	4.424	1.055	1.285	3.395
600	4.899	1.523	1.708	4.246
700	5.273	2.032	2.128	5.030
800	5.585	2.575	2.536	5.755
900	5.852	3.147	2.932	6.429
1000	6.085	3.744	3.313	7.058
1100	6.287	4.363	3.681	7.647
1200	6.463	5.001	4.035	8.202
1300	6.617	5.655	4.376	8.726
1400	6.750	6.324	4.704	9.221
1500	6.867	7.005	5.021	9.691
1600	6.969	7.697	5.327	10.137
1700	7.058	8.398	5.623	10.563
1800	7.137	9.108	5.908	10.968
1900	7.206	9.825	6.185	11.356
2000	7.268	10.549	6.453	11.727
2100	7.322	11.278	6.713	12.083
2200	7.371	12.013	6.965	12.425
2300	7.414	12.752	7.209	12.754
2400	7.453	13.496	7.447	13.070

However, the crystal samples were prepared by very different methods. The American Potash boron I was prepared⁹ by a hot wire deposition process. It is believed that the U. S. Borax boron II was prepared by a process involving the recrystallization of a commercial "amorphous" boron at high temperatures. If some of the amorphous boron still remains in boron II, this would tend to explain the higher heat content.

The high temperature data reported here may be combined with the low temperature data of Johnston, Hersh and Kerr¹ to yield heat capacity equations for crystalline and amorphous borons of the form

$$C_p/R = D(\theta_D/T) + 2E_1(\theta_1/T) + E_2(\theta_2/T)$$

(9) D. K. Stern and L. Lynds, *J. Electrochem. Soc.*, **105**, 676 (1958).

where the characteristic temperatures have the values $\theta_D = 875$; $\theta_1 = 1075$ and $\theta_2 = 4000$ for crystalline boron and $\theta_D = 750$, $\theta_1 = 1150$ and $\theta_2 = 4050$ for amorphous boron. These equations yield the thermodynamic functions in Tables VII and VIII.

Acknowledgments.—The authors wish to acknowledge the financial support of this work by the Bureau of Aeronautics, U. S. Navy, through its contractor the Callery Chemical Company, and the du Pont Company. Also, we acknowledge the aid of Dr. M. V. Evans for spectrographic analyses.

Samples of boron for study were furnished by the American Potash and Chemical Corporation, by the U. S. Borax Company and by Dr. Robert J. Thorn of the Argonne National Laboratory.

COMPARATIVE STUDIES ON THE DECARBOXYLATION OF MALONIC ACID AND THE TRICHLOROACETATE ION

BY LOUIS WATTS CLARK

Department of Chemistry, Saint Mary of the Plains College, Dodge City, Kansas

Received February 18, 1960

Kinetic data are reported for the decarboxylation of malonic acid in molten trichloroacetic acid and of the trichloroacetate ion in decanoic acid. The constants of the Eyring equation are evaluated. A comparison of these results with those previously obtained for the reaction of these two reagents with a wide variety of polar solvents indicates that the malonic acid tends to evoke favorable electromeric and inductive effects which produce a decrease in ΔH^\ddagger , whereas the negative charge on the trichloroacetate ion tends to evoke unfavorable electromeric and inductive effects which cause an increase in ΔH^\ddagger . An explanation is advanced for the fact that the aromatic amines are an exception to this pattern of behavior. Finally, a possible mechanism is suggested for the decarboxylation of molten trichloroacetic acid at high temperatures.

The mechanism of the decarboxylation of malonic acid in nucleophilic solvents has been well established.¹ Evidence has been presented which strongly indicates that the trichloroacetate ion likewise decomposes in similar solvents by essentially the same mechanism as does malonic acid.² The rate-determining step of both reactions appears to be the formation, prior to cleavage, of a transition complex, the polarized carbonyl carbon atom of the reactant coordinating with a pair of unshared electrons on the nucleophilic atom of a solvent molecule. If the cumulative inductive effects of three alpha halogens are considered, the effective positive charge on the carbonyl carbon atom of the trichloroacetate ion is evidently greater than that in the case of malonic acid. Therefore, since an increase in the attraction between two reagents lowers the ΔH^\ddagger of the reaction,³ it would be predicted that, in identical solvents, the ΔH^\ddagger would be less for the decomposition of the trichloroacetate ion than for malonic acid. Comparison of data on the two reactions in five aromatic amines reveals that this anticipated result is actually obtained.² For example, in aniline, ΔH^\ddagger (in kcal.) for the decarboxylation of malonic acid is 26.9, for the trichloroacetate ion, 24.5; in quinoline corre-

sponding figures are 26.7 and 24.0; in *o*-toluidine 25.7 and 23.8.

However, when the reactions were carried out in several of the monocarboxylic acids and their derivatives, it was found that ΔH^\ddagger was higher in each case for the decarboxylation of the trichloroacetate ion than for malonic acid.⁴ For example, in propionic acid, ΔH^\ddagger (in kcal.) for the decomposition of malonic acid is 33.4, for the trichloroacetate ion, 35.3; in butyric acid, 32.3 and 35.1; in monochloroacetic acid, 31.7 and 48.9.

These results suggest that a fundamental difference in electron activation obtains between reactions of malonic acid and the trichloroacetate ion in acid media. The source of this difference may be traced to the difference in the nature of the two reagents. In malonic acid we are dealing with a neutral molecule containing a polarizable, electrophilic carbonyl group. The electrophilic carbonyl carbon atom may have two effects: (1) it may coordinate with an unshared pair of electrons on the nucleophilic atom of the solvent molecule, and (2) it may attract mobile electrons present in the solvent molecule—in other words it may evoke a favorable electromeric effect at the moment of reaction.

In the case of the trichloroacetate ion, however, the electrophilic carbonyl carbon atom is bound to two oxygen atoms which share, through resonance, a negative ionic charge. This negative charge will

(1) G. Fraenkel, R. L. Belford and P. E. Yankwich, *J. Am. Chem. Soc.*, **76**, 15 (1954).

(2) L. W. Clark, *THIS JOURNAL*, **63**, 99 (1959).

(3) K. J. Laidler, "Chemical Kinetics," McGraw-Hill Book Co., Inc., New York, N. Y., 1950, p. 138.

(4) L. W. Clark, *ibid.*, **63**, 1760 (1959).

tend to repel any mobile electrons which may be conjugated with the nucleophilic center of the solvent molecule so that, at the moment of reaction, the electron density on the nucleophilic atom of the solvent will be reduced, thus necessitating the acquisition of additional energy in order to form the activated complex.

If these principles are applied to the case of the two reactions taking place in acid solvents, it will be deduced that the trichloroacetate ion will tend to repel electrons away from the point of attack, thus evoking a $-E$ effect on the carbonyl oxygen atom of the solvent. Hence the effective positive charge on the carbonyl carbon atom will be increased, electrons will then be withdrawn from the hydroxyl group, and more energy will be needed to form the activated complex. In the case of the reaction with malonic acid, on the other hand, a $-E$ effect will not be called into play at the moment of reaction, hence the activation energy will be expected to be lower.⁵

In order to further test the above postulates, further kinetic studies have been carried out in this Laboratory, as: (1) the decarboxylation of malonic acid in molten trichloroacetic acid, and (2) the decarboxylation of the trichloroacetate ion in decanoic acid. Results of this investigation are reported herein.

Experimental

(a) **Reagents.**—The malonic acid, trichloroacetic acid and potassium trichloroacetate used in this research were Reagent Grade, 100.0% assay. The decanoic acid was "Highest Purity" grade. The usual precaution was taken of distilling this solvent at atmospheric pressure directly into the reaction flask immediately before the beginning of each decarboxylation experiment.

(b) **Apparatus and Technique.**—The details of the apparatus and technique have been described previously.⁶ Temperatures were controlled to within $\pm 0.01^\circ$ and were determined by means of a thermometer calibrated by the U. S. Bureau of Standards. In studying the decomposition of malonic acid in molten trichloroacetic acid, 60 g. of trichloroacetic acid were placed in a 100-ml. reaction flask which was then immersed in the constant-temperature oil-bath, and 0.1857 g. of malonic acid (the amount required to produce 40.0 ml. of CO_2 at STP on complete reaction) was introduced in the usual manner. In studying the decomposition of the trichloroacetate ion in decanoic acid, 330 mg. of potassium trichloroacetate (the amount required to furnish 40.0 ml. of CO_2 at STP on complete reaction) was added to 70 ml. of solvent.

Results

1. The Decarboxylation of Malonic Acid in Molten Trichloroacetic Acid.—It has been found that, when 1 mole (163.8 g.) of trichloroacetic acid is heated at temperatures of about 156° and above, carbon dioxide is evolved at an appreciable rate.⁷ Since the temperature coefficient of the reaction is about 5.4, the volume of CO_2 evolved with time falls off rapidly as the temperature is decreased below about 156° . When smaller quantities (50–60 g.) of trichloroacetic acid are heated at temperatures considerably below 156° very little volume change occurs during the period of time required to study the decomposition of malonic acid therein.

(5) A. E. Remick, "Electronic Interpretations of Organic Chemistry," 2nd Ed., John Wiley and Sons, Inc., New York, N. Y., pp. 62, 53 and 54.

(6) L. W. Clark, *THIS JOURNAL*, **60**, 1160 (1956).

(7) L. W. Clark, *J. Am. Chem. Soc.*, **77**, 3130 (1955).

However, in determining the rate constants for the decarboxylation of malonic acid in trichloroacetic acid, allowance was made for the small increment of volume change due to this factor. Experiments were carried out, in duplicate, at three different temperatures over a 16° range. The average rate constants, in sec.^{-1} , calculated in the usual manner from slopes of the experimental logarithmic plots, were as follows: at 131.60° , 0.203×10^{-4} ; at 138.14° , 0.407×10^{-4} ; at 147.39° , 1.065×10^{-4} . Average deviations were less than 1% in each case. On the basis of these results, ΔH^\ddagger for the reaction was found to be 34.9 kcal., and $\Delta S^\ddagger + 5.5$ e.u.

2. The Decarboxylation of the Trichloroacetate Ion in Decanoic Acid.—The decarboxylation of the trichloroacetate ion was first order in decanoic acid, and followed very nearly the same pattern of behavior as was found previously for the reaction in acetic acid, propionic acid and butyric acid.⁴ Experiments were carried out, in duplicate, at three different temperatures over a 16° range. The average rate constants, in sec.^{-1} , calculated from the slopes of the experimental logarithmic plots, were as follows: at 121.62° , 1.19×10^{-4} ; at 132.13° , 4.68×10^{-4} ; at 137.70° , 9.58×10^{-4} . Average deviations were not more than 1% in each case. The value of ΔH^\ddagger for the reaction was found to be 41.4 kcal.; the value of $\Delta S^\ddagger + 27.7$ e.u.

Discussion

The reasons for the selection of the particular systems for investigation reported in this research will become apparent from a study of Table I.

TABLE I

ENTHALPIES OF ACTIVATION FOR THE DECARBOXYLATION OF MALONIC ACID AND OF THE TRICHLOROACETATE ION IN VARIOUS LIQUIDS

System	ΔH^\ddagger , kcal.
(1) Molten malonic acid ⁸	33.0
(2) Malonic acid in propionic acid ⁹	33.6
(3) Malonic acid in monochloroacetic acid ⁹	31.7
(4) Malonic acid in trichloroacetic acid ^a	34.9
(5) Malonic acid in decanoic acid ¹⁰	26.6
(6) Trichloroacetate ion in acetic acid ⁴	35.5
(7) Trichloroacetate ion in propionic acid ⁴	35.3
(8) Trichloroacetate ion in monochloroacetic acid ⁴	48.9
(9) Molten trichloroacetic acid ⁷	62.0
(10) Trichloroacetate ion in decanoic acid ^a	41.4

^a Present research.

On going from acetic acid to monochloroacetic acid, ΔH^\ddagger for the decomposition of the trichloroacetate ion increases from 35.5 to 48.9 kcal. (see lines 6 and 8 of Table I)—a result which has been attributed to a $-I$ effect of the halogen evoked by the ionic negative charge on the trichloroacetate ion.⁴

On going from propionic acid to monochloroacetic acid, the ΔH^\ddagger for the decomposition of malonic acid decreases from 33.6 to 31.7 kcal. (see lines 2 and 3 of Table I)—a result which has been attributed to a $+E$ effect of the halogen evoked by the effective

(8) C. N. Hinshelwood, *J. Chem. Soc.*, **117**, 156 (1920).

(9) L. W. Clark, *THIS JOURNAL*, **64**, 41 (1960).

(10) L. W. Clark, *ibid.*, **64**, 692 (1960).

positive charge on the polarized carbonyl carbon atom of the neutral malonic acid.⁹

It has been suggested that, in the decomposition of molten malonic acid, the transition complex is formed by the coordination of a polarized carbonyl carbon atom of one molecule of malonic acid with an unshared pair of electrons on the hydroxyl oxygen atom of a second molecule of malonic acid.¹⁰ A study of the data shown in lines 6, 8 and 9 of Table I sheds light on the probable mechanism of the decomposition of molten trichloroacetic acid. Inasmuch as un-ionized trichloroacetic acid is stable, and since, in molten trichloroacetic acid, especially at elevated temperatures near the boiling point, some trichloroacetic ions are undoubtedly present, it may be inferred that the electrophilic carbonyl carbon atom of the ion coordinates with one of the unshared pairs of electrons on the hydroxyl group of one of the un-ionized trichloroacetic acid molecules forming a transition complex similar to that in the case of monochloroacetic acid. The very high activation energy for the reaction (62.0 kcal.) is in line with the strong electron withdrawing power of the three alpha halogen atoms, none of which can release its mobile electrons because of the electron repelling effect of the negative charge on the attacking ion. The increase in ΔH^\ddagger for the reaction on going from monochloroacetic acid to trichloroacetic acid (13.1 kcal.) is almost exactly equal to the increase on going from acetic acid to monochloroacetic acid (13.4 kcal.). In other words, three halogen atoms on the same carbon atom have only about twice the inductive effect as does one halogen. This is in line with the fact that in cases of multiple substitution on the same atom the inductive effect is not cumulative but diminishes with successive substitution.¹¹

For the decarboxylation of malonic acid in molten trichloroacetic acid ΔH^\ddagger is only 3.2 kcal. greater than it is in monochloroacetic acid (lines 3 and 4 of Table I). This indicates that, in the reaction with trichloroacetic acid as in that with monochloroacetic acid, the malonic acid evokes on the chlorine atoms at the moment of reaction a +E effect, which tends partially to restore to the nucleophilic center those electrons which have been removed by the inductive effect of the halogens.

In molten trichloroacetic acid the ΔH^\ddagger for the decomposition of the trichloroacetate ion is nearly twice that for malonic acid (lines 4 and 9 of Table I). Again it appears strongly evident that, in the case of the trichloroacetate ion, the halogens are exerting a -I effect since the negative charge on the attacking ion prevents a +E effect from taking place, whereas in the case of malonic acid, the halogens manifest a +E effect, evoked by the effective positive charge on the carbonyl carbon atom of the attacking agent.

The data for the reactions in propionic acid and in decanoic acid (lines 2, 5, 7 and 10 of Table I) also are consistent with the postulate that the trichloroacetate ion evokes a -E effect on the carbonyl oxygen atom of the solvent, whereas no -E effect can take place in the presence of malonic acid.

The strong hydrogen bonding in the dimer of the lower fatty acids results in a withdrawal of electrons from the hydroxyl group somewhat analogous to that which would be produced by a -E effect on the carbonyl oxygen atom of the monomer. Therefore, the electron repelling effect of the negative charge on the trichloroacetate ion is able to produce only a small additional decrease in the electron density on the nucleophilic atom of propionic acid. The electron density on the hydroxyl group of the undimerized decanoic acid is normally greater than that in the case of propionic acid since in the former no electrons are being called into play to form hydrogen bonds.

Additional evidence in support of these deductions is furnished by a study of data obtained by Verhoek on the decomposition of sodium trichloroacetate ion in ethanol.¹² According to his results, ΔH^\ddagger for the reaction is 31.1 kcal., as compared with 27.2 kcal. for the decomposition of malonic acid in 1-butanol.¹³ It appears evident from these figures that the ΔH^\ddagger for the decomposition of the trichloroacetate ion in the aliphatic alcohols will be higher than will be that for malonic acid. In the reaction with malonic acid the alkyl groups of the alkanols can exert a -I effect, whereas, with the trichloroacetate ion, such a +I effect is prevented from taking place because of the electron repulsion of the negative ion.

These results indicate that, in the attempted coordination between malonic acid and a polar molecule, the effective positive charge on the polarized, electrophilic, carbonyl carbon atom of the neutral malonic acid molecule will attract mobile electrons, in other words it will evoke favorable inductive and electromeric effects, in such a way as always to increase the electron density on the nucleophilic center at the moment of reaction, thus bringing about a decrease of ΔH^\ddagger . In other words, the solvent molecule will always tend to respond to the advances of the attacking reagent.

In the attempted coordination between the trichloroacetate ion and a polar molecule, on the other hand, the negative charge on the ion will tend to repel mobile electrons, in other words it will evoke unfavorable inductive and electromeric effects, in such a way as always to decrease the electron density on the nucleophilic center at the moment of reaction, thus bringing about an increase of ΔH^\ddagger . In other words, the solvent molecule will always tend to resist the advances of the attacking reagent.

The only class of compounds so far investigated which does not follow the above pattern is the aromatic amines.³ Evidently, in these liquids, the effective positive charge on the carbonyl carbon atom of the malonic acid is not sufficiently strong to evoke a -E effect on the nitrogen atom—in other words it is not able to attract back to the nitrogen those electrons which have been withdrawn from it by the powerful resonance effect of the aromatic nucleus. Since the negative charge on the trichloroacetate ion prevents a -E effect from taking place on the nitrogen atom the electron density on the nucleophilic center of these solvents will not be

(11) E. A. Braude and F. C. Nachod, "Determination of Organic Structures by Physical Methods," Academic Press, Inc., New York, N. Y., 1955, p. 579.

(12) F. H. Verhoek, *J. Am. Chem. Soc.*, **56**, 571 (1934).

(13) L. W. Clark, *ТРИС ЖУРНАЛ*, **64**, 508 (1960).

affected appreciably by the field effects of the different electrophilic reagents.

Further work on this problem is contemplated.

Acknowledgments.—This research was supported by the National Science Foundation, Washington, D. C.

ACTIVITY COEFFICIENTS FOR THALLOUS SULFATE IN AQUEOUS SOLUTION AT 25°

BY J. M. CREETH¹

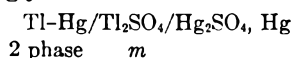
Contribution from the Department of Physical and Inorganic Chemistry of the University of Adelaide, South Australia

Received February 22, 1960

Measurements of the e.m.f. of the cell Tl, Hg (2 phase)/Tl₂SO₄(*m*)/Hg₂SO₄(s), Hg have been made over the concentration range 0.005 to 0.1 molal, and by combination with the literature value for the appropriate standard potential have been used to calculate stoichiometric activity coefficients. In the lowest concentrations investigated (0.005–0.01 *m*) anomalous effects were observed, and failure of the Hg₂SO₄ electrode suspected. In general, the activity coefficients are considerably lower than, for example, those of the alkali metal sulfates, in conformity with results obtained on other thallosulfates. By applying the Bjerrum theory and a model equation for the activity coefficients, a series of values have been calculated for the apparent "dissociation constant" for the TlSO₄⁻ ion: by this means a comparison is made possible with results previously obtained on this system. It is concluded that ion-association greater than is compatible with the Bjerrum theory occurs, in agreement with the previous findings. The limits of applicability of the model activity coefficient equation are discussed in the light of their effect on the value of the dissociation constant.

In connection with studies² of the transport properties of the thallosulfate-water system, information concerning the variation of the activity coefficient with concentration was required; accordingly a limited series of measurements of the activity coefficient was undertaken, the results of which are reported here as they have some general interest and applicability.

For the concentration region of interest, a method based on e.m.f. measurements has advantages, and accordingly the cell



was used: this has an e.m.f., *E*, given by

$$E = E^0 - \frac{3RT}{2F} \ln 4^{1/2} m \gamma_{\pm}$$

Here *m* is the molality of Tl₂SO₄, γ_{\pm} the stoichiometric mean activity coefficient on the molal scale and the coefficient of the logarithmic term has its usual significance. Measurements were made between 0.005 and 0.10 *m*, the lower limit being dictated by the characteristics of the Hg₂SO₄ electrode^{3,4} and the upper by the limited solubility of Tl₂SO₄.

Experimental

Materials.—Commercial thallosulfate (BDH, Ltd., England) was twice recrystallized from conductivity water and dried *in vacuo* over phosphorus pentoxide. Metallic thallium was prepared by electrolysis, following the general procedure of Richards and Daniels,⁵ and mixed immediately with the appropriate amount of mercury (twice redistilled) to give a composition of approximately 57% Tl. The mixture thus prepared was clearly two-phase (the solubility of Tl in Hg is approximately 44% by weight⁶ at 25°); it was stored under boiled conductivity water. Mercurous sulfate

was prepared in the form of an intimate mixture of the salt and mercury by the method of Hattox and de Vries.⁶ It was stored in the dark after thorough drying.

Solutions.—These were prepared by weight, employing the appropriate air buoyancy corrections and density data.

The Cell for E.M.F. Determination.—The design of this unit must allow a completely oxygen-free⁷ solution of thallosulfate (of precisely known composition) to be placed in contact with the thallium amalgam electrode: the latter reacts instantly with atmospheric oxygen and so is normally covered, if dry, by a black film of thallosulfate which immediately dissolves on the addition of an aqueous solution. The cell shown in Fig. 1 was therefore used; it is operated as follows. The dry amalgam is placed in the bottom of the cell compartment C through which a platinum wire E-1 is sealed (a tube, not shown, leads this directly to the potentiometer terminals). The mercury-mercurous sulfate electrode E-2 is then assembled separately with dry materials⁴; about 1 ml. of the Tl₂SO₄ solution to be used is then cautiously added to it and all air bubbles removed by alternately sucking and blowing with a capillary pipet. The electrode is then inserted into the cell arm F, connection to the potentiometer being made as before. The reservoir R (which holds about 25 ml.) is then filled with the Tl₂SO₄ solution; by opening the tap T-1 briefly, bubbles are removed from the tube joining R and C and simultaneously the surface of the amalgam in C is rinsed. Most of the solution in C is then removed, but enough is left to cover the surface of the amalgam. The remaining parts of the assembly are then put in place, and all taps are shut. In this state the cell is transferred to the thermostat ($T = 25.00 \pm 0.005^\circ$), and the solution in R deoxygenated at constant composition by the passage of purified hydrogen through a conventional pre-saturating system. During this time taps T-1 and T-4 are closed, T-2 and T-3 open; after about half an hour T-3 is closed and T-4 opened so ensuring that the cell is thoroughly cleared of air. As the junction of the tube D with the cell occurs at a point just above the surface of the amalgam, most of the (slightly contaminated) solution left above the amalgam is displaced to D, from which it is removed. The amalgam is then rinsed four to six times with clean solution from the reservoir; this is done by closing T-2 and T-4 and opening T-1 and T-3, until the cell is half full, when T-1 and T-3 are closed and T-2 and T-4 opened to displace the solution again to D. Finally the cell is filled completely by closing T-2 and T-4 and opening T-1 and T-3; if this is done cautiously, there is no disturbance of the layer of mercurous sulfate.

(1) Lister Institute of Preventive Medicine, London S.W. 1, England.

(2) To be published shortly.

(3) G. N. Lewis and M. Randall, "Thermodynamics and the Free Energy of Chemical Substances," McGraw-Hill Book Co., Inc., New York, N. Y., 1923, p. 356.

(4) H. S. Harned and R. D. Sturgis, *J. Am. Chem. Soc.*, **47**, 945 (1925).

(5) T. W. Richards and F. Daniels, *ibid.*, **41**, 1732 (1919).

(6) E. M. Hattox and T. de Vries, *ibid.*, **58**, 2126 (1936).

(7) The sensitivity of the thallium amalgam electrode to atmospheric oxygen has been discussed by G. N. Lewis and C. L. von Ende, *J. Am. Chem. Soc.*, **78**, 4520 (1956).

The e.m.f.'s were measured with a precision vernier potentiometer (Messrs. Pye, Ltd., Cambridge, England), which could be read to 0.00001 v. The values of E obtained when the cell was first completed were fairly stable, a slow and roughly constant decrease with time of about 0.0001 v. per day ensuing. As the value after, e.g., 3 days was not sensibly changed by replacement of the liquid over the Tl amalgam (the reservoir holds enough to allow for one such replacement), it was assumed that the change with time was due either to the spreading of grease from the taps over the electrodes, or to gradual hydrolysis of the Hg_2SO_4 ; in either case, the initial stable value should be closest to the desired reversible e.m.f. The values quoted are therefore those obtained within the first 3 hours of completing the cells.

Results

The experimental results obtained in this work are summarized in Table I, columns 1, 2, 5 and 6.

TABLE I

E.M.F. DATA FOR THE CELL $\text{Tl}, \text{Tl}_2\text{SO}_4(m), \text{Hg}_2\text{SO}_4, \text{Hg}$ AT 25° , AND DERIVED ACTIVITY COEFFICIENTS

1	2	3	4	5	6	7
$10^3 \times m^a$	E^b	γ_{\pm}^c	γ_{\pm}^d	$10^3 \times m$	E	γ_{\pm}^c
5.404	1.1376 ₆	(0.85)	0.75	21.433	1.0990 ₆	0.58 ₆
6.298	1.1332 ₄	(.82)	.74	24.561	1.0950 ₆	.56 ₆
6.661	1.1317 ₆	(.80)	.73	34.212	1.0861 ₆	.510
7.465	1.1287 ₇	(.78)	.71	42.219	1.0805 ₆	.478
8.541	1.1246 ₆	(.75)	.70	50.047	1.0762 ₆	.451
10.415	1.1194 ₆	(.71)	.68	63.090	1.0702 ₆	.418
12.639	1.1131 ₄	.68 ₆		79.552	1.0655 ₆	.374
15.663	1.1075 ₆	.64 ₆		101.012	1.0593 ₆	.346

^a m values calculated on the basis of $M = 504.85$. ^b Last figures quoted are probably not significant, due to reasons discussed in Experimental section, but retained here to avoid later accumulation of errors. ^c Stoichiometric activity coefficient γ_{\pm} calculated on basis of $E^0 = 0.9480$; values in parentheses may not be reliable. ^d Calculated from equation 4 (see text).

In order to calculate activity coefficients, a value must be assigned to E^0 ; it is not to be expected, however, that any reliable extrapolation can be made from the data of Table I. For an unsymmetrical electrolyte, particularly one which exhibits ion association, there is no form of activity coefficient equation which can be used with confidence at concentrations greater than 0.01 m , and the e.m.f.'s obtained at concentrations below this are, experimentally, the least reliable. In this situation the best course is to combine the literature values for the standard potentials of Tl (satd. amalgam), Tl^+ and $\text{Hg}(\text{l}), \text{Hg}_2\text{SO}_4(\text{s}), \text{SO}_4^{2-}$. This should be a valid procedure, in view of the nature of the electrodes. The value for E^0 thus obtained was 0.9480 v., on the basis of $E^0_{\text{Tl}(\text{Hg})}, \text{Tl}^+ = 0.3339$, and $E^0_{\text{Hg}, \text{Hg}_2\text{SO}_4, \text{SO}_4^{2-}} = -0.6141$ v., the former being based on Lewis and Randall's⁸ figures of 0.3336–0.3340 v.⁹ and the latter on data of Shrawder, Cowperthwaite and La Mer.¹⁰ Although Lewis and Randall's value depends on the figure -0.2700 v. for the normal calomel elec-

(8) Ref. 3, p. 413.

(9) The thallose azide cell investigated by M. L. Brouty (*Compt. rend.*, **214**, 258 (1942)) gave $E^0_{\text{Tl}(\text{Hg}), \text{Tl}^+} = 0.3353$ v., but this rests on assigning the value $E^0 = -0.2945$ v. to the AgN_3 -Ag electrode, a figure which is not yet confirmed. The value 0.3336 may be obtained by combining the results of I. A. Cowperthwaite, V. K. La Mer and J. Barksdale (*J. Am. Chem. Soc.*, **56**, 544 (1934)) on the cell $\text{Tl}(\text{s})/\text{TlCl}(m) \text{AgCl}(\text{s}), \text{Ag}$ with those of R. H. Gerke (*Chem. Revs.*, **1**, 377 (1924)) for $\text{Tl}(\text{s}), \text{Tl}(\text{Hg})$ and H. S. Harned and R. W. Ehlers (*J. Am. Chem. Soc.*, **54**, 1350 (1932)) for $\text{Ag}(\text{s}), \text{AgCl}(\text{s}), \text{Cl}^-$.

(10) J. Shrawder, I. A. Cowperthwaite and V. K. La Mer, *J. Am. Chem. Soc.*, **56**, 2348 (1934).

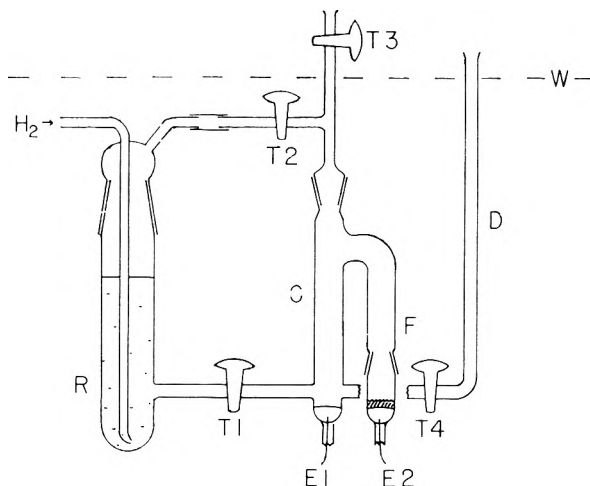


Fig. 1.—Cell for e.m.f. determination: W represents level of water in the thermostat; symbols and mode of operation are explained in text.

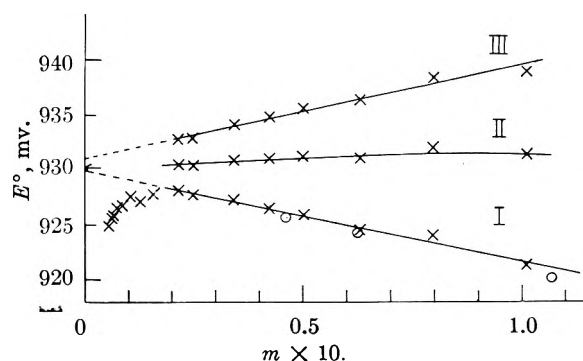


Fig. 2.—Various representations of the e.m.f. data for Tl_2SO_4 : for curve I ordinate $E^{\circ'} = E + (3RT/2F) \ln m - (2.303RT/2F) 2A \sqrt{3d_0 m}$; for curve II $E^{\circ'} = E + (3RT/2F) \ln m - (2.303RT/2F) 2A \sqrt{3d_0 m} / (1 + B\delta \sqrt{3d_0 m})$ with $\delta = 1.4 \text{ \AA}$, and for curve III, $E^{\circ'} = E + (3RT/2F) \ln m - (2.303RT/2F) \{ [2A \sqrt{3m} / (1 + \sqrt{3m})] - B'm \}$, with $B' = -0.93$. (Values of the fundamental constants were obtained from ref. 14, pp. 468, 469). Arrow at $E^{\circ'} = 0.9302$ v. indicates expected value from previous data. Points \circ in curve I are from data of Ishikawa.

trode, a figure since revised to -0.2680 ,^{11,12} a corresponding revision for the value cited above for the thallium electrode is not indicated.¹¹ This value of E^0 was then substituted in equation 1, when the stoichiometric activity coefficients shown in Table I, columns 3 and 7, were calculated.

This E^0 value is, in fact, quite close to that obtained by applying conventional extrapolation procedures¹³ to the data (for the less dilute solutions) of Table I: thus curves I and II are based on the Debye-Hückel equation¹⁴

$$-\log \gamma_{\pm} = \frac{2A \sqrt{3md_0}}{1 + B\delta \sqrt{3md_0}} \quad (2)$$

(d_0 is the density of water at 25°) using, respec-

(11) M. Randall and L. E. Young, *ibid.*, **50**, 989 (1928).

(12) D. G. Hills and D. J. G. Ives, *J. Chem. Soc.*, 318 (1951).

(13) See, e.g. H. S. Harned and B. B. Owen, "The Physical Chemistry of Electrolytic Solutions," 3rd Ed., Reinhold Publ. Corp., New York, N. Y., 1958, pp. 431, 458 *et seq.*

(14) Numerical values of the constants A and B were taken from R. A. Robinson and R. H. Stokes, "Electrolyte Solutions," 2nd Ed., Academic Press, Inc., New York, N. Y., 1959, p. 468.

tively, $\bar{a} = 0.0$ and $\bar{a} = 1.4 \text{ \AA}$. (Higher, and thus more realistic, values of \bar{a} give lines of increasing positive slope.) From curve I, the limiting value at $m = 0$ is 0.9299, while $E^0_{\text{calcd}} - (RT/2F)\ln 4 = 0.9480 - 0.0178 = 0.9302 \text{ v}$. Also shown on curve I are three points obtained from the e.m.f. values reported by Ishikawa¹⁵ for a cell apparently identical with the one investigated here: the agreement is excellent. Finally curve III represents the formulation for γ_{\pm} proposed by Guggenheim,^{16,17} which becomes for the case of a 1:2 electrolyte

$$-\log \gamma_{\pm} = \frac{2A\sqrt{3m}}{1 + \sqrt{3m}} - B'm \quad (3)$$

the value of B' used here (obtained by the method of least squares) was -0.93 .

In the case of curves II and III only those values for $m > 0.015$ have been used: at lower concentrations, these curves show a similar behavior to that of curve I, where it is most evident that the e.m.f. values for m lower than 0.015 lie progressively further from the straight line. While one cannot dismiss them *solely* on this score, the deviations may indicate failure of the mercurous sulfate electrode.

In attempting to assess the reliability of the results in this region the following points must be considered: (a) the concentration range in question is well above that where the Hg_2SO_4 electrode is known to fail^{3,4}; (b) in the case¹⁸ of $\text{In}_2(\text{SO}_4)_3$, where failure of the Hg_2SO_4 electrode was suspected at concentrations around 0.01 m , spuriously high values of E were obtained, and (c) the effect of ion association is as yet unestablished, but qualitatively is not incompatible with the shape of the curve (*cf.* Bates¹⁹ results on CdBr_2). With the information at present available, no final decision can be made concerning the results in this region, but it does seem possible, at least, to specify the degree of uncertainty: thus the linear relation of curve I, extrapolated to the region 0.0 to 0.01 m , can be used to define activity coefficients which probably represent a lower limit. (In terms of γ_{\pm} , this relation may be expressed simply as

$$-\log \gamma_{\pm} = \sqrt{3m} - 0.852m \quad (4)$$

a form which is useful for approximate calculations, as it represents the activity coefficient information obtained, with an error not greater than 0.006 in γ_{\pm} , for $m = 0.015 - 0.10$.) The values in column 4 of Table I have been obtained from (4): the differences are quite marked in the range 0.005 to 0.008 m .

The extrapolation procedure of Harned and Fitzgerald²⁰ demands data on the degree of dissociation at low concentrations which cannot readily be obtained from cells employing the Hg_2SO_4 electrode.

(15) F. Ishikawa, *Bull. Chem. Soc. Japan*, **2**, 294 (1927); see also E. Cohen, F. Ishikawa and A. L. T. Moesveld, *Z. physik. Chem.*, **105**, 155 (1923).

(16) E. A. Guggenheim, *Phil. Mag.*, **19**, 588 (1935).

(17) E. A. Guggenheim and J. C. Turgeon, *Trans. Faraday Soc.*, **51**, 747 (1955).

(18) M. H. Lietzke and R. W. Stoughton, *J. Am. Chem. Soc.*, **78**, 4520 (1956).

(19) R. Bates, *ibid.*, **61**, 308 (1939).

(20) H. S. Harned and M. E. Fitzgerald, *ibid.*, **68**, 2624 (1936).

Discussion

It is recognized that the activity coefficients of thalious salts are lower than those, for example, of the alkali metals (*cf.* Robinson's results²¹ on TlNO_3 , TlClO_4) and so far as comparison is possible, the results of this investigation bear out the generalization (*cf.* information on Li, Na, K sulfates summarized in ref. 13, p. 553). One explanation for this behavior is that the thalious salts are incompletely ionized in solution,²² and it would be of considerable interest to see whether the results of this investigation can help to decide whether this is the case for Tl_2SO_4 . While a final answer is not possible in the present state of electrolyte theory, a preliminary interpretation may be made, and is presented in the remainder of this paper. Following Guggenheim,²³ the criterion of incomplete ionization will be taken as the demonstration that there occurs ion-association materially in excess of that required by the Bjerrum²⁴ theory of electrostatic interaction.

In brief, the route is as follows: the Bjerrum theory has been used to compute an expected value of the equilibrium constant K for the reaction $\text{TlSO}_4^- = \text{Tl}^+ + \text{SO}_4^{2-}$, while an experimental estimate of K has been derived by combining the results of this investigation with a model equation for the activity coefficients.

(a) The 'Bjerrum value' of K .—The sum of the crystal radii for Tl^+ and SO_4^{2-} ions must be somewhat less than the mean ionic diameter, a , in solution, so that the K obtained will represent a lower limit: this is desirable from the viewpoint of the comparison to be made. K is formulated as

$$K = \frac{[\text{Tl}^+]^2[\text{SO}_4^{2-}]\gamma_{12}^3}{[\text{Tl}]^+[\text{TlSO}_4^-]\gamma_{11}^2} = \frac{m\gamma_{12}^3\alpha(1 + \alpha)}{\gamma_{11}^2(1 - \alpha)} \quad (5)$$

where the brackets represent actual ionic concentrations, γ_{12} is the mean ionic activity coefficient for Tl^+ and SO_4^{2-} ions at the actual concentrations, γ_{11} the same quantity for Tl^+ and TlSO_4^- ions, and α is the degree of dissociation for TlSO_4^- . At very low concentrations both γ 's and $\alpha \rightarrow 1$ so that $K^{-1} = (1 - \alpha)/2m$. Taking a as 4.34 \AA ,²⁵ and applying the conventional form²⁶ of the Bjerrum equation we obtain $b = 3.29$, $Q(b) = 0.39_5$, leading to the result $K = 0.23 \text{ mole kg.}^{-1}$.

(b) The 'Experimental Value' of K .—The necessary relation between the operationally defined stoichiometric activity coefficient γ_{\pm} and the hypothetical "real" mean ionic activity coefficient of equation 5 is²⁰

$$\gamma_{\pm}^3 = \alpha(1 + \alpha)^2\gamma_{12}^3 \quad (6)$$

It is impossible to proceed without making an assumption concerning the behavior of the activity

(21) R. A. Robinson, *ibid.*, **59**, 84 (1937).

(22) This interpretation presents some difficulties: the presence of a covalent bond is normally inferred if a substance is incompletely ionized, but in the case of TlOH no such bond could be detected by Raman spectroscopy. Should the absence of covalent bonds be shown generally, it would be necessary to place the thalious salts in a special category in the classification of electrolytes. *cf.* C. W. Davies, *Disc. Faraday Soc.*, **24**, 83 (1957).

(23) E. A. Guggenheim, *ibid.*, **24**, 53 (1957).

(24) N. Bjerrum, *Kgl. Danske Vidensk. Selskab.*, **7**, No. 9 (1926).

(25) L. Pauling, "Nature of the Chemical Bond," Cornell University Press, Ithaca, N. Y., 1939.

(26) Ref. 14, equation 14.2, p. 396.

coefficients γ_{11} and γ_{12} . In general, an equation of the form

$$-\log \gamma_{ij} = 0.50 |z_i z_j| \left[\frac{I^{1/2}}{1 + kI^{1/2}} - CI \right] \quad (7)$$

has been used, where z_i and z_j are the ion valences, and I is the "real" ionic strength given (for a 1:2 electrolyte) by

$$I = m(1 + 2\alpha) \quad (8)$$

The most frequently used choice of coefficients (due to Davies²⁷) is $k = 1.0$, $C = 0.20$. The general use of (7) with these coefficients is open to criticism on several grounds,^{23, 28-30} and indeed, on one view, with $k = 1$, a value $C = 1.3$ is indicated. Under these circumstances three sets of values of α and K have been calculated for different choices of the coefficients in (7). In (i) the values suggested by Davies were used for both γ_{11} and γ_{12} ; this set, the results of which are shown in Table II, columns 3 and 4, is thus directly comparable with previous

TABLE II

ILLUSTRATIVE CALCULATIONS OF THE APPARENT DEGREE OF DISSOCIATION AND DISSOCIATION CONSTANT OF Tl_2SO_4

m	γ_{\pm}^a	Set (i) ^b		Set (iii) ^b	
		α	$K \times 10^2$	α	$K \times 10^2$
0.003	0.809	0.93 ₁	5.6
.010	.684	0.91 ₁	10.3	.85 ₀	6.3
.020	.592	.83 ₇	8.3	.74 ₈	5.6
.060	.423	.61 ₅	5.1	.50 ₂	4.0
.100	.345	.47 ₈	4.0	.37 ₈	3.6

^a Values of γ_{\pm} have been calculated from equation 4 and may therefore differ slightly from those interpolated from Table I. ^b Set (i) obtained by use of $k_{11} = k_{12} = 1.0$, $C_{11} = C_{12} = 0.2$; set (iii) from $k_{11} = 1.4$, $k_{12} = 2.3$, $C_{11} = C_{12} = 0$. ^c Units are mole kg.⁻¹.

data interpreted on the same basis. It is clear from the table that a marked variation of K occurs as m increases, and accordingly the values of α and K quoted can have little significance. Set (ii) was based on assigning the values $k_{11} = k_{12} = 1.0$, while C_{11} and C_{12} (denoting the coefficients used for γ_{11} and γ_{12}) were varied over the ranges -0.2 to $+0.7$ and 0.0 to 1.5 , respectively. For every combination attempted the values of K varied somewhat with m , but the extremes always lay in the range 0.11 to 0.02. The variation of K with m was considerably reduced in combinations where $C_{12} = 2C_{11}$ (these have greater physical significance) and the extremes were much less scattered (approximate range 0.08-0.04). Set (iii) was designed to be consistent with the use of the Bjerrum analysis to obtain the "expected value" of K . Since this analysis implies that all Tl^+ ions distant further than 7.1 Å. (= q) from a given SO_4^{2-} ion are free and obey the Debye-Hückel expression, it is logically necessary to use this distance (or its equivalent in terms of k) in interpreting the experimental data to determine whether or not it is in agreement with the Bjerrum model.^{30a} Thus the values $k_{11} = 1.4$,

$k_{12} = 2.3$, $C_{11} = C_{12} = 0$, were used³¹; the results of this set are shown in columns 5 and 6 of Table II. It is evident that while some variation of K with m remains, this is not extreme, and a reasonable extrapolation to $K = 0.06$ may be made: thus this choice of parameters allows a satisfactory and reasonably self-consistent interpretation to be made, and more confidence can be placed in the values of α and extrapolated K . (The remaining variation may be ascribed to the neglect of small linear terms in the equations for γ_{11} and γ_{12} : it is not expected that an equation with a single adjustable parameter should be applicable over such a wide variation of I . Moreover, the calculations evidently embody two steps where a small change in γ_{12} produces a large effect on K .)

It seems safe to conclude that K can be stated as 0.06 ± 0.05 , for within these limits the value is independent of the choice of the parameters k and C over the wide range tried. It is probable that these limits are unduly wide, but this is unimportant with respect to the comparison to be made: it is sufficient that the experimental results give K values significantly lower than the "Bjerrum value." It is therefore to be inferred that ionic association, beyond that considered by this theory, must occur. (This conclusion is also implied by the magnitude of the term B' in equation 3; when $B' = -0.97$, the coefficient $\beta(\text{Tl-SO}_4) = -0.80$. The limit corresponding to ordinary "Bjerrum-type" interaction does not seem to be well established for 1:2 electrolytes.) In the terms of the definition adopted, Tl_2SO_4 is therefore incompletely ionized in aqueous solution at 25°.

This conclusion, and the numerical magnitude of K , are in general agreement with previous results: thus Bell and George³² found $K = 0.042$ from measurements of the solubility of Tl_2O_3 in K_2SO_4 solutions, K being constant over the "rea." ionic strength range 0.002-0.08 (*i.e.*, comparable with the first three rows of Table II). Bell and George used $k = 1$, $C = 0.2$ throughout, but in view of the lower ionic strength range the value of C is less important. The lack of closer agreement between their result and the comparable figures of Table II may not be significant, in view of the rather different nature of the experiments, particularly the fact that solubility studies are necessarily conducted in mixed electrolyte systems.

The only other comparable information on the Tl_2SO_4 - H_2O system comes from the spectrophotometric study by Panckhurst and Woolmington³³: although marked departures from Beer's law were found (indicative of ion-association), the limits of

(30a) Cf. ref. 14, p. 412.

(31) The use of values of k different from unity is allowable in three-ion systems of one solute component, but cannot be extended to mixed electrolyte systems (E. A. Guggenheim, "Thermodynamics," North Holland Publishing Co., Amsterdam, 1950, p. 313). At the higher I values the form of the curve given by $k = 2.3$, $C = 0$, differs quite markedly from that for $k = 1.0$, $C = 1.3$, while the two curves for γ_{11} are essentially identical.

(32) R. P. Bell and J. H. B. George, *Trans. Faraday Soc.*, **49**, 619 (1953); see also earlier work of a similar nature by H. E. Blyden and C. W. Davies, *J. Chem. Soc.*, 549 (1930), which gave $K = 0.038$; E. C. Righellato and C. W. Davies, *Trans. Faraday Soc.*, **26**, 592 (1930), obtained $K = 0.047$ from conductivity measurements.

(33) M. H. Panckhurst and K. G. Woolmington, *Proc. Roy. Soc. (London)*, **A244**, 124 (1958).

(27) C. W. Davies, *J. Chem. Soc.*, 2093 (1938); a summary of results is given by this author in "The Structure of Electrolytic Solutions," John Wiley and Sons, Inc., New York, N. Y., 1959.

(28) P. M. G. Brown and J. E. Prue, *Proc. Roy. Soc. (London)*, **A232**, 320 (1955).

(29) W. G. Davies, R. J. Otter and J. E. Prue, *Disc. Faraday Soc.*, **24**, 103 (1957).

(30) H. A. C. McKay, *ibid.*, **24**, 80 (1957).

K could not be defined. Quoting " K " values of 0.125 and 0.087 for $k = 1$, and $C = 0.2$ and 0.4, respectively, as being compatible with the experimental data, they emphasize³⁴ that no significance can be attached to values whose magnitude is determined by the choice of C ; it is evident that their results, while indicative of a higher K than was found by Bell and George, are not inconsistent with the results of this investigation. Presumably an interpretation of the conclusion (*i.e.*, of incomplete

(34) Cf. O. Redlich, *Chem. Revs.*, **39**, 342 (1946).

ionization) must be sought either in terms of molecular structure or of inadequacy of the Bjerrum approximations.

Acknowledgments.—The author was privileged to be able to discuss various aspects of this work with several authorities: he is particularly indebted to Professor R. H. Stokes of the University of New England, Australia; to Dr. M. Spiro of the University of Melbourne, Australia; and to Professors L. J. Gosting, E. L. King and J. W. Williams, of the University of Wisconsin.

ASBESTOS ORE BODY MINERALS STUDIED BY ZETA POTENTIAL MEASUREMENTS

BY EDWARD MARTINEZ AND GORDON L. ZUCKER

Central Research Laboratories, American Smelting and Refining Company, South Plainfield, New Jersey, and Texas Instruments Incorporated, Dallas, Texas

Received February 29, 1960

The zeta potentials of chrysotile (asbestos) and lizardite were measured using the streaming potential method. It was found that chrysotile had an equilibrium zeta potential of +93 mv., compared to +2 mv. for lizardite, a non-fibrous serpentine mineral. The pH had a large effect on the potentials; highly alkaline solutions produced negative potentials, whereas in more acidic media the potentials were positive. The isoelectric points (zero potentials) were at a pH of 11.8 for chrysotile and 9.6 for lizardite. Additions of sodium silicate resulted in reversals from positive to negative zeta potentials with both minerals. Similar concentrations of sodium carbonate and sodium phosphate decreased but did not reverse the polarity with chrysotile. This study was undertaken in an attempt to characterize the surface properties of these two serpentine minerals which may lead to a better understanding of their singular and mutual behavior while in aqueous suspensions.

Introduction

Chrysotile (asbestos) and lizardite are two minerals in the serpentine group which have strikingly different physical and chemical properties. Both are hydrated magnesium silicates [$Mg_3(OH)_2Si_2O_5$] varying only slightly in chemical composition but having vastly different crystal structures. Much research on the chemical and structural properties has been reported in the literature. The present study was undertaken to determine the surface electrical properties of these minerals, and the effects of pH and some electrolytes on these properties. This information may be of value in understanding and controlling the behavior of these minerals in aqueous suspensions.

The streaming potential method was selected to measure the zeta potentials because of recent interest in that method and the noteworthy information derived by several investigators utilizing this technique. The recent discovery and solution to the problems of irreproducible data arising from electrode flow polarization effects¹ further satisfied the authors as to the usefulness of the method.

Experimental Methods and Materials

The streaming potential method consists of streaming a liquid through a porous plug of solids held between two electrodes and measuring the potential difference between the ends of the plug. The zeta potential can be calculated from the streaming potential data by the equation^{2,3} in which

$$\zeta = \frac{-4\pi\eta}{\epsilon} \times \frac{E\lambda}{P}$$

η is the viscosity, ϵ the dielectric constant, E the streaming potential, λ the specific conductance, and P the applied pressure difference. In aqueous solutions at 25°, the equation becomes

$$\zeta = -0.097 \times \frac{E\lambda}{P} \text{ mv.}$$

where E is the streaming potential in millivolts, P is the driving pressure in centimeters of mercury, and λ the specific conductance of the solution within the plug in micro-mhos/cm. Experimentally these three have to be measured.

In these experiments, the non-fibrous serpentine was a closely sized 35 × 48 mesh and the chrysotile was in a fibrous form having a larger surface area and smaller pores in the plug. The chrysotile also exhibited a greater surface conductance than the lizardite. These two factors would tend to lower the zeta potentials measured for chrysotile.^{3,4} However, the data obtained can still be interpreted satisfactorily.

The streaming potential and gas purification apparatus used were similar to that described by Fuerstenau.^{4,5} The cell, Fig. 1, consisted of a Pyrex tube 1.90 cm. in internal diameter in which is mounted a perforated bright platinum disc of the same diameter and 0.10 cm. thick. The electrode had twenty perforations 0.05 cm. in size and the face was covered with 80 mesh platinum gauze. A duplicate electrode was constructed on the face of the inner member of a 24/40 glass joint. The electrodes were 6.70 cm. apart in parallel planes. Before use the electrodes were removed from the plug soaked in hot concentrated hydrochloric acid, washed, steamed, fired and washed before silver plating in silver cyanide solution at low current density. This coating was anodically chloridized in hydrochloric acid. A solution of 10^{-6} *N* potassium chloride was used as the streaming liquid. The streaming potentials were measured with a d.c. battery electrometer designed by Professor A. O. Nier, University of Minnesota. It

(1) G. L. Zucker, Sc.D. thesis, Columbia University, 1959.

(2) D. W. Fuerstenau, Sc.D. thesis, Massachusetts Institute of Technology, 1953.

(3) L. A. Wood, *J. Am. Chem. Soc.*, **68**, 432 (1946).

(4) D. W. Fuerstenau, *This Journal*, **60**, 981 (1956).

(5) D. W. Fuerstenau, *Trans. A.I.M.E.*, **203**, 834 (1956).

incorporated an electrometer tube with a maximum of 10^{-14} ampere and an input resistance of a million megohms (10^{12} ohms). The instrument was direct reading and eliminated the necessity for a d.c. potentiometer bridge circuit and provided for measuring currents of 10^{-12} ampere even at voltages of 1000 mv. Triply distilled conductivity water was used to make up all solutions, and all solutions were bubbled with nitrogen to remove carbon dioxide and oxygen. Nitrogen passed through KOH, alkaline pyrogallol and water scrubbers was used as the driving gas for the KCl solution in the apparatus.

The chrysotile came from the Lake Asbestos of Quebec Mine in the Thetford region of Quebec, Canada, and is considered a "semi-harsh" type. The sample was fiberized in a Mikro Samplmill which did not grind the fibers down to a small particle size. Samples checked with a Stone differential thermal analysis unit (D.T.A.) and Chevenard thermobalance (T.G.A.) did not indicate the presence of other minerals. A typical chrysotile X-ray pattern was obtained. Approximately 2.5 g. was used for each run.

The non-fibrous serpentine also came from the Lake Asbestos orebody. Pieces were broken from a large chunk, ground in the Samplmill and screened to obtain a sample of 35×48 mesh particles. The 35×48 mesh sample was passed through a Frantz Isodynamic Separator to remove those particles containing magnetite. D.T.A. and T.G.A. indicated approximately 3% brucite, $Mg(OH)_2$, was present. An X-ray pattern was obtained and indicated that the sample was "lizardite."

Experimental Results

Preliminary Measurements.—The zeta potentials of the minerals were obtained as $10^{-5} N$ potassium chloride was swept through the packed samples in the cell. Chrysotile and lizardite each had a relatively high positive potential initially which decreased as the solution streamed through. Chrysotile reached an equilibrium potential of +93 mv., compared to +2 mv. for lizardite.

pH and Zeta Potentials.—The effect of pH on the zeta potential was determined by changing the pH of the streaming solutions by additions of hydrochloric acid and sodium hydroxide. Two samples of each mineral were used, one for the acid and the other for alkaline additions. The curves for chrysotile and lizardite (Figs. 2 and 3) are similar in that highly alkaline solutions produced negative potentials, whereas in more acidic media the potentials were positive. However, the isoelectric point with lizardite was at a pH of approximately 9.6 compared to 11.8 for chrysotile. Chrysotile exhibited a very sharp rise in potential when the pH was dropped from 7 to 3; further lowering of the pH caused a sharp decrease in the potential. Lizardite showed a gradual decrease in potential as the pH was lowered from 8 to 3.

Polyvalent Ions.—Chrysotile and lizardite were tested adding increasing concentrations of sodium silicate to the streaming solution. The results are shown in Fig. 4. At low concentrations of sodium silicate both minerals had positive potentials, but as the concentration of silicate increased the positive potentials decreased and then reversed to negative values. The pH of the solution increased with the silicate additions, but the final pH at 10^{-2} mole per liter was still below the isoelectric pH for chrysotile. The zeta potential at this concentration of sodium silicate was a negative 30 mv. Two further tests were run with chrysotile adding 10^{-2} mole per liter each of sodium carbonate and sodium phosphate to the streaming solution. Both produced a decrease in potential, but no reversal of sign.

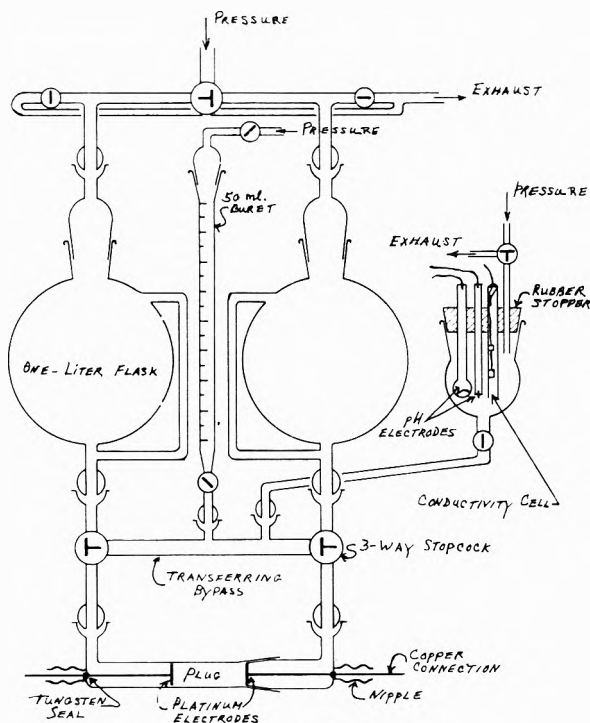


Fig. 1.—Streaming potential cell.

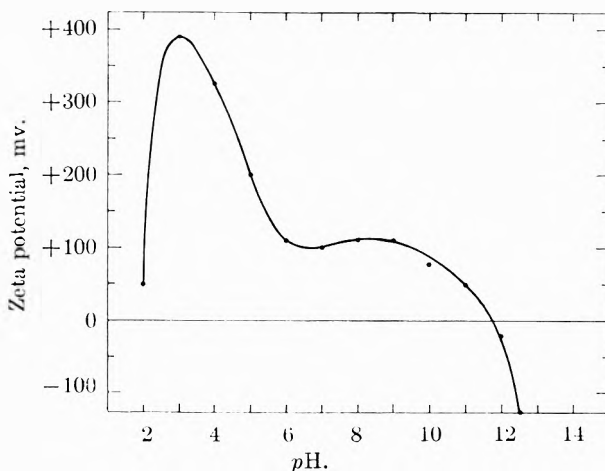


Fig. 2.—Zeta potential of chrysotile as a function of pH.

Discussion

Since chrysotile and lizardite are approximately the same in chemical composition [$Mg_6(OH)_3Si_4O_{10}$], the differences noted in this study are probably due to other factors. Chrysotile is believed by some to be in the form of hollow tubes several hundred ångströms in diameter with magnesium hydroxide as the outer layer and silicon-oxygen as an inner layer.⁶⁻⁹ Lizardite is considered to be platy with layers of magnesium hydroxide and silicon-oxygen. The very sharp increase in potential obtained with chrysotile as the pH was decreased from 7 to 3 may be due to the removal of hydroxyl ions by the acid leaving mag-

(6) J. Hillier and J. Turkevich, *Anal. Chem.*, **21**, 475 (1949).

(7) W. Noll and H. Kircher, *Naturwissenschaften*, **37**, 540 (1950).

(8) T. F. Bates, L. B. Sand and J. F. Mink, *Science*, **111**, 512 (1950).

(9) T. F. Bates, Circular No. 51, Col. of Mineral Industries, Pennsylvania State Univ., 21 (1958).

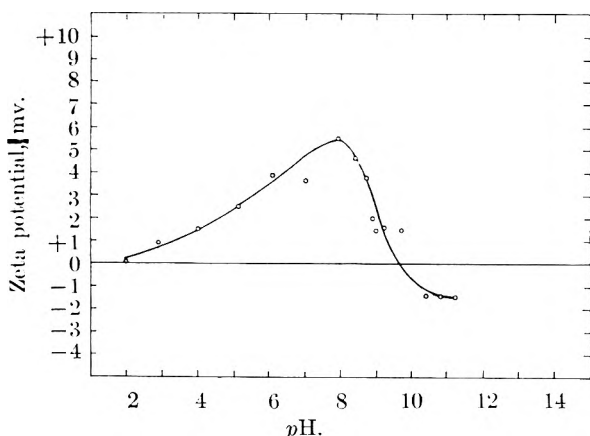


Fig. 3.—Zeta potential of lizardite as a function of pH .

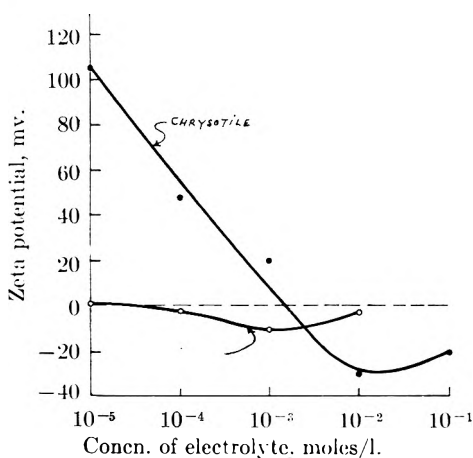


Fig. 4.—Effect of sodium silicate on zeta potentials of chrysotile and lizardite (lower curve).

nesium ions exposed on the surface. In contrast, a gradual decrease in potential resulted with lizardite as acid was added decreasing the pH below 8.0. This indicates that the magnesium-hydroxyl layers in the lizardite are not as exposed to the action of the hydronium ion compared to chrysotile. Much lower conductivities in acid solutions were observed with lizardite. The results obtained are in agreement with reported data on the higher acid resistance of platy serpentine with relation to chrysotile^{10,11} and the differences noted in titration behavior.¹² The very steep decrease in potential obtained with chrysotile as the pH is dropped from 3 to 2 may be due to the completion of the leaching of the magnesium hydroxide leaving a hydrated silica.

Pundsack¹³ found that highly alkaline solutions produced negative potentials with chrysotile, whereas in more acidic ones the potentials were positive. The streaming potential measurements

indicate an isoelectric pH of 11.8 compared to 10.1 reported by Pundsack, whose value was inferred from turbidity measurements on suspensions of finely ground chrysotile. The pH at minimum turbidity was called the isoelectric point. The streaming potential method did not require fine grinding of the sample and the measurements were made on a sample similar in its fibrous characteristics to that of commercially produced fiber.

The differences in the isoelectric pH 's measured for chrysotile and lizardite, 11.8 and 9.6, respectively, may play a part in the suspension behavior when these two are together. In the pH range from 9.6 to 11.8, chrysotile has a positive potential and lizardite is negative, and the tendency would be toward flocculation. If the pH is adjusted to a value below 9.6 or above 11.8, both would have potentials of the same polarity, a condition tending to produce dispersion.

The reversal of the zeta potential polarity from positive to negative with the addition of sodium silicate (Fig. 4) indicates that the silicate ion in solution is specifically attracted and held to the solid surface by chemical as well as electrostatic forces. Other electrolytes, such as sodium phosphate and sodium carbonate, reduce the value of the zeta potential by compression of the double layer, but do not reverse the polarity. The reversal produced by the sodium silicate indicates that this electrolyte may be useful in controlling the behavior of asbestos in aqueous suspensions, since flocculation and dispersion, precipitation of other ions or molecules on the surface, etc., are to a large extent dependent on the zeta potentials of the particles.

Since both chrysotile and lizardite are silicates, it is reasonable to assume that the silicon-oxygen portion of the crystal structure may influence the potentials measured. If this assumption is correct, the inference then may be made that the potentials measured are the resultants of the two portions of the minerals, the magnesium-hydroxyl and silicon-oxygen layers. Results obtained with other minerals indicate the silicate would tend to produce negative potentials. Therefore, the following is a possible explanation for the considerably higher positive potentials obtained with chrysotile: The greater exposure of the magnesium-hydroxyl outer layer surrounding the silicon-oxygen in chrysotile produces high positive potentials. In contrast, the more intimate mixing of the layers in lizardite allows the silicon-oxygen layer to have a larger effect on the potential, relative to chrysotile, tending to decrease the magnitude of the positive potentials.

Acknowledgment.—The authors wish to acknowledge the assistance of Professor Nathaniel Arbiter, School of Mines, Columbia University, for his counsel on streaming potential measurements; and to Dr. Max Hollander of American Smelting and Refining Company for his helpful comments and suggestions.

(10) B. Nagy and T. F. Bates, *Am. Mineralogist*, **37**, 1055 (1952).

(11) B. Nagy and G. T. Faust, *ibid.*, **41**, 817 (1956).

(12) F. L. Pundsack and G. Reimschuessel, *THIS JOURNAL*, **60**, 1218 (1956).

(13) F. L. Pundsack, *ibid.*, **59**, 892 (1955).

HEATS OF COMBUSTION, FORMATION AND ISOMERIZATION OF THE *cis* AND *trans* ISOMERS OF HEXAHYDROINDAN¹

BY CLARENCE C. BROWNE² AND FREDERICK D. ROSSINI

Chemical and Petroleum Research Laboratory, Carnegie Institute of Technology, Pittsburgh 13, Pennsylvania

Received March 9, 1960

A new thermochemical laboratory for making precise calorimetric measurements of heats of reaction was assembled. Measurements were made of the heats of combustion of the *cis* and *trans* isomers of hexahydroindan (hydrindan) in the liquid state. Values were calculated for the heats of combustion, formation and isomerization of the two isomers for both the liquid and gaseous states.

I. Introduction

A new thermochemical laboratory for making precise calorimetric measurements of heats of reaction was assembled. Measurements were made of the heats of combustion of the *cis* and *trans* isomers of hexahydroindan (hydrindan), with the energy equivalent of the calorimeter system being determined with standard benzoic acid. These data, along with values for the heats of vaporization, permit calculation of the heats of formation and isomerization of the two isomers for both the liquid and gaseous states. The relation of energy with the molecular structure of the two isomers is discussed.

The thermochemical method employed is the substitution method in which a standard calorimeter is used as the absorber and comparator of two kinds of energy, one of which is the heat evolved in the combustion of a measured amount of the reaction of combustion of the "unknown" and the other of which is the heat evolved in the combustion of a measured amount of the reaction of combustion of standard benzoic acid.

II. Calorimetric Apparatus

The calorimeter is one available commercially.³ The general design was made at the National Bureau of Standards by Prosen and Rossini and is a modification of the original Dickinson design,⁴ the important difference being that the container for the calorimeter can is sealed and immersed in the jacket water during the experiment.

The water jacket, containing approximately 38 liters of water, is maintained near 30.1° at a constant temperature within a few thousandths of a degree by means of an automatic regulator system.

The calorimeter can, supported on three pointed Lucite pins, contains in each experiment a standard amount of water (4450.00 ± 0.02 g.), the stirrer, platinum resistance thermometer, heater and the bomb with its contents. The stirrer is operated at approximately 300 r.p.m. with a flexible shaft drive from a synchronous motor.

The calorimeter heater, which fits snugly on the bomb, is similar to the one described by Prosen and Rossini⁵ and was made of a cylinder of 26 gage copper, 7.8 cm. in diameter and 6.4 cm. in height.

The thermometric system included a platinum resistance thermometer of the regular flat calorimetric type,⁶ a Type G-2 Mueller resistance bridge,⁶ a high sensitivity galvanom-

eter,⁶ and a lamp and scale assembly. The thermometric sensitivity is such that 1 mm. on the scale corresponds to about 0.0003° when the current through the platinum resistance thermometer is 5 milliamperes.

III. Chemical Apparatus

The oxygen combustion bomb⁷ is a commercially available modification of the bomb previously described by Prosen and Rossini,⁵ and had an internal volume of 380 ml. Important features of the present bomb are the Teflon head gasket and valve packing, the inlet tube and electrodes made of 10% iridium-platinum, and the provision of snap-on fittings at the inlet valve and of standard taper fittings at the outlet valve. A short section of platinum wire was attached to each electrode. The twelve headless steel set screws in the cap were tightened with a calibrated torque wrench.

The chemical train for purifying the oxygen and filling the bomb is quite similar to the one previously described,⁵ and includes the following: A, oxygen cylinder; B, pressure gage, needle valve, and safety valve assembly; C, high-pressure steel tube, electrically heated and filled with copper oxide to oxidize combustible impurities in the oxygen; D, high-pressure steel cooling coil, immersed in water; E, high-pressure steel purifying tube, filled with Ascarite to remove all carbon dioxide from the oxygen; F, Bourdon-type pressure gage; G, the combustion bomb; H, a flow meter. The temperature of the heated oxidizing tube was measured with a chromel-alumel thermocouple.

The chemical train for analysis of the products of combustion is similar to that previously described⁵ and includes the following: A, cylinder of oxygen used for flushing the train; B, a two-stage pressure regulator; C, a Pyrex-glass pressure safety trap, containing mercury; D, an electrically heated furnace, with quartz tube containing copper oxide to oxidize combustible impurities in the oxygen; E, a Pyrex-glass purifying tube containing Ascarite, to remove carbon dioxide; F, the combustion bomb; G, a flexible glass coil, to facilitate transfer of the bomb into or out of the train; H, a Pyrex-glass absorption tube, to remove water, containing anhydrous magnesium perchlorate backed with phosphorus pentoxide; I, a Pyrex-glass weighed absorption tube, to remove carbon dioxide, which contains Ascarite, backed, in order, with anhydrous magnesium perchlorate and phosphorus pentoxide; J, a duplicate of D; K, a duplicate of H; L, a duplicate of I; M, a Pyrex-glass guard tube containing, in order, phosphorus pentoxide, anhydrous magnesium perchlorate and Ascarite, to prevent back diffusion of water vapor or carbon dioxide; N, a flow meter. The safety-trap, C, prevents excessive build up of pressure in the train while oxygen from the cylinder is flowing and facilitates adjustment of the needle valve to the setting required for the proper rate of flow of oxygen during the flushing period. The temperature of each furnace is measured with chromel-alumel thermocouples, with the power to the furnace being controlled with a variable transformer.

The absorption tube is the same as that previously described,⁸ with a cylindrical body in place of the former U-tube. The absorption tubes were flushed out and filled with helium free of water vapor and carbon dioxide before each weighing, in a train designed to avoid contamination of the absorption tube and its contents.

(1) This investigation was supported in part by a grant from the National Science Foundation. Submitted in partial fulfillment of the requirements for the degree of Doctor of Philosophy in Chemistry at the Carnegie Institute of Technology.

(2) Du Pont Fellow in Chemistry for 1952-1953.

(3) Catalog No. 3028, Precision Scientific Company, Chicago, Illinois.

(4) H. C. Dickinson, *Bull. Bur. Standards*, **11**, 189 (1915).

(5) E. J. Prosen and F. D. Rossini, *J. Research Natl. Bur. Standards*, **27**, 289 (1941).

(6) Catalog Numbers 8160A, 8069, and 2284-C, respectively, Leeds and Northrup Company, Philadelphia, Pennsylvania.

(7) Catalog No. 1002, Parr Instrument Company, Moline, Illinois.

(8) E. J. Prosen and F. D. Rossini, *J. Research Natl. Bur. Standards*, **33**, 255 (1944).

IV. Calorimetric Procedure

Ignition was accomplished by the use of standard iron fuse wire, 5 cm. in length, weighing approximately 8 mg. The total ignition energy was about 0.02% of the heat evolved in a calorimetric combustion experiment.

The procedure followed in the calorimetric combustion experiments was substantially the same as previously described.^{5,8} A standard mass of water, 4450.00 ± 0.02 g., was used in each experiment. 1.00 ml. of water was placed in the bottom of the bomb before each combustion experiment.

The calorimetric observations were divided into the usual three parts: a "fore" period of 20 minutes, with observations of the steady state being made every 2 minutes; a "reaction" period of 16 minutes, in which the combustion occurred, followed by re-establishment of the steady state; and an "after" period of 20 minutes, with observations of the steady state being made every 2 minutes. In the first five minutes of the "reaction" period, observations were recorded of the time, to the nearest hundredth of a minute, at which the resistance of the thermometer attained certain preselected values.

The value of ΔR_c , the corrected increase in temperature of the calorimetric system, expressed as the increase in resistance in ohms of the given platinum thermometer at the mean temperature of 29°, as measured on the given resistance bridge, was determined substantially as previously described.^{6,9} Although the nature of the substitution method employed makes it unnecessary, formal calculation was made of the contribution to the rise of temperature from stirring, etc., and the heat flow from the jacket to the calorimeter. The contribution from stirring, etc., was taken as μ ohms/min., the total contribution for an entire experiment, for the reaction period of 16 minutes, being

$$U = 16 \mu \text{ ohms} \quad (1)$$

The heat leak constant was taken as k ohms/min.-ohm, or k /min., the total contribution for an entire experiment, for the reaction period of 16 minutes, being

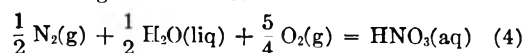
$$K = kA \text{ ohms} \quad (2)$$

where A is the area, in ohm-minutes, between the curves of the calorimeter resistance and the jacket resistance, from the 20th to the 36th minute.

The corrected temperature rise is then given by

$$\Delta R_c = (R_{36} - R_{20}) - K - U \text{ ohms} \quad (3)$$

The value of Δr_n , the rise in temperature produced by the heat evolved in the formation of a small amount of nitric acid, according to the reaction



was calculated from the amount of nitric acid formed, using the value 59 kJ./mole for the heat evolved in the formation of dilute aqueous nitric acid in the bomb process.^{5,8}

V. Chemical Procedure

The compounds measured in the present investigation were API Research hydrocarbons made available through the API Research Project 44 at the Carnegie Institute of Technology. These samples had the purities in mole per cent.: *cis*-hexahydroindan, 99.95 ± 0.02 ; *trans*-hexahydroindan, 99.71 ± 0.11 . The purification and determination of purity of these samples already has been described.¹⁰

The ampoules in which the hydrocarbon material was sealed prior to combustion were similar in dimensions to those previously described,⁵ but were made with one opening instead of two. Details of these ampoules and the filling of them are described elsewhere.¹¹ The average mass of the ampoules used in the present investigation was 0.23 g.

For combustion in the bomb, the filled and sealed glass ampoule was laid on one of its two flat sides in the crucible. The iron fuse wire, 5 cm. in length, was placed with its central coil 1 to 2 mm. distance from the upper flat side of the ampoule. An alternating current at 21 volts from an ignition unit¹² supplied the energy for ignition of the fuse

wire. After a combustion, the glass of the ampoule was found in the bottom of the crucible in the form of one or more globules, varying from clear to dark in appearance. As discussed previously,⁵ the heat effect associated with the darkening was believed to be not significant.

The oxygen used for the combustion was ordinary commercial oxygen, freed of combustible impurities as previously reported⁵ with the apparatus described in Section III of this paper. The initial pressure of oxygen for each experiment, corrected to 25°, was 30 atmospheres.

The products of each hydrocarbon combustion experiment were examined to determine the amount of carbon dioxide formed in the main reaction of combustion in the bomb, the amount of aqueous nitric acid formed by oxidation of some of the nitrogen in the oxygen used for combustion, and the amount of carbon dioxide formed by subsequent oxidation of any products of incomplete combustion. The products of each benzoic acid combustion experiment were examined only to determine the amount of aqueous nitric acid formed. In each case, the detailed procedures were substantially as previously described.⁶

The mass of carbon dioxide collected in each hydrocarbon combustion experiment was near 2.8 g., on the average. It has been shown previously^{5,13} that no significant amount of nitric acid is lost from the bomb during the removal of the carbon dioxide.

The absorption tubes were handled as described previously,⁹ and were weighed on a keyboard type analytical balance¹⁴ using as a counterpoise a substantially identical absorption tube, closed, containing some glass beads and a fixed mass of air. The counterpoise tube had a total mass of about 135 g., approximately the same as that of the working absorption tube before absorption of carbon dioxide. The weights used on the balance pan were brass, while those added from the keyboard were gold with some smaller ones in aluminum. The following expression was used to obtain the true mass (*in vacuo*) of the carbon dioxide absorbed¹⁵

$$m(\text{CO}_2) = 1 + 0.00007\Delta m(\text{total}) - 0.00014\Delta m(\text{brass}) - 0.00007\Delta m(\text{gold}) - 0.00044\Delta m(\text{aluminum}) \quad (5)$$

In this equation, $\Delta m(\text{total})$ is the total mass of the brass and keyboard weights (after absorption) minus the total mass of the brass and keyboard weights used in the first weighing (before absorption). The factor 0.00007 by which $\Delta m(\text{total})$ is multiplied corrects for the decreased amount of helium present in the tube at the second weighing because of expansion of the Ascarite in the amount of 0.45 cm.³ per g. of carbon dioxide absorbed.¹⁵ The last term in the foregoing equation is negligible because the largest aluminum piece was 0.03 g.

The amount of reaction in a given calorimetric hydrocarbon combustion experiment was determined from the mass of carbon dioxide collected in the given experiment, as determined above. For conversion to moles of hydrocarbon, the molecular weight of carbon dioxide was taken as 44.010 g./mole.

The small amount of nitric acid formed during the combustion experiment was determined, after the removal of the gaseous products of combustion from the bomb, by carefully washing the inside of the bomb with water and titrating the aqueous solution with standard 0.01 *N* aqueous sodium hydroxide using phenolphthalein as the indicator.

VI. Data of the Present Investigation

The energy equivalent of the calorimeter, for the temperature interval 28 to 30°, was determined by burning NBS Standard Sample benzoic acid, No. 39g, in the bomb, using the value 26433.8 joules per gram mass for the heat of combustion of this sample under the conditions of the standard bomb process at 25° with appropriate corrections for the differences between the actual and standard bomb processes. The results of the calibration experiments are shown in Table I. The symbols

(9) F. D. Rossini, *J. Res. Natl. Bur. Stds.*, **6**, 1 (1931).

(10) A. J. Streiff, A. R. Hulme, P. A. Cowie, N. C. Krouskop and F. D. Rossini, *Anal. Chem.*, **27**, 411 (1955).

(11) H. F. Bartolo and F. D. Rossini, *THIS JOURNAL*, in press.

(12) Catalog No. 2901, Parr Instrument Company, Moline, Illinois.

(13) R. S. Jessup, *J. Research Natl. Bur. Standards*, **18**, 115 (1937).

(14) Type TC, No. 25877, Wm. Ainsworth and Sons, Denver, Colorado.

(15) F. D. Rossini, *J. Research Natl. Bur. Standards*, **6**, 37 (1931).

TABLE I
 RESULTS OF THE CALIBRATION EXPERIMENTS WITH BENZOIC ACID

Expt.	Mass of benzoic acid, g.	k , min. ⁻¹	K , ohm	U , ohm	ΔR_c , ohm	q_i , j.	q_n , j.	E_i , j./ohm	Deviation from mean, j./ohm
1	1.54125	0.001611	0.000836	0.000186	0.198207	87.5	17.7	206041	+32
2	1.53741	.001592	.000839	.000037	.197685	88.9	2.2	206001	-8
3	1.54049	.001588	.000857	.000046	.198075	89.3	1.5	206005	-4
4	1.54020	.001578	.000846	.000136	.198061	90.1	9.1	206023	+14
5	1.54273	.001601	.000861	.000067	.198415	88.1	10.6	205990	-19
6	1.54051	.001589	.000838	.000056	.198123	88.4	9.0	205991	-18
								Mean 206009	..
								Standard deviation of the mean	±8

 TABLE II
 RESULTS OF THE COMBUSTION EXPERIMENTS ON *cis*-HEXAHYDROINDAN (*cis*-HYDRINDAN)

Expt.	Mass of CO ₂ form. d, g.	k , min. ⁻¹	K , ohm	U , ohm	ΔR_c , ohm	Δr_i , ohm	Δr_n , ohm	B , ohm/g. CO ₂	Dev. from mean, ohm/g. CO ₂
1	2.763873	0.001581	0.001024	0.000082	0.191717	0.000431	0.000009	0.0692107	+0.0000196
2	2.876832	.001602	.000772	.000120	.199481	.000432	.000010	.0691920	+ .0000010
3	2.892734	.001602	.000793	.000187	.200562	.000430	.000012	.0691853	- .0000057
4	2.911151	.001581	.000813	.000208	.201751	.000419	.000010	.0691607	- .0000304
5	2.718551	.001595	.001066	.000123	.188577	.000438	.000011	.0692064	+ .0000153
								Mean 0.0691910
								Standard deviation of the mean	±0.0000089

at the heads of the columns are defined as follows: ΔR_c = the corrected increase in temperature of the calorimeter system, expressed as the increase in resistance in ohms of the given platinum resistance thermometer at a mean temperature of 29°, as measured with the given resistance bridge; q_i = the heat evolved, in absolute joules, by the ignition process of heating and burning the iron wire; q_n = the heat evolved, in absolute joules, by the formation of the small amount of nitric acid in the combustion; E_i = the energy equivalent, over the temperature interval 28 to 30°, of the initial calorimeter system used in the calibration experiments, obtained as the ratio $(-\Delta E + q_i + q_n)/\Delta R_c$, where $-\Delta E$ is the heat evolved by combustion of the given mass of benzoic acid under the conditions of the experiment.

The mean value of the energy equivalent E_i is for an initial system containing a benzoic acid pellet having a mass equal to the mean of the masses of the pellets used in the experiments. However, the desired energy equivalent for the hydrocarbon experiments is that for a system containing no pellet, but containing instead a mass of soft glass equal to the mean mass of the glass ampoules used in the hydrocarbon experiments. The following expressions were used in calculating the desired energy equivalent, E_{si}

$$E_{si} = E_i - D(1.21m_s - 0.711m_g) \quad (6)$$

Here, D = number of degrees Celsius (centigrade) equivalent to one unit of the temperature scale used (9.93 degrees per ohm for the thermometric system used in our experiments); m_s = the mean mass, in grams, of the pellets of benzoic acid used in the calibration experiments (1.54 g.); m_g = the mean mass of the soft glass ampoules used in the hexahydroindan experiments (0.233 g.). In the above equations, E_i and E_{si} are expressed in joules per ohm. With the value of E_i equal to

206009 ± 8 joules per ohm, the value of 205992 ± 8 joules per ohm was obtained for E_{si} .

The results of the combustion experiments on *cis*-hexahydroindan and *trans*-hexahydroindan are shown in Tables II and III. The symbols at the heads of the columns are defined thusly: Δr_i = the increase in temperature of the calorimeter system, expressed as the increase in resistance in ohms of the platinum thermometer, produced by the ignition process of heating and burning the iron wire; Δr_n = the increase in temperature of the calorimeter system, expressed as the increase in resistance of the platinum thermometer, produced by the formation of the small amount of nitric acid in the combustion; $B = [(\Delta R_c - \Delta r_i - \Delta r_n)/m_{CO_2}][1 + (C + \delta)/E_{si}]$; m_{CO_2} = the mass of carbon dioxide formed in the combustion of the hydrocarbon; C = the heat capacity of the amount of hydrocarbon placed in the bomb, expressed as joules per ohm increase in resistance of the given platinum resistance thermometer; δ = a correction term, too small to be significant in this series of experiments, expressed as joules per ohm increase in resistance of the given platinum resistance thermometer, to take account of (a) the variations in mass of the glass ampoule from the "standard" value of 0.233 g., and (b) variations in the mean temperature of an experiment from the standard value of 29°.

VII. Heats of Combustion, Formation and Isomerization of the *cis* and *trans* Isomers of Hexahydroindan

In Table IV are presented the resulting values of the standard heats of combustion of the *cis* and *trans* isomers of hexahydroindan from this investigation. There are given the values of the constant B for 30°, in ohms per gram of carbon dioxide formed, $-\Delta E_B$, the heat evolved in the bomb process at 30° in kilojoules per mole of

TABLE III
 RESULTS OF THE COMBUSTION EXPERIMENTS ON *trans*-HEXAHYDROINDAN (*trans*-HYDRINDAN)

Expt.	Mass of CO ₂ formed, g.	k, min. ⁻¹	K, ohm	U, ohm	ΔR _o , ohm	Δr _i , ohm	Δr _n , ohm	B, ohm/g. CO ₂	Dev. from mean, ohm/g. CO ₂
1	2.816677	0.001727	0.001061	0.000086	0.195195	0.000431	0.000026	0.0691424	-0.0000101
2	2.904492	.001594	.000786	.000067	.201336	.000399	.000026	.0691775	+ .0000250
3	2.854443	.001684	.000913	.000054	.197772	.000427	.000024	.0691326	- .0000199
4	2.743043	.001597	.000954	.000195	.190191	.000428	.000024	.0691757	+ .0000232
5	2.813633	.001612	.000912	.000154	.194959	.000430	.000024	.0691344	- .0000181
								Mean 0.0691525
								Standard deviation of the mean ±0.0000100

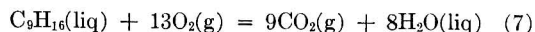
TABLE IV

 VALUES^a OF THE STANDARD HEATS OF COMBUSTION FOR *cis*-HEXAHYDROINDAN (*cis*-HYDRINDAN) AND *trans*-HEXAHYDROINDAN (*trans*-HYDRINDAN)

Compound			B at 30° ohm/g. CO ₂	-ΔE _B at 30° kj./mole	-ΔE° at 30° kj./mole	-ΔH° at 30° kj./mole	-ΔH° at 25° kj./mole	-ΔH° at 25° kcal./mole
Name	Formula	State						
<i>cis</i> -Hexahydroindan (<i>cis</i> -hydrindan)	C ₉ H ₁₆	Liq.	0.0691910 ±0.0000178	5645.39 ± 1.52	5643.30 ± 1.52	5653.38 ± 1.52	5655.10 ± 1.52	1351.60 ± 0.36
<i>trans</i> -Hexahydroindan (<i>trans</i> -hydrindan)	C ₉ H ₁₆	Liq.	0.0691525 ±0.0000200	5642.25 ± 1.69	5640.16 ± 1.69	5650.24 ± 1.69	5651.99 ± 1.69	1350.86 ± 0.40

^a All the uncertainties in this table are equal to twice the standard deviation.

hydrocarbon; $-\Delta E^0$ the decrease in internal energy for the ideal reaction at 30°, with all reactants and products in their standard states; $-\Delta H^0$ the decrease in heat content (or heat evolved in the ideal combustion at constant pressure) for the ideal reaction at 30°; and $-\Delta H^0$ for the ideal reaction at 25°. The recorded values of $-\Delta E^0$ and $-\Delta H^0$ apply to the reaction, with each substance in its standard state



The correction which was applied to $-\Delta E_B$ in obtaining $-\Delta E^0$ was calculated by the method of Washburn,¹⁶ using, where possible, values for 30°, and taking advantage of more recent expressions for the solubility of oxygen and carbon dioxide in nitric acid solutions.¹⁷ The value for this correction was -0.037% or + 2.09 kj. per mole for both isomers. Conversion from $-\Delta E^0$ to $-\Delta H^0$, at 30°, involved + 10.08 kj. per mole for $-\Delta(PV)^0$. Conversion to $-\Delta H^0$ at 25° involved + 1.72 kj. per mole for *cis*-hexahydroindan and +1.75 kj. per mole for *trans*-hexahydroindan. The over-all uncertainty assigned to each final value of the heat of combustion of a compound was taken as the square root of twice the resulting standard deviation of the mean, including both the combustion experiments and the calibration experiments.¹⁸

Values for the standard heat capacities (at 25°) of O₂(g), CO₂(g) and H₂O(liq), as well as values for the standard heats of formation (at 25°) of CO₂(g) and H₂O(liq), were obtained from the tables of the API Research Project 44.¹⁹ The values in joules were converted to the defined

(16) E. W. Washburn, *ibid.*, **10**, 525 (1933).

(17) W. N. Hubbard, D. W. Scott and G. Waddington, *This Journal*, **58**, 152 (1954).

(18) F. D. Rossini and W. E. Deming, *J. Wash Acad. Sci.*, **29**, 416 (1939).

(19) F. D. Rossini, K. S. Pitzer, R. L. Arnett, R. M. Braun and G. C. Pimentel, "Selected Values of Physical and Thermodynamic Properties of Hydrocarbons and Related Compounds," Carnegie Press, Pittsburgh, Pennsylvania, 1953.

thermochemical calorie using the relation: 1 calorie = 4.184 (exactly) joules.

Table V gives the values for the standard heats of formation of the two isomers for both the liquid and gaseous states. For the latter values, use is made of the values of heats of vaporization at 25°, calculated from vapor pressure data, with some extrapolation.²⁰ For the heats of vaporization at 25°, the values are 11.00 ± 0.30 and 10.70 ± 0.30, kcal./mole, respectively, for the *cis* and

TABLE V

 VALUES OF THE STANDARD HEATS OF FORMATION AND ISOMERIZATION OF *cis*-HEXAHYDROINDAN AND *trans*-HEXAHYDROINDAN

Compound			Heat of formation, ΔH° _{298.15} , kcal./mole	Heat of isomern. (referred to the <i>trans</i> -isomer) ΔH° _{298.15} , kcal./mole
Name	Formula	State		
<i>cis</i> -Hexahydroindan	C ₉ H ₁₆	Liq.	-41.41 ± 0.36	0.74 ±0.52
<i>cis</i> -Hexahydroindan	C ₉ H ₁₆	Gas	-30.41 ± 0.47	1.04 ±0.53
<i>trans</i> -Hexahydroindan	C ₉ H ₁₆	Liq.	-42.15 ± 0.40	0.00
<i>trans</i> -Hexahydroindan	C ₉ H ₁₆	Gas	-31.45 ± 0.50	0.00

trans isomers. The difference in the heats of vaporization is taken as 0.30 ± 0.10 kcal./mole.

VIII. Results of Previous Investigation

Only one report of the heats of combustion of *cis*- and *trans*-hexahydroindan has appeared in the literature, and that as an incidental part of another investigation,²¹ with Becker and Roth²¹

(20) D. L. Camin, Chemical and Petroleum Research Laboratory, Carnegie Institute of Technology, unpublished data.

(21) W. Hüchel, E. Kamenz, A. Gross and W. Tappe, *Ann.*, **533**, 1 (1937).

reported marking three combustion experiments with each of the compounds. From their meager data, one calculates a value of $\Delta H = +1.5 \pm 0.9$ kcal./mole for the heat of isomerization, in the liquid state, of the *trans* isomer to the *cis* isomer. Because of a number of uncertainties, it is difficult to recover an absolute value for the heat of combustion of the isomers from the little information supplied. Within the limits of uncertainty, the heat of isomerization derived from Becker and Roth²¹ is in accord with the value from the present investigation.

IX. Discussion

The data of the present information yield $\Delta H^0 = 1.04 \pm 0.53$ for the heat of isomerization of the *trans* isomer to the *cis* isomer in the gaseous state at 25°, making the *trans* isomer more stable. As discussed by a number of investigators,^{22,23} a five-membered cycloparaffin ring and a six-membered cycloparaffin ring may be fused together through two adjacent carbon atoms common to both rings either through (a) one equatorial and one axial bond or (b) two equatorial bonds. In the former case, the *cis* isomer of hydrindan is formed and in the latter case the *trans* isomer. It is expected that, on the basis of the conformation, the *trans* isomer would be more stable energetically, that is, have a lower energy content, as shown by the experimental data. However, without other complicating factors, a simple substitution of one equatorial bond for one axial bond, in going

(22) W. G. Dauben and K. S. Pitzer, Chapter in "Steric Effects in Organic Chemistry," M. S. Newman, Editor, John Wiley and Sons, Inc., New York, N. Y., 1956.

(23) E. L. Eliel and C. Pillar, *J. Am. Chem. Soc.*, **77**, 3600 (1955).

from the *cis* isomer to the *trans* isomer, should give a difference of energy nearly twice that observed. As previously pointed out,^{22,23} the explanation lies in the fact that the six-membered ring requires some distortion in order to bring together the desired bonds for the fusion of the two rings. This distortion is not much for the *cis* isomer but is appreciable for the *trans* isomer. This introduces additional strain which keeps the energy of the *trans* isomer from becoming as low as it might otherwise become, and hence makes the difference in energy of the two forms less than originally expected. Similar considerations may be inquired into in the case of (a) the *cis* and *trans* isomers of decahydronaphthalene, formed by a like fusion of two six-membered cycloparaffin rings, and (b) the *cis* and *trans* isomers of bicyclo-[3.3.0]octane, formed by a like fusion of two five-membered cycloparaffin rings.

McCullough and co-workers²⁴ have measured calorimetrically the entropies of the *cis* and *trans* isomers of hexahydroindan and find the entropy of the *cis* form to be greater than that of the *trans* form by 1.68 ± 0.10 cal./deg. mole, for the liquid state at 25°. From this value, and the heat of isomerization determined in the present investigation, the standard free energy of isomerization of the *trans* form to the *cis* form is calculated to be

$$\Delta F_{298-16}^0 = 0.24 \pm 0.52 \text{ kcal./mole} \quad (8)$$

This result indicates that, within the limits of uncertainty, the two isomers have substantially the same free energy in the liquid state at 25°.

(24) J. P. McCullough, U. S. Bureau of Mines, Bartlesville, Oklahoma - private communication.

NOTES

EFFECT OF A NOBLE GAS ON THE LABELING OF *n*-HEXANE BY EXPOSURE TO TRITIUM

By A. Y. MOTT LAU

Esso Research and Engineering Company, Linden, New Jersey

Received September 16, 1959

When the tritiated products from the labeling of liquid *n*-hexane by exposure to tritium gas¹ were examined in this Laboratory with a radio-assaying gas chromatograph, the proportion of labeled compounds in the C₆ fraction was found to be considerably less than that reported by Riesz and Wilzbach² using only gaseous *n*-hexane. Table I compares the two sets of data.

It can be seen that in our work not only was there less labeling of the C₆ fraction but also a much greater amount of the tritium ended up in the heavier fractions. Our sample handling procedure did allow some small loss of compounds lighter than C₄

(1) K. E. Wilzbach, *J. Am. Chem. Soc.*, **79**, 1013 (1957).

(2) P. Riesz and K. E. Wilzbach, *This Journal*, **62**, 6 (1958).

TABLE I
VARIATION IN TRITIATED PRODUCT YIELD

Source	Distribution of radioactivity in fractions, % Physical state ^a	Distribution of radioactivity in fractions, %				
		C ₃	C ₄	C ₅	C ₆	C ₇
Riesz and Wilzbach	Gas	48	27	9	11	5
This work	Gas and					
	liquid	39	15.5	10	19.5	16

^a During exposure to tritium.

due to evaporation, but the effect of this on product distribution was quite small.

There appear to be only two differences between the labeling procedures used by Riesz and Wilzbach and by ourselves important enough to account for the quite different yields of tritiated C₆ obtained: (1) In the former work the hydrocarbon was entirely in the vapor state; in ours both liquid and vapor phases were present. (2) The tritium used by Riesz and Wilzbach contained 50% helium-3; ours contained much less than 10%.

The possibility that helium could have had an effect on product distribution seemed worth investi-

gating. The noble gases, argon and helium, have ionization potentials higher than those of T₂ and *n*-hexane. They can therefore ionize, by charge transfer, either of those molecules. Furthermore, the noble gases possess metastable states having lives comparable to ions. These metastable atoms can ionize *n*-hexane on collision. Argon rather than helium was chosen for this study because, having a higher density, it would absorb a larger fraction of the β -ray energy and thus enhance energy-transfer effects, if any.

Into each of three ampoules was introduced 1.0 ml. of *n*-hexane (Research Grade) and 150 mm. of tritium. One of the ampoules was sealed without argon; to the second and third were added 150 and 300 mm. of argon, respectively, before sealing. The 150 mm. of tritium represented an activity of three curies. After the ampoules had been shaken for 2 weeks at room temperature the hexane and the radiolysis products were frozen with liquid nitrogen and the fixed gases were pumped off. To minimize the evaporation loss referred to in the earlier experiment, the samples were chilled with Dry Ice during handling.

Tritium distribution, as C₆, lighter than C₆, and heavier than C₆, was determined for each of the samples using the radioassaying gas chromatograph. This instrument is similar to that used by Riesz and Wilzbach.¹ The results are summarized in Table II.

TABLE II

Argon mm. Hg	Tritium dist., %			Sp. act. (mc./ ml.)	Millicuries by fractions		
	C ₁₋	C ₆	C ₇ thru C ₁₀		C ₁₋	C ₆	C ₇ thru C ₁₀
0	39	18	43	71	28	13	31
150	27	25	48	92	25	23	44
300	29	25	46	53	15	13	24

The data indicate that argon dilution does increase by almost 40% (from 18 to 25%) the proportion of tritium incorporated in the C₆ fraction. Also the specific activity of the product is increased from 71 to 92 mc./ml. Note that the distribution obtained in the sample without argon dilution is substantially the same as that obtained in our earlier experiment, shown in Table I. This indicates satisfactory experimental reproducibility.

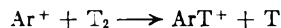
Doubling the amount of argon in the system causes no further improvement in the tritiation selectivity. Furthermore, there appears to be an optimum concentration beyond which a serious reduction in the total amount of tritiation is experienced; note the sharp drop in the specific activity of the total product when the argon content was doubled.

The effect of argon on the distribution of tritiated products can be more easily visualized by studying the total millicuries of labeled hydrocarbons formed in each fraction, also given in Table II. These values were obtained by multiplying the specific activity of each sample by the tritium distributions. It appears that a 1:1 argon-to-tritium dilution has little effect on the C₃-compounds formed; a slight reduction is indicated. The C₆ and heavier compounds are markedly increased,

however. A further dilution with argon to 2:1 causes a pronounced and proportional decrease in tritiated products in each fraction.

The beneficial effect of argon in the system is probably related to the characteristics of its ions and metastable atoms. When tritium and hexane are sealed in an ampoule without argon, the β -energy is dissipated by the formation of ions and excited molecules of both constituents and by loss to the wall. In the case of a continuously wet wall as in the present system, wall loss should be small. When argon is present in the system, the β -energy is again spent in the formation of ions and excited molecules but now part of these are the ions and long-lived metastable atoms of argon. The former quickly ionize either T₂ or C₆H₁₄ by charge transfer and the latter ionize only C₆H₁₄ because the energy of the metastable argon atom (11.6 e.v.) lies between the ionization potentials of *n*-hexane (10.4 e.v.) and H₂ (15.6 e.v.). One effect, then, of argon addition is to increase the ratio of ionized to excited reactants in the system.

Another probable effect of argon addition is to increase the proportion of energy supplied to the tritium. Lampe, *et al.*,³ found the ionization cross section (by 75 volt electrons) of argon to be three times that of hydrogen, normal hexane to be almost twenty times that of hydrogen. If we assume these values to be at least roughly representative of the ionization cross sections by tritium β -rays, argon would increase the proportion of energy supplied to the tritium as a result of the reaction⁴



It is to be noted that, in addition to the formation of the molecule-ion containing tritium, this reaction produces tritium atoms that could also contribute to the labeling process. An increased concentration of tritium ions and atoms in the system might be expected to be a contributing factor to the altered product composition observed with argon addition.

The increased yield of labeled products with argon addition, coupled with the observations of Stevenson and Schissler⁴ on the ready occurrence of ion-molecule reactions and of Thompson and Schaeffer⁵ on their role in the radiation-induced exchange between H₂ and D₂, lend support to the hypothesis that ion-molecule reactions contribute to the formation of labeled products in the present process.

The decrease in product yield with increase in argon concentration beyond an optimum can be explained on the basis of an increasing probability of metastable atom decay and ion neutralization before a useful collision (one leading to product formation) has occurred.

The use of hexane in the liquid state in this work—compared to the vapor phase work by Riesz and Wilzbach—also has an effect. Using gaseous hexane, only about 25% of the fixed tritium is

(3) F. W. Lampe, J. L. Franklin and F. H. Field, *J. Am. Chem. Soc.*, **79**, 6129 (1957).

(4) D. P. Stevenson and D. O. Schissler, *J. Chem. Phys.*, **29**, 282 (1958).

(5) S. O. Thompson and O. A. Schaeffer, *J. Am. Chem. Soc.*, **80**, 553 (1958).

found in the heavier-than- C_6 fraction. Using liquid hexane, this fraction amounts to 48%. It is to be expected that the cage effect in the liquid phase would lead to the formation of labeled products of higher molecular weight.

Acknowledgment.—Helpful discussion with Dr. K. E. Wilzbach on the reaction mechanisms involved in this work is gratefully acknowledged.

AN APPROXIMATE METHOD FOR MEASURING THE SELF-INTERACTION CONSTANT OF NON-ELECTROLYTES IN TWO-COMPONENT SOLVENTS¹

BY ERNEST GRUNWALD² AND GEORGE BAUGHMAN

Chemistry Department, Florida State University, Tallahassee, Florida

Received November 13, 1959

For moderately dilute solutions of a non-electrolyte in a solvent of fixed composition, the molal activity coefficient γ_i of the non-electrolyte may be expressed as a function of its molal concentration m_i by equation 1

$$\ln \gamma_i = k_i m_i \quad (1)$$

In typical cases, the constant k_i is negative and may be regarded as an approximate measure of the self-interaction of the non-electrolyte in the given solvent.

Long and McDevit, in their analysis of activity coefficients of non-electrolytes in aqueous salt solution, have concluded that the term $k_i m_i$ is in general not negligible.³ However, experimental values of k_i are available only for relatively few systems, largely because of experimental difficulties. This is particularly true for non-volatile non-electrolytes. Here the measurement of k_i is extremely difficult except at the freezing point or boiling point of the solvent.

For this reason, we have tried to find a more convenient method for measuring k_i . Some years ago we reported⁴ a modification of the dynamic method of vapor pressure measurement⁵ which permits the precise determination of the activities of the solvent components in two-component solvents containing non-volatile solutes. We now apply this method, in conjunction with solubility data, to obtain fairly accurate estimates of k_i for non-electrolytes in two-component solvents.

Method

We shall consider a solution consisting of two solvent components, 1 and 2, and a solute component, 3. It is convenient to express the solvent composition by the mole fractions Z_1 and $Z_2 (= 1 - Z_1)$, where $Z_1 = n_1/(n_1 + n_2)$, and n_1 and n_2 are mole numbers. Furthermore, it is convenient

(1) Work supported by the Office of Naval Research. Reproduction in whole or in part is permitted for any purpose of the United States Government.

(2) Alfred P. Sloan Fellow, 1959.

(3) (a) F. A. Long and W. F. McDevit, *Chem. Revs.*, **51**, 119 (1952); (b) W. F. McDevit and F. A. Long, *J. Am. Chem. Soc.*, **74**, 1090 (1952).

(4) (a) A. L. Bacarella, A. Finch and E. Grunwald, *THIS JOURNAL*, **60**, 573 (1956); (b) E. Grunwald and A. L. Bacarella, *J. Am. Chem. Soc.*, **80**, 3840 (1958).

(5) E. W. Washburn and E. O. Heuse, *ibid.*, **37**, 309 (1915).

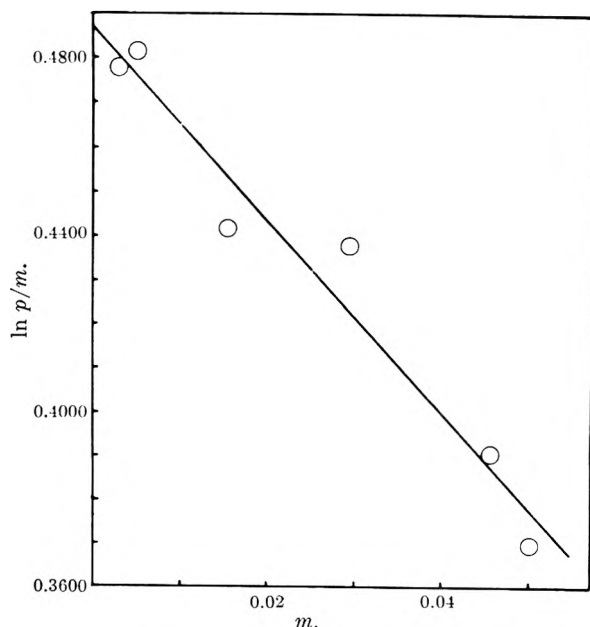


Fig. 1.—Plot of $\ln(p_3/m_3)$ for naphthalene as a function of molal concentration; 50.00 wt. % dioxane-water solvent, 25.00°.

to write the partial molal free energy of the solute in the form of equation 2, where F_{3m}^0 is the standard partial molal free energy (on the molal scale).

$$\bar{F}_3 = F_{3m}^0 + RT \ln m_3 + RT \ln \gamma_3 \quad (2)$$

We define γ_3 so that $RT \ln \gamma_3$ approaches zero as m_3 approaches zero at constant solvent composition. By virtue of this definition, F_{3m}^0 is a function of the solvent composition, and $\ln \gamma_3$ is given by equation 1. Thus we obtain

$$\bar{F}_3 = F_{3m}^0 + RT \ln m_3 + k_3 m_3 \quad (3)$$

In attempting to measure k_3 , we proceed as follows. First, we measure the molal solubility s_3 as a function of Z_1 . Since, for the saturated solution, $\bar{F}_3 = F_3(\text{solid})$, $d\bar{F}_3/dZ_1 = 0$, and differentiation of equation 3 leads to equation 4

$$\frac{-d \ln s_3}{dZ_1} = \frac{1}{RT} \frac{dF_{3m}^0}{dZ_1} + k_3 s_3 \frac{d \ln s_3}{dZ_1} + s_3 \frac{dk_3}{dZ_1} \quad (4)$$

The three terms on the right in equation 4 have been arranged in sequence of decreasing order of magnitude. If the smallest term, $s_3(dk_3/dZ_1)$, be neglected, equation 5 is obtained for k_3 .

$$k_3 = \frac{-1}{s_3} \left[1 + \frac{dF_{3m}^0/dZ_1}{RT d \ln s_3/dZ_1} \right] \quad (5)$$

The value $0^- dF_{3m}^0/dZ_1$ required in equation 5 is obtained from vapor pressure data. As reported elsewhere,⁴ the quantity

$$\ln \frac{a_1 a_2^*}{a_2 a_1^*}$$

can be obtained with good precision by the dynamic vapor pressure method, where

a_1 = activity of component 1 in a soln. consisting of the solute and the two-component solvent of composition Z_1

a_1^* = activity of component 1 in the two-component solvent of composition Z_1 , in the absence of solute

and analogous definitions apply for a_2 and a_2^* .

TABLE I
THERMODYNAMIC DATA FOR NAPHTHALENE AND 1-NAPHTHOIC ACID IN THE SYSTEM DIOXANE-WATER, 25°

Wt. % dioxane	Z_1	$s_3(m)$	$\frac{\delta \ln s_3}{\delta Z_1}$	$\frac{d \ln s_3}{dZ_1}$	$\frac{dF_{3m}^0}{dZ_1}/RT$	k_3
Naphthalene						
46.319	0.8500	0.04014	-21.46
50.000	.8302	.0614 ^a	-21.59	-21.53 ^b	18.85	-2.03
53.422	.8100	.0950
1-Naphthoic Acid						
40.00	.8800	.05071 ^a	-24.03
50.00	.8302	.1678 ^a	-15.34	-20.25 ^b	18.43	-0.536
60.00	.7653	.4541 ^a
46.319	.8500	.1056	-22.17
50.000	.8302	.1638	-18.64	-20.42 ^b	18.43	-0.595
53.422	.8100	.2387

^a Reported by A. F. Butler.⁷ ^b Calculated on the assumption that $d \ln s_3/dZ_1$ varies linearly with Z_1 in this interval. Note that, in the case of 1-naphthoic acid, the size of the interval has been more than doubled without significant effect on the calculated derivative.

Upon substitution of equation 1 in equation 11 of reference 4b and integration at constant Z_1 , we obtain

$$\frac{1000}{M_{12}} \ln \left(\frac{a_1 a_2^*}{a_2 a_1^*} \right) = \left[\frac{1}{RT} \frac{dF_{3m}^0}{dZ_1} - r \right] m_3 - \frac{rk_3 m_3^2}{2} + (dk_3/dZ_1) m_3^2/2 \quad (6)$$

where $r = (M_1 - M_2)/M_{12}$, and $M_{12} = Z_1 M_1 + Z_2 M_2$. The three terms on the right in equation 6 have been arranged in sequence of decreasing order of magnitude. If the third and smallest term be again neglected, we have an equation involving only experimental quantities and the two parameters, $(dF_{3m}^0/dZ_1 - rRT)/RT$ and $rk_3/2$.

Although in principle k_3 is obtainable from vapor pressure data alone *via* equation 6, in practice the term $rk_3 m_3^2/2$ barely exceeds the experimental error even at moderate solute concentrations. On the other hand, dF_{3m}^0/dZ_1 is obtained with good precision and differs sufficiently from $RT d \ln s_3/dZ_1$ in equation 5 so that k_3 can be derived with reasonable accuracy. In computing dF_{3m}^0/dZ_1 and k_3 *via* equations 5 and 6, it is best to use a method of successive approximations. In the first approximation, the term $rk_3 m_3^2/2$ is neglected in (6). The resultant value of dF_{3m}^0/dZ_1 leads to a first estimate of k_3 *via* equation 5, which is then used to obtain a second estimate of dF_{3m}^0/dZ_1 *via* equation 6, and so on. Convergence is rapid.

To illustrate the use of this method, some data for naphthalene and 1-naphthoic acid are given in Table I. The method fails to be satisfactory only if excessive curvature of the plot of $\ln s_3$ *vs.* Z_1 makes it difficult to evaluate the derivative. In the case of naphthalene, it is possible to evaluate k_3 by an independent method, since the partial pressure of this substance is sufficiently large for precise measurement. Experimental values of $\ln(p_3/m_3)$ are plotted *vs.* m_3 in Fig. 1 for naphthalene in 50.00 wt. % dioxane-water at 25°. The slope of this line, which is equal to k_3 , has been evaluated by the method of least squares as -2.18, in excellent agreement with the value of -2.03 obtained by the approximate method in Table I.⁶

(6) The accuracy of the data plotted in Fig. 1 is supported by the following comparison: If the linear relationship of $\ln(p_3/m_3)$ *vs.* m_3 is extrapolated slightly to $m_3 = s_3$, the vapor pressure of naphthalene in the saturated solution is found to be 0.0874 mm. The vapor

Experimental

The purification of dioxane, water, naphthalene and 1-naphthoic acid, and the apparatus used for the dynamic vapor pressure measurements, have been reported elsewhere.^{4,7} Values of $(a_1 a_2^*/a_2 a_1^*)$ were calculated from the mass ratios of the vapor condensates,⁴ due correction being made for the volatility of 1-naphthoic acid (almost negligible) and naphthalene (significant). The concentrations of these substances in the vapor condensates were measured spectrophotometrically.

Solubilities were measured in sealed ampoules under a nitrogen atmosphere in order to prevent changes in solvent composition during the long shaking periods (48-96 hours) required for saturation. All measurements were made in thermostats maintained at 25.00°.

pressure of pure solid naphthalene is 0.087₅ mm. at 25° ("International Critical Tables," Vol. III, p. 208).

(7) A. F. Butler, Ph.D. Thesis, Florida State University, Tallahassee, 1956.

THE EFFECT OF PRESSURE ON THE MELTING POINTS OF ISOTACTIC POLYPROPYLENE AND POLYETHYLENE OXIDE

By L. R. FORTUNE AND G. N. MALCOLM

University of Otago, Dunedin, New Zealand

Received December 7, 1959

The determination of the entropies of fusion of isotactic vinyl polymers is of considerable interest as a means of examining their molecular structure. If these substances possess comparatively stiff molecular chains¹ their entropies of fusion should be fairly small. However the entropy of fusion of isotactic polypropylene recently has been found to be 5.8 ± 0.2 e.u. per mole of crystalline repeating units² which is almost as large as the value 5.85 e.u. which has been reported for poly-(ethylene oxide).³ But both these entropy values include not only the change of configurational entropy on melting but also the entropy of volume change on melting.⁴ Only if this latter quantity can be determined will a comparison of the changes of configurational entropies on melting be possible.²

(1) G. Gee, *Proc. Chem. Soc. (London)*, 111 (1957).

(2) F. Danusso, G. Moraglio and E. Flores, *Atti. Acc. naz. Lincei. Rend. Classe Sci. fis. mat. nat.*, **26**, 520 (1958).

(3) L. Mandelkern, *J. Appl. Phys.*, **26**, 443 (1955).

(4) P. J. Flory, "Principles of Polymer Chemistry," Cornell Univ. Press, Ithaca, N. Y., 1953, p. 575.

The entropy of volume change on melting is given by the expression $\Delta S = (\partial P/\partial T)_V \Delta V_u$ where $(\partial P/\partial T)_V$ is the thermal pressure coefficient of the polymer at its melting point and ΔV_u is the volume change on melting per mole of crystalline repeating units. The latter quantity is related to the total entropy of fusion by the Clapeyron-Clausius equation

$$dT_m/dP = \Delta V_u/\Delta S_u \quad (1)$$

where T_m is the temperature of melting.

We report here some measurements of the effect of pressure on the melting points of isotactic polypropylene and poly-(ethylene oxide) from which the volume changes on melting have been calculated by means of equation 1. Measurements of the thermal pressure coefficients of these polymers are being made at the present time.

Experimental

Apparatus.—The polymer sample was melted into a glass tube which was placed with its open end dipping into a pool of mercury inside a steel pressure bomb. The bomb was connected through a pressure gauge to a compressor which consisted of a cylindrical steel chamber into which a thin rod was inserted through a packing gland. The rod could be screwed into or out of the cylinder, and its exact position could be observed through a travelling microscope. The bomb containing the polymer was placed inside a large well-lagged aluminum heating block which could be maintained at any temperature up to 250° to within $\pm 0.1^\circ$. After assembly the apparatus was evacuated and filled with freshly distilled water. The pressure was raised to the required value by screwing the rod into the compressor, after which the aluminum block was heated to some convenient starting temperature and the system allowed to reach equilibrium. A small adjustment in the pressure was made if necessary after equilibrium had been attained. Subsequently the temperature of the block was raised in small steps and the increase in volume of the contents of the pressure bomb caused by thermal expansion was counteracted by winding the rod out of the compressor so that the pressure in the system remained at the required value. Plots were made of the position of the rod against temperature and showed a sharp decrease in slope at the melting point. The temperature was raised extremely slowly through the last ten degrees below the melting point and was kept just below the melting point for 12 to 24 hours to allow equilibrium to be attained. The temperatures were read to 0.1° and the pressures to within 5 p.s.i.

Materials.—The isotactic polypropylene was kindly supplied by I.C.I. Plastics Division, Welwyn City, England, and the poly-(ethylene oxide) by Messrs. Oxirane Ltd. of Manchester, England. The number average molecular weight of the poly-(ethylene oxide) was given as 5000.

Results

The melting points of the two polymers were determined at pressures of 19, 95.5, 190 and 380 atmospheres. At least three experiments were performed at each pressure and gave results which agreed with one another within 0.5°. The observed linear dependence of the melting points on pressure can be represented closely by the equations $T_m = 171.0 + 0.040(P - 50)$, isotactic polypropylene (2) and

$$T_m = 62.0 + 0.021(P - 50), \text{ poly-(ethylene oxide)} \quad (3)$$

where T is in °C. and P is in atmospheres.

The results for isotactic polypropylene extrapolate to a melting point at atmospheric pressure of 169° which is lower than either of the values 174.5 and 176° reported by Danusso, Moraglio and Flores² for two of their samples of this polymer. Although care was taken to hold samples at tem-

peratures just below the melting point for prolonged periods it was not possible to obtain melting points higher than those shown in the figure. Small differences between the melting points of different samples of isotactic polymers also have been observed by Krigbaum, Carpenter and Newman⁵ who obtained values for isotactic polystyrene about 6° lower than those reported by Danusso and Moraglio. According to a recent discussion by Coleman⁶ it is possible that these differences in melting points arise from small differences in the degree of chain regularity of the different samples of the isotactic polymers.

The results for poly-(ethylene oxide) give a melting point at atmospheric pressure of 61°. A value of 66° for this polymer has been reported by Mandelkern,³ but this was for a sample with a number average molecular weight of 10,000 whereas the molecular weight of the present sample was only 5000.

From equations 2 and 3 the values of the pressure coefficients of the melting point are 0.040 deg. atm.⁻¹ for isotactic polypropylene and 0.021 deg. atm.⁻¹ for poly-(ethylene oxide). Combination of these values with the entropies of fusion^{2,3} according to equation 1 leads to values of the volume changes on melting shown in Table I.

TABLE I

THE VOLUME CHANGE ON MELTING PER MOLE OF CRYSTALLINE REPEATING UNITS, ΔV_u

Polymer	ΔV_u , cc.
Polypropylene (isotactic)	9.6
Poly-(ethylene oxide)	5.1

The value of ΔV_u obtained for poly-(ethylene oxide) is very close to the value 5.7 cc. which has been estimated for linear polyethylene.⁷ The much larger value of ΔV_u for the isotactic polypropylene is interesting in view of the unexpectedly large value of the entropy of fusion which was found for this polymer. Further discussion of these results will be possible when the thermal pressure coefficients of the polymers have been determined.

We wish to thank Professor Gee of Manchester University, England, for helpful discussion of these results.

(5) W. R. Krigbaum, D. K. Carpenter and S. Newman, *THIS JOURNAL*, **62**, 1586 (1958).

(6) B. D. Coleman, *J. Poly. Sci.*, **31**, 155 (1958).

(7) F. A. Quinn and L. Mandelkern, *J. Am. Chem. Soc.*, **80**, 3178 (1958).

THE INFLUENCE OF ETHANE ON THE POLYMERIZATION RATE OF ETHYLENE

BY CHITA EDEN AND HANS FEILCHENFELD

Petrochemistry Laboratory of the Research Council of Israel and of the Department of Physical Chemistry, Hebrew University, Jerusalem, Israel

Received December 11, 1959

While working on the polymerization of ethylene in the presence of $TiCl_3-Al(C_2H_5)_3$ catalyst it was found that ethane has an inhibiting effect. This effect proved to be reversible.

The experiments were carried out in the absence of a solvent at a temperature of 21°. The reaction

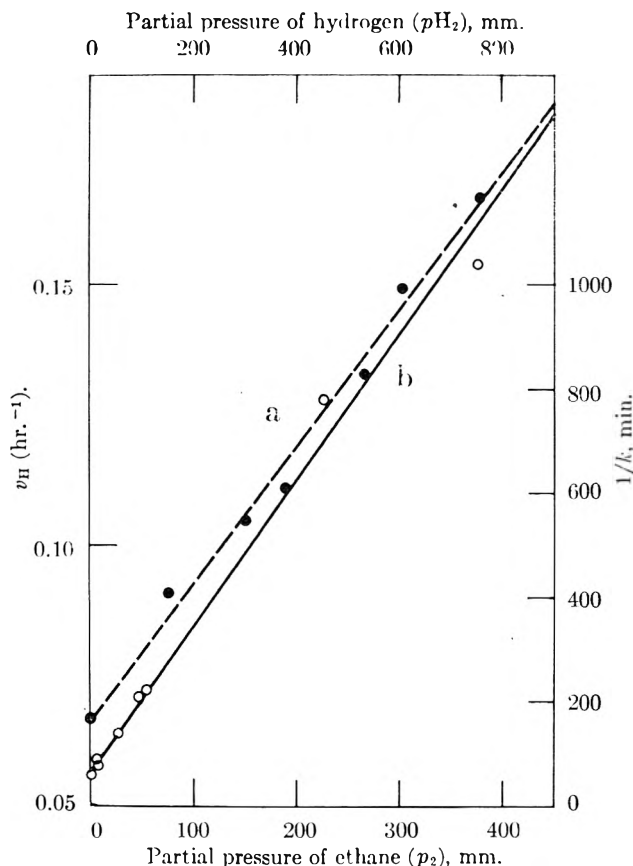


Fig. 1.—(a) ●●— — —, the inverse of the apparent rate constant of polymerization of ethylene as a function of the partial pressure of ethane, catalyst, $\text{TiCl}_3\text{-Al}(\text{C}_2\text{H}_5)_3$; (b) ○○——, the inverse of the rate of polymerization of propylene as a function of the partial pressure of hydrogen as calculated from results published by Natta, *et al.*⁴

followed a first-order law with regard to ethylene (p_1)

$$r = kp_1 \quad (1)$$

This is in accord with earlier works in which a solvent was used.^{1,2}

The apparent rate constant k was found to be a function of the partial pressure of ethane (p_2) and to obey the law (Fig. 1a) (2).

$$\frac{1}{k} = a + bp_2 \quad (2)$$

It has been customary to attribute inhibition by gases not participating in the reaction to competition for adsorption sites.³ In the present case this explanation cannot be true in this simple form and needs some further elaboration. For, the first-order implies that most adsorption sites are vacant. It should therefore make little difference that ethane molecules also occupy a few sites. This can easily be seen from Langmuir's isotherm

$$\theta_1 = \frac{K_1 p_1}{1 + K_1 p_1 + K_2 p_2} \quad (3)$$

where θ_1 is the fraction of catalyst surface occupied by ethylene molecules. Since it must be assumed

(1) G. Natta, I. Pasquon and E. Giachetti, *Angew. Chem.*, **69**, 213 (1957).

(2) H. Feilchenfeld and M. Jeselson, *THIS JOURNAL*, **63**, 720 (1959).

(3) K. J. Laidler, "Kinetic Laws in Surface Catalysis," in "Catalysis," Vol. 1, Reinhold Publ. Corp., New York, N. Y., 1954, p. 119.

for chemical reasons that ethane will not be adsorbed more strongly than ethylene, it should follow that also for a mixture of ethane and ethylene the fraction of the occupied catalyst sites must be small; both $K_1 p_1$ and $K_2 p_2$ should be small as compared with 1, and the constant b in equation 2 should tend to 0; this is in contradiction with the experimental evidence.

The ethane effect can be explained if it is assumed that the true rate constant for the polymerization of ethylene is larger than that for the adsorption of ethylene. The number of active sites occupied by ethylene may then be smaller than that occupied by ethane even if K_2 is not greater than K_1 .

This qualitative argument can be put into a quantitative form: In the steady state the rate of adsorption of ethylene must equal the sum of the rates of desorption and polymerization. If suffix 1 signifies ethylene and suffix 2 ethane, α the rate constant of adsorption, β the rate constant of desorption and k_1 the true rate constant of polymerization of ethylene on the catalyst then

$$\theta_1(\beta_1 + k_1) = (1 - \theta_1 - \theta_2)\alpha_1 p_1$$

$$\theta_2 \beta_2 = (1 - \theta_1 - \theta_2)\alpha_2 p_2$$

Solving the two simultaneous equations for θ_1

$$\theta_1 = \frac{p_1}{\frac{1}{K_1} + \frac{k_1}{\alpha_1} + p_1 + \left(\frac{K_2}{K_1} + \frac{k_1 K_2}{\alpha_1}\right) p_2}$$

where $K = \alpha/\beta$. The first order of the reaction for pure ethylene proves that

$$p_1 \ll \frac{1}{K_1} + \frac{k_1}{\alpha_1}$$

therefore

$$\theta_1 = \frac{p_1}{\frac{1}{K_1} + \frac{k_1}{\alpha_1} + \left(\frac{1}{K_1} + \frac{k_1}{\alpha_1}\right) K_2 p_2}$$

Since the measured rate of the polymerization of ethylene $k p_1 = \theta_1 k_1 A$, A being the area of the catalyst, it follows that

$$\frac{1}{k} = \frac{\left(\frac{1}{K_1} + \frac{k_1}{\alpha_1}\right) (1 + K_2 p_2)}{A k_1} = a + b p_2 \quad (4)$$

Therefore

$$a = \frac{1}{A} \left(\frac{1}{K_1 k_1} + \frac{1}{\alpha_1}\right) \text{ and} \\ b = \frac{K_2}{A} \left(\frac{1}{K_1 k_1} + \frac{1}{\alpha_1}\right) \quad (5)$$

and $b/a = K_2$. Inserting a and b from Fig. 1a, K_2 works out to be 32 atm.⁻¹.

It should be mentioned that recently Natta and co-workers⁴ have published results on the influence of hydrogen on the polymerization of propylene with a similar catalyst dispersed in *n*-heptane. As can be seen from Fig. 1b their results fit equation 2 closely. However, they prefer a relation of the form

(4) G. Natta, G. Mazzanti, P. Longi and F. Bernadini, *Chim. ind.*, **41**, 513 (1959).

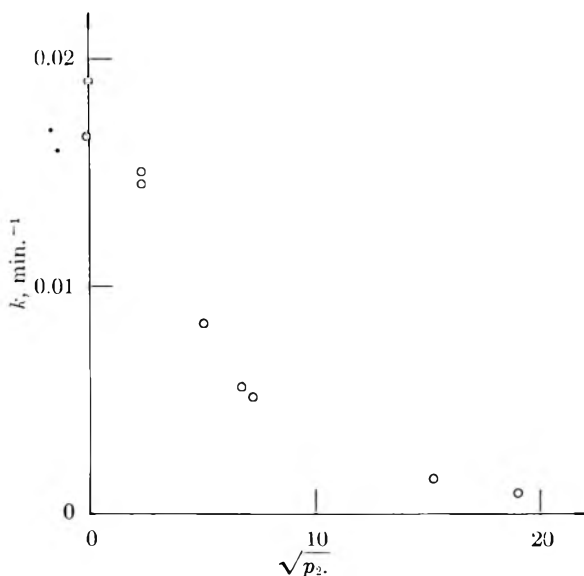


Fig. 2.—The apparent rate constant of polymerization of ethylene as a function of the square root of the partial pressure of ethane.

$$v_H = v_0 - \frac{p_{H_2}}{\lambda} \quad (6)$$

where v_H and v_0 are the reaction rates at constant propylene partial pressure in the presence and absence of hydrogen, respectively, p_{H_2} is the partial pressure of hydrogen and λ an arbitrary constant. They assume that hydrogen causes hydrogenolysis of bonds between the catalyst and the growing polymer chains. For algebraic reasons the difference between equations of types (2) and (6) is well within the experimental error for the conditions of Natta's experiments. The results of this paper will, however, not fit Natta's hypothesis as can be seen from the plot in Fig. 2. Admittedly the two systems are different. Still it is possible that also with hydrogen in heptane solution, hydrogen will occupy an appreciable portion of the active sites while those occupied by propylene are vacated by polymerization in preference to desorption. If this is the case, equation 2 must be expected to hold also for Natta's case.

As to the polymerization of ethylene, the experimental evidence shows that this is a case where the rate-determining step is the adsorption of ethylene on the catalyst surface, the actual polymerization proceeding rather fast. As Laidler³ has pointed out, the tacit assumption in discussing surface catalysis that adsorption equilibrium is in fact established is rarely supported by evidence. In this instance, at least, the experimental evidence is all against this assumption.

HEAT AND ENTROPY OF FUSION AND CRYOSCOPIC CONSTANT OF SILVER NITRATE

BY GEORGE J. JANZ, DAVID W. JAMES AND JEROME GOODKIN

Department of Chemistry, Rensselaer Polytechnic Institute, Troy, N. Y.

Received January 21, 1960

Cryoscopy in silver nitrate solvent has been studied by a number of workers both from the aspect

of a qualitative test of species present¹ and a quantitative test of the solvent-solute interactions and behavior.² For quantitative evaluation of behavior in the dilute region (concentration $< 10^{-2} m$) it is essential to know the heat of fusion accurately from a direct measurement. Two calorimetrically measured values for the heat of fusion of silver nitrate are known. Goodwin and Kalmus³ obtained the value 2580 cal. mole⁻¹ while Magnus and Oppenheimer⁴ obtained a value of 2757 cal. mole⁻¹. In 1936, Kelley¹ published a mean value of 2550 cal. mole⁻¹ based on an assessment of the available cryoscopic data at that time. Attention is also drawn by Kelley⁵ to a value of 2755 cal. mole⁻¹ empirically derived from a formula quoted by Juptner.⁶ The present communication reports the results of a redetermination of the heat of fusion for silver nitrate by the method of drop calorimetry.

Experimental

Calorimeter and Accessories.—The calorimetric assembly designed to yield results with an accuracy of $\pm 2\%$ for heats of fusion in the range 2–4 kcal./mole, and the recording differential potentiometer for the temperature-time measurements were the same as described elsewhere in detail.^{7,8}

Silver Nitrate.—Finely powdered silver nitrate (reagent grade) was vacuum dried for several days under a stream of dry nitrogen with progressive elevation of the temperature to a point just below the fusion point of the salt. This maximum of temperature was maintained for 24 hr., after which the sample was cooled under a stream of dry gas and stored in a sealed container protected from the light. The appearance of the $AgNO_3$ was important after this drying technique. If the drying is not complete the traces of water will react with the salt to give nitric acid and silver oxide at the elevated temperatures. The silver oxide will cause discoloration of the salt and very small traces of oxide can be visually distinguished. If thermal decomposition of the salt takes place traces of silver or silver oxide will be deposited depending on the decomposition process. These deposits will also be visible in trace amounts. The appearance of the salt thus indicated both dryness and whether or not decomposition had taken place. It was found that fusion points of the best selected samples were sharp and deviated by less than 0.1° from the fusion temperature of 209.6° .

Results

The procedures for calibration of the calorimeter and measurement of the heat of fusion have been described in the earlier papers.^{7,8} Table I summarizes the data and results for a series of eleven determinations of the enthalpy change between 430 and $590^\circ K.$ below and above the melting point. The analysis of the data is similar to that followed for previous calculations.⁹ Since there was a scatter of experimental points, particularly above the melting point, 95% confidence limits were adopted and a least squares analysis was made. From the graph so obtained of enthalpy change *vs.* initial temperature of the sample the heat of fusion of

(1) E. Kordes, W. Bergmann and W. Vogel, *Z. Elektrochem.*, **55**, 600 (1951).

(2) Y. Doucet, J. A. LeDuc and G. Pannetier, *Compt. rend.*, **236**, 1018 (1953).

(3) H. M. Goodwin and H. T. Kalmus, *Phys. Rev.*, **28**, 1 (1909).

(4) A. Magnus and F. Oppenheimer, *Z. anorg. allgem. Chem.*, **168**, 305 (1928).

(5) K. K. Kelley, *Bull. U. S. Bur. Mines*, No. 371, Washington, 1936.

(6) H. Juptner, *Stahl u. Eisen*, **18**, 1039 (1898).

(7) J. Goodkin, C. Solomons and G. J. Janz, *Rev. Sci. Instr.*, **29**, 105 (1958).

(8) C. Solomons and G. J. Janz, *Anal. Chem.*, **31**, 623 (1959).

(9) C. Solomons, J. Goodkin, H. J. Gardner and G. J. Janz, *This Journal*, **62**, 243 (1958).

silver nitrate at its melting point was found to be 2960 ± 60 cal./mole.

Discussion

The values for the heat of fusion of silver nitrate reported from 1898 onward are summarized in Table II, together with the value from the present investigation. In view of the markedly higher value gained from the present calorimetric measurements, an evaluation of the factors possibly contributing to the differences in the previously determined values is of interest.

TABLE I

ENTHALPY OF SILVER NITRATE AT VARIOUS TEMPERATURES (T_1) RELATIVE TO STANDARD TEMPERATURE (300°K .)

Sample	Initial temp., T_1 , $^\circ\text{K}$.	Final temp., $^\circ\text{K}$.	Calorimeter temp. change	Cal. evolved by 1 mole AgNO_3	Corrn. to 298.15°K .	$H_T - H_{298.15}$, cal./mole
	587.2	302.3	4.83	10945.61	41.22	11036.83
	547.7	301.3	3.43	9316.53	68.98	9385.51
	517.3	301.3	3.36	9245.78	68.98	9314.76
	503.3	303.0	2.90	7916.64	106.79	8023.43
	500.2	305.8	2.89	7913.53	168.99	8082.55
	491.5	304.1	2.82	7733.45	131.25	7864.70
	483.2	300.2	1.99	5221.68	44.52	5266.40
	479.4	300.9	1.74	4479.91	60.09	4540.00
	460.2	300.6	1.59	4110.81	53.41	4164.22
	450.2	301.8	1.52	3939.52	80.10	4029.62
	438.4	300.1	1.44	3752.74	42.29	3795.03

Wt. of AgNO_3 sample, g. 30.0256
 Wt. of Pt crucible, g. 16.0315
 Heat equiv. of calorimeter 1st expt. 441.07 cal./deg.; remaining expt. 539.10 cal./deg.

TABLE II

VALUES FOR HEAT OF FUSION FOR AgNO_3

Investigator	Method	ΔH_f° , cal./mole	Ref.
H. Juptner (1898)	Estimated	2755	6
H. Goodwin and H. Kalmus (1909)	Calorimetry	2580	3
A. Magnus and F. Oppenheimer (1928)	Calorimetry	2757	4
K. Kelley (1936)	2550	5
Present investigation (1959)	Calorimetry	2960	

It has been realized only recently how difficult it is to remove all traces of water from a crystalline salt; in the present investigation a rigid vacuum-elevated temperature technique was employed as the most efficient drying method. Magnus and Oppenheimer⁴ used an isothermal calorimetric method in which the sample was open to the air at all times. The presence of water thus possible in their samples would contribute to a lower value for ΔH_f . In the work of Goodwin and Kalmus,³ in addition to this factor, a heat loss owing to chimney convection in the design of drop calorimeter used is seen possible and would contribute to the low result. The melting point for AgNO_3 is reported as 219° by Goodwin and Kalmus³ (cf. 209.6°) and this may indicate that all temperatures in this work were incorrect.

The value attributed to Juptner⁶ was obtained not by direct measurement but is a value calculated by use of the empirical relation

$$\Delta H = 0.00167K \left(1 + \frac{2}{\sqrt{\rho}} \right)$$

where K is the modulus of elasticity and ρ is the density of the salt. No information relative to the temperature at which the modulus or density were measured is given. The agreement of this estimated value with other results must be regarded as fortuitous. Further tests of this expression to evaluate its applicability would seem of interest.

The value by Kelley⁵ is based on seven sets of cryoscopic data varying from 2,300 to 2,800 cal. mole⁻¹. Assumptions relative to the thermodynamic ideality of the solutions and the dissociation processes for the solutes are implicit in the calculations of the heats of fusion from the above cryoscopic results. For theoretical discussions of cryoscopic behavior of solutes in silver nitrate a value of the heat of fusion (and thus the cryoscopic constant) independently derived by a different experimental technique is almost essential.

The values for the heat of fusion (2960 cal./mole) entropy of fusion (6.74 e.u./mole) and cryoscopic constant (26.47 deg./mole/1000 g.) derived from the present calorimetric measurements are recommended for practical and theoretical calculations.

Acknowledgment.—This work was made possible in part by support received from U. S. Air Force, Air Research and Development Command, Office of Scientific Research. Active participation in the earlier phases of this study and continued interest by Dr. Cyril Solomons is gratefully acknowledged.

THE PREPARATION OF SINGLE CRYSTALS OF CERTAIN TRANSITION METAL FLUORIDES

BY H. GUGGENHEIM

Bell Telephone Laboratories, Incorporated, Murray Hill, New Jersey
 Received January 22, 1960

Single crystal NiF_2 was grown from the melt using a modification of Stockbarger's¹ method. NiF_2 is reported² to have a vapor pressure of one atmosphere at about 1000° and a melting point over 1300° . For these reasons it is impractical to grow it from the melt using conventional methods, but a sealed platinum container has been found to overcome the difficulties. Dry NiF_2 was prepared by passing HF over "low cobalt" NiCl at 850° for 16 hours. The resulting material was a light greenish-yellow. The Pt-10% Rh alloy tube was used. To facilitate pinching off of the tube, a smaller Pt tube was welded to the larger tube after charging with NiF_2 . To prevent moisture and oxygen contamination, the tube was heated to 250° while connected to a vacuum line. The vacuum was broken with argon and then the small tube was pinched off near the top with barrel jaw pliers. The pinched end was welded with a gas flame and the tube was placed inside an alumina tube attached to a clock motor by a sprocket chain. The tube was lowered through a hot zone (1420°) at 0.075" per hour. After 100 hours the tube was removed at room temperature and opened by cutting along the length with a circular diamond saw. The NiF_2 boule was emerald green, weighing 56 g., and was 2

(1) D. C. Stockbarger, *Rev. Sci. Instr.*, **10**, 205 (1939).

(2) C. Poulenc, *Ann. Chem. Phys.*, **2**, 41 (1894).

inches long and $3/4$ inch in diameter. Although there were many cracks, there were clear areas as large as a $1/2$ inch cube which were shown to be single crystal. The Pt tube was easily repaired for reuse. The cracking might best be minimized or eliminated by slowly cooling the boule in a uniform temperature zone after the last part has crystallized in the temperature gradient.

The growth of mixed fluorides in a hydrothermal bomb has been illustrated by the preparation in a sealed vessel of Cu compounds which normally dissociate or form oxides in air. K. Knox³ has grown crystals of KCuF_3 and K_2CuF_4 from the melt. These crystals were very small and the KCuF_3 invariably twinned. By analogy with the KF-NiF_2 ⁴ and KF-MgF_2 ⁵ systems, it is expected that KCuF_3 and K_2CuF_4 will exist in the KF-CuF_2 system, the former congruently and the latter incongruently melting. An additional factor in the Cu system is the fact that copper(II) fluoride,⁶ and presumably potassium-copper-fluorides, have an appreciable dissociation pressure of fluorine at the melting point, so that in an open system loss of fluorine and reduction of the copper occur. The copper system should be several hundred degrees lower than the KF-NiF_2 and KF-MgF_2 systems. Because of oxide formation and the dissociation problem, the system was investigated in a sealed vessel. KHF_2 was used instead of KF because it is less hygroscopic, and has a melting point much below the dissociation temperature of CuF_2 . The melting point of KHF_2 is 195° , at which temperature it begins to liberate HF . Because of the build up of pressure when heating over 200° , a steel bomb⁷ with a platinum liner was used. This autoclave was designed for hydrothermal experimentation and was constructed to withstand pressures up to about 7000 p.s.i. A corrosion resistant steel was used which can be heated to 600° without creep. Reagent grade $\text{CuF}_2 \cdot 2\text{H}_2\text{O}$ was dried in dry HF at 400° . Above this temperature decomposition takes place. A typical run was made as follows: The bomb, which has a capacity of 30 ml., was charged with 30 g. of liquid KHF_2 prepared by heating the powder in a platinum crucible. After solidification, 10 g. of dry CuF_2 was added. A 0.005 inch thick platinum disc was placed over the top of the liner and the steel plunger was forced down on the disc by tightening the head in a vise. The bomb was heated in a muffle furnace to 500° for 16 hours. The temperature then was lowered at a rate of 3° per hour to 200° , at which temperature the bomb was removed from the furnace. This mixture of 20 mole % CuF_2 and 80 mole % KHF_2 yielded single crystal plates of KCuF_3 , about 0.5 cm^2 . They could be separated by dissolving the KF matrix in warm H_2O which had no effect on the KCuF_3 . Single crystal plates of K_2CuF_4 were grown using the same procedure but changing the mole ratio to 13% CuF_2 and 87% KHF_2 . These crystals were the same size and habit as the KCuF_3 crystals. In this case, the flux could not be removed with H_2O be-

cause the K_2CuF_4 hydrolyzed as evidenced by a change in color from clear colorless to opaque blue; however, the crystals could be separated mechanically without difficulty. The crystals were shown to be KCuF_3 and K_2CuF_4 , respectively, by X-ray powder and single crystal pictures.

Finally, single crystals of MnF_2 , ZnF_2 and KMnF_3 have been grown by zone melting in an inert atmosphere. A significant reduction in the impurity content of the crystals, as well as quantitative impurity doping of the crystal, were accomplished by this method.

The author is indebted to K. Knox for helpful discussions on KCuF_3 and K_2CuF_4 and J. W. Nielsen and E. Dearborn for useful discussions on the Stockbarger technique.

THE ASSOCIATION EQUILIBRIUM IN THE METHYL BROMIDE-ALUMINUM BROMIDE SYSTEM. ESTIMATED BONDING STRENGTHS OF ALUMINUM BROMIDE-ADDITION MOLECULES WITH METHYL BROMIDE, PENTENE AND BENZENE

By D. G. WALKER

Research and Development Division, Humble Oil & Refining Company, Baytown, Texas

Received January 25, 1960

Brown and Wallace¹ have reported an excellent and thoroughgoing study of the addition compounds of aluminum halides with alkyl halides. They obtained experimental vapor pressure-composition data for the system methyl bromide-aluminum bromide at -80 , -64.4 , -45.8 , -31.3 and 0° and concluded that the aluminum bromide in solution was present in the form of an additional molecule $\text{CH}_3\text{Br}:\text{AlBr}_3$.

A redetermination of the vapor pressure-composition curve for methyl bromide-aluminum bromide at 0° was made in the course of some other work. In the homogeneous liquid phase, excellent agreement was found with the results of Brown and Wallace. Also, in agreement with their results, the appearance of a solid phase was found to occur at a $\text{CH}_3\text{Br}:\text{AlBr}_3$ liquid-phase ratio of 1.19 and at a system pressure of 235 mm. However, a well-defined pressure plateau was obtained between $\text{CH}_3\text{Br}:\text{AlBr}_3$ ratios of 1.19 to zero whereas Brown and Wallace found no such pressure plateau in this region corresponding to compound formation in the solid phase. They concluded that solid solution phenomena must be present. Possibly they did not allow adequate time for the system to equilibrate between withdrawals of methyl bromide. It seemed that if aluminum bromide was the solid precipitate, the system might be simple enough that considerable information of interest could be gained by a further study.

Results and Discussion

In Fig. 1 is plotted the system vapor pressure versus composition obtained experimentally at 0° . If one assumes that only the addition mole-

(3) K. Knox, *J. Chem. Phys.*, **30**, 991 (1959).

(4) G. Wagner and D. Balz, *Z. Elektrochem.*, **56**, 576 (1952).

(5) R. C. DeVries and R. Roy, *J. Am. Chem. Soc.*, **75**, 2481 (1953).

(6) H. v. Wartenberg, *Z. anorg. Chem.*, **241**, 381 (1939).

(7) G. W. Morey, *Am. Min.*, **22**, 1121 (1957).

(1) H. C. Brown and W. J. Wallace, *This Journal*, **76**, 6279 (1953).

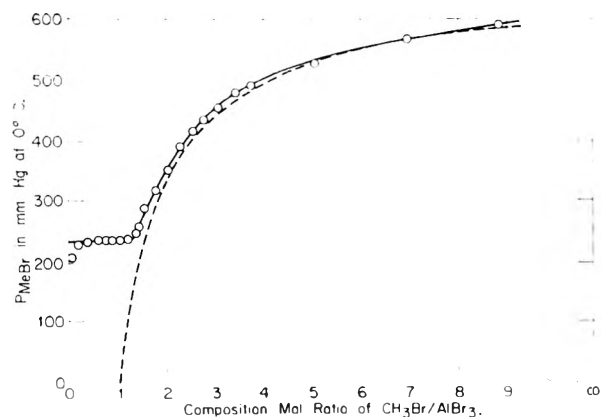


Fig. 1.—Vapor pressure of the methyl bromide-aluminum bromide system at 0°. $P_{\text{CH}_3\text{Br}}$ at 0° = 659.5 mm. Experimental: —, theoretical assuming: (a) only CH_3Br and $\text{CH}_3\text{Br}:\text{AlBr}_3$ (non-volatile) are present; (b) Raoult's law is obeyed. —, Theoretical assuming: (a) equilibrium $K = \frac{(\text{Al}_2\text{Br}_6)^{1/2}(\text{CH}_3\text{Br})}{[\text{CH}_3\text{Br}:\text{AlBr}_3]} = 0.216$; (b) Al_2Br_6 solubility = 0.073 mole fraction; (c) Raoult's law.

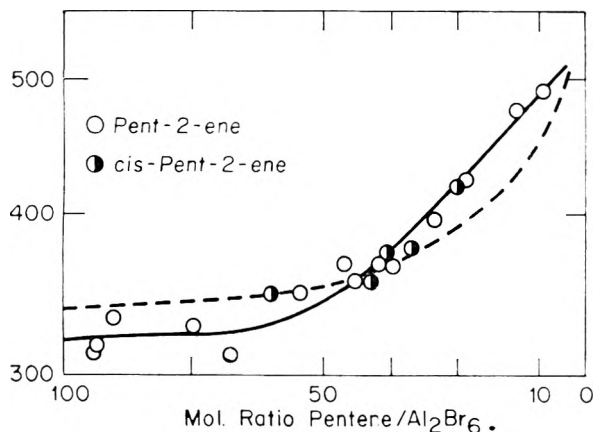


Fig. 2.—Molecular weight of aluminum bromide in olefin solution (experimental work of Fairbrother and Field⁶). Calculated assuming: (1) only the equilibrium olefin- $\text{AlBr}_3 \rightleftharpoons \frac{1}{2}\text{Al}_2\text{Br}_6 + \text{olefin}$ exists; (2) $K_{\text{equil}} = 3$ at 0°.

cule, $\text{CH}_3\text{Br}:\text{AlBr}_3$, and CH_3Br exist in the liquid phase, that only CH_3Br has an appreciable volatility and that Raoult's law is obeyed, a vapor pressure curve corresponding to the dotted line in Fig. 1 is predicted. As may be seen, the calculated line is in very good agreement with experiment for dilute solutions of $\text{CH}_3\text{Br}:\text{AlBr}_3$ in CH_3Br and falls surprisingly close to the experimental values even in more concentrated solutions. The pressure plateau, which exists between $\text{CH}_3\text{Br}:\text{AlBr}_3$ ratios of 1.19 to zero, shows that solid aluminum bromide first precipitates at a composition ratio of 1.19 and correspondingly an invariant liquid phase of $\text{CH}_3\text{Br}:\text{AlBr}_3$, CH_3Br and Al_2Br_6 exist in equilibrium with solid Al_2Br_6 . These data may be used to calculate an equilibrium constant at this temperature (Fig. 1).

Al_2Br_6 and CH_3Br have identical solubility parameters ($\delta = 9.3$) and would be expected to form an ideal solution. The fact that the addition molecule $\text{CH}_3\text{Br}:\text{AlBr}_3$ (δ unknown) forms nearly ideal solutions with methyl bromide (see Fig. 1) is extremely interesting. This addition molecule must

have very nearly the same intermolecular attraction in the liquid phase as the two parent species and by no means should be thought of as an ionic or even a very polar compound.

Data on the vapor pressure-composition of methyl bromide-aluminum bromide mixtures similar to that of Fig. 1 were obtained at three other temperatures. The composition at which Al_2Br_6 was observed to precipitate as well as the plateau pressure of the invariant liquid region was used to calculate an equilibrium constant for (1) at each experimental temperature (Table I).

$$K = \frac{(\text{CH}_3\text{Br})(\text{Al}_2\text{Br}_6)^{1/2}}{(\text{CH}_3\text{Br}:\text{AlBr}_3)} \quad (1)$$

In Table II the calculated composition at four temperatures of the invariant liquid phase, saturated with Al_2Br_6 , is given. The corresponding ideal solubility of Al_2Br_6 as calculated from

$$\log X_{\text{Al}_2\text{Br}_6} = \frac{\Delta H_{\text{fusion}}}{2.3(R)} \left(\frac{1}{T} - \frac{1}{T_{\text{m.p.}}} \right) = 1180 \left(\frac{1}{T} - 2.7012 \times 10^{-3} \right)$$

is shown in the last column of Table II. The general agreement of this value with that found from the calculated equilibrium constants for (1) is an independent confirmation of the fact that the three molecular species of (1) must form a nearly ideal solution.

TABLE I
EXPERIMENTAL DATA ON CH_3Br -ALUMINUM BROMIDE MIXTURES EQUILIBRIUM CONSTANT AS A FUNCTION OF TEMPERATURE

T, °C.	Vapor pressure CH_3Br , mm.	Compn. $\text{CH}_3\text{Br}:\text{AlBr}_3^a$	Exptl. plateau pressure, mm.	Calcd. K for eq. 1
5.3	804	1.08	280	0.256
0	659.5	1.19	235	.216
-8.1	505	1.30	170	.137
-23.9	233	1.30	67	.076

^a At which Al_2Br_6 precipitates.

TABLE II

T, °C.	COMPOSITION IN LIQUID PHASE			Ideal $N(\text{Al}_2\text{Br}_6)$
	$N(\text{CH}_3\text{Br}:\text{AlBr}_3)$	$N(\text{CH}_3\text{Br})$	$N(\text{Al}_2\text{Br}_6)$	
5.3	0.510	0.348	0.141	0.089
0	.538	.356	.106	.073
-8.1	.602	.337	.060	.054
23.8	.678	.288	.033	.028

The slope of the usual type plot of the logarithm of K (from Table I) vs. $1/T$ gives a value of 5.69 kcal./mole for the heat of reaction of (1), and an entropy of reaction of +17.7 e.u. Thus in the liquid phase

$$K = \frac{(\text{CH}_3\text{Br})(\text{Al}_2\text{Br}_6)^{1/2}}{(\text{CH}_3\text{Br}:\text{AlBr}_3)} = e^{17.71R} e^{5.690/RT} \quad (2)$$

Fischer and Rahlfs² found in the gas phase

$$K = \frac{(\text{AlBr}_3)^2}{(\text{Al}_2\text{Br}_6)} = e^{39.41R} e^{26.560/RT} \quad (3)$$

By neglecting any heat of solution of monomeric AlBr_3 in the liquid phase of (2), equations 2 and 3 can be combined to yield

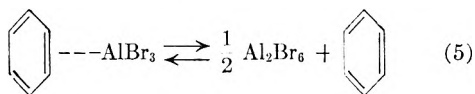
(2) W. Fischer and O. Rahlfs, *Z. anorg. allgem. Chem.*, **205**, 37 (1932).

$$K = \frac{(\text{CH}_3\text{Br})(\text{AlBr}_3)}{\text{CH}_3\text{Br}:\text{AlBr}_3} = e^{37.4/R} e^{19,950/RT} \text{ (liquid phase)} \quad (4)$$

The bonding strength of $\text{CH}_3\text{Br}:\text{AlBr}_3$ is then $\cong 19$ kcal.

Other aluminum bromide solutions may be interpreted in a similar manner.

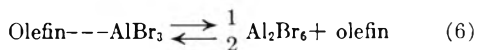
Nespital³ by the use of dipole measurements found that an addition molecule, --- AlBr_3 , existed in small concentration in benzene solutions of aluminum bromide. Ulrich,⁴ by cryoscopic measurements in very dilute solutions of aluminum bromide in benzene, obtained results consistent with the conclusions of Nespital. Both of these studies are consistent with the equilibrium



for which $K = 700 @ 20^\circ$. This, combined with an estimated (Sackur-Tetrode equation) $\Delta S = +17.9$ e.u., yields an estimated bond strength of

the addition compound --- AlBr_3 of 14.6 kcal.

The vapor pressure measurements of Fairbrother and Field⁵ on solutions of aluminum bromide in *cis*-pent-2-ene at 0° also can be interpreted as due to the existence of an addition molecule between an olefin and AlBr_3 in equilibrium with Al_2Br_6 and free olefin. In Fig. 2 are plotted the apparent molecular weights of aluminum bromide in pentene solution as were experimentally determined by Fairbrother and Field. The dotted line represents calculated values of this same molecular weight function assuming that equilibrium (6) exists in the liquid phase



and has a value of 3.0 at 0° . Again combining an estimated $\Delta S = +17.5$ kcal. with this value for the $K_{\text{equilibrium}}$, a bond strength of 17.5 kcal. is estimated for the pentene- AlBr_3 molecule.

Experimental

Apparatus.—All of the experiments were carried out with high vacuum apparatus and techniques in which the materials came in contact only with glass and mercury.

Procedure.—A weighed amount of synthesized aluminum bromide was re-sublimed several times into a glass vessel under dry nitrogen. The vessel was attached to the vacuum system and evacuated. A measured amount of methyl bromide was condensed on the aluminum bromide and the vessel was agitated until solution was complete. Temperature control was by the use of appropriate slush baths. Pressure was read from a mercury manometer. The composition was varied by allowing fractional portions of the vapor to transfer to the vacuum system. Compositions reported as " $\text{CH}_3\text{Br}/\text{AlBr}_3$ ratio" were corrected for the presence of CH_3Br in the vapor space above the system.

The vapor pressure of the methyl bromide recovered after a given experiment was identical to that recorded before the experiment. The volume of gas recovered also was very nearly identical to that charged.

(3) W. Nespital, *Z. physik. Chem.*, **B16**, 153 (1932).

(4) H. Ulrich, *ibid.*, **B15**, 427 (1931).

(5) F. Fairbrother and K. Field, *J. Chem. Soc.*, 2614 (1956).

THE GROWTH OF BARIUM TITANATE SINGLE CRYSTALS FROM MOLTEN BARIUM FLUORIDE

BY R. C. LINARES

Bell Telephone Laboratories, Inc., Murray Hill, New Jersey

Received January 26, 1960

Single crystals of barium titanate have been of interest for ferroelectric studies. Most of these crystals have been grown from molten salts, and at moderate temperatures (1000 – 1250°), because BaTiO_3 undergoes a change from the cubic to hexagonal form at 1460° .¹ Some of the solvents successfully used include: BaCl_2 ,² KF ,³ PbF_2 ,⁴ PbO^4 and Na_2CO_3 .⁵ Of these, the KF process has been the most widely used; however, potassium from the solvent and platinum from the crucible enter the crystals as impurities. The purpose of this paper is to report the solubility of BaTiO_3 in BaF_2 and point out that BaTiO_3 crystals can be grown from BaF_2 solutions. Although this method has some drawbacks, which will be discussed, crystals can be grown free of potassium and platinum.

Solubility Curve.—An approximate phase diagram for the system BaF_2 – BaTiO_3 was determined by a simple quenched melt technique. A charge of barium titanate and barium fluoride was heated in an electric furnace for four hours at a temperature 20° above the desired temperature. At the end of the time the temperature was dropped 20° and held for another two hours. Next the temperature close to the crucible was determined with a Pt–Pt 10% Rh thermocouple probe, the crucible was removed from the furnace, and the melt was poured off and quenched in a platinum crucible. Only those runs in which there was an excess of barium titanate in the crucible at the time of pouring were used for the solubility determination.

The eutectic mixture was made by heating a mixture of 30 g. of BaTiO_3 and 60 g. of BaF_2 to 1350° and cooling slowly to 1200° . The BaTiO_3 crystals were removed mechanically leaving the eutectic mixture and the melting point of this mixture was determined in a platinum wound micro furnace. The average of seven readings was taken as the melting point and was found to be 1260° with the maximum deviation being $\pm 4^\circ$.

The composition of the melts was determined by analysis for barium and titanium by an X-ray fluorescence technique.⁶ The results are considered to be correct to within 1%. The molar composition was calculated on the assumption that barium and titanium were present only as BaF_2 and BaTiO_3 . Although X-ray pictures show only these two phases present in low temperature runs, long runs (24 hr.) at high temperatures (1420°) show a small amount of an unidentified third phase. Also if the weight per cent. of barium titanate and barium fluoride in these samples is calculated, these total slightly more than 100% indicating the possible presence of another phase. It is possible that this phase is a barium platinum oxide formed by slow decomposition of BaF_2 to BaO which would attack the platinum crucible.

The proposed phase diagram for the system BaF_2 – BaTiO_3 is given in Fig. 1. This shows the solubility of BaTiO_3 to range from 16.5 mole % at the eutectic point of 1260° to 49.2 mole % at 1393° . The accuracy of the curve has been confirmed by observations made during crystal growth by pulling. When using a melt of a given composition, crystallization began very near the temperature predicted by the solubility curve as drawn.

The vapor pressure of BaF_2 is quite low even at elevated

(1) Phase Diagrams for Ceramists, 1956, p. 42.

(2) Blattner, Matthias, Merz and Scherrer, *Helv. Chim. Acta*, **20**, 225 (1947); *Experientia*, **3**, 4 (1947).

(3) J. P. Remoika, *J. Am. Chem. Soc.*, **76**, 940 (1954).

(4) J. W. Nielsen, personal communication.

(5) Shozo Sawada, Choichiro Nomura and Shin'ichi Fujii, *Rept. Inst. Sci. Technol., Univ. Tokyo*, **5**, 7 (1951).

(6) T. C. Loomis, unpublished work.

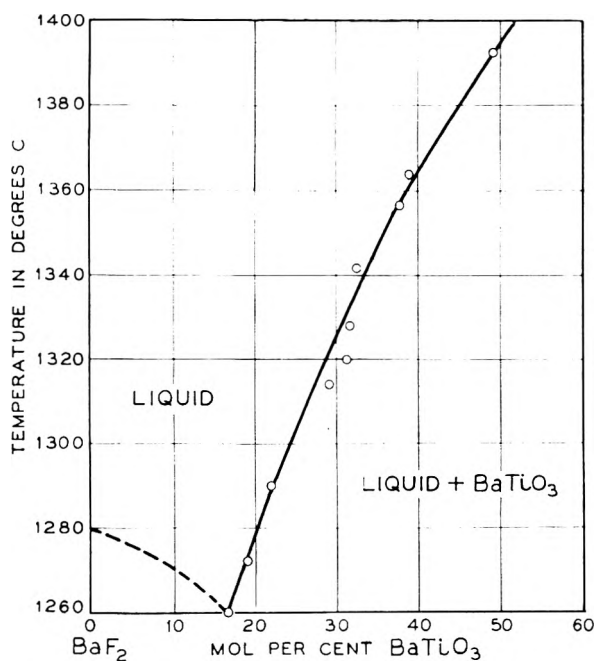


Fig. 1.

temperatures which makes it desirable as a solvent. The attack on the platinum crucible is only slight⁷ but any contamination of the BaF₂-BaTiO₃ melt with silicates causes rapid attack on the crucible and eventual failure.

Growth of Crystals. Butterfly Twins.—A typical crystal growth run was made by heating a mixture of 50 g. of BaTiO₃ and 50 g. of BaF₂ at 1350° for 4 hours in a Pt crucible. At the end of this time, a crucible containing 5 g. of BaTiO₃ was placed in the furnace and allowed to reach furnace temperature (about 10 minutes). Then the molten solution was poured onto the BaTiO₃ powder and the growth cycle was begun. The growth cycle consisted of holding the temperature constant from 0 to 2.5 hours, followed by cooling at rates from 1 to 25° per hour. At the end of the cooling cycle (1270 to 1300°) the crucible was removed from the furnace and the melt was poured off. In the bottom of the crucible were the dark blue barium titanate butterfly twins and cubes.

Discussion of Twin Growth.—The barium titanate crystallized from barium fluoride melts is dark blue to black in color. This is due to an oxygen deficiency in the crystal like that of BaTiO₃ grown from KF in a nitrogen atmosphere.⁸ Attempts were made to grow clear twins from barium fluoride by growing in an oxygen atmosphere. The crystals appeared no lighter in color, indicating that the oxygen pressure of the transparent crystals at these temperatures may be greater than one atmosphere. These crystals and others were heated in an oxygen atmosphere for 4 days at 1000° with no indication of losing their dark color. However, by raising the temperature to 1050–1100° some lightening in color did occur after a week of oxidation. Dark blue crystals grown from KF oxidize more rapidly under those same conditions. This would indicate that the oxygen defect concentration in the barium fluoride grown crystals is considerably greater than the defect concentration in potassium fluoride grown crystals.

Growth on Seeds.—While barium fluoride is an excellent solvent for barium titanate, it is very difficult to remove from the crystals and from the crucible. For this reason it was decided to explore the possibility of pulling the BaTiO₃ from a BaF₂ melt while slowly cooling the melt. It was also thought that the method itself should be explored to determine its usefulness in other systems.

A crystal was grown by first preparing a saturated BaTiO₃-BaF₂ solution at about 1360° in a platinum crucible. Then a seed was lowered to, and rotated on the surface of the melt,

and cooling was begun of 2.5 degrees per hour; at 1275–1300° the grown crystal was withdrawn from the melt, and allowed to cool slowly to room temperature. Crystals up to 7.5 g. have been grown in this manner.

Both butterfly twins and cubes were used as seed material in these runs. No appreciable difference could be found in the growth behavior between the two type seeds; however, the orientation of the seed was very important. The crystal has a great tendency to grow as a cube or a rectangular parallelepiped; thus the (111) and (110) faces cap out rapidly leaving the crystal bounded by (100) faces. A crystal grown from the (110) face capped out quickly in that direction and then grew in steps as a pile of cubes. Crystals grown from the (100) face were more regular, and although they grew slightly stepped on the side they were sound internally.

Despite the slow growth rate there was a great tendency for the crystals to twin. For this reason the crystal could not actually be pulled during growth; the slowest practical pulling rate was faster than the rate of deposition at the desirable cooling rate.

Conclusions

Barium titanate butterfly twins and cubes can be grown from molten BaF₂. BaTiO₃ single crystals can be grown on a rotating seed by slowly cooling moderately concentrated solutions of BaTiO₃ in BaF₂. This method of growing a crystal allows the crystal to be removed from the melt when the growth is completed and allows one large crystal rather than many small ones to be grown from a melt. This procedure should also prove useful in other systems where the solvent is difficult to remove from the crystals. The solubility of the material need not be high provided that the slope of the solubility curve is such that a reasonable amount of material can be deposited during the cooling cycle and that the transport can be accurately controlled.

Acknowledgments.—The author wishes to thank J. W. Nielsen for his helpful discussions and suggestions on this work. Thanks are also due to W. Hartmann and T. C. Loomis for their excellent chemical analysis and to Miss A. D. Mills for X-ray identification of melt phases.

THE FLUORESCENCE OF ACETALDEHYDE VAPOR¹

By E. MURAD²

Department of Chemistry, University of Rochester, Rochester, N. Y.
Received January 27, 1960

Previous work on the fluorescence of acetaldehyde has been cursory and limited to visual observation of the fluorescence.^{3,4} This visible emission has been attributed by Matheson and Zabor⁵ to the sensitized emission of biacetyl, which is a product of the photochemical decomposition of acetaldehyde vapor.

(1) This work was supported in part by the United States Air Force through the Air Force Office of Scientific Research of the Air Research and Development Command, under Contract No. AF 18(600) 1528. Reproduction in whole or in part is permitted for any purpose by the United States Government.

(2) Department of Chemistry, University of Wisconsin, Madison 6, Wis.

(3) P. A. Leighton and F. E. Blacet, *J. Am. Chem. Soc.*, **55**, 1766 (1933).

(4) G. K. Rollefson and D. C. Grahame, *J. Chem. Phys.*, **7**, 775 (1939).

(5) M. S. Matheson and J. W. Zabor, *ibid.*, **7**, 536 (1939).

(7) Analysis of three separate samples of crystals showed less than 0.005% platinum.

(8) J. W. Nielsen, to be published.

Experimental

Reagents. Acetaldehyde.—Eastman grade acetaldehyde was purified by bulb to bulb distillation on the vacuum line, a middle fraction being used. Analysis on the mass spectrometer showed the absence of any impurities, and, in particular, the absence of biacetyl.

Biacetyl.—Eastman grade biacetyl was dried over Anhydron for three hours; a middle third then was taken after distillation. Analysis by vapor phase chromatography (Perkin-Elmer Model 154) showed that the impurities were not more than 1%.

Oxygen.—Research grade oxygen in a one-liter bulb was obtained from Air Reduction Co.

Propane.—C.P. grade propane from the Matheson Co. was purified by bulb to bulb distillation and a middle third was used.

Apparatus.—The apparatus for the photoelectric study of the fluorescence and the vacuum line were similar to those described by Hecklen.⁶

Photographs of the fluorescence spectrum were taken with a Hilger quartz spectrograph, Model E-484, which was kindly loaned to the author by Professor A. B. F. Duncan. Kodak plates No. 103a-B were used to photograph the emission spectrum of acetaldehyde-biacetyl mixtures. Kodak plates No. 103a-0 were used to photograph the emission spectrum of pure acetaldehyde. No filters were introduced between the fluorescence window and the spectrograph. The scattered 3130 Å. line was used as a reference line in assigning a wave length scale to the emission.

The flow system was similar to that used by Luckey, *et al.*⁷ The temperatures of the two bulbs in this flow system were 0 and -10°.

The light source was a medium pressure mercury lamp (British Thomson-Houston 250 watt ME/D 3-pin lamp) which was operated on direct current. Various wave lengths were isolated with a Bausch and Lomb grating monochromator.⁸

Results

Fluorescence Spectrum.—The fluorescence spectrum of acetaldehyde extends from 3515 to about 4700 Å. It consists of a broad diffuse emission with bands superimposed on it, and has a maximum at about 4000 Å. The resolution was such that measurement of the fine structure of the emission was not possible. A microphotometer tracing showed peaks at 3565, 3640 and 3783 Å. A banded emission with band heads at 5100, 5600 and 6000 Å. was present in static runs but almost absent in flow runs. This banded system is attributed to biacetyl.⁸ This observation confirms the conclusion of Matheson and Zabor⁶ that the strong visible fluorescence which has been reported for acetaldehyde is due to biacetyl. Upon addition of small amounts of biacetyl, the bands at 5100, 5600 and 6000 Å. became very pronounced. The addition of oxygen to acetaldehyde did not affect the acetaldehyde spectrum, while the bands due to biacetyl were completely removed. This observation is due either to the removal of triplet biacetyl emission by oxygen⁶ or to the reaction of acetyl radicals with oxygen.

It should be pointed out that the short wave length fluorescence limit at 3515 Å. is very close to the long wave length absorption limit which had been reported to be at 3483 Å.^{3,9,10}

(6) J. Hecklen, *J. Am. Chem. Soc.*, **81**, 3853 (1959).

(7) G. W. Luckey, A. B. F. Duncan and W. A. Noyes, Jr., *J. Chem. Phys.*, **16**, 407 (1948).

(8) G. M. Almy, H. Q. Fuller and G. D. Kinzer, *ibid.*, **8**, 37 (1940).

(9) S. A. Schou, *J. chim. phys.*, **26**, 27 (1929).

(10) V. R. Rao and I. A. Rao, *Indian J. Phys.*, **28**, 489 (1954).

These authors found absorption to begin at 3485 Å., but concluded that the O-O band is at 3204.1 Å.

Fluorescence Efficiencies.—Before considering the variation of fluorescence efficiency with various parameters, a remark is in order. It has been pointed out by Noyes and Henriques^{11,12} and more recently by Stevens¹³ that the geometry of the cell may give rise to false trends when the absorption is high. Noyes and Henriques suggested a method of correcting this apparent trend. Their method was, however, tedious and the results obtained in the present investigation were not precise enough to warrant their use. A simpler correction was made by correcting the apparent values of Q (the fluorescence efficiency) to a standard per cent. absorption in the vicinity of the fluorescence window by the use of Beer's law. The apparent values of Q were obtained as

$$Q = \frac{F - F_0}{I_1 - I_2}$$

where F is the fluorescence reading with the cell full, F_0 the fluorescence reading with the cell empty, I_1 the intensity of the light transmitted through the cell when it is empty, and I_2 the intensity of the light transmitted through the cell when it is full. The values of Q thus obtained are in arbitrary units; they are proportional to the actual quantum yields of fluorescence.

Fluorescence at 3340 Å.—The fluorescence at 3340 Å. was studied at two temperatures, 26 and 52°. A plot of $1/Q$ vs. pressure is shown in Fig. 1. Within experimental error Q is independent of temperature. The addition of oxygen did not affect Q .

Fluorescence at 3130 Å.—The variation of Q (both corrected and uncorrected) with pressure at 3130 Å. at 26° is shown in Fig. 2. In the presence of oxygen at 3130 Å., Q was reduced by 10% at acetaldehyde pressures of a few hundred millimeters and by 25% at a pressure of about 30 mm. The effect of oxygen on the fluorescence efficiency of acetaldehyde (*i.e.*, emission of wave lengths shorter than 5000 Å.) is (pressure of acetaldehyde 100 mm., T 25°)

P_{O_2} (mm.)	0.16	0.26	0.46	0.55	1.09	2.00	3.58	20.00
Q (relative)	61	60	57	56	57	54	54	55

Although there is some scatter, it can be seen that a constant value of Q is reached when the pressure of oxygen is about 2 mm. Similar results were obtained at oxygen pressures of 50 and 200 mm. When an inert gas (propane) was added and the pressure of acetaldehyde kept constant (at 100 mm. and at 60 mm.) Q increased with increasing pressure of inert gas (data not shown). Reducing the intensity to a tenth of its value increased the fluorescence efficiency (data not shown). The fluorescence efficiency also was studied at 50 and 90° (data not shown). The oxygen-sensitive emission was strongly temperature-dependent, and, in fact, at 90° it was very close to zero. The oxygen-sensitive emission was independent of temperature.

(11) W. A. Noyes, Jr., and F. C. Henriques, Jr., *J. Chem. Phys.*, **7**, 767 (1939).

(12) F. C. Henriques Jr., and W. A. Noyes, Jr., *J. Am. Chem. Soc.*, **62**, 1038 (1940).

(13) R. Stevens, *Chem. Revs.*, **57**, 439 (1957).

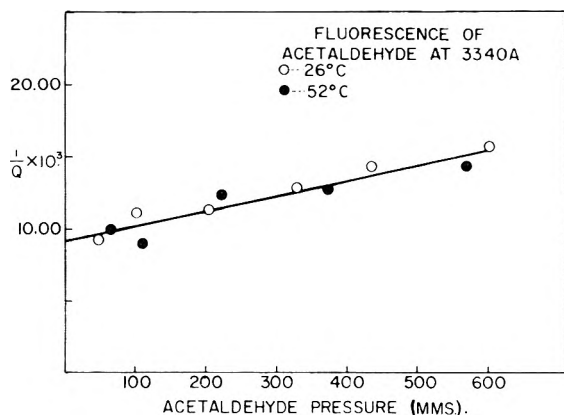


Fig. 1.—Fluorescence of acetaldehyde at 3340 Å.

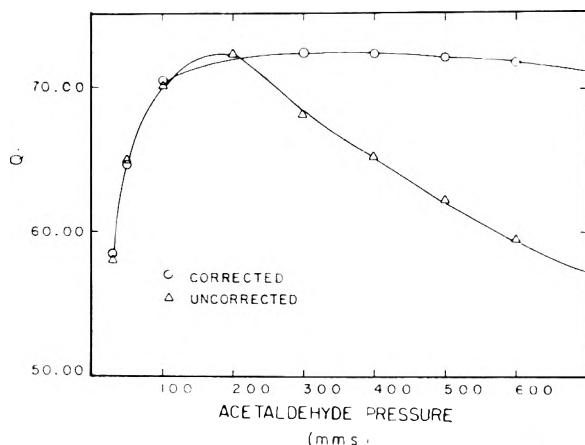


Fig. 2.—Fluorescence of acetaldehyde at 3130 Å.

Fluorescence at 3020 and 2980 Å.—A cursory study of the fluorescence efficiency of acetaldehyde as a function of pressure at 3020 and at 2980 Å. was made. At these wave lengths the trend of Q with pressure was the same as at 3130 Å., although a steady value was not reached until higher pressures. Oxygen had a slight effect at these wave lengths—as at 3130 Å. The effect of oxygen on the fluorescence efficiency at several acetaldehyde pressures at 3020 Å. and 25° is shown by the data

Acetaldehyde pressure (mm.)	520	411	285	203	102	52	34
$Q(\text{cor.})(P_{O_2} = 0)$	70	69	63	59	54	43	17
$Q(\text{cor.})(P_{O_2} = 4 \text{ mm.})$	70	66	59	55	47	38	10

The data at 2980 Å. were similar and are not shown. A study of the fluorescence at shorter wave lengths was prevented by the strong fluorescence of quartz which obscured the fluorescence of acetaldehyde.

The Effect of Biacetyl.—Biacetyl was added to acetaldehyde and the sensitized phosphorescence of biacetyl was studied with a Corning Filter No. 3486, which transmits only wave lengths longer than 5000 Å. At 3130 Å. the pressure of biacetyl was varied from less than 0.1 mm. to a few millimeters, while that of acetaldehyde was kept constant. While there was some scatter in the data, there was strong phosphorescence. For example,

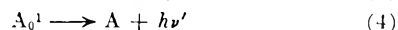
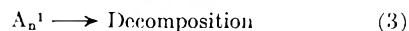
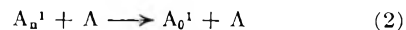
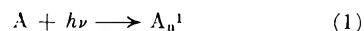
when the pressure of acetaldehyde was 50 mm. and that of biacetyl only 0.035 mm., the value of Q_{3000} (efficiency of biacetyl phosphorescence) was six times that of pure acetaldehyde. Similar results were obtained when the incident radiation was 3340 Å.

Discussion

The data at 3340 Å. (Fig. 1) can be explained by a competition of the fluorescence process with collisional deactivation and decomposition. Since oxygen had no effect on the fluorescence efficiency, the excited state which emits radiation must be a singlet. The sensitized phosphorescence of biacetyl when acetaldehyde is irradiated with 3340 Å. indicates that a triplet state of acetaldehyde is formed, but that it does not emit.

The data at 3130 Å. show that the behavior of acetaldehyde at this wave length is similar to that of biacetyl at 3660 Å. and acetone at shorter wave lengths.⁶ A triplet state must exist, although it seems not to emit radiation. Evidence for this statement is: (1) the effect of oxygen is small, and (2) the phosphorescence of biacetyl (which is from a triplet state) is sensitized by acetaldehyde. The formation of a triplet state of biacetyl may be due to either of the following processes: (a) singlet acetaldehyde molecules transfer energy to produce singlet biacetyl molecules which then undergo the usual processes including triplet state formation; or (b) triplet acetaldehyde molecules produce triplet biacetyl molecules by direct energy transfer. It is not possible to rule out mechanism (a) since the lifetime of the singlet acetaldehyde molecule has not been measured. However, if it is similar to that of acetone (about 10^{-6} second) then the first mechanism is highly unlikely. On the basis of similar work on acetone,^{14,15} the second mechanism is the more attractive. The triplet state of acetaldehyde must disappear by internal conversion rather than emission. Recently, Calvert and Hanst¹⁶ estimated that oxygen at high pressures deactivates 76% of the excited acetaldehyde molecules, and these are, presumably, all in the triplet state.

The following mechanism fits the data at 3130 Å. and at shorter wave lengths



where A_n^1 is an excited singlet state acetaldehyde molecule in an upper vibrational level; A_0^1 is one in the lowest vibrational level. Other steps leading to the formation and disappearance of a triplet state must be included, but the present data do not allow an unambiguous choice of such a mechanism. Further discussion is unwarranted at the present time, although this investigation is being continued in this Laboratory.

(14) H. Okabe and W. A. Noyes, Jr., *J. Am. Chem. Soc.*, **79**, 801 (1957).

(15) J. Heicklen and W. A. Noyes, Jr., *ibid.*, **81**, 3858 (1959).

(16) J. G. Calvert and P. L. Hanst, *Can. J. Chem.*, **37**, 1671 (1959)

Acknowledgment.—The author wishes to thank Professor W. Albert Noyes, Jr., for his many helpful and kind suggestions during the course of this investigation.

DISSOCIATION CONSTANT AND LIMITING CONDUCTANCE OF LiBr IN LIQUID SO₂ AT 0.22°: EVIDENCE FOR THE SOLVATION OF Li⁺

BY NORMAN N. LICHTIN AND K. NARAYANA RAO

Chemistry Department, Boston University, Boston, Mass.

Received February 5, 1960

Previous work has revealed that Bjerrum distances of closest approach² calculated from the dissociation constants of KCl, KBr and KI in liquid SO₂ solution correspond to an unprecedented degree to the sums of the respective crystallographic radii and that the limiting conductances of these ionophores correspond equally closely to the values calculated by employing crystallographic radii in conjunction with Stokes' equation.^{3,4} Lithium bromide provides an interesting addition to this series because of the evidence derived from limiting conductance data⁵ that lithium ion is strongly solvated in many solvents.

Experimental

The conductance bridge,^{3,6} experimental procedures^{3,6} and conductance cell¹ have been described previously.

LiBr was prepared by adding concentrated aqueous HBr (J. T. Baker Analyzed Reagent) dropwise to Li₂CO₃ (Mallinckrodt Analytical Reagent) in a platinum crucible until effervescence ceased, evaporating to dryness and heating to incipient fusion, treating the solidified product with an additional two drops of aqueous HBr, evaporating to dryness once more and fusing the resulting product. The product was cooled and stored under vacuum in a desiccator.

It was found that LiBr is less soluble in liquid SO₂ than has been reported by Jander.⁷ No attempt was made to determine the solubility accurately but it was estimated to be about one third the reported value. Its low solubility and hygroscopicity render the preparation of solutions from directly weighed portions of LiBr very difficult. Samples were therefore introduced into the conductance cell in the form of weighed aliquots of ethanolic solution. The solvent was removed by vacuum distillation. The residual solid subsequently was pumped at 10⁻⁴ mm. pressure for about 12 hours before admission of the solvent.

Because of the high initial dilution (>4.6 × 10³ l. mole⁻¹) and the necessity of restricting the data to a dilution range where the solvent conductivity was relatively small (less than 3% of the solution conductivity) the internal dilution procedure^{3,6} was limited to provide no more than two useful points per run.

Data and Discussion

Conductance data are presented in Table I. These data were analyzed by Shedlovsky's procedure⁸ with the aid of Daggett's table⁹ of $S(z)$

(1) Paper VIII in the Series "Ionization and Dissociation Equilibria in Liquid SO₂," *cf. J. Am. Chem. Soc.*, **81**, 4520 (1959), for Paper VII.

(2) *cf. H. S. Owen and B. B. Owen, "The Physical Chemistry of Electrolytic Solutions," Reinhold Publ. Corp., New York, N. Y., 1958, pp. 70-74.*

(3) N. N. Lichtin and H. P. Leftin, *This Journal*, **60**, 160 (1956).

(4) More recent data suggest that the agreement with respect to both quantities is considerably better for KCl than was originally reported. For a preliminary report, *cf. N. N. Lichtin and P. Pappas, Trans. N. Y. Acad. Sci.*, **20**, 143 (1957).

(5) *cf. Ref. 2, pp. 697-704.*

(6) N. N. Lichtin and H. Glazer *J. Am. Chem. Soc.*, **73**, 5537 (1951).

(7) G. Jander, "Die Chemie in Wasserähnlichen Lösungsmitteln," Springer, Berlin, 1949, p. 231, reports a value of 6 × 10⁻³ mole kg.⁻¹.

values to yield $K_d = (2.65 \pm 0.28) \times 10^{-5}$ mole l.⁻¹ and $\Lambda^0_{exp} = 189 \pm 9$, mhos cm.² mole⁻¹, where the indicated uncertainties are (variances)^{1/2} calculated for 95% confidence limits and $n = 15$. The Bjerrum distance of closest approach, $a_{Bjerrum}$, calculated from K_d is 2.70 ± 0.03 Å. This may be compared with the sum of Pauling's "ionic radii,"¹⁰ 2.55 Å., or with the experimental¹¹ crystallographic interionic distance, 2.75 Å. The value of Λ^0_{exp} may be compared with $\Lambda^0_{Stokes} = 482$, calculated from Stokes law,¹² Pauling's "ionic radii" and the viscosity of the solvent which was taken as 4.01×10^{-3} poise.

TABLE I
CONDUCTANCE OF LiBr IN SO₂ AT 0.22°

V ^a	Λ ^b	V ^a	Λ ^b
4602 ^c	59.7	12630	85.9
5515	63.2	15520	91.4
5919	64.9	16250	91.8
6214	66.4	17205	93.3
6638	68.4	17690	96.0
7631	71.2	21010	102.4
8218	73.3	22580	103.9
10645	80.0		

^a In l. mole⁻¹. ^b In mhos cm.² mole⁻¹, corrected for solvent conductivity. ^c The maximum value of $\kappa_a = 0.03$, where κ is the reciprocal of the average radius of the ionic atmosphere.

The value of K_d for LiBr is sufficiently small that it is not necessary to evaluate it by means of the Fuoss procedure based on the extended Onsager-Fuoss conductance equation nor can an a -value be derived directly from the conductance data.¹³ Shedlovsky's procedure is appropriate for this ionophore and for KCl, KBr and KI as well. The value of $a_{Bjerrum}$ for LiBr falls between the sum of the Pauling radii and the experimental interionic distance in the LiBr crystal. Thus, this ionophore resembles KCl, KBr and KI in its association behavior; the data provide no reason for concluding that solvation of the lithium cation impedes its association with bromide anion to an extent that differs significantly from that obtaining with the potassium salts. The simplest explanation is that the anions penetrate the solvation sheaths of both K⁺ and Li⁺.

In contrast, the mobility of the lithium ion appears to be drastically reduced by solvation; Λ^0 for LiBr is substantially less than that of (C₂H₅)₄NBr (215 at 0.16°⁴). Thus the hydrodynamic behavior of Li⁺ is radically different from that of all other ions we have investigated in liquid SO₂ solution. In no other case has Λ^0_{exp} been more than 10% less than Λ^0_{Stokes} calculated from Pauling ionic radii or (for quaternary ammonium ions) from bond distances and angles and van der Waals radii. Indeed, for all the 1:1 ionophores

(8) T. Shedlovsky, *J. Franklin Inst.*, **225**, 739 (1938).

(9) H. M. Daggett, *J. Am. Chem. Soc.*, **73**, 4977 (1951).

(10) L. Pauling, "Nature of the Chemical Bond," Cornell University Press, Ithaca, N. Y., 1948, p. 346.

(11) *Ref. 10, p. 358.*

(12) *Ref. 2, p. 284.*

(13) *cf. R. M. Fuoss and F. Accascina, "Electrolytic Conductance," Interscience Publishers, New York, N. Y., 1959, Chapter XVII.*

we have studied in SO_2 where the cation is a bulky organic ion, Λ^0_{exp} is substantially larger than $\Lambda^0_{\text{Stokes}}$.^{3,4}

ON THE CONCENTRATION-DEPENDENCE OF THE MOBILITY OF INCOMPLETELY-DISSOCIATED UNSYMMETRICAL ELECTROLYTES IN DIFFUSION

BY J. M. CREETH AND R. H. STOKES

Department of Chemistry, University of Wisconsin, Madison, Wisconsin
and
Department of Chemistry, University of New England, Armidale, N.S.W., Australia

Received February 8, 1960

It is known that a satisfactory explanation of the concentration-dependence of the diffusion coefficient of weak or incompletely-dissociated symmetrical electrolytes may be found by expressing the mobility term in the diffusion equation¹ as a function of the individual ion mobilities, the mobility of the neutral molecule and the degree of dissociation.²⁻⁴ The analogous case of unsymmetrical electrolytes presents greater difficulties in interpretation insofar as the Onsager-Fuoss series approximation for the electrophoretic correction does not converge satisfactorily, but there is, in addition, a further complication arising from the fact that the association product is itself an ion. Thus a three-ion system arises, and it is no longer possible to equate the individual ion-velocities. Since it appears that much of the concentration dependence of the mobility of such electrolytes may be accounted for in terms of incomplete dissociation, it has seemed worth while to derive a solution in this form; the following treatment applies specifically to the case of 1:2 electrolytes (and, by reversal of indices, to 2:1 electrolytes) but could be extended to the general case without excessive difficulty.

For the case $\text{M}_2\text{X} \rightleftharpoons \text{M}^+ + \text{MX}^- \rightleftharpoons 2\text{M}^+ + \text{X}^-$

where the second dissociation proceeds to the extent α , these relations are self-evident

$$c_1 = c(1 + \alpha); \quad c_2 = c\alpha; \quad c_3 = c(1 - \alpha) \quad (1)$$

$$\mu_3 = \mu_1 + \mu_2; \quad \mu = 2\mu_1 + \mu_2 \quad (2)$$

where c represents molar or ionic concentration, μ_i chemical potential of a single i-ion, 1, 2, 3 the ionic species M^+ , X^- and MX^- , and the absence of an index denotes the neutral electrolyte as a whole. By introducing the ionic velocities v_i in terms of expressions

$$v_i = u_i[-(\partial\mu_i/\partial x) + z_i e\psi] \quad (3)$$

where u_i are mobilities, z_i ion valences, e the electronic charge and ψ the potential gradient due to incipient charge separation, and substituting appropriately for z_i , one obtains the relations

$$\frac{v_1}{u_1} + \frac{v_2}{u_2} = \frac{v_3}{u_3} \quad (4)$$

(1) I. Onsager and R. M. Fuoss, *This Journal*, **36**, 2689 (1932), (Equation 4-12-5).

(2) H. S. Harned and R. M. Hudson, *J. Am. Chem. Soc.*, **73**, 5880 (1951).

(3) B. F. Wishaw and R. H. Stokes, *ibid.*, **76**, 2065 (1954).

(4) G. T. A. Muller and R. H. Stokes, *Trans. Faraday Soc.*, **53**, 642 (1957).

and

$$\frac{2v_1}{u_1} + \frac{v_2}{u_2} = -\frac{\partial\mu}{\partial x} \quad (5)$$

Equation 4 describes the restrictions on the velocities in a three-ion system of one solute component.

The flow J , expressed in moles of solute per unit area per unit time, may be written either as

$$J = (c_1v_1 + c_3v_3)/2 \quad (6)$$

or as

$$J = c_2v_2 + c_3v_3 \quad (7)$$

here we choose to use the form (6). Thus the fundamental flow equation becomes

$$J = \frac{c}{2} [(1 + \alpha)v_1 + (1 - \alpha)v_3] \quad (8)$$

Since there can be no net transport of charge, $\sum J_i z_i = 0$, or

$$(1 + \alpha)v_1 - 2\alpha v_2 - (1 - \alpha)v_3 = 0 \quad (9)$$

The operational definition of the diffusion coefficient is

$$D = -J/(\partial c/\partial x) \quad (10)$$

while its theoretical formulation may be represented as

$$D = u \cdot c \left(\frac{d\mu}{dc} \right) \quad (11)$$

so that we obtain the conventional expression for the electrolyte mobility

$$u = -\frac{J}{c(\partial c/\partial x)(d\mu/dc)} \quad (12)$$

Substituting appropriately from (5) and (8) we find

$$u = \frac{1}{2} \left[\frac{(1 + \alpha)v_1 + (1 - \alpha)v_3}{2(v_1/u_1) + v_2/u_2} \right] \quad (13)$$

and the use of equations 4 and 9 enables the v_i to be eliminated. After some manipulations one finally obtains

$$u = \frac{u_1 u_3 (1 + \alpha)(1 - \alpha) + u_1 u_2 \alpha (1 + \alpha) + u_2 u_3 \alpha (1 - \alpha)}{u_1 (1 + \alpha) + 4\alpha u_2 + u_3 (1 - \alpha)} \quad (14)$$

which is the desired solution. We note the two limiting cases

$$(u)_{\alpha \rightarrow 0} = \frac{u_1 u_2}{u_1 + 2u_2} \quad \text{and} \quad (u)_{\alpha \rightarrow 1} = \frac{u_1 u_3}{u_1 + u_3}$$

which are, respectively, the standard formulations for completely dissociated 1:2 and 1:1 electrolytes, as required.

In the use of equation 14 to substitute in the relation

$$D = 3ukT[1 + cd \ln y_{\pm}/dc]$$

(where y_{\pm} is the stoichiometric mean ionic activity coefficient on the c scale) it is apparent that the mobilities appropriate to the particular ionic strength (in this case $I = c(1 + 2\alpha)$) are required; however, as it seems that the greatest uncertainty will generally lie in the magnitude of α , it is likely that the limiting values derived from ion conductances ($u_i^0 = N\lambda_i^0/F^2|z_i|$, where the symbols have their usual significance) will be sufficiently accurate. An application of this theory to the case of thallosulfate will be published shortly.

Acknowledgments.—It is a pleasure to thank Professors L. J. Gosting and J. W. Williams for their comments and criticism of the manuscript. The work was supported in part (J.M.C.) by a grant from the National Institutes of Health (RG 4912).

THE APPLICATION OF GAS-LIQUID PARTITION CHROMATOGRAPHY TO PROBLEMS IN CHEMICAL KINETICS. ACID-CATALYZED METHANOLYSIS OF ENOL ACETATES

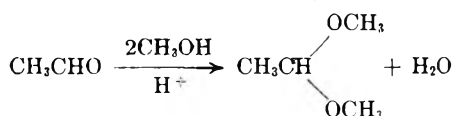
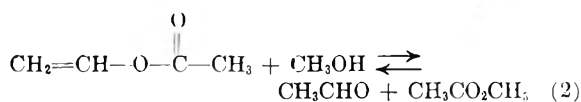
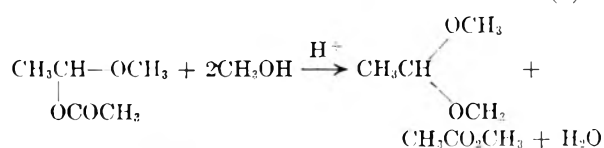
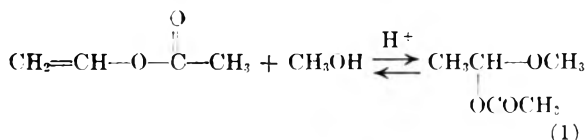
BY E. V. KRING,¹ G. I. JENKINS¹ AND V. L. BACCHETTA

E. I. du Pont de Nemours & Co., Inc., Electrochemicals Department, Niagara Falls Research Laboratory, Wilmington, Delaware

Received February 10, 1960

Gas-liquid partition chromatography as an analytical tool is ideal for studying many organic reactions because the reaction mixture is not disturbed by the removal of the minute samples required in analysis using this technique. These techniques are being used in varied problems in chemical kinetics.²⁻⁴

The acid-catalyzed reactions of enol acetates with methanol may be explained by many different mechanisms. Two possible mechanisms are



The reactions of vinyl acetate and isopropenyl acetate with methanol were studied in order to obtain information on the variations in energy and entropy of activation when an α -hydrogen is replaced by $-\text{CH}_3$ in this little-studied reaction. The relationship between rate and acid concentrations was also studied.

Experimental

1. Materials.—Spectral grade methanol from Eastman Kodak Co., Rochester 3, New York, was used as received. A vapor chromatography scan was obtained on each bottle to assure its purity. These scans showed no methyl acetate, dimethylacetal or acetone.

Vinyl acetate from E. I. du Pont de Nemours & Co.,

(1) E. I. du Pont de Nemours & Co., Inc., Electrochemicals Department, Chestnut Run, Wilmington, Delaware.

(2) C. M. Drew, J. R. McNesby, Presented at Pittsburgh Conference on Analytical Chemistry and Applied Spectroscopy, Dec., 1956.

(3) A. B. Callear, R. J. Cventanovic, *Can. J. Chem.*, **33**, 1256 (1955).

(4) L. F. Hatch, Proceedings of ISA International Symposium on Gas Chromatography, 1957, p. 9.

Inc., Electrochemicals Dept., was used after redistillation. Vapor chromatography showed the material to be free of acetic acid and acetaldehyde. This purified vinyl acetate was kept refrigerated until used.

Isopropenyl acetate was used as received from Eastman Kodak Co., Rochester 3, New York. Vapor chromatography scans were used to establish the purity of this chemical.

2. Reaction Rate Studies.—Reaction rate studies were carried out in a 250-ml. round-bottom flask connected to a spiral reflux condenser. Methanol, cooled by passing through a trichloroethylene-Dry Ice bath, was used in the condenser.

The reaction mixture consisted of 99.0 g. of spectral grade methanol and 1.00 g. of either vinyl acetate or isopropenyl acetate. Immediately after mixing, the solution was cooled to -68° , and either 1.5, 3.0 or 6.0 ml. of a freshly made 1% solution of H_2SO_4 in methanol was then added depending on the acid concentration desired. The reaction mixture was analyzed at the start and as often as possible during each run.

3. Analysis.—Analyses were carried out in a Perkin-Elmer Model 154 Vapor Fractometer using a 4-meter column operated at $94-96^\circ$. The column contained Carbowax 600 on Celite or Carbowax 1500 on firebrick for the vinyl acetate studies and dimethylsulfolane on Celite for the isopropenyl acetate studies. Samples (0.02 ml.) were withdrawn with an Agla micrometer syringe and injected into the helium carrier gas stream. The ratio of the areas under the peaks were used as a measure of the concentration of reactants and products present. By analyzing standard samples, it was shown that for the products being analyzed, and under the above conditions, this was correct to within 2-3%.

The elution time for the various components in the reaction mixture was established in separate experiments. In addition methyl acetate was identified in the eluted gas by mass spectral analysis, and acetone by the 2,4-dinitrophenylhydrazone derivative.

4. Calculation of the Thermodynamic Quantities for the Reactions.—Kinetic data were obtained at three different temperatures, 30, 49 and 65° , for each of three concentrations of acid (0.245, 0.490 and 0.980 meq. acid/gram of acetate). The log of concentration of unreacted acetate was plotted *versus* time for each temperature and acid concentrations. Figure 1 is included to illustrate the type of data obtained. The reactions under the conditions described were all first order with respect to the acetate concentration. The method of least squares was used to calculate the specific reaction rate constants for the first-order expression $C_t = C_0e^{-kt}$. The calculated reaction rate constants were found to increase both with increase in temperature and in acid concentration (see Table I).

TABLE I
COMPARISON OF KINETIC DATA FOR VINYL AND ISOPROPENYL ACETATE

Acid concn., meq. H^+ / g. acetate	Reaction temp., $^\circ\text{C}$.	$k(\times 10^3)$ min. ⁻¹	—Isopropenyl acetate—	
			Reaction temp., $^\circ\text{C}$.	$k(\times 10^3)$ min. ⁻¹
0.245	31.1	1.24 ± 0.05	32.4	0.75 ± 0.04
	49.0	$3.32 \pm .16$	49.9	$3.01 \pm .10$
	64.6	$8.97 \pm .32$	67.6	$7.47 \pm .10$
0.490	30.1	$2.33 \pm .47$	31.9	$1.68 \pm .14$
	30.8	$1.37 \pm .21$	49.0	$7.73 \pm .82$
	31.4	$1.78 \pm .21$	65.3	$16.52 \pm .51$
	49.9	$6.58 \pm .16$	66.3	25.25 ± 2.16
	65.8	$14.60 \pm .55$		
0.980	66.1	21.68 ± 1.06		
	30.7	3.58 ± 0.23	30.4	2.88 ± 0.15
	49.0	15.42 ± 0.73	30.2	3.28 ± 0.12
	66.4	28.70 ± 2.30	49.1	12.52 ± 1.01
	67.2	28.13 ± 2.15	65.2	27.69 ± 1.23
			67.4	31.22 ± 2.74

5. Generalized Rate Equation.—A general rate equation for the methanolysis reactions was derived by employing all the experimental data.

TABLE II

VALUES OF ΔH^* , ΔS^* , ΔF^* OBTAINED FROM KINETICS DATA FOR VINYL ACETATE AND ISOPROPENYL ACETATE IN TABLE I USING ARRHENIUS EQUATION FORM $k = A[H^+]^b e^{-E/RT}$

Reactant	Acid concn., meq. H ⁺ /g. acetate	<i>E</i> _{act.} kcal./mole	Log <i>PZ</i>	$\frac{\Delta H^*}{(E_{act}-nRT)}$, kcal./mole	ΔS^*		
					<i>T</i> = 303°K.	cal./deg./mole 322°K.	338°K.
Vinyl acetate	0.245		4.01		38.9	39.0	39.9
	.490	12.6	4.26	11.9	38.4	38.5	38.6
	.980		4.52		37.9	38.0	38.1
Isopropenyl acetate	.245		4.69		37.1	37.2	37.3
	.490	13.8	5.00	13.1	35.7	35.8	35.9
	.980		5.31		34.3	34.4	34.5

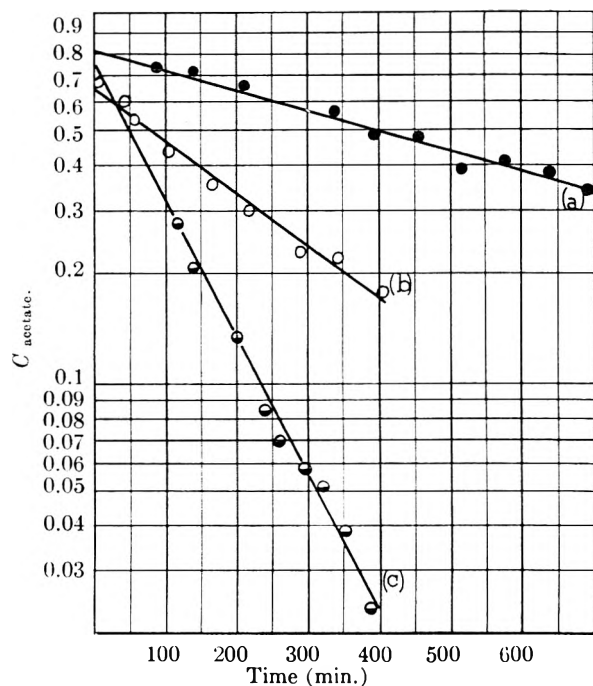


Fig. 1. Acid-catalyzed reaction of vinyl acetate and methanol (1:99) weight ratio using 0.245 meq. acid/g. acetate: (a) $t = 31.1^\circ$, (b) $t = 49.0^\circ$, (c) $t = 64.6^\circ$.

Since

$$\text{rate of reaction} = k[\text{acetate concn.}]$$

$$\text{and } k = A[H^+]^b e^{-E/RT}$$

then

$$\ln k = \ln A + B \ln [H^+] - \frac{E}{R} \left(\frac{1}{T} \right) \quad (1)$$

Using the experimental values of $\ln k$, $\ln [H^+]$ and T available, equation 1 may be solved for the constants $\ln A$, b and E by the method of least squares. For the vinyl acetate-methanol reaction

$$\ln k = 14.51431 + 0.85014 \ln [H^+] - 6334.929 \left(\frac{1}{T} \right) \quad (2)$$

with a standard deviation $s_{\ln k} = 0.20219$; and for the isopropenyl acetate-methanol reaction

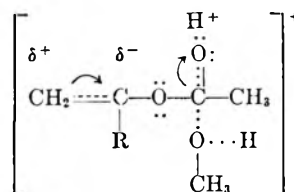
$$\ln k = 16.33806 + 1.03410 \ln [H^+] - 6960.318 \left(\frac{1}{T} \right) \quad (3)$$

with a standard deviation $s_{\ln k} = 0.20442$ were obtained.

From the values of b in these equations, it is clear that the reaction rates approach first order with respect to acid concentration in each case.

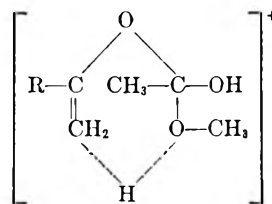
The thermodynamic quantities ΔH^* , and ΔS^* obtained from these calculated values of $\ln k$ (Table II) agree very well with those obtained directly from the experimental k values.

6. Discussion.—A mechanism for the attack of methanol on the protonated enol acetate might involve an activated complex



Molecular models indicate more steric strain in the complex involving isopropenyl acetate than in the vinyl acetate; however, the probability factor ($\log PZ$), determined experimentally, increases from vinyl to isopropenyl acetate. This suggests that an electronic effect exists which has more influence than the steric effect.

In the methanolysis reaction a negative entropy of activation was obtained meaning that the activated state has a more ordered structure than the ground state for the reactants. One such ordered structure that could be envisaged for the activated state is



The literature cites numerous examples whereby cyclic compounds have lower entropies of formation than their linear isomers.

The decrease in entropy in going to the activated complex was greater in the case of vinyl acetate than in the case of isopropenyl acetate. It is suggested that the methyl group increases the number of degrees of freedom in the cyclic activated structure to a greater extent than it does in the linear ground state structure. This theory supports the relationship between molal entropy and molecular structure tabulated by Parks and Huffman.⁵ Their calculations show that substitution of a $-\text{CH}_3$ group for a $-\text{H}$ group in a straight chain compound (to give branching) and in a ring compound increases the entropy by approximately 3.2 and 7.7 e.u., respectively. There is a greater increase amounting to 4.5 e.u. for the ring compound. In this work a difference of 4.9 e.u. was obtained; i.e., the increase in entropy when $-\text{CH}_3$ replaces $-\text{H}$ is greater for the activated complexes than it is for the ground state by 4.9 e.u. The close agreement between experimental and theoretical values is a justification for postulating a ring structure as the activated complex.

The data show that the energy of activation for the isopropenyl acetate methanolysis is greater than that for the vinyl acetate methanolysis. This can be explained on the basis of the energy contents of the protonated complexes. The inductive methyl group will stabilize the isopropenyl acetate protonated complex so that its energy content is less than that for vinyl acetate.⁶ This effect will be less

(5) (a) Parks and Huffman, "Free Energies of Some Organic Compounds," Am. Chem. Soc. Monograph Series, No. 60, Chemical Catalog Co., New York (1932); (b) Rossini, *J. Research Natl. Bur. Standards*, **13**, 21, 189 (1934).

pronounced in the activated complex. An analogy is found in the $H_2 + D_2$ reactions. The differences in ground state energies for H_2 and D_2 account for the differences in their activation energy for hydrogenation.⁷

Summary

1. The experimental evidence points to a mechanism in which the attack of the methanol takes place at the carbonyl carbon in both acetates studied. Steric hindrance is not a predominant factor.

2. A suitable criterion for elucidation of reaction mechanism results in the evaluation of the entropy of activation as well as in the energy of activation.

3. Gas-liquid partition chromatography lends itself to studies in chemical kinetics.

Acknowledgments.—The authors are indebted to members of the research staff of the Electrochemicals Department for their encouragement. The work of Mr. J. A. Love who conducted many of the experiments is also appreciated.

(6) C. K. Ingold, *Chem. Revs.*, **15**, 225 (1934).

(7) S. Glasstone, "Textbook of Physical Chemistry," D. Van Nostrand Co., Inc., New York, N. Y., 1940, p. 1104.

THE TWO CRYSTAL FORMS OF (ETHYLENE-DINITRIL)-TETRAACETIC ACID

By R. B. LeBLANC AND H. L. SPELL

Texas Division, The Dow Chemical Company, Freeport, Texas

Received February 11, 1960

A very great number of papers have appeared in the literature on (ethylene-dinitrilo)-tetraacetic acid (EDTA). Most of them concern the analytical applications of this compound and the chelation of it with metal ions.^{2,5}

The properties, including acid-base constants, have been studied.^{3,4} The infrared spectrum of this compound has been reported,¹ but no mention was made that it has more than one form.

During a routine infrared analysis of some EDTA precipitated by addition of acid to a solution of the sodium salt a spectrum was obtained which did not match the standard spectrum of EDTA. Chemical analysis proved the compound to be EDTA with a "different" spectrum. Further work was done to substantiate that there are two forms of EDTA.

Experimental

When EDTA is precipitated by acid addition to a solution of one of its sodium salts at room temperature, the low temperature form (α) is produced. Precipitation at a temperature near the boiling point of water produces the high temperature form (β). Most commercially available EDTA is the β -form since high temperature precipitation usually gives a purer product. The published infrared spectrum¹ is for the β -form.

The α -form can be converted to the β -form by suspending some of the former in water and boiling for a short time. Attempts to convert the β -form to the α -form by a similar

(1) D. Chapman, *J. Chem. Soc.*, 1766 (1955).

(2) H. Flaschka, "EDTA Titrations," Pergamon Press, New York, N. Y., 1959.

(3) G. Schwarzenbach and H. Ackermann, *Helv. Chim. Acta*, **30**, 1798 (1947).

(4) G. Schwarzenbach and H. Ackermann, *ibid.*, **31**, 1029 (1948).

(5) F. J. Welcher, "The Analytical Uses of Ethylenediaminetetraacetic Acid," D. Van Nostrand Co., Princeton, N. J., 1958.

method (stirring a suspension of the β -form in water at room temperature for 24 hours) were unsuccessful. This conversion probably would take place by this method if sufficient time were allowed.

The refractive indexes of the two forms were measured by microscopy. These values are

α -form: 1.53–1.54

β -form: 1.576–1.620

The infrared spectrum of the α -form is shown in Table I. The infrared spectrum of the β -form was determined by Chapman.¹

TABLE I

INFRARED SPECTRUM OF THE α -FORM OF EDTA

The wave numbers in cm^{-1} and the strengths of the bands are listed: vw = very weak, w = weak, m = medium, s = strong, vs = very strong.

670w	1059w shoulder	1380m
713s	1072w	1465m
814vw	1094m	1690vs
856m	1217m	2655w
910s	1235m	2860vw
933w	1260s	2995w
1040w shoulder	1282m	3020m
	1348s	

The X-ray diffraction patterns for the two forms are shown in Table II.

TABLE II

X-RAY DIFFRACTION PATTERNS FOR THE TWO FORMS OF (ETHYLENEDINITRIL)-TETRAACETIC ACID

The diffraction data were obtained with a Norelco X-ray diffractometer using iron $K\alpha$ radiation. $d\text{\AA}$. is listed followed by I/I_1 in parentheses.

α Form			β Form		
7.13(16)	3.61(39)	2.41(5)	8.0(13)	3.61(42)	2.48(4)
6.90(62)	3.42(26)	2.35(3)		3.45(9)	2.43(11)
5.58(100)	3.17(7)	2.28(5)	6.65(5)	3.32(13)	2.39(6)
5.03(11)	3.02(28)	2.22(7)	5.41(4)	3.09(9)	2.21(4)
4.68(12)	2.94(8)	2.14(5)	5.14(5)	3.02(10)	2.14(2)
4.10(40)	2.76(13)	2.12(6)	4.96(28)	2.95(2)	2.10(1)
3.99(9)	2.75(8)	2.02(3)	4.42(20)	2.79(16)	2.07(1)
3.84(16)	2.58(12)	1.97(3)	4.01(100)	2.71(4)	1.97(1)
3.65(56)	2.50(7)	1.83(3)	3.79(8)	2.58(4)	1.93(4)
		1.80(4)			

Discussion

No difference in chemical properties was observed for the two forms of EDTA nor was any difference observed in the physical properties in solution. The difference in physical properties of the two forms can be attributed to two different crystalline structures.

Acknowledgment.—The X-ray diffraction work and the refractive index work were done by Knud C. Poulsen and Dr. A. A. Levinson, respectively, both of The Dow Chemical Company.

FLAME TEMPERATURE AND COMPOSITION IN THE ALUMINUM- POTASSIUM NITRATE REACTION

By A. W. BERGER, D. GOLOMB AND J. O. SULLIVAN

Geophysics Corporation of America, Boston 15, Massachusetts

Received February 3, 1960

For the purpose of artificial electron cloud generation at high altitudes,¹ potassium vapors were re-

(1) F. F. Marmo, L. M. Asehenbrand and J. Pressman, *Planet. Space Sci.*, **1**, 227 (1959), *et seq.*

TABLE I
APPROXIMATE FLAME COMPOSITION AND TEMPERATURE IN KNO_3 -Al SYSTEMS

	Mole ratio Al/KNO ₃	Reaction conditions	Flame composition in moles ^a						Flame temp., °K.
			Al ₂ O ₃ (c)	Al ₂ O(g)	AlO(g)	Al(g)	O ₂ (g)	O(g)	
1	2	$V_c = 0.165$ l. $P_t = 4400$ atm.	0.959	0.039	...	0.002	0.023	0.037	5500
2	2	$V_c = 1$ l. $P_t = 770$ atm.	.876	.116	0.001	.010	.068	.115	5200
3	2.66	$P_c = 500$ atm.	.819	.496029	.008	.036	4900
4	2	$P_c = 100$ atm.	.848	.145015	.080	.160	4600
5	3	$P_c = 100$ atm.	.733	.745044	.002	.003	4000
6	3	$P_c = 1$ atm.	.717	.783024	.162	3600

^a In addition the flame consists also of 1 mole K(g) and 0.5 mole N₂(g) per mole of KNO₃.

leased from rocket-borne canisters, by the reaction of aluminum powder with potassium nitrate. In order to estimate the number of free electrons in the flame, obtained by ionization of potassium, flame temperatures were calculated for various conditions of release.

The following reaction products are considered to be involved in simultaneous equilibria:^{2,3} Al₂O₃(c), Al₂O(g), AlO(g), O₂(g), and O(g), where c represents condensed and g gaseous phase. N₂(g) and K(g) are assumed to act as inert diluents only. Minor products such as NO, N, K⁺ and e⁻ are neglected in estimating flame composition and temperature.⁴ Minimizing, thus, the number of products and assuming ideal gas behavior, desk calculation of equilibrium conditions is feasible.⁵ Equilibrium concentrations are calculated in the usual way from the mass balance relations and equilibrium equations. The heat of reaction is then compared with the enthalpy change (from the initial temperature) of the assumed equilibrium products. The temperature at which heat balance is achieved is defined as the flame temperature.

Equilibrium constants were calculated from tabulated free energy functions.^{6,7} The heat of formation of the elements in their standard state at 298.16°K. is taken as zero. For Al₂O₃(c) and Al₂O(g), $\Delta H_f^0 = -400.1$ and -39.4 kcal./mole, respectively, were adopted.³ AlO(g) is usually present in negligible amounts. For KNO₃(c) and O(g), $\Delta H_f^0 = -117.9$ and $+59.16$ kcal./mole were taken, respectively.⁸ Since all alkali nitrates have similar heats of formation and the enthalpies of the gaseous alkalis are alike (except Li)—no great difference is expected in flame temperature and

composition by substituting other alkalis for potassium.

Table I gives the product composition and flame temperature in KNO₃-Al mixtures at constant volume (V_c) or constant pressure (P_c). For the constant volume reactions the total pressure (P_t) in the vessel is also calculated. The volume of 165 ml. in Row 1 is the capacity of the canister necessary to hold (without pressing) a mixture of 2 moles of aluminum powder (≈ 200 mesh) and one mole of potassium nitrate (≈ 20 mesh). Row 6 gives the equilibrium conditions at 1 atm. constant pressure. However, preliminary experiments have shown the reaction to be extinguished at atmospheric pressure. In sealed bombs explosions are produced.⁹

According to Table I, the flame temperature increases with increased pressure in the vessel and decreases with increasing Al/KNO₃ ratio. The highest (calculated) flame temperatures are obtained in the 2Al:1KNO₃ systems—which is the stoichiometric ratio.

As a first approximation, equilibrium electron concentrations are calculated readily from a given flame temperature and the ionization potential of potassium by means of the Saha equation.¹⁰ The number thus calculated, however, is reduced during the expansion of the products, due to recombination processes. An elementary treatment of this problem will be presented elsewhere.

Acknowledgment.—This research was supported in part under U. S. Army Signal Corps Contract DA-36-039-SC-78971.

(9) A. W. Berger and L. Aschenbrand, Geophysics Corp. of America, Boston 15, Mass., unpublished results.

(10) R. H. Fowler, "Statistical Mechanics," Cambridge Univ. Press, London, 1936, 2nd edition, p. 372.

(2) M. A. Cook, "The Science of High Explosives," Reinhold Publ. Corp., New York, N. Y., 1956, p. 389.

(3) "Preliminary Report on the Thermodynamic Properties of Li, Be, Mg and Al," Natl. Bureau of Standards, Report 6297, 1959.

(4) For instance in a 4900°K. flame at 500 atm. the equilibrium mole fraction of electrons is about 0.003. The heat of ionization will not alter substantially the flame temperature. On the other hand, such an electron concentration is detected easily by radiolar techniques.

(5) S. S. Penner, "Chemistry Problems in Jet Propulsion," Chapt. 13, Pergamon Press, New York, N. Y., 1957.

(6) E. A. Mickle, "Collected Thermodynamic Properties of 88 Possible Products of Reaction," General Electric Co., Evandale, Ohio, DF58AGT 111, 1957.

(7) R. Altman, "Thermodynamic Properties of Propellant Combustion Products," Rocketdyne Publication, R-669, 1959.

(8) "Selected Values of Chemical Thermodynamic Properties," Natl. Bureau of Standards, Circular 500, 1952.

THE CALCULATION OF EQUILIBRIUM CONSTANTS FROM SPECTROPHOTOMETRIC DATA

By C. P. NASH

Department of Chemistry, University of California, Davis, California
Received February 16, 1960

Very recently there has been a revival of interest in methods for treating visible and ultraviolet spectral data to obtain equilibrium constants for

complex formation.¹ The equation deduced by Benesi and Hildebrand,² or modifications thereof,³⁻⁵ has been most commonly employed in this connection. These expressions all have a common failing. Namely, they require an auxiliary quantity, the molar absorptivity for the complex, to be determined before the object of primary interest, the equilibrium constant, can be obtained. The equation of Nakagura⁶ does not have this objection, but it is not well suited to other than pairwise analyses of a series of data. From a practical point of view, an application of the expression given recently by Rose and Drago⁷ would require many auxiliary calculations to be made before an equilibrium constant could be obtained. A more serious objection, however, is that their method in the general case does not include a rapid means of verifying the existence of a unique complex in order to justify a detailed treatment of the data.

In many cases, complex formation is accompanied by the appearance of a new spectral peak, *e.g.*, the "charge transfer" absorption of the molecular complexes of the halogens. In many other cases, such as the "blue shift" absorption of these same complexes or the absorption of hydrogen bonded complexes, considerable overlap with the existing peaks of non-complexed molecules occurs. It is the purpose of the present note to develop an expression which will treat spectral data specifically in the overlap region and permits a direct evaluation of the equilibrium constant with a minimum of computational labor.

Theoretical

We assume the existence of a chemical equilibrium of the form



where D is any donor molecule and S is an acceptor substrate. For purposes of orientation we assume that only S and SD absorb in the wave length region of interest, and for temporary mathematical convenience we assume the concentration of S to be very small relative to that of D.

The equilibrium constant appropriate to reaction 1 is given in concentration units by

$$K_c = \frac{C_c}{C_s C_d} \quad (2)$$

where C_c is the equilibrium concentration of SD complex and C_s and C_d are the final concentrations of S and D. If both S and SD obey Beer's law at a given wave length, the total absorbance per cm. of path (A) is given by

$$A = \epsilon_s C_s + \epsilon_c C_c \quad (3)$$

where ϵ_s and ϵ_c are the molar absorptivities of species S and SD, respectively. In the absence

- (1) S. P. McGlynn, *Chem. Revs.*, **58**, 1113 (1958).
- (2) H. A. Benesi and J. H. Hildebrand, *J. Am. Chem. Soc.*, **71**, 2703 (1949).
- (3) J. A. A. Ketelaar, *et al.*, *Rec. trav. chim.*, **71**, 1104 (1952).
- (4) R. L. Scott, *ibid.*, **75**, 787 (1956).
- (5) R. M. Keefer and L. J. Andrews, *J. Am. Chem. Soc.*, **74**, 1891 (1952).
- (6) S. Nakagura, *ibid.*, **76**, 3070 (1954).
- (7) N. J. Rose and R. S. Drago, *ibid.*, **81**, 6138 (1959).

of complexing agent D the total absorbance per cm. is given by

$$A^0 = \epsilon_s C_s^0 \quad (4)$$

where C_s^0 is the initial concentration of S. If we divide eq. 3 by eq. 4 and substitute for C_c from eq. 2 we find

$$\frac{A}{A^0} = \frac{C_s}{C_s^0} \left[1 + \frac{\epsilon_c}{\epsilon_s} K C_d \right] \quad (5)$$

By introducing conservation of species S

$$C_s^0 = C_s + C_c \quad (6)$$

and invoking eq. 2 a second time we find

$$\frac{C_c}{C_s^0} = (K C_d + 1)^{-1} \quad (7)$$

When eq. 7 is substituted into eq. 6 there results

$$\frac{A}{A^0} = \frac{1 + \frac{\epsilon_c}{\epsilon_s} K C_d}{1 + K C_d} \quad (8)$$

For manipulative ease let us define

$$\frac{A}{A^0} = Z \quad (9)$$

$$K \epsilon_c / \epsilon_s = \alpha \quad (10)$$

$$C_d = 1/Y \quad (11)$$

so that eq. 8 becomes

$$Z = \frac{(1 + \alpha/Y)}{(1 + K/Y)} \quad (12)$$

Equation 12 may be solved explicitly for Y to obtain

$$Y = \frac{KZ - \alpha}{1 - Z} \quad (13)$$

When we now define

$$X \equiv 1/(1 - Z) \quad (14)$$

and substitute eq. 14 into eq. 13 there results the linear equation

$$Y = X(K - \alpha) - K \quad (15)$$

The physical significance of eq. 15 is quite clear. When the reciprocal of the donor concentration is plotted against the reciprocal of (one minus the absorbance ratio), a straight line should result if 1:1 complex formation occurs. The intercept of this line is the negative of the equilibrium constant, and the slope is related to the molar absorptivity of the complex. Equation 15 may be generalized to include the formation of a single, more complicated complex SD_n simply by raising Y to the n 'th power. In addition, either concentration units or mole fractions may be used to express the amount of D present without altering the form of the final equation.

Discussion

In order to demonstrate the utility of eq. 15 in the determination of equilibrium constants we have selected several sets of data from the literature and applied our method to them. The data of Ketelaar, *et al.*,^{3,8} on the system dioxane-iodine in carbon tetrachloride solution recently have been reanalyzed by Drago and Rose.⁹ Because the original data are very complete, this system af-

(8) J. A. A. Ketelaar, *et al.*, *Rec. trav. chim.*, **70**, 499 (1951).

(9) R. S. Drago and N. J. Rose, *J. Am. Chem. Soc.*, **81**, 6141 (1959).

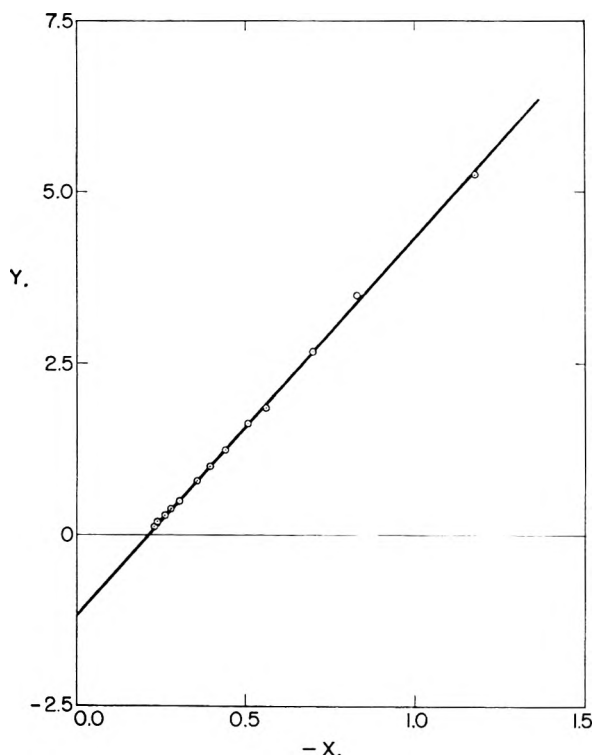


Fig. 1.—Dioxane-iodine spectrophotometric data of Ketelaar³ plotted according to eq. 15.

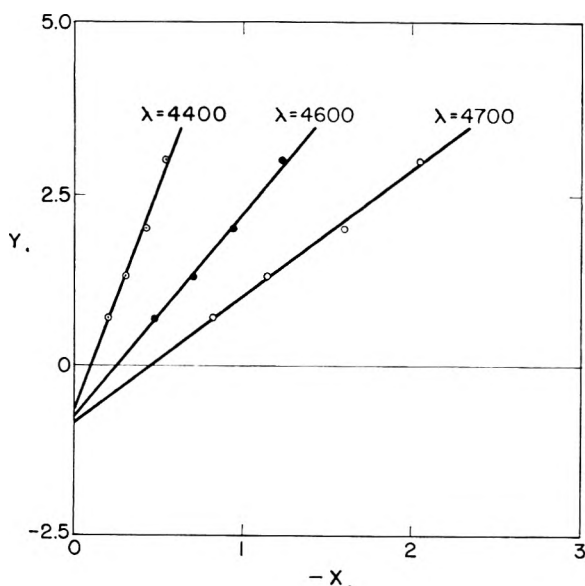


Fig. 2.—Dibutyl ether-iodine spectrophotometric data of Keefer and Andrews¹¹ plotted according to eq. 15.

fords a particularly good test of our method. In Fig. 1 we have plotted the Ketelaar data at 4514 Å., expressed in concentration units, according to eq. 15. When all the points are included, we obtain an equilibrium constant, by least squares analysis, of $K_c = 1.17 \pm 0.04$ and a molar absorptivity of the complex of $\epsilon_c = 957 \pm 8$. These values are to be compared with Ketelaar's values of $K_c = 1.05$ and $\epsilon_c = 988$. Drago and Rose report the values of $K_c = 1.14 \pm 0.03$ and $\epsilon_c = 979 \pm 10$. It is to be noted that our analysis and that of Drago and Rose lead to values of the prod-

uct $K_c \epsilon_c$ (a fundamental quantity in the Benesi-Hildebrand and Ketelaar equations) which are virtually identical, and which exceed Ketelaar's own value for this quantity by some 7%. Evidently our method and that of Rose and Drago simply apportion this product between the two component factors in a slightly different manner.

It has been noted previously⁹ that the iodine-dioxane spectra do not form an isosbestic point with the pure iodine spectrum when the dioxane concentration exceeds 1 M. We find that the dilute solution data yield an equilibrium constant of 1.18 ± 0.04 while the data at concentrations 1 M and above are best fit by a constant having magnitude 1.08 ± 0.02 . These results are again within the limits of error given by Drago and Rose. It is tempting to attribute the change in equilibrium constant to the formation of a second dioxane complex. However, when the data are analyzed in this fashion (by subtracting out the absorbance due to free iodine from the experimental value and using the calculated absorbance of the 1:1 complex as A^6 in eq. 8), the scatter is extremely bad and constants ranging from +0.2 to -0.5 can be obtained. In addition, it is reasonable to suppose that the neglect of dioxane activity coefficients could contribute about as much to the change in K_c as would a second complex. Dioxane and the solvent carbon tetrachloride have been shown to form a compound in the solid state.¹⁰ Interaction between dioxane and the solvent would have the largest relative depressant effect on the dioxane activity in the most dilute solutions, and it is in these that the largest equilibrium constants for complex formation with iodine are observed.

According to eq. 15, data taken at various wave lengths should yield a family of straight lines having a common intercept and different slopes. To illustrate, we have plotted in Fig. 2 the data of Keefer and Andrews¹¹ on the system dibutyl ether-iodine in cyclohexane solution. The three lines corresponding to data at wave lengths 4400, 4600 and 4700 Å. have nearly the same intercepts and yield an equilibrium constant $K_c = 0.79 \pm 0.05$. Keefer and Andrews¹² have reported the value 0.74.

To illustrate the applicability of our expression to hydrogen bonding equilibria, and also to indicate the errors which may arise when the assumption that the non-absorbing species is present in very large excess is not justified, we have examined the data of Nakagura and Gouterman¹³ on the system phenol-triethylamine in *n*-heptane. The data were taken from Fig. 5 of their paper. The excesses of triethylamine over phenol which they used ranged roughly from 25 to 500-fold. If the concentrations of triethylamine are not adjusted to correct for complexing, we obtain an average equilibrium constant of 78.6 based on data at 2740 and 2800 Å. If a cyclic procedure is adopted to correct the amine concentration, however, a value of 82.0 is obtained.

(10) S. M. S. Kennard and P. A. McCusker, *ibid.*, **70**, 3375 (1948).

(11) R. M. Keefer and L. J. Andrews, unpublished data.

(12) R. M. Keefer and L. J. Andrews, *J. Am. Chem. Soc.*, **75**, 3561 (1953).

(13) S. Nakagura and M. Gouterman, *J. Chem. Phys.*, **26**, 881 (1957).

The latter value agrees well with the figure 83.8 cited for this system, when the errors inherent in obtaining the data from small scale graphs are considered.

The necessity for a cyclic procedure when insufficient excesses of complexing agent are encountered is not a serious deterrent to the general utility of the present method, for the data at the two or three highest concentrations will serve to establish immediately the order of magnitude of the constant. Furthermore, during the refinement process the movement of a particular point on a plot of the defined variables X and Y will be always in the direction of increasing Y at constant X , with the greatest displacement occurring at values of X farthest from the origin. Hence the first approximation to the value of the equilibrium constant will yield a value which is too small. The ability to predict the direction in which K will go upon improving the calculations is of considerable value in analyzing the data. It should be mentioned also that refinements in the calculations affect only two of the four sums required to carry out least squares treatments, and we have found this method to be nearly as rapid as graphical techniques for obtaining numerical results. Also, the long extrapolations sometimes required to obtain an intercept graphically can introduce several per cent. error into the equilibrium constant, even when the variables do not need to be adjusted for concentration differences due to complexing.

Acknowledgment.—The author is indebted to Professors R. M. Keefer and L. J. Andrews for supplying their data on the dibutyl ether-iodine system, and for valuable discussions on the subject matter of this note.

INFRARED ANISOTROPY OF TRICLINIC *trans*-8-OCTADECENOIC ACID

BY ANNE S. JAHN AND H. SUSI

Eastern Regional Research Laboratory,¹ Philadelphia, Penna.

Received February 22, 1960

A previous investigation with polarized infrared radiation indicated that crystalline *trans*-11-octadecenoic acid has a more regular structure than any of the known forms of saturated normal fatty acids.² The present communication reports the results of a similar study on *trans*-8-octadecenoic acid. Powder diffraction work has shown that in the *trans*-6 through *trans*-12-octadecenoic acids all odd and all even acids have a similar structure but substantial differences exist between the two groups.³ It became obvious at the beginning of the present investigation that *trans*-8-octadecenoic acid crystallizes in the triclinic system. Application of polarized infrared methods to molecular crystals is complicated by the fact that structurally significant directions are defined inside the absorbing medium, whereas the propagation direction and polarization of the radiation beam is easily identified only out-

side the medium.⁴ Particular care is necessary with triclinic systems and the results must be expected to be of a more qualitative nature than in the case of crystals with higher symmetry.^{4,5} Additional experimental work on triclinic crystals should help to evaluate the usefulness and/or limitations of such studies.

Experimental

The sample has been described.⁶ An oriented film between rock-salt plates was prepared by previously discussed methods.² A Perkin-Elmer Model 21 instrument equipped with a rock-salt prism and silver chloride polarizer was used. It was not possible to specify the exact orientation of the sample. It was assumed that the layers of the end-groups were parallel to the planes of the sample, as found for previously investigated acids,² and parallel to the ab planes as in all known saturated acids.⁷ This assumption is supported by the polarization of the OH stretching band which is very similar to form C stearic acid.² The band is apparently polarized in a unique direction, which we call c' . The projection of c' on the plane of the sample is designated a , the direction perpendicular to a and to c' is called b . a , b and c' coincide with corresponding directions in Fig. 1 of reference 2. Bold face letters are used to avoid confusion with crystallographic axes. Spectra were first obtained with the electric vector ϵ along a , b , a' , a'' , b' and b'' . (The nomenclature is identical with the one used in earlier work.²) Additional data were obtained with perpendicular incidence and the electric vector at 15° increments, parallel to the sample plane. The directions of the electric vector refer to the beam before it enters the sample.

Result

The spectra obtained with tilted radiation beams revealed no planes or glide planes of symmetry, in contrast to the previously studied *trans*-11 acid and the saturated parent compound, stearic acid.² CH_2 rocking and bending bands around 720 and 1470 cm^{-1} were not found to be split and polarized in the manner which is characteristic for orthorhombic hydrocarbon substructure.^{2,8} Absence of an in-phase C=O stretching band, known from Raman measurements to occur around 1650 cm^{-1} ,⁹ suggests centrosymmetric dimers, as in all previously studied carboxylic acids.

These observations indicate that centrosymmetric dimers are packed into a triclinic system in such a way that no orthorhombic hydrocarbon substructure results. The highest possible space group symmetry is $C_1^1\text{-P}\bar{1}$.

Because of the low over-all and substructure symmetry, the polarization of all the numerous absorption bands is not discussed; nor is a detailed assignment attempted. The spectra observed with ϵ along a and b (perpendicular incidence) and the spectra with ϵ approximately parallel or perpendicular to c' (within the ac plane, nonperpendicular incidence) are shown in Fig. 1. a , b and c' have been defined in the Experimental section. Some qualitative suggestions about the shape and packing of the molecules are made on the basis of splitting and polarization of well-known group-fre-

(4) R. Newman and R. S. Halford, *J. Chem. Phys.*, **18**, 1276 (1950).

(5) (a) R. Newman and R. M. Badger, *ibid.*, **19**, 1147 (1951); (b) H. Susi, *Spectrochim. Acta*, 1063 (1959).

(6) D. Swern, L. P. Witnauer, S. A. Fusari and J. B. Brown, *J. Am. Oil Chemists' Soc.*, **32**, 539 (1955).

(7) E. v. Sydow, *Arkiv Kemi*, **9**, 231 (1956).

(8) S. Krimm, C. Y. Liang and G. B. B. M. Sutherland, *J. Chem. Phys.*, **25**, 549 (1956).

(9) J. H. Eibben, *Chem. Revs.*, **18**, 1 (1936).

(1) Eastern Utilization Research and Development Division, Agricultural Research Service, U. S. Department of Agriculture.

(2) H. Susi, *J. Am. Chem. Soc.*, **81**, 1535 (1959).

(3) E. S. Lutten and D. G. Kolp, *ibid.*, **73**, 2733 (1951).

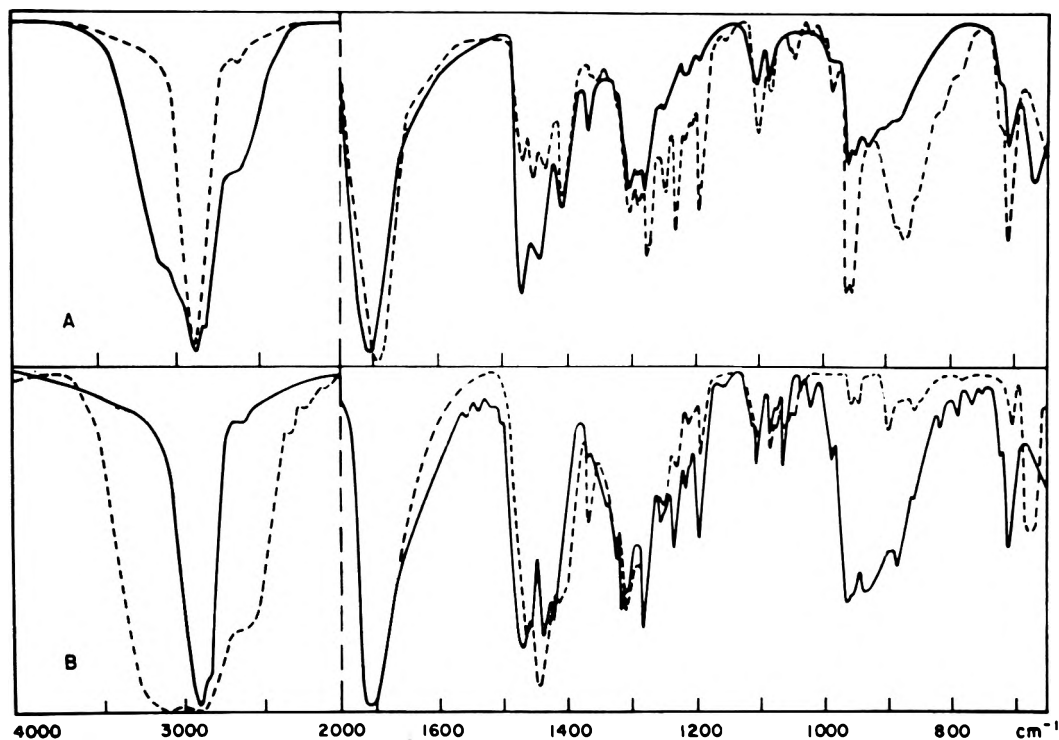


Fig. 1.—Infrared spectrum of *trans*-8-octadecenoic acid: A, electric vector along *a* (solid line) and *b* (dotted line); B, electric vector within the *ac'* plane, approximately perpendicular to *c'* (solid line) and parallel to *c'* (dotted line).

quency bands listed in Table I. Bands which are sufficiently free from extensive overlap have been chosen.

TABLE I

POSITION AND POLARIZATION OF SOME GROUP-FREQUENCY BANDS

Description	Cm. ⁻¹	Polarization	
		ab plane	ac plane
(Carboxyl bands)			
OH str.	3100	<i>a</i>	to <i>c'</i>
C=O	1706	<i>a</i>	to <i>c'</i>
	1693	<i>b</i>	
OH o.o.p. bend.	940	<i>a</i>	⊥ to <i>c'</i>
	881	<i>b</i>	⊥ to <i>c'</i>
COO def.	676	<i>a</i>	to <i>c'</i>
(CH ₂ bands)			
CH ₂ sym. str.	2850	<i>a</i> + 30°	⊥ to <i>c'</i>
CH ₂ bend	1469	<i>a</i> + 30°	⊥ to <i>c'</i>
CH ₂ rock	719	<i>b</i> + 30°	⊥ to <i>c'</i>
(trans-HC=CH— bands)			
HC=CH o.o.p. bend.	966	<i>a</i> ± 75°	⊥ to <i>c'</i>
	959	<i>a</i> - 75°	⊥ to <i>c'</i>

All OH bonds seem roughly parallel to each other and to the main axes of the molecules. The splitting of the C=O stretching and OH out of plane (o.o.p.) bending bands into oppositely polarized branches indicates two sets of carboxyl groups with non-parallel planes. The frequency difference between the 940 and 881 cm.⁻¹ branch of the OH bending band is much larger than is usually observed for factor group splitting and could mean that non-equivalent sites are occupied. The relative polarization of the CH₂ bands is correct and suggests that the major portions of the hydrocarbon

chains are parallel to each other, but probably not parallel to the planes of any of the carboxyl groups. The —HC=CH— o.o.p. bending band is split into a doublet, both components being polarized the same way: perpendicular to the chains but neither perpendicular nor parallel to CH₂ or carboxyl bands.

The molecules, like the ones of the previously studied *trans*-11 acid,² seem to be considerably twisted, but the resulting structure must be different: roughly parallel hydrocarbon chains (strongly tilted with respect to the layers of end groups³) connected to non-parallel carboxyl groups in a triclinic over-all structure.

EVIDENCE FROM INTRINSIC VISCOSITY AND SEDIMENTATION FOR HYPERCOILED CONFIGURATIONS OF STYRENE-MALEIC ACID COPOLYMER

By WALTER DANNHAUSER, WILLIAM H. GLAZE,
RAY L. DUELTGEN AND KAZUHIKO NINOMIYA

Departments of Chemistry, University of Wisconsin, Madison, Wisconsin,
and University of Buffalo, Buffalo, New York

Received February 13, 1960

Some data concerning the viscometric behavior of styrene-maleic acid copolymer (SYMA) in aqueous solutions have been reported previously by Ferry and co-workers.¹ In pure water, the reduced viscosity curves are concave upward, typical of a polyelectrolyte. On addition of hydrochloric acid, the curves flatten and extrapolate to progressively smaller intrinsic viscosities. A sample of $M = 190,000$ in 0.006 *N* HCl at 25° had $[\eta] = 0.09$, for example. On further addition of

(1) J. D. Ferry, D. C. Udy, F. C. Wu, G. E. Heckler and D. B. Fordyce, *J. Colloid Sci.*, **6**, 429 (1951).

hydrochloric acid, phase separation occurred. In fact, it was found later that fractionation of a sample could be effected by progressive acidification of an aqueous solution.²

From the thermodynamic theory of phase separation³ it might be expected that 0.006 N HCl should be close to a Θ -solvent at 25°. However, Flory's expression⁴ for the intrinsic viscosity, $[\eta] = KM^{1/2}\alpha^3$, predicts that the intrinsic viscosity in a Θ -solvent ($\alpha = 1$) will be the smallest observed; and estimation with a reasonable value of $K = 8 \times 10^{-4}$ gives $[\eta]_{\Theta} = 0.35$ for $M = 190,000$. Thus the observed intrinsic viscosity is smaller than the theoretical minimum by a factor of 4. We wish to report some preliminary experiments aimed at resolving this apparent anomaly. The polymer was taken from the same source as in the earlier study.

In order to obtain directly the properties of the uncharged molecule, for which hydrodynamic theories are well developed, it was necessary to find a non-ionizing Θ -solvent. Exploratory studies established the utility of *sec*-butyl alcohol for this purpose, and from phase separation studies with fractions of different molecular weights in the usual manner³ the Flory temperature was determined to be 40°. The Θ point was further confirmed by absence of a second virial coefficient in the concentration dependence of osmotic pressure. Added hydrochloric acid had no effect on the viscosity in this solvent. Intrinsic viscosities and sedimentation constants were obtained for two well-characterized fractions of SYMA in *sec*-butyl alcohol at 40° and also in a 0.006 N HCl-0.008 N KCl aqueous solution at 25°. The latter solvent composition was chosen to give a stable solution in which the upsweep of the reduced viscosity curves was almost completely repressed. The potassium chloride was added to the ionizing solvent to minimize the sedimentation drag of the counterions.⁵ The aqueous acid solutions were water clear and remained so for at least several days. They then gradually became turbid and eventually a precipitate formed. Molecular weights were determined osmotically in *sec*-butyl alcohol at 40°. The experimental results, as well as some derived parameters, are given in Table I. Here f is the friction coefficient.⁵ (Results for two other, less precisely characterized fractions were in qualitative agreement with those reported here.)

The viscometric and sedimentation data in *sec*-butyl alcohol are in general accord with current theories and there is little doubt that they are characteristic of the unperturbed random coil. The extremely small intrinsic viscosities and abnormally large sedimentation constants found in

(2) A blend of relatively low molecular weight was fractionated from 0.5% aqueous solution by successive additions of hydrochloric acid; the successive HCl normalities yielded percentages precipitated with intrinsic viscosities as follows: 0.0150 N, 60%, 0.51 dl./g.; 0.0175 N, 23%, 0.48 dl./g.; 0.0300 N, 5%, 0.31 dl./g.; 0.0500 N, 2%, 0.26 dl./g. The intrinsic viscosities refer to the polyacid in 90% aqueous dioxane at 25°. This experiment was suggested by Dr. E. R. Garrett.

(3) P. J. Flory, "Principles of Polymer Chemistry," Cornell University Press, Ithaca, N. Y., 1953, Chapter XIII.

(4) Reference 3, p. 612.

(5) T. Svedberg and K. O. Pedersen, "The Ultracentrifuge," Oxford University Press, New York, N. Y., 1940, Chapter 2.

TABLE I

Polymer fraction	4A	B2-RHB
\bar{M}_n	74,000	200,000
$[\eta]_{\Theta}$, <i>sec</i> -butyl alcohol, 40°	0.35	0.55
$[\eta]$, aqueous HCl-KCl, 25°	.049	.061
$\alpha^3 = [\eta]/[\eta]_{\Theta}$.140	.111
α	.52	.48
$s_0 \times 10^{13}$, <i>sec</i> -butyl alcohol, 40°	2.69	4.41
$s_0 \times 10^{13}$, aqueous HCl-KCl, 25°	9.7 ₅	26.6
$(f/\eta_0) \times 10^{-6}$, <i>sec</i> -butyl alcohol, 40°, η_0 = solvent viscosity	4.8	7.2
$(f/\eta_0) \times 10^{-16}$, aqueous HCl-KCl, 25°	1.6	1.6

the aqueous system indicate that we have here a truly hypercoiled configuration. Assuming that the intrinsic viscosity of the tightly coiled molecule still has the same functional dependence on molecular parameters as does the random coil, we see that the coil has contracted by a factor of two. Comparison of the friction factors leads to qualitatively similar conclusions but large experimental uncertainties in these data preclude a more detailed analysis.

Summary.—The inordinately small intrinsic viscosity of SYMA in acidified aqueous solution is due to the fact that the solvent is actually much poorer than a Θ -solvent. Precipitation, when it occurs, probably is based on kinetic rather than thermodynamic relations. Because of the metastability of the solution, it has been possible to study a polymer in which the expansion factor α is appreciably smaller than unity.

Acknowledgments.—This work was supported in part by a grant from Esso Research and Engineering Company to the University of Wisconsin, and in part by the Office of Naval Research under Contract N701R-28509. We wish to thank Professor Robert L. Baldwin, formerly of the Department of Biochemistry, University of Wisconsin, and Professor Sidney Shulman, School of Medicine, University of Buffalo, for their assistance with the ultracentrifuge experiments; and Professor John D. Ferry for helpful discussions.

SPECTROSCOPIC EVIDENCE OF AN ALUMINA CATALYZED SURFACE REACTION BETWEEN AMMONIA AND CARBON DISULFIDE

BY E. P. PARRY AND H. RUBALCAVA

Union Oil Company of California, Research Center, Brea, California
Received February 23, 1960

During some preliminary studies of the infrared spectra of various gases adsorbed on aluminas, a reaction between carbon disulfide and ammonia was observed. Our data can be interpreted in terms of the alumina catalyzed reaction



This reaction is known in solution but the rate of reaction is small. Carbon disulfide and excess concentrated aqueous ammonia react very slowly at room temperature to give ammonium thiocya-

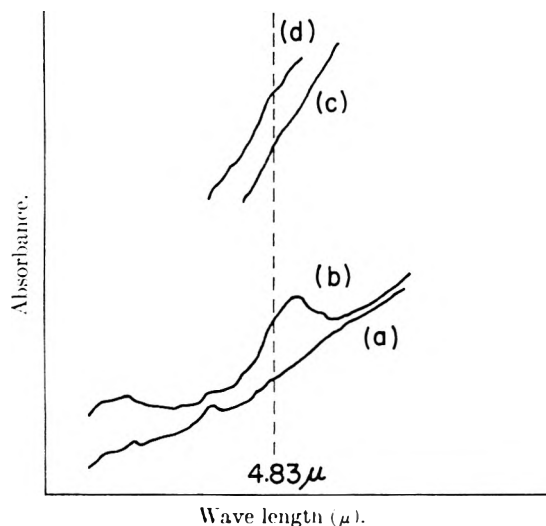


Fig. 1.—(a) η -alumina background; (b) after exposure to $\text{NH}_3\text{-CS}_2$ mixture then pumping off at room temperature; (c) γ -alumina background; (d) same as (b) for γ -alumina.

nate.¹ In the gas phase the reaction does not go except at "red heat."²

When mixtures of ammonia and carbon disulfide are exposed to an infrared transparent disc of partially dried η (or γ) alumina for 5 to 10 minutes, then the gases pumped off, an absorption band at 2090 cm.^{-1} is found in the spectrum. This band does not appear when either gas is used alone, or when silica is used as adsorbent. The band increases in intensity with increasing carbon disulfide concentration. Under optimum conditions, the band can just be detected with a carbon disulfide concentration of about 0.03%. Miller and Wilkens³ have reported that the thiocyanate ion has a strong absorption band in the region 2020 to 2090 cm.^{-1} . We suggest that our experimental facts are consistent with the occurrence of a surface reaction similar to reaction 1 with the alumina acting as catalyst.

If, after exposure of the alumina disc to the gases, the cell is evacuated ($< 10^{-4}\text{ mm.}$) and slowly heated to about 200° , the intensity of the band increases markedly, indicating that reaction 1 goes further to the right with increasing temperature. The removal of the absorption band at 2090 cm.^{-1} is not easily done, requiring temperatures of up to 350° with concomitant evacuation for two hours or more. This implies that the ammonium thiocyanate formed by reaction 1 is strongly chemisorbed to the alumina surface.⁴

If excess carbon disulfide and a small amount of ammonia are used, the spectrum is complicated by an additional band at 2070 cm.^{-1} which is easily removed upon evacuation. This weakly adsorbed species is probably carbonyl sulfide which has a fundamental vibration in the gas phase at 2060 cm.^{-1} . Whether this is formed by the direct reaction of carbon disulfide with alumina⁵ or results from the

hydrolysis of HSCN on the surface,^{6,7} cannot be decided with the data available.

Our data indicate that η -alumina is better than γ -alumina as a catalyst for this reaction at room temperature. The figure shows spectra obtained after admitting ammonia containing 0.07 mole % carbon disulfide to two similar (*i.e.*, approximately the same thickness, surface area, prior treatment and infrared transmission in the region of $5\ \mu$) discs of η - and γ -alumina for 5 to 10 minutes, then evacuating for 45 minutes. The 2090 cm.^{-1} band is quite prominent when η -alumina is used as an absorbent, while it cannot be seen with γ -alumina. However, the intensities of the two bands are approximately equal after each absorbent-adsorbate mixture is heated slowly to 200° . This variation in reactivity may be caused by differences in Lewis acidity between the two aluminas.

The various adsorbents were used in the form of thin self-supporting wafers.⁸ Surface areas of about $200\text{ m.}^2/\text{g.}$ and disc thicknesses of about 20 mg./cm.^2 were typical. The reactions were made in an *in situ* cell somewhat like that of Eischens, *et al.*⁹ and the spectra were obtained with a modified Beckman IR-2A spectrophotometer employing sodium chloride optics.

(5) L. A. Munro, *et al.*, *Trans. Roy. Soc. (Can.)*, **III**, **28**, 29 (1934); *Can. J. Res.*, **9**, 124 (1933).

(6) N. V. Sidgwick, "The Chemical Elements and their Compounds," Vol. I, Clarendon Press, Oxford, 1950, p. 675.

(7) T. Moeller, "Inorganic Chemistry," John Wiley and Sons, Inc., New York, N. Y., 1952, p. 690.

(8) R. H. Lindquist and D. G. Rea, paper presented before the Physical and Inorganic Division of the American Chemical Society, September, 1957.

(9) R. P. Eischens, S. A. Francis and W. A. Pliskin, *THIS JOURNAL*, **60**, 194 (1956).

REACTION OF N^1, N^2 -DISALICYLIDENE-1,2-PROPANEDIAMINE WITH COPPER(II) IONS IN AQUEOUS ISOPROPYL ALCOHOL SOLUTION

BY KERMIT B. WHETSEL

Tennessee Eastman Co., Division of Eastman Kodak Co., Kingsport, Tenn.

Received February 4, 1960

The reaction of N^1, N^2 -disalicylidene-1,2-propanediamine (A) with copper (II) is generally recognized to result in the formation of a 1:1 violet complex.¹ In the course of working with these reactants in 50% aqueous isopropyl alcohol solution, it became apparent that more than one reaction was taking place. The potentiometric and spectrophotometric work which subsequently was carried out in order to clarify the course of the reaction in the mixed solvent system is described in this note.

Experimental

Apparatus and Materials.—Spectra were measured with a Cary Model 14 spectrophotometer using 1.00-cm. silica cells. Apparent pH readings in 50% (by volume) aqueous isopropyl alcohol solution, hereafter called the solvent, were measured with a Beckman Model G pH meter standardized with aqueous buffers.

(1) (a) A. E. Martell and M. Calvin, "Chemistry of Metal Chelate Compounds," Prentice-Hall, Inc., New York, N. Y., 1952, pp. 289-292; (b) J. C. Bailar, Jr., "The Chemistry of the Coordination Compounds," Reinhold Publ. Corp., New York, N. Y., 1956, p. 223.

(1) E. Wertheim, *J. Am. Chem. Soc.*, **48**, 826 (1926).

(2) J. W. Mellor, "A Comprehensive Treatise of Inorganic and Theoretical Chem.," Vol. VI, Longman's, Green and Co., London, 1925, p. 112.

(3) F. A. Miller and C. H. Wilkens, *Anal. Chem.*, **24**, 1254 (1952).

(4) H. J. Callomon, *et al.*, *Proc. Roy. Soc. (London)*, **208A**, 341 (1951).

Stock solutions of all reagents were prepared in 50% aqueous isopropyl alcohol solution. A recrystallized sample of A, m. p. 52–53°, and distilled samples of salicylaldehyde and 1,2-propanediamine were used. An aqueous stock solution of Merck reagent grade copper(II) chloride was standardized by the iodine–thiosulfate method.² The acetate buffer was a 10:1 mixture of 0.42 *M* acetic acid and sodium hydroxide solutions, and the borate buffer was a 6:1 mixture of 0.22 *M* boric acid and sodium hydroxide solutions. The 2,2,4-trimethylpentane was Eastman Kodak Spectro Grade.

Preparation of Samples.—Except where otherwise noted, the following procedure was used to prepare samples for apparent *pH* and absorbance measurements. To each of a series of 50-ml. volumetric flasks were added, in order, the desired aliquots of 2.35×10^{-2} *M* solutions of A, salicylaldehyde and/or 1,2-propanediamine, 5 ml. of 0.08 *N* hydrochloric acid, the desired aliquot of 2.35×10^{-2} *M* copper(II), and enough solvent to make the volume about 35 ml. Acetate buffer, sodium hydroxide or hydrochloric acid solution was added to give the desired apparent *pH*, and the volume was then brought to 50 ml. with solvent.

In the potentiometric titration of mixtures of copper(II) and A, the sodium hydroxide was added in one increment when the ratio of base to metal was less than 6:1; for the more alkaline solutions six moles of base per mole of metal were added initially, and a second addition of base was made 2 hours later. This procedure prevented the precipitation of copper hydroxide except in the very alkaline solutions.

Mole ratio³ and continuous variation⁴ experiments were carried out at apparent *pH* 4.5 using 10 ml. of the acetate buffer for the initial *pH* adjustment and a small amount of 0.5 *N* hydrochloric acid or sodium hydroxide solution, added a few hours later, for the final adjustment. The spectra were measured immediately and after 22 and 48 hours. Similar data were obtained at apparent *pH* 8.8 by mixing, in order, 20 ml. of the borate buffer, 14 ml. of solvent, the desired aliquots of copper(II) and of A, and enough solvent to bring the volume to 50 ml. Much of the copper(II) precipitated in the buffered solution, but the precipitate gradually disappeared after A was added. The spectra were measured 16 hours after mixing. The formation of the violet complex was incomplete when the buffer was added to acidic solutions of the reactants and when copper(II) was added to buffered solutions of A.

The reaction of copper(II) with 1,2-propanediamine and/or salicylaldehyde was studied using a series of solutions having reactant ratios of 1:0:0, 1:0:2, 1:1:0, 1:1:1, 1:1:2, and 1:1:4. The apparent *pH* was adjusted to 4.5 with sodium hydroxide solution three times over a two-day period before measuring the spectra (Fig. 1). The apparent *pH* then was adjusted to 8.5 with alkali, and the spectra were measured at intervals over the next month (Fig. 2).

Using acetate buffer to maintain the apparent *pH* at 4.5, four solutions were prepared in which the ratios of copper(II), 1,2-propanediamine, and salicylaldehyde were (1) 1:1:0.5; (2) 1:1:1; (3) 1:1:2; and (4) 0:0:1. A fifth solution in which the reactant ratios were the equivalent of 1:1:2 was prepared by mixing equimolar amounts of copper(II) and A. The concentration of salicylaldehyde in solution 4 and of copper(II) in the other solutions was 2.35×10^{-3} *M*. After being allowed to stand overnight, the solutions were extracted three times with 2,2,4-trimethylpentane (the blue complex remained in the aqueous layer). The ultraviolet spectra of the extracts were measured and the concentrations of salicylaldehyde were calculated. The extraction efficiency, determined with sample 4, was 91%.

Results

Between apparent *pH* 2.8 and 4.0, only a blue complex having an absorption maximum at 620 $m\mu$ was formed. This reaction was almost complete within 2 hours and three protons were released for each copper(II) ion present. Both the potentiometric and the spectrophotometric data

(2) F. P. Treadwell and W. T. Hall, "Analytical Chemistry," Vol. II, 9th ed., John Wiley and Sons, Inc., New York, N. Y., 1942, p. 611.

(3) (a) J. H. Yoe and A. L. Jones, *Ind. Eng. Chem., Anal. Ed.*, **16**, 111 (1944); (b) J. H. Yoe and A. E. Harvey, Jr., *J. Am. Chem. Soc.*, **70**, 648 (1948).

(4) (a) P. Job, *Ann. Chim.*, [10] **9**, 113 (1928); (b) W. C. Vosburgh and A. R. Cooper, *J. Am. Chem. Soc.*, **63**, 437 (1941).

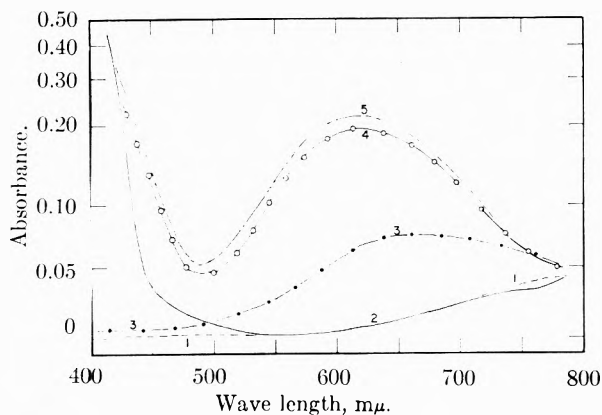


Fig. 1.—Spectra of mixtures of copper(II), 1,2-propanediamine and salicylaldehyde at apparent *pH* 4.5; 2.35×10^{-3} *M* Cu(II); Cu(II): amine: aldehyde ratios of: (1) --- 1:0:0; (2) — 1:0:2; (3) ··· 1:1:0; (4) ○—○ 1:1:1; and (5) - - - 1:1:2.

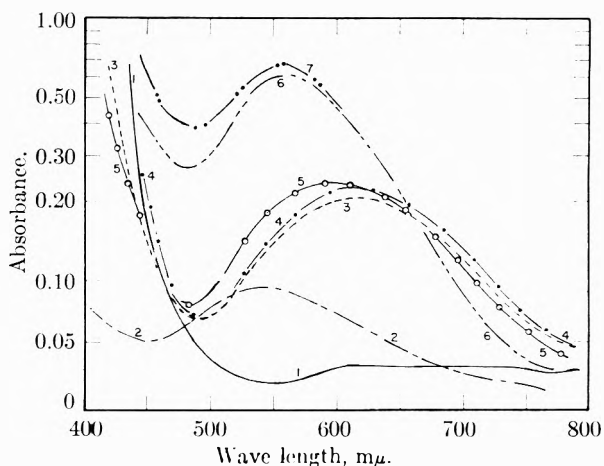


Fig. 2.—Spectra of mixtures of copper(II), 1,2-propanediamine and salicylaldehyde at apparent *pH* 8.5; 2.35×10^{-3} *M* Cu(II); Cu(II): amine: aldehyde ratios of: (1) — 1:0:2; (2) - - - 1:1:0; (3) ··· 1:1:1 immediately after *pH* adjustment; (4) - - - 1:1:2 immediately after *pH* adjustment; (5) ○—○ 1:1:1 34 days after curve 3, *pH* 8.2; (6) — 1:1:2 after 3 adjustments of *pH* to 8.5; and (7) - - - 1:1:4 after 3 adjustments of *pH* to 8.5.

indicated that the reaction was half complete at apparent *pH* 3.2. A violet complex with an absorption maximum at 560 $m\mu$ was formed immediately when the apparent *pH* was 6.7 or higher. In the apparent *pH* range of 4.0 to 6.7, the blue complex was formed at first, but over a period of several days it was converted to the violet one with an accompanying decrease in apparent *pH*. The proton release per copper(II) ion reached a maximum of 3.7 at apparent *pH* 4.5 and then decreased almost linearly to 2.0 at apparent *pH* 8.8. Similar results were obtained with 1:1 mixtures of copper(II) and A between apparent *pH* 2.6 and 5.0. The 1:1 mixtures at apparent *pH* above 5 were not studied because of the excessive time required for equilibrium to be established.

The mole ratio and continuous variation data indicated 1:1 metal to ligand ratios for both the blue and the violet complexes. Similar results were obtained in unbuffered solutions by repeatedly adjusting the *pH* with sodium hydroxide solution.

The curves plotted in Fig. 1 show that salicyl-

aldehyde does not form a colored complex with copper(II) at apparent pH 4.5, but that 1,2-propanediamine forms a complex having a weak absorption maximum near 675 $m\mu$. When all three reactants are present in 1:1:1 ratios, the absorption is much stronger and the maximum is at 620 $m\mu$. Thus, at apparent pH 4.5 the three reactants form a complex that is more stable than the simple copper(II)-amine complex. Another mole of salicylaldehyde does not alter the nature of the complex but increases its concentration through the mass action effect. Under the same conditions, the spectrum of a 1:1 mixture of copper(II) and A is almost identical to curve 5 of Fig. 1.

The effects of raising the apparent pH of these solutions to 8.5 are shown in Fig. 2. When only copper(II) and salicylaldehyde were present, copper(II) was precipitated. The blue 1:1 complex of copper(II) and the amine was converted to the 1:2 violet one (curve 2), and the excess copper was precipitated.⁵ Very little precipitation occurred in the solution containing the three reactants in 1:1:1 ratios, and only minor changes of absorption and apparent pH occurred over a period of 34 days (curve 5). No precipitation occurred in the solution containing copper(II), 1,2-propanediamine and salicylaldehyde in ratios of 1:1:2, but the absorption increased with time and the maximum shifted to 560 $m\mu$ (curve 6); the apparent pH of this solution also decreased with time. The absorption of the 1:1:4 mixture increased faster than that of the 1:1:2 mixture, and it was still the stronger of the two after a month (curve 7). A 1:1 mixture of copper(II) and A behaves in the manner described for the 1:1:2 mixture.

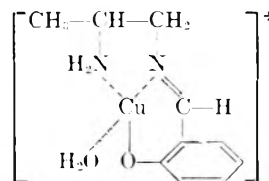
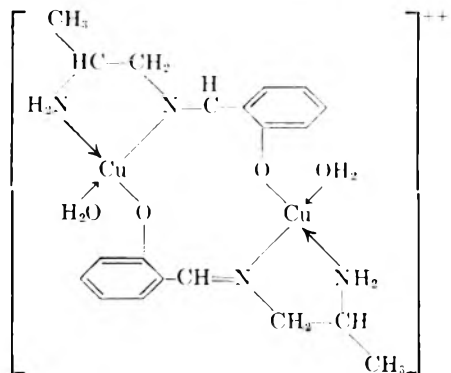
With samples containing copper(II), 1,2-propanediamine and salicylaldehyde in ratios of 1:1:0.5, 1:1:1, and 1:1:2, the salicylaldehyde in the trimethylpentane extracts was 10, 18 and 49%, respectively, of the amounts added. The salicylaldehyde extracted from a 1:1 mixture of copper(II) and A was equivalent to one mole for each mole of A added.

Discussion

From the foregoing results, it is believed that the blue complex has the formula⁶

(5) Similar behavior of the copper(II)-ethylenediamine system was described by H. B. Jonassen and T. H. Dexter, *J. Am. Chem. Soc.*, **71**, 1553 (1949).

(6) Placing the salicylideneamino group on N¹ rather than on N² seems reasonable for steric considerations, although there is no direct experimental evidence on this point. One of the referees has pointed out that the complex might be a dimeric species with the formula



When the apparent pH of the copper(II)-A system is raised above 4.1, the second mole of salicylaldehyde reacts with the free amine group of the blue complex and the product coordinates with the phenolic group to form the violet complex. The number of protons released per metal ion fails to reach the theoretical value of 4, because the formation of the violet complex is incomplete in the apparent pH range of 4.1 to 4.5.

The results obtained upon mixing copper(II) and A in 50% aqueous isopropyl alcohol solutions can be explained once the effects of time, pH and ratio of reactants are understood. When copper(II) is added to an unbuffered solution of A, the violet complex is the sole reaction product until the metal-to-ligand ratio exceeds 0.5:1 slightly. At this stage of the reaction the apparent pH has dropped to about 4.5, and a large part of the unchelated A has been hydrolyzed. The violet complex continues to be formed as more copper(II) is added until the apparent pH drops below 4, at which point the blue complex begins to be formed. By the time that the ratio of copper(II) to A reaches 1:1, however, the apparent pH is in the neighborhood of 3, and most of the blue complex has been hydrolyzed. Thus, the violet complex appears to be the only reaction product, but its concentration is considerably below that expected for complete reaction.

THE VOLATILITY OF ACTINIUM

BY K. W. FOSTER^{1a} AND L. G. FAUBLE^{1b}

Monsanto Chemical Company, Mound Laboratory,² Miamisburg, Ohio

Received March 9, 1960

The scarcity of actinium in natural ores and the exceptional radiation hazards connected with its handling have been obstacles to the determination of many of the element's chemical and physical properties. The general chemical nature of the element and the radioactive behavior of its various isotopes have been known for some time,³ but practically none of the physical properties have been measured until relatively recently. As yet no measurements of the vapor pressure or the boiling point have been found by the authors.

During the course of some related classified research at this Laboratory, several 5-10 mg. samples of actinium-227 metal were prepared from purified salts by the lithium reduction of actinium

(1) (a) Monsanto Chemical Co., Research and Engineering Div., Dayton, Ohio; (b) Monsanto Chemical Co., South Kearny, New Jersey.

(2) Mound Laboratory is operated by Monsanto Chemical Co., for the United States Atomic Energy Commission under Contract No. AT-33-1-GEN-53.

(3) Gmelin, "Handbuch der Anorganischen Chemie," 8 Auflage, System-Nummer 10, Actinium und Isotope (MsTh₂), Verlag Chemie, G.m.b.H., Berlin, 1942, p. 29.

fluoride.⁴ Thin specimens of the element were obtained by volatilization of the actinium from molybdenum crucibles onto hemispherical nickel collectors. Following completion of these volatilization experiments it was found that sufficient data had been accumulated to permit a calculation of an approximate value of the vapor pressure of the element at the volatilization temperature.

The vapor pressure was computed from the rate of evaporation by means of an equation given by Langmuir⁵

$$\log P_{\text{mm}} = 1.2340 + \log W + 0.5 \log T/M$$

where P_{mm} is the vapor pressure in millimeters of mercury, W is the rate of evaporation of material in $\text{g. cm.}^{-2} \text{ sec.}^{-1}$; M is the molecular weight of the substance; and T is the absolute temperature.

The volatilizations were made at 1600° , which is well above the melting point of the element, given by Stites⁴ as $1050 \pm 50^\circ$. The rate of evaporation, W , was determined from the gain in weight of the nickel collector during the time of heating and from the average surface area of the molten metal in the crucible. The crucibles were heated by electron bombardment techniques⁶ and the temperatures were measured with an optical pyrometer.

Table I shows the results of six runs during which actinium was volatilized at 1600° *in vacuo* of 10^{-4} to 10^{-5} mm. Five of these runs were performed primarily to achieve maximum material transfer and, therefore, were carried nearly to completion. The average surface area of the melt in these runs was assumed to be the area of the bottom of the crucible since molten metal was observed to cover the bottom during most of each run. The five-minute run was made primarily to establish a more precise value for the rate of evaporation at the operating temperature. This run was kept short in order to avoid appreciable changes in the surface area of the molten actinium during evaporation. Since the vapor pressure value computed for this short run agreed, within a reasonable factor, with the results of the longer runs, it was decided that the data from these longer runs were equally valid. Therefore, the arithmetic mean of the vapor pressure values for the six runs, 0.006 mm., was used to determine the boiling point of the element from Loftness' chart.⁷ The boiling point of actinium was found to be 3200° with an estimated error of $\pm 300^\circ$. The error is defined by a range of vapor pressure values within a factor of ten of 0.006 mm.

Since the crucible-collector configuration had been varied significantly between runs, the most difficult factor to determine with any precision in this experiment was the evaporation surface area and the various associated crucible effects.

(4) J. G. Stites, M. L. Salutsky and B. D. Store, *J. Am. Chem. Soc.*, **77**, 237 (1955).

(5) I. Langmuir, *Phys. Rev.*, **2**, 329 (1913).

(6) (a) H. M. O'Bryan, *Rev. Sci. Instr.*, **5**, 125 (1934); (b) J. Yarwood, "High Vacuum Technique," John Wiley & Sons, Inc., New York, N. Y., 1946, p. 87.

(7) R. L. Loftness, "A Vapor Pressure Chart for Metals," NAA-SR-132, July, 1952.

However, the range of vapor pressure values in Table I indicates that the effect of these variables is not exceptionally serious. In all configurations the collection of volatilized actinium apparently was accomplished with relatively negligible loss since only minute radioactive contamination of the remainder of the vacuum system resulted. Also, the entire crucible was observed to be at approximately the volatilization temperature, whereas the temperature of the collector was never above 200° . Visual examination of the crucibles after firing indicated that the only wetting that occurred was on the crucible bottom, so it was concluded that refluxing was negligible. It was estimated that the various crucible and area effects could not affect the values for the vapor pressure by more than a factor of two or three.

TABLE I

ACTINIUM VOLATILIZATION EXPERIMENTS AT 1600°			
Ac in crucible, mg.	Time of run, min.	Collector gain, mg.	Computed min. v.p., mm.
6.80	30	4.81	0.004
6.48	30	5.37	.005
9.76	30	9.38	.008
4.98	30	4.62	.004
6.07	30	5.86	.005
6.48	5	1.76	.007

Subsequent neutron emission determinations of the vacuum deposited films of actinium⁸ indicated that the amount of actinium fluoride, the most likely volatile impurity was less than 0.2 atomic % in any one of the samples. It was, therefore, assumed with reasonable assurance that the vapor pressure values in Table I represent minimum values since sources of error other than actinium fluoride contamination would tend to depress the apparent vapor pressure rather than enhance it. Refractory impurities and loss of material not deposited on the nickel collector could affect the results in this manner, but their effects are considered to be within the measuring precision of the experiment. The actinium was kept in a dry helium environment at all times to inhibit the formation of actinium oxide. Also, the material was volatilized as soon as possible after the separation of the actinium to reduce the effects of contamination by daughter products of the radioactive decay of actinium-227. It is felt that the cumulated errors in these experiments did not affect the values obtained for the vapor pressure by more than a factor of ten, which would not affect the value for the boiling point by more than 300° .

It is realized by the authors that this measurement is a side result from related experimentation and is, at best, a crude determination of the boiling point of the element. However, because of the extensive radiation protection equipment and associated health monitoring services required for any work with significant quantities of this element, it does not appear likely that any precise evaluation of its physical properties will be forthcoming in the near future.

(8) K. W. Foster and J. G. Stites, *THIS JOURNAL*, **60**, 1017 (1956).

Acknowledgment.—The authors are indebted to E. H. Daggett, A. W. Wotring, D. U. Wright and R. G. Olt for their contributions to this experiment.

COMMUNICATION TO THE EDITOR

FARADAIC RECTIFICATION AND ELECTRODE PROCESSES¹

Sir:

A theory of faradaic rectification extending and clarifying results of previous investigators² was developed. It was shown that two types of control must be considered, namely, control of the total mean current density (\bar{I}) or the mean electrode potential (\bar{E}). In practice, $\bar{I} = 0$ or $\bar{E} = E_e$, E_e being the equilibrium potential. The shift of mean potential $\Delta\bar{E}$ for control of \bar{I} at zero is the same whether the alternating current or voltage is controlled as a practically harmonic-free sinusoidal function of time. Conversely, the mean current for control of \bar{E} at E_e is the same whether there is alternating current or voltage control.

The time variation of $\Delta\bar{E}$ was derived by noting that the sum of the mean faradaic and non-faradaic (double layer charging) current densities is equal to zero ($\bar{I} = 0$). It was shown that $\Delta\bar{E} \approx \Delta\bar{E}_{t \rightarrow \infty}$ even after as short a time as 10^{-3} sec. provided that reactant concentrations are large enough. Times longer than 10^{-3} sec. may be required for dilute solutions (perhaps $10^{-3}M$). The build-up and decay curves for $\Delta\bar{E} = f(t)$ when the alternating current is switched on once and switched off are the images of each other. The influence of the cell resistance on the time variations of \bar{I} with control of \bar{E} at E_e was shown to be the same as in the voltage-step potentiostatic method, and \bar{I} is equivalent to the current in the latter method when a

potential step $-\Delta\bar{E}_{t \rightarrow \infty}$ is applied while the kinetic parameters remain those at E_e .

A general equation in terms of first and second partial derivatives of \bar{I} with respect to \bar{E} , C_O , and C_R was derived for $\Delta\bar{E}$ and \bar{I} for any type of I - E characteristic for the electrode reaction $O + ne = R$. A particular form is

$$\Delta\bar{E}_{t \rightarrow \infty} = \frac{nF}{RT} V^2 \left\{ \frac{2\alpha - 1}{4} + \frac{\tau_F[(1 - \alpha)r_O - \alpha r_R] + x_F[(1 - \alpha)x_R - \alpha x_O]}{2(\tau_F^2 + x_F^2)} \right\} \quad (1)$$

where V is the amplitude of the alternating voltage, α the transfer coefficient, r_F and x_F the real and imaginary parts of the total faradaic impedance, respectively, and r_i ($i = O$ or R) and x_i the corresponding components of the faradaic impedance for substances O or R . Values of the r 's and x 's obtained in the classical faradaic impedance theory for a variety of processes (simple discharge, discharge with preceding chemical reaction, etc.) can be directly introduced in eq. (1). Properties of $\Delta\bar{E}$ and \bar{I} are readily deduced.

An instrument with application of the alternating voltage for a short duration (10^{-3} to 10^{-1} sec.) and oscilloscopic recording of $\Delta\bar{E}$ (single pulse) was designed for frequencies up to 2 megacycles per sec. Heating of electrolyte near the working electrode is minimized by this method, and frequencies above 2 megacycles per sec. undoubtedly could be utilized.

Theory and experimental results will be published.

(1) Investigation sponsored in part by the Office of Naval Research and the National Science Foundation.

(2) For references, see H. Matsuda and P. Delahay, *J. Am. Chem. Soc.*, **82**, 1547 (1960).

COATES CHEMICAL LABORATORY
LOUISIANA STATE UNIVERSITY
BATON ROUGE 3, LA.

P. DELAHAY
M. SENDA
C. H. WEIS

RECEIVED JUNE 3, 1960

Announcing the second edition of . . .

THE RING INDEX

**A List of Ring Systems
Used in Organic Chemistry**

**by AUSTIN M. PATTERSON
LEONARD T. CAPELL
DONALD F. WALKER**

Until this book first appeared in 1940 there was no single source in any language where structural formulas, names and numberings of the thousands of parent organic ring systems could be found.

FEATURES

This new edition of the Ring Index lists 7727 organic ring systems—almost a hundred percent increase over the first edition. The book now has been enlarged to 1456 pages to cover the abstracted literature through 1956. Each ring system contains: (1) A structural formula showing the standard numbering system in accord with the 1957 Rules for Organic Chemistry of the IUPAC. (2) Other numberings that have appeared in the literature. (3) A serial number which identifies the system. (4) The preferred name and other names given to the system. (5) Identifying references to the original literature.

ARRANGEMENT

The ring systems are arranged from the simplest to the most complex, beginning with single rings, then systems of two rings and so on up to twenty-two ring complexes.

USES

The Ring Index is an indispensable reference work for organic chemists and for others who have to do with cyclic organic compounds. Some of its uses are: (1) Determining accepted structure of a ring system. (2) Finding name or names of the system if structure is known. (3) Finding the numbering of a system. (4) Identifying a system if there are two or more isomeric forms. (5) Discovering what systems have been reported in the literature and where. (6) Naming and numbering a newly discovered ring system. (7) As a reference book in teaching.

Cloth bound

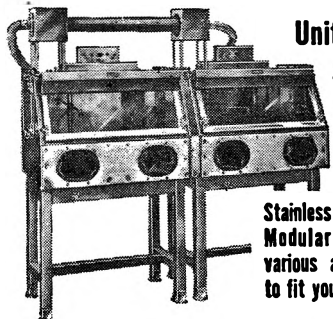
1456 pages

\$20.00

Order from

Special Issues Sales Department, American Chemical Society
1155 Sixteenth Street, N.W., Washington 6, D. C.

22 types of Safety Enclosures for Handling Hazardous Substances



Unitized SAFETY ENCLOSURES

Stainless Steel, All Purpose:
Modular adaptability with various adaptor accessories to fit your needs.

DRY RADIOACTIVE WASTE CONTAINER

All-welded stainless steel construction with stainless steel inner container.

Write for illustrated folder describing these and 20 other kinds of enclosures. S. Blickman, Inc., 9007 Gregory Avenue, Weehawken, New Jersey.



BLICKMAN SAFETY ENCLOSURES

Look for this symbol of quality



Announcing . . . 1959 EDITION

American Chemical Society DIRECTORY of GRADUATE RESEARCH

INCLUDES: Faculties, Publications, and Doctoral Theses in Departments of Chemistry, Biochemistry, and Chemical Engineering at United States Universities

- All institutions which offer Ph.D. in chemistry, biochemistry, or chemical engineering
- Instructional staff of each institution
- Research reported at each institution for past two years
- Alphabetical index of approximately 3,000 faculty members and their affiliation; alphabetical index of 258 schools.

The ACS Directory of Graduate Research, prepared by the ACS Committee on Professional Training, is the only U.S. Directory of its kind. The 4th edition includes all schools and departments, known to the Committee, which are concerned primarily with chemistry, biochemistry, or chemical engineering, and which offer the Ph.D. degree.

The Directory is an excellent indication not only of research reported during the last two years by the staff members at these institutions but also of research done prior to that time. Each faculty member reports publications for 1958-59; where these have not totaled 10 papers, some articles prior to 1958 are reported. This volume fully describes the breadth of research interest of each member of the instructional staff.

Because of the indexing system, access to information is straightforward and easy—the work of a moment to find the listing you need. Invaluable to anyone interested in academic or industrial scientific research and to those responsible for counseling students about graduate research.

Compared to the 1957 edition, this new volume will contain 118 more pages, list approximately 200 additional faculty members, and include 22 additional schools.

Special Offer: Save \$2.50. Copies of the 1957 edition of the Directory, formerly \$3.50 each, may be purchased in combination with the current edition for a total price of \$5.00 for the two volumes. Possession of both copies provides continuity of reference information. Orders for 1957 editions only will be billed at the regular \$3.50 rate.

Paper bound 752 pages \$4.00

ORDER FROM: Special Issues Sales

American Chemical Society

1155 - 16th Street, N.W. • Washington 6, D.C.

CA TODAY

This informative 130 page clothbound volume describes for the reader the interworkings of the world's largest and most successful abstracting undertaking.

All scientists and organizations interested in producing abstracts and/or indexes will find this book on the production of CHEMICAL ABSTRACTS an invaluable aid.

- Increasingly, authors are asked to prepare abstracts of their papers to accompany the complete papers when published in primary journals.
- Scientists must frequently index their own books.
- Industrial organizations routinely build collections of abstracts and indexes with emphasis on their own special interests.

CA Today tells how source material is gathered, explains the assignment of abstracts, and the problems of recording, editing, and classifying abstracts. Indexing procedures are explained, methods of printing are discussed, and research, administration, housing and equipment, nomenclature, and records are amply described in separate chapters. The total concept behind the development of successful abstracting is presented for the first time in one reference.

Clothbound 130 pages \$3.50

order from

Special Issues Sales

AMERICAN CHEMICAL SOCIETY

1155 16th Street, N. W.

Washington, D. C.